2007-12-14

Probing the Structural Topology of HIV-1 Virion Infectivity Factor (VIF): A Dissertation

Jared R. Auclair
University of Massachusetts Medical School

PROBING THE STRUCTURAL TOPOLOGY OF

HIV-1 VIRION INFECTIVITY FACTOR (VIF)

A Dissertation Presented

By

Jared R. Auclair

Submitted to the Faculty of the
University of Massachusetts Graduate School of Biomedical Sciences, Worcester
In partial fulfillment of the requirement for the degree of

DOCTOR OF PHILOSPOHY

December 14, 2007

Biochemistry and Molecular Pharmacology

PROBING THE STRUCTURAL TOPOLOGY OF

HIV-1 VIRION INFECTIVITY FACTOR (VIF)

A Dissertation Presented by

Jared R. Auclair

The signatures of the Dissertation Defense Committee signifies
completion and approval as to the style and content of the Dissertation.

_____
Celia A. Schiffer Ph.D., Thesis Advisor

_____
Mohan Somasundaran Ph.D., Thesis Advisor

_____
Paul Clapham Ph.D., Member of Committee

_____
Reuben Harris Ph.D., Member of Committee

_____
C. Robert Matthews Ph.D., Member of Committee

_____
Mary Munson Ph.D., Member of Committee

The signature of the Chair of the Committee signifies that the written dissertation meets
the requirements of the Dissertation Committee

_____
Phillip Zamore Ph.D., Chair of Committee

The signature of the Dean of the Graduate School of Biomedical Sciences signifies
that the student has met all graduation requirements of the school.

_____
Anthony Carruthers, Ph.D.,
Dean of the Graduate School Biomedical Sciences

Interdisciplinary Graduate Program

December 14, 2007

ACKNOWLEDGEMENTS

I would like to acknowledge all those who have helped me on my path to completing my graduate work. I would like to start by thanking my thesis research advisory committee: Dr. Phillip Zamore, Dr. Mary Munson, Dr. Mario Stevenson, and Dr. Mohan Somasundaran for keeping me on track and helpful discussions over the years. In particular, I would like to thank Phil and Mary for always challenging me to ask the right questions, critically think about my hypothesis, problem solve, and to design experiments that would address the question I was asking. In addition, to my thesis research advisory committee I would like to thank my dissertation examination committee: Dr. Phillip Zamore, Dr. Mary Munson, Dr. Paul Clapham, Dr. C. Robert Matthews, and Dr. Reuben Harris. I especially thank Dr. Harris for making the trip from Minnesota to serve as my external examiner. Finally, I thank Dr. Sean Ryder for his helpful discussions on peptide competition experiments and agreeing to serve as a back-up DEC committee member.

The Schiffer lab has been instrumental in my success over the last 6 and half years. The supportive environment of the lab is second to none. I truly enjoyed coming to work every day, it has been a great place to work and I will miss coming in each day. When I first joined the lab I was the fifth person and we were still on the 7th floor of the medical school, now we have around 15 people in the lab which is a sign of the supportive environment created by Dr. Schiffer. I would like to thank both Alex and Van, two undergraduate students, for there help with my project and giving me the opportunity to teach them. Thank you to Dr. Moses Prabu for critically reading drafts of this thesis

and for always making lab fun and interesting. Thank you Madhavi Nalam for helping me map my cross-linking data onto the theoretical HIV-1 Vif models in Chapter I. In addition, I would like to thank Claire Baldwin for critically reading this thesis. Finally, thanks to Shiven Shandilya for discussions on HIV-1 Vif and his help in advancing the HIV-1 Vif project as a whole.

A few people in the lab and Biochemistry department I would like to thank specifically. First, I would like to thank Tiffanie Covello for being a great friend, helping keep me organized, and just making my job easier in general. Karen Welch has been an amazing friend and extremely supportive over the last six plus years. She has always been there for me professional and personal; going to work without her around will not be the same. Along with many other things, I will miss Karen, Ellen, and I's Weenie Wednesdays. I also cannot even begin to express my thanks to Ellen Nalivaika. She has always been one of my biggest supporters, and over the years we have become really great friends. There are few people in the world who understand and know me as well as she does and I'm truly grateful for that because without her, getting through graduate school would not have been as fun and it would have been much more difficult. I'll be sending many emails with my brain-dead calculation questions!

Of course, I have to thank all my great friends for their support and putting up with me and my "moods" over the last six years. Jenn Murzycki, a former labmate, has been a great friend and without her I could not have done this. Coffee breaks with Dianne Schwarz helped keep me sane over the years and she is one of my closest friends from graduate school. Thanks to Melonnie Furgason for listening to me complain, we

share a common bond of torturous projects, and for critical reading my thesis. Thanks to my bowling friends (Kapil, Evan, Dan, Mike, Jay, and Steve) without our weekly bowling league graduate school just would not have been the same. In addition to weekly bowling, Wednesday night get togethers with Jes, Chris, Crytal and Dave also helped keep me sane through this whole process. They are some of my oldest friends and I appreciate all the support they have given me; I would truly do anything for them.

I do not even know where to begin in thanking both Dr. Celia Schiffer and Dr. Mohan Somasundaran. Celia has been an amazing mentor who has given me every opportunity to succeed. I'm most grateful for her support both scientifically and personally and faith in me. She has always given me all the tools I need to be successful and has taught and allowed me to guide my own research. She not only has been a great mentor but colleague and friend. Mohan is the person I have known the longest at UMass, and he is responsible for sparking an excitement in me for research during my senior year at WPI that persists to this day. Without his support and guidance I could not have done this! I not only consider him an amazing mentor, but an amazing person and friend!

Finally, I would like to thank my family for without there love and support I could have never done this. My Mom and Dad have always been supportive of everything I do; even this crazy thing called graduate school. They have given me the tools and drive to be successful and I'm proud to be their son. I thank my sister, Heather, and my brother, Tyler, for all their support as well. I know that I have not always been the easiest person to get along with but regardless they have always been there for me. I looking forward to

sharing many more of life's adventures with them; and I'm always here for them no matter what. I also would like to thank my cousin Madeleine for all her support over the years; I could not have done this without her support as well. I thank my grandparent's for their support as well; just knowing they are thinking of me helped me through some tough times. I also thank Mr., Mrs., and Adam Grabowski for their support in my quest to get a Ph.d.; and for raising an amazing woman, Melissa.

I thank my wife, Melissa, for all her love and support over the years. You are my best friend and I am blessed to have you in my life. You know me better than anyone else, and I am so happy we were able to share this experience together. There is no doubt in my mind that I could not have done this without you. You are an amazing person and I love you with all my heart. I look forward to the next chapters in our life together and the experiences that lay ahead including the birth of our daughter, Madison. I cannot wait to meet you Madison and love you. Finally, as I finish these acknowledgements I remember all those family and friends who have died and take a moment to pause and remember them and thank them for helping make me the person I am today!

ABSTRACT

Human Immunodeficiency Virus Type 1 (HIV-1), the virus that causes Acquired Immunodeficiency Syndrome (AIDS), attacks the immune system leaving patients susceptible to opportunistic infections that eventually cause death. Highly Active Antiretroviral Therapy, HAART, is the current drug strategy used to combat HIV. It is a combination therapy that includes HIV-1 Reverse Transcriptase and HIV-1 Protease inhibitors. Drug resistant strains arise that evade current HAART treatments; therefore novel drugs are needed.

HIV-1 regulatory proteins such as Tat, Rev, Nef, Vpr, Vpu, and Vif are attractive new drug targets. Of particular interest is the HIV-1 Vif protein and its cellular binding partner APOBEC3G. In the absence of HIV-1 Vif, APOBEC3G, a cytidine deaminase, is able to mutate the viral cDNA and render the virus noninfectious. HIV-1 Vif binds to APOBEC3G and targets it for proteosomal degradation through an interaction with a Cullin-RING ligase complex. Blocking the HIV-1 Vif APOBEC3G interaction would allow APOBEC3G to perform its antiviral function.

An attractive strategy to target the HIV-1 Vif APOBEC3G interaction would be a structure-based one. To apply structure-based drug design approaches to HIV-1 Vif and APOBEC3G, I attempted to collect high resolution structural data on HIV-1 Vif and APOBEC3G. My attempts were unsuccessful because the milligram quantities of soluble protein required were not obtained.

Therefore, in Chapter III I used chemical cross-linking and mass spectrometry to probe the structural topology of HIV-1 Vif obtaining low resolution structural data.

Chemical cross-linking formed HIV-1 Vif multimers including dimers, trimers, and tetramers. Analysis of the cross-linked monomer revealed that HIV-1 Vif's N-terminal domain is a well-folded, compact, globular domain, where as the C-teriminal domain is predicted to be disordered. In addition, disorder prediction programs predicted the C-terminal domain of HIV-1 Vif to be disordered. Upon oligomerization the C-terminal domain undergoes a disorder-to-order transition that not only facilitates oligomerization but may facilitate other protein-protein interactions. In addition, HIV-1 Vif oligomerization bring Lys34 and Glu134 in close proximity to each other likely creating one molecular surface forming a "hot spot" of biological activity.

In Chapter IV I confirmed my low resolution structural data via peptide competition experiments where I identified peptides that can be used as scaffolds for future drug design. HIV-1 Vif oligomerization is concentration dependent. The HIV-1 Vif peptides Vif(29-43) and Vif(125-139) were able to disrupt HIV-1 Vif oligomerization, which confirms the low resolution structural data. HIV-1 Vif peptides Vif(25-39) and Vif(29-43) reduced the amount of APOBEC3G immobilized on the Protein A beads, reduced the amount of HIV-1 Vif interacting with APOBEC3G, or degraded APOBEC3G itself. These peptides could be used as scaffolds to design novel drugs that disrupt the function of HIV-1 Vif and or APOBEC3G.

Therefore, low resolution structural data and peptide competition experiments were successful in identifying structurally important domains in HIV-1 Vif. They also provided insight into a possible mechanism for HIV-1 Vif function where a disorder-to-order transition facilitates HIV-1 Vif's ability to interact with a diverse set of macromolecules. These data advance our structural understanding of HIV-1 Vif and they will facilitate future high-resolution studies and novel drug designs.

. TABLE OF CONTENTS

LIST OF TABLES

LIST OF FIGURES

ABBREVIATIONS

α-cyano	α-cyano-4-hydroxycinnamic acid matrix
AGM	African Green Monkey
APOBEC3G, APO3G	Apolipoprotein B mRNA Editing Enzyme, Catalytice Polypeptide-like 3G
AIDS	Acquired Immunodeficiency Syndrome
Cul5	Cullin5
co-IP	co-Immunoprecipitation
EDC	1-ethyl-3-[3-dimethylaminopropyl]carbodiamide
EIAV	equine infectious anemia virus
EloB	elongin B
EloC	elongin C
Env	HIV-1 envelope protein
ER	endoplasmic reticulum
ESI	electrospray ionization
FRET	fluorescence resonance energy transfer
FT-ICR	fourier transform ion cyclotron resonance
GPMAW	General Protein Mass Analysis for Windows
HAART	Highly Active Antiretroviral Therapy
HDL	high density lipoprotein
HMM	high molecular mass

HIV-1	Human Immunodeficiency Virus Type-1
IAP	Intracisternal A-Particle
LB	luria broth
LINE	long interspersed nuclear elements
LMM	low molecular mass
LTR	long terminal repeat
MALDI/MS	matrix-assisted laser desorption/ionization-mass spectrometry
MALDI-Tof	matrix-assister laser desorption/ionization-time of flight
MAPK	mitogen-activated protein kinase
MS	mass spectrometry
MW	molecular weight
m/z	mass-to-charge ratio
NarL	nitrate/nitrite response regulator
NC	HIV-1 nucleoside
NESI	nanoelectrospray
NRTI	nucleotide or nucleoside reverse-transcriptase inhibitors
NNRTI	nonnucleoside reverse-transcriptase inhibitors
PAWS	Protein Analysis Worksheet
PBL	peripheral blood lymphocytes
PIC	preintegration complex
PONDR®	Predictors of Natural Disordered Regions

ppm	parts-per-million
PR	HIV-1 protease
RRE	Rev Response Element
RT	HIV-1 reverse transcriptase
RU	response unit
SAXS	small angle x-ray scattering
SEC-LS	size exclusion chromatography-laser light scattering
(SCF)-like complex	Skp1-Cullin-F-box-like complex
SOCS	suppressor of cytokine signaling
sor	short open-reading frame
SPR	surface plasmon resonance
SU	HIV-1 surface domain
sulfo-NHS	sulfo-N-hydroxysuccinimide
TB	terrific broth
TFA	trifluoroacetic acid
TM	HIV-1 transmembrane domain
TRF	time resolved fluorescence
UNAIDS	United Nations Programme on HIV/AIDS
VHL	von Hippel-Lindau tumor suppressor protein
Vif	HIV-1 virion infectivity factor
vRNA	viral RNA
WHO	World Health Organization

PREFACE

Chapter III has been previously published as:

Auclair, J.R., Green, K.M., Shandilya, S., Evans, J.E., Somasundaran, S., and Schiffer, C.A. Mass spectrometry analysis of HIV-1 Vif reveals an increase in ordered structure upon oligomerization in regions necessary for viral infectivity (2007). *Proteins* 69(2): 270-84.

Contributions to this work: A number of people contributed to this work. In Chapter I, Madhavi Nalam generated the figures (Figure 1.2D/E) where my cross-linking data was mapped onto the theoretical HIV-1 Vif models. In Chapter III, both James Evans, Karin Green, and Jinal Patel of the UMass Proteomics Core Facility helped run the mass spectrometers and aided in data analysis. Jennifer Saporita helped quantitate the cross-linked bands in Chapter III. Ellen Nalivaika helped run western blots of the serial dilution experiments in Chapter IV. In my attempts to try to obtain soluble protein (Appendix I), Mohan Somasundaran helped infect sf9 insect cells and maintained the cultures. In Appendix II, Kara Herlihy (the application scientist for Biacore) helped run the Biacore analysis of NusA-Vif and APOBEC3G. Ewa Folta-Stogniew, a research scientist at the Yale Keck Facility, was instrumental in collecting and analyzing the SEC-LS data presented in Appendix II.

CHAPTER I

INTRODUCTION

Human immunodeficiency virus type 1 (HIV-1), the retrovirus that causes acquired immunodeficiency syndrome (AIDS), has become epidemic over the last 30 years. The virus devastates a patient's immune system by killing macrophages, CD4 T cells, and dendritic cells, leaving the patient susceptible to opportunistic infections that eventually cause death. To combat the virus, drug strategies have been created and administered to patients. Most patients currently receive highly active antiretroviral therapy (HAART), which includes inhibitors of both viral reverse transcriptase and protease and has effectively prolonged the lives of HIV-1-infected individuals. However, due to the high infidelity of the reverse transcriptase and selective pressures caused by current drug regimens, viruses resistant to HAART have emerged, creating a need for new viral targets.

Attractive new viral targets include HIV-1 regulatory proteins such as Tat, Rev, Vpu, Nef, Vpr, and Vif (Flexner, 2007). In the past, regulatory proteins were thought to be unessential to the viral life cycle, and therefore not considered valuable drug targets. However, in recent years, the roles of regulatory proteins have become better understood, and many of them are necessary for viral production. Two regulatory proteins, Tat and Vpr, have previously been targeted in clinical trials, but these inhibitors showed no antiviral activity (Haubrich, 1995; Para, 2006; Flexner, 2007). Further investigation into regulatory proteins as potential drug targets are needed. An interesting candidate is the HIV-1 Vif protein and its cellular binding partner, apolipoprotein B mRNA editing enzyme, catalytic polypeptide-like 3G (APOBEC3G or simply, APO3G), which HIV-1 Vif targets for proteosomal degradation (Marin, 2003; Sheehy, 2003; Stopak, 2003). In

the absence of HIV-1 Vif, APO3G acts as an endogenous antiretroviral agent hypermutating the viral genome and rendering the virus noninfectious (Harris, 2003; Lecossier, 2003; Mangeat, 2003; Sheehy, 2003; Zhang, 2003; Bishop, 2004; Bishop, 2004; Harris, 2004; Liddament, 2004; Wiegand, 2004; Zheng, 2004; Doehle, 2005; Holmes, 2007). Therefore, blocking the Vif-APO3G interaction would allow APO3G to carry out its antiviral activity.

Traditional drug therapies have relied on inhibitors designed to disrupt a specific protein/enzyme's activity; however, a more effective approach to drug design might be structure-based. In structure-based drug design, the development of inhibitors is based on specific interactions between a potential inhibitor and its target (protein/enzyme). This approach has been successful in developing antiviral inhibitors of HIV-1 protease. In this case, the design of inhibitors has been based on their interaction with the protease's active site. In particular, the Schiffer lab has focused on designing new inhibitors to fit inside the "substrate envelope," a volume into which the majority of protease substrates fit. The Schiffer lab hypothesized that if inhibitors fill that envelope, they will more effectively avoid drug resistance by HIV-1 protease (Prabu-Jeyabalan, 2002).

To apply structure-based drug design strategies towards the HIV-1 Vif-APO3G interaction, I sought to obtain high-resolution crystallographic information. My attempts were unsuccessful; therefore, I utilized mass spectrometry and cross-linking methods to obtain low-resolution data on the structure of HIV-1 Vif (Auclair, 2007). This low-resolution structural mapping revealed that HIV-1 Vif had a compact, globular N-terminal domain and a disordered C-terminal domain. The C-terminal disorder was also

predicted by disorder prediction programs. Mapping of higher order HIV-1 Vif oligomers suggests that oligomerization occurs in a head-to-tail fashion, with the C-terminus subsequently undergoing a disorder-to-order transition. This transition may be a general mechanism allowing HIV-1 Vif to interact with a host of viral and cellular proteins. In addition, my mass spectrometry analysis identified a "hot spot" for biological activity between residues 34 and 134, which was supported by a previous mutational analysis (Simon, 1999). I then confirmed my structural information with peptide-competition experiments, mapping regions of structural importance. Peptides mapping to the hot spot of biological activity disrupt oligomerization and N-terminal peptides found in the hot spot have an unknown influence on HIV-1 Vif and APO3G (Auclair, unpublished). Although high-resolution structural data were not obtained for structure-based drug design, low-resolution structural data, in conjunction with peptide-competition experiments, give new insights into HIV-1 Vif's structural mechanisms and highlight potential regions for drug design.

In this chapter, I will give a brief overview of the AIDS epidemic and the stages of the HIV-1 life cycle. After describing AIDS, I will give a detailed description of HIV-1 Vif, including structural models, post-translational modifications, and protein-protein interactions. APOBEC3G will then be described, including its role as an antiviral agent via cytidine deamination and/or blocking retrotransposition. Finally, the HIV-1 Vif and APO3G interaction will be discussed, with a focus on proteosomal degradation of APO3G by its interaction with HIV-1 Vif and the Cullin-RING ligase complex.

AIDS

Acquired immunodeficiency syndrome is caused by the human immunodeficiency virus. HIV-1 patients are classified as progressing to AIDS when their CD4+ T cell count drops below 200 per μl of blood, and the patients develop opportunistic infections (Centers for Disease Control, www.cdc.gov). The median progression from HIV-1 to AIDS in untreated individuals is 9-10 years, and after diagnosis of AIDS a patient's life expectancy is approximately 9 months. HIV-1 is transmitted by three major routes: (1) sexual contact, (2) exposure to infected bodily fluids, including intravenous drugs, and (3) mother-to-child transmission.

AIDS patients have a weakened immune system, making them vulnerable to lethal opportunistic infections. An opportunistic infection is caused by an organism that would not infect a person with a healthy immune system. Common opportunistic infections observed in AIDS patients include tuberculosis, Epstein-Barr virus, and Kaposi's sarcoma-associated herpes virus. A patient's AIDS classification is not changed even if the opportunistic infection is cured or the level of CD4+ T cells rise.

The Global AIDS Epidemic

AIDS has grown into a global epidemic even with advances in education and ability to treat the disease. According to the Joint United Nations Programme on HIV/AIDS (UNAIDS) and the World Health Organization (WHO), the number of adults and children living with AIDS increased from 36.9 million (31.9-43.8 million) in 2004 to 39.5 million (34.1-47.1 million) in 2006. In addition to the overall increase in adults and

children living with AIDS, UNAIDS and WHO reported that new infections increased from 3.9 million (3.3-5.8 million) in 2004 to 4.3 million (3.6-6.6 million) in 2006. The number of deaths due to AIDS rose from 2.7 million (2.3-3.2 million) in 2004 to 2.9 million (2.5 million-3.5 million) in 2006. Over the last few decades public education and the advent of new treatments have helped prolong the lives of HIV-1-infected individuals. Even with these advances in education and treatment, however, the increase in new infections reported is most striking. These numbers suggest AIDS is still a growing worldwide problem needing to be addressed through both new public education programs and treatments.

The numbers released by UNAIDS and the WHO have recently been the subject of controversy (www.unaids.org). For example, the number of adults and children living with AIDS was adjusted in 2006 from 39.5 million (34.1-47.1 million) to 33.2 million (30.6-36.1 million). All the numbers released by the UNAIDS and WHO have been updated, including the numbers for previous years. This discrepancy in numbers was due to an audit of the methodologies used to compute them and to increased accuracy in numbers reported from such places as India. Although, the original estimated numbers were high, the adjusted numbers do not negate the validity of AIDS as a global epidemic that needs to be addressed.

HIV-1 and the Viral Life Cycle

HIV-1, the virus that causes AIDS, is a retrovirus classified as a member of the family *retroviridae* of the genus lentivirus. HIV-1 has two copies of single-stranded,

positive-sense RNA encoding all nine of its viral genes. Of these nine genes, three, i.e., *gag*, *pol*, and *env*, encode structural proteins, two envelope proteins, and three enzymes. The remaining six genes, i.e., *tat*, *rev*, *nef*, *vpr*, *vpu*, and *vif*, code for the six regulatory proteins. The viral life cycle consists of entry, reverse transcription, integration, nuclear export, budding, and maturation (Figure 1.1).

Entry

The HIV-1 virion infects macrophages, CD4+ T cells, and dendritic cells, causing cell death after virion budding. The HIV-1 virion first infects a cell by the interaction of the viral envelope (env) protein, gp160, with host cell receptors. The gp160 protein comprises a transmembrane domain (TM or gp41) and a surface domain (SU or gp120). The SU protein, gp120, binds to the N-terminal immunoglobulin domain of a CD4+ receptor on the host cell membrane. After interacting with the CD4+ receptor, the *env* glycoprotein then interacts with a chemokine co-receptor, typically CCR5 or CXCR4. These interactions cause a conformational change in gp41, resulting in membrane fusion between the viral and cellular membrane and release of the viral genome into the host cell (Frankel, 1998).

Reverse Transcription

After release, the viral RNA is uncoated and reverse transcribed by the viral protein, reverse transcriptase (RT). Reverse transcription is first initiated by base pairing of the cellular $tRNA_3^{lys}$ primer, thus allowing synthesis of a (-)-strand DNA molecule. The RNase H domain of RT degrades the (+)-sense RNA molecule used to synthesize the (-)-strand DNA, which is then used as a primer to synthesize the (+)-strand DNA. This

Figure 1.1

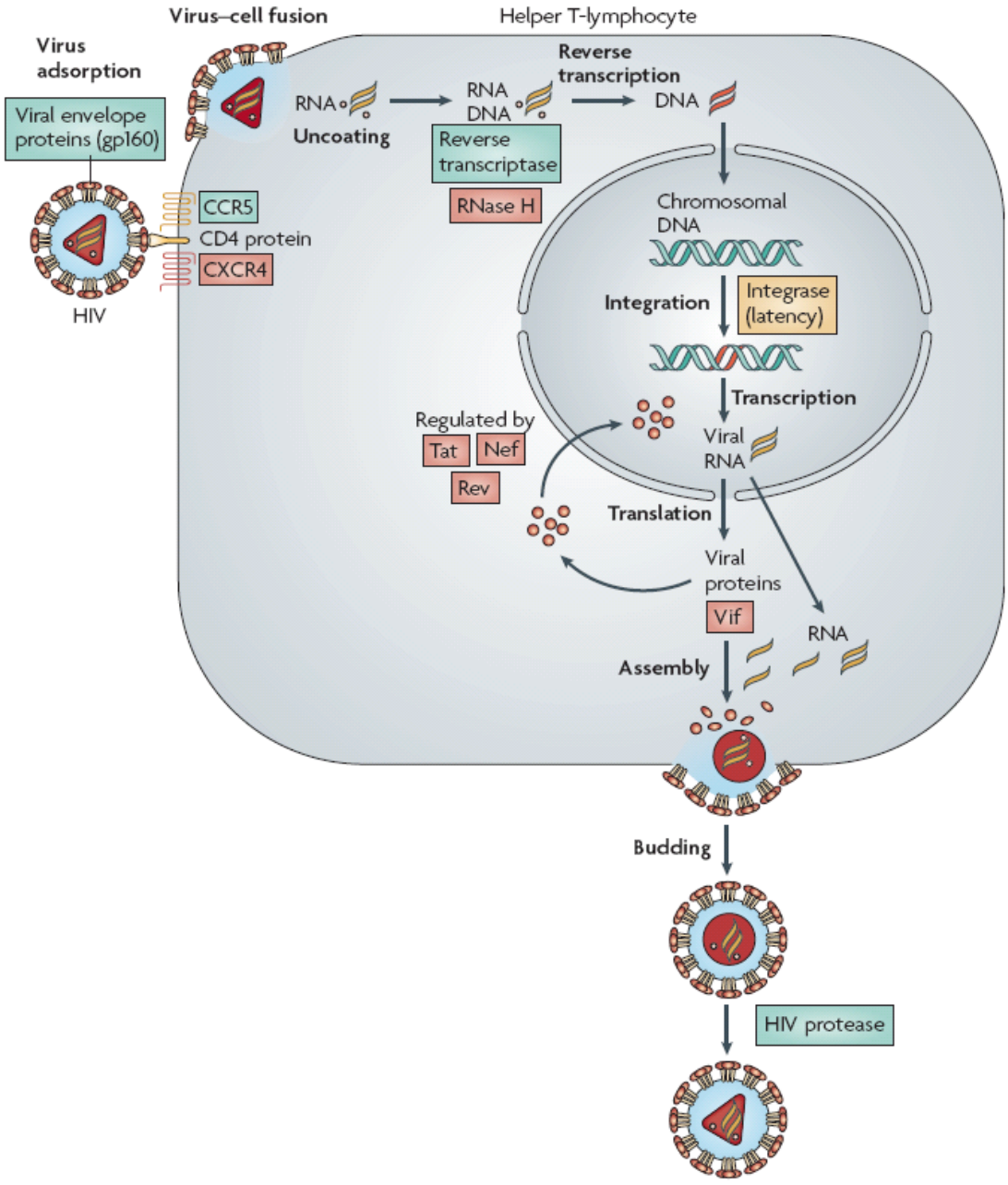

Figure 1.1: HIV-1 Life Cycle. The virion first interacts with a CD4+ receptor and a chemokine co-receptor, typically CCR5 or CXCR4, through its envelope glycoprotein (**entry**). After binding, the viral core is released into the host cell, uncoated, and reverse transcribed into the viral cDNA (**reverse transcription**). The viral cDNA is then transported to the nucleus and integrated into the host cell genome (**integration**). After transcription, viral mRNAs are transported to the cytoplasm and translated into the viral proteins (**nuclear export**). The structural proteins and enzymes are transported to the site of budding at the plasma membrane (**budding**). After budding, HIV-1 protease cleaves Gag and Gag-Pol polyproteins, leading to a mature virion (**maturation**). Proteins in green boxes are currently targeted by antiviral drugs, yellow boxes indicate targets in clinical trials, and red boxes indicate potential drug targets (Flexner, 2007).

newly formed DNA double helix or viral cDNA is capable of integrating into the host genome. This HIV-1 RT-mediated transcription of viral cDNA is a target of retroviral therapy (Frankel, 1998; Castro, 2006).

Reverse transcription results in a large number of mutations in the newly synthesized viral cDNA due to the infidelity of HIV-1 reverse transcriptase. In addition, host cell proteins, such as the cytidine deaminase APOBEC3G, cause mutations in viral cDNA (Harris, 2003; Lecossier, 2003; Mangeat, 2003; Sheehy, 2003; Zhang, 2003; Bishop, 2004; Bishop, 2004; Harris, 2004; Liddament, 2004; Wiegand, 2004; Zheng, 2004; Doehle, 2005; Holmes, 2007).

Integration

The newly synthesized DNA double helix forms a nucleoprotein complex, or preintegration complex (PIC). Along with reverse transcriptase, the PIC contains other viral proteins such as matrix, Vpr, and integrase. The PIC is transported to the nucleus by the nuclear import machinery, importin-α and nucleoporins. The viral integrase integrates the viral cDNA into the host cell genome by inserting it into the host cell chromosomes (Frankel, 1998; Castro, 2006).

Nuclear Export

After integration and transcription, both spliced and unspliced mRNAs are transported to the cytoplasm where they are translated into viral proteins. The Tat, Rev, and Nef proteins are synthesized first. Once synthesized, HIV-1 Rev enters the nucleus, binds the Rev response element (RRE) of unspliced mRNA and transports it out of the

nucleus using the nuclear export machinery. Once exported from the nucleus, the mRNAs are translated into viral proteins (Frankel, 1998).

Budding

The Env proteins, gp120 and gp41, are synthesized in the endoplasmic reticulum (ER) as is the CD4+ receptor. To avoid Env binding to CD4+ in the cytoplasm and on the ER, CD4+ is targeted for degradation by two viral proteins: Vpu and Nef. Vpu targets CD4+ via the ubiquitin-proteosome pathway, and Nef targets CD4+ via endosomal degradation. The degradation of CD4+ facilitates the transport of Env proteins to the site of the newly forming virion. Simultaneously, structural proteins such as Gag and Gag-Pol, whose synthesis is caused by a -1 ribosomal frameshift (Jacks, 1988), are transported to the plasma membrane of the host. The viral matrix protein is myristoylated and anchored to the cellular membrane. Along with the structural proteins and enzymes, two copies of the unspliced viral genome are transported to the bud site and incorporated into the virion. The newly created virion buds from the host cell in an immature, noninfectious, state (Frankel, 1998).

Maturation

After the immature virion buds from the host cell, the viral protease cleaves the Gag and Gag-Pol polyprotein, resulting in the release of viral enzymes, rearrangement of structural proteins, and maturation of the virion. This mature virion is now able to infect the next cell and repeat the viral life cycle (Frankel, 1998). Traditional drug treatments include inhibitors targeting the HIV-1 protease, thus preventing cleavage and viral maturation.

Antiviral Therapy, Drug Resistance, and Novel Drug Targets

Although AIDS cannot currently be cured, AIDS patients can be treated by a drug regimen, HAART. HAART typically consists of drugs targeting two proteins in the viral life cycle: reverse transcriptase and HIV-1 protease. When traditional HAART becomes ineffective, patients are treated with newer inhibitors that target viral entry. These inhibitors include two types of reverse transcriptase inhibitors (nucleoside or nucleotide reverse-transcriptase inhibitors [NRTI], and non-nucleoside reverse-transcriptase inhibitors [NNRTI]), 10 protease inhibitors, and 2 inhibitors of viral entry. These inhibitors are prescribed as a combination of drugs to minimize the effects of drug resistance; as resistance to one drug-treatment regimen arises, patients are treated with a new combination of drugs (Flexner, 2007).

Treatment has caused the emergence of drug-resistant strains, which likely existed before treatment and were selected by the drug-induced selective stress. Drug resistance is due to a change in molecular recognition so that a previously effective inhibitor becomes ineffective in treating the disease. Several drug-resistant mutants have already been described for both HIV-1 reverse transcriptase and protease, leading to the development of second- and third-generation RT and PR inhibitors less susceptible to resistance. Although, the current HAART therapy is necessary to sustain HIV-1-infected patients, this therapy is no longer sufficient due to drug-resistant viruses (Coffin, 1995; Gruttola, 2006; Flexner, 2007).

Emergence of these drug-resistant strains has resulted in the need to identify new drug targets. Potential new drug targets include viral proteins in the viral life cycle or

cellular proteins playing a role in that cycle. Targeting viral enzymes such as integrase or RNase H are two potential strategies, but a more attractive group of targets may be the regulatory proteins Tat, Rev, Nef, Vpr, Vpu, and Vif (Cochrane, 2004; Federico, 2004; Zhao, 2004; Barbaro, 2005; Reeves, 2005; Yu, 2005; Harrich, 2006). Regulatory proteins have not been considered valuable drug targets because they were originally considered nonessential proteins. Many of these proteins, however, have recently been shown to be necessary for infectivity (Rouzic, 2005; Ehrlich, 2006; Nekhai, 2006; Lindwasser, 2007). Regulatory proteins have also not been considered because targeting them would disrupt the large surface of a protein-protein interaction, producing pharmacological problems. For example, an antagonist to Vpr, which inhibits cell division, had no anti-HIV-1 activity (Para, 2006). Although targeting an enzyme's active site may be simpler than targeting a protein-protein interface, the emergence of drug resistance has made it necessary to tackle this complex problem (Flexner, 2007).

Other potential drug targets are host cellular proteins involved in the viral life cycle such as the chemokine co-receptors CXCR4 and CCR5, which are necessary for viral entry. CXCR4 is less likely to be a candidate for antiviral therapies due to its importance in normal cell development, but the role of CCR5 in normal cellular processes appears less crucial. Furthermore, a natural population of patients has a 32-amino acid deletion in their CCR5 protein that makes them resistant to infection and does not appear to affect any cellular processes, strengthening the case for CCR5 inhibitors (Paxton, 1996; Flexner, 2007).

Along with targeting and blocking the activity of cellular proteins involved in the life cycle, another promising area for drug development is enhancing or enabling the activity of naturally occurring host defenses. One example is APOBEC3G (APO3G), a cellular cytidine deaminase that causes G-to-A hypermutations in the plus strand of the viral cDNA, rendering the virus noninfectious (Harris, 2003; Lecossier, 2003; Mangeat, 2003; Sheehy, 2003; Zhang, 2003; Bishop, 2004; Bishop, 2004; Harris, 2004; Liddament, 2004; Wiegand, 2004; Zheng, 2004; Doehle, 2005; Holmes, 2007). Therefore, enhancing the activity of APO3G is a possible strategy to fight the virus. In the case of APO3G, HIV-1 has developed a protein, Vif, which counteracts the endogenous antiviral properties of APO3G. Thus, neutralizing Vif is another potential and attractive treatment strategy.

HIV-1 Virion Infectivity Factor (Vif)

HIV-1 Vif, originally called *sor* (short open-reading frame), is a 23 kDa, highly basic protein conserved in all lentiviruses except equine infectious anemia virus (EIAV) (Kan, 1986; Lee, 1986; Sodroski, 1986). EIAV may lack Vif because an equine cytidine deaminase has not yet been described. Even if an equine cytidine deaminase did exist, another EIAV gene might have a Vif-like function. Early in the fight against AIDS, HIV-1 Vif was recognized as essential for virus infectivity (Strebel, 1987). However, HIV-1 Vif was only recently shown to be important in degrading the endogenous antiviral protein APO3G through an interaction with a Cullin-RING ligase complex (Harris, 2003; Lecossier, 2003; Mangeat, 2003; Sheehy, 2003; Zhang, 2003; Bishop,

2004; Bishop, 2004; Harris, 2004; Liddament, 2004; Wiegand, 2004; Zheng, 2004; Doehle, 2005; Holmes, 2007).

The development of first-, second-, and third-generation small-molecule inhibitors of HIV-1 protease has been successful due to structure-based drug design. However, the three-dimensional structure is not available for HIV-1 Vif. This lack of structural information is due to an inability to bacterially express milligram quantities of soluble HIV-1 Vif proteins. Due to this lack of structural information, traditional structure-based drug design techniques cannot be applied to HIV-1 Vif. However, understanding the molecular mechanism and biochemical properties of HIV-1 Vif will aid in its development as a therapeutic target.

Insights into the structure of HIV-1 Vif have been gained through homology models. Mutational analysis has highlighted HIV-1 Vif residues necessary for infectivity and can give insights into regions that are potential drug targets. In addition, HIV-1 Vif infectivity has been shown to be correlated to several biochemical properties, including multimerization, phosphorylation, and binding partners such as APOBEC3G. However, more structural and biochemical data are needed in order to exploit HIV-1 Vif as a therapeutic target. Through mass spectrometry and peptide-competition experiments, I have collected low-resolution structural data and new biochemical data revealing a novel mechanism for HIV-1 Vif action and possibly its native tertiary structure.

The subsequent sections provide an overview of the characterization of HIV-1 Vif to date. Structural models, a mutational analysis, multimerization, and phosphorylation

will be considered. Finally, evidence will be given for HIV-1 Vif binding to a host of other macromolecules.

Structural Models

Although no HIV-1 Vif structural data are available from crystallographic or NMR studies, several homology models have been created. HIV-1 Vif has no known structural homologs; therefore, no sequence can be used to model the whole HIV-1 Vif protein. To create a homology model, the HIV-1 Vif sequence was divided into C- and N-terminal domains (Lv, 2007). The C-terminal domain (residues 142-177) was modeled using von Hippel-Lindau tumor-suppressor protein (VHL) because both VHL and HIV-1 Vif have been proposed to contain a suppressor of cytokine signaling (SOCS) box domain, they have similar conserved key residues, they have similar predicted secondary structures, and VHL is the only SOCS-box protein structure available. The SOCS-box was first described in the SOCS family of proteins as a 40-amino acid region of homology thought to be involved in targeting proteins for ubiquitination through interactions with the Elongin BC complex (Stebbins, 1999).

The N-terminal domain (residues 1-143) of HIV-1 Vif was modeled using nitrate/nitrite response regulator (NarL) from *Escherichia coli* because its predicted secondary structure is similar to that of HIV-1 Vif, it is functionally similar to HIV-1 Vif in terms of multimerization and phosphorylation, and the NarL C-terminal domain is similar to that of VHL. Residues 178-192 of HIV-1 Vif were not included in the model because they were not similar to either NarL or VHL and were considered to lack functional importance (Lv, 2007). However, my cross-linking data (Chapter III) and the

large number of proteins that bind to the HIV-1 Vif C-terminus (Auclair, 2007) lead me to hypothesize that the C-terminus is important for HIV-1 Vif function and should not have been omitted from the model.

The homology model created by Lv *et al.* gave insight into HIV-1 Vif structure and its interaction with the Elongin B/C complex. For example, two helices forming a concave surface in Elongin C interacted with the SLQ residues of HIV-1 Vif. In addition, the cysteines in HIV-1 Vif (C114 and C133) were predicted to be in two adjacent loops, creating a groove with a heavily, negatively charged center that could allow interactions with other proteins (Figure 1.2A) (Lv, 2007). However, when considering this structural model, one must keep in mind that the templates were two different proteins with little sequence homology to HIV-1 Vif. In addition, these two proteins were selected based on their predicted secondary structure, and the C-terminal tail of HIV-1 Vif was excluded from the analysis.

Another homology model of HIV-1 Vif was created using isopenicillin N synthase from *Aspergillus nidulans* (Figure 1.2B, (Balaji, 2006)). This model was based on 25% sequence homology and similar secondary structure predictions between HIV-1 Vif and isopenicillin N synthase. Unlike the previous model of HIV-1 Vif, this model was created using one protein sequence and structure. This model suggested that the C-terminus of HIV-1 Vif (150-192) is exposed on the protein surface and is thus available to kinases. The model also identified that the HIV-1 Vif C-terminus contains helices able to self-associate, suggesting that HIV-1 Vif can dimerize and may facilitate the formation of higher-order oligomers. Finally, a positive surface is created with a hooklike structure

partially obstructed by S146, which has been shown to be phosphorylated (Balaji, 2006). As for the previous model, this model is based on secondary structure predictions and is built on a sequence with low identity to HIV-1 Vif. Therefore, one must be cautious in overanalyzing the significance of this model. In addition, the model itself contains many unideal geometries (Balaji, 2006), bringing into question the validity of the model itself. Although, these two models can be used to guide further studies, without experimental structures or structural data, structure-based drug design is difficult.

Both of these HIV-1 Vif models (Figure 1.2A and 1.2B) were created using two different templates and are drastically different from each other. Therefore, it is unlikely that both models accurately represent the HIV-1 Vif structure. The model of Balaji *et al.* (Figure 1.2B) more accurately predicts the number of beta sheets and alpha helices than the model of Lv *et al.* (Figure 1.2A), but the latter model presents a more likely structure based on the order of helices and sheets (Figure 1.2C). I obtained the pdb files for each homology model (1VZF.pdb and vif-b-c.pdb) and mapped my intra-molecular cross-links (Chapter III) onto them (Figure 1.2D and E). In order for an EDC cross-link to occur between a lysine and glutamic or aspartic acid they must be within 5 angstroms of each other (Kalkhof, 2005). Based on the distances generated by mapping my intra-molecular cross-links it can be seen that the majority of the distances observed are around above 5 angstroms for each respective model. This suggests that neither model is well described by my cross-linking data, and therefore not likely to be the actual structure of HIV-1 Vif. Therefore, it is likely that some aspects of each model are correct, however this cannot be confirmed without a high resolution structure of HIV-1 Vif.

Figure 1.2A

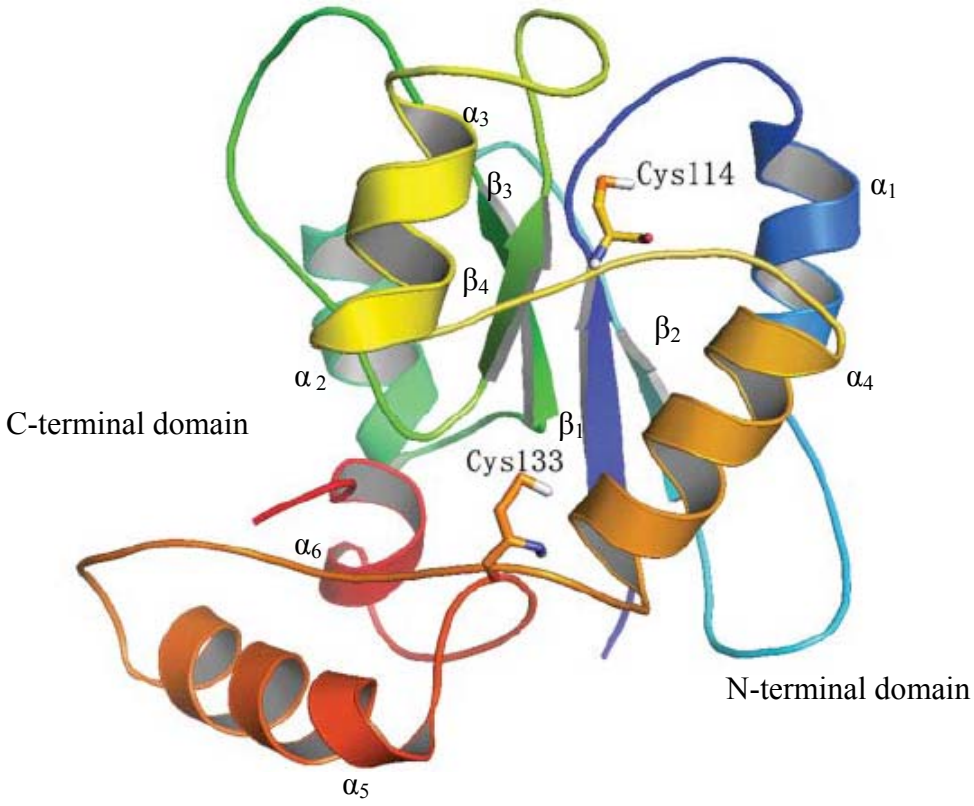

Lv, W. *et al.* (2007). Three-dimensional structure of HIV-1 Vif constructed by comparative modeling and the function characterization analyzed by molecular dynamics simulations. Organic and Biomolecular Chemistry 5(4): 617-626. Reproduced by permission of The Royal Society of Chemistry.

Figure 1.2B

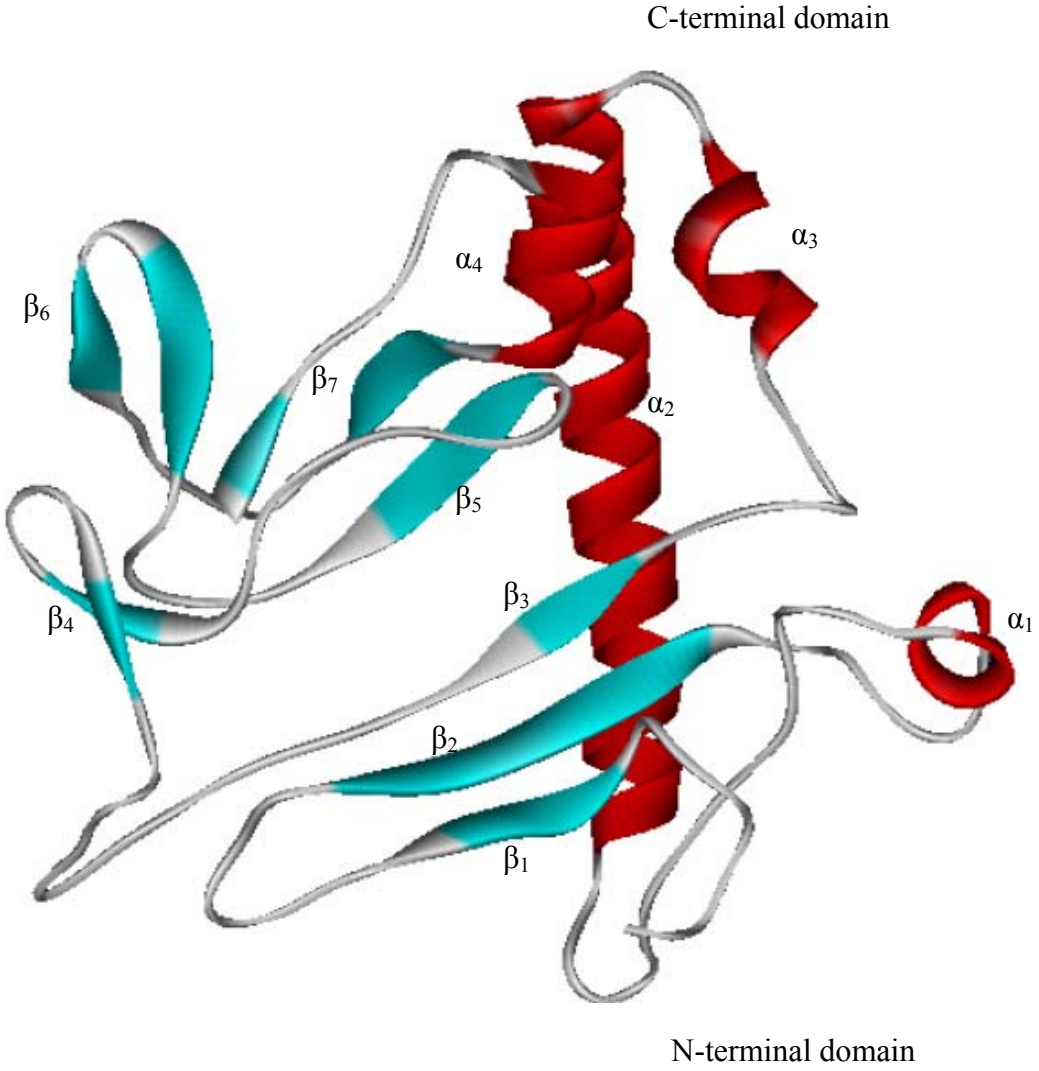

Balaji, S. R., *et al.* (2006) Paradigm development: Comparative and predictive 3D modeling of HIV-1 virion infectivity factor (Vif). Bioinformation 1(8): 290-309.

Figure 1.2C


Conf:
Pred:
Pred: CCCEEEEEEEEEECHHHHHHHHHHHHHCCEECCCCCCCEE
AA: MENRWQVMIVWQVDRMRIRTWKSLVKHHMYVSGKARGWFY
10 20 30 40
Conf:
Pred:
Pred: CCCEECCCCEEEEEEEEECCCEEEEEEECCCCCCCCCCC
AA: RHHYESPHPRISSEVHIPLGDARLVITTYWGLHTGERDWH
50 60 70 80
Conf:
Pred:
Pred: CCCCEEEEEECCEEEECHHHHHHHHHHHHCCCCCHHHH
AA: LGQGVSIEWRKKRYSTQVDPELADQLIHLYYFDCFSDSAI
90 100 110 120
Conf:
Pred:
Pred: HHHHCCCEECCCCCCCCCCCCCCHHHHHHHHHHHCCCCCC
AA: RKALLGHIVSPRCEYQAGHNKVGSLQYLALAALITPKKIK
130 140 150 160
Conf:
Pred:
Pred: CCCCCEECCCCCCCCCCCCCCCCCCCCCCCCC
AA: PPLPSVTKLTEDRWNKPQKTKGHRGSHTMNGH
170 180 190
Legend:
- helix
- strand
- coil
Conf:
- confidence of prediction
Pred: predicted secondary structure
AA: target sequence

Figure 1.2D

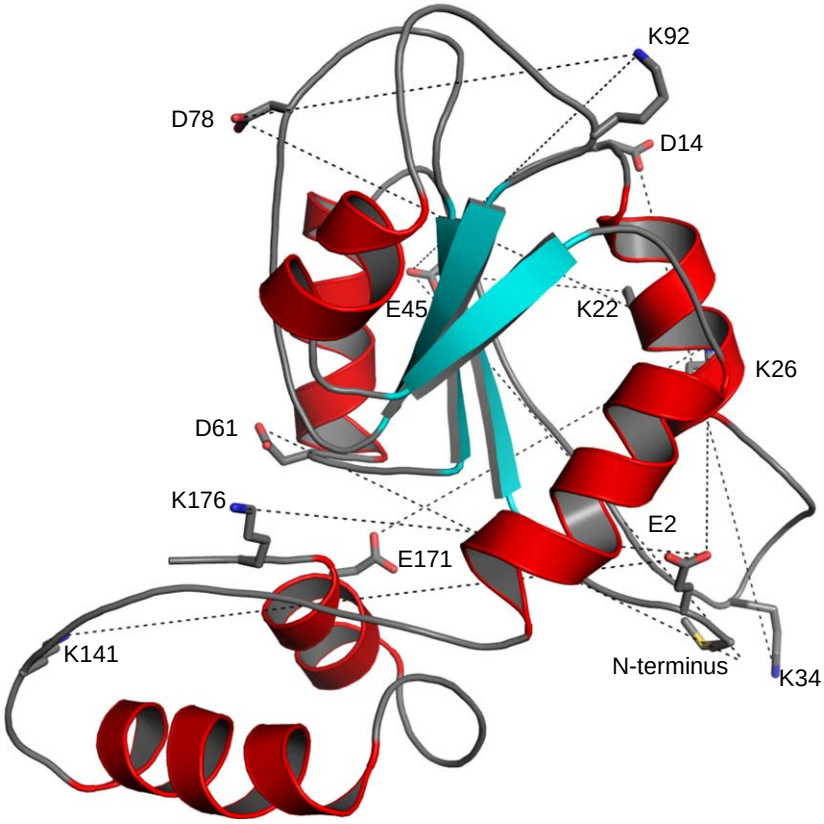

Cross-link Residue	Cross-link Residue	Distance (Angstroms)
Termini	E45	31.42
Termini	D61	30.39
E2	K26	17.44
E2	K141	36.35
E2	K176	25.37
D14	K34	31.19
K22	E45	13.31
K26	D78	32.24
K26	E171	22.74
E45	K92	29.17
D78	K92	22.31
E171	K181	N/A

Figure 1.2E

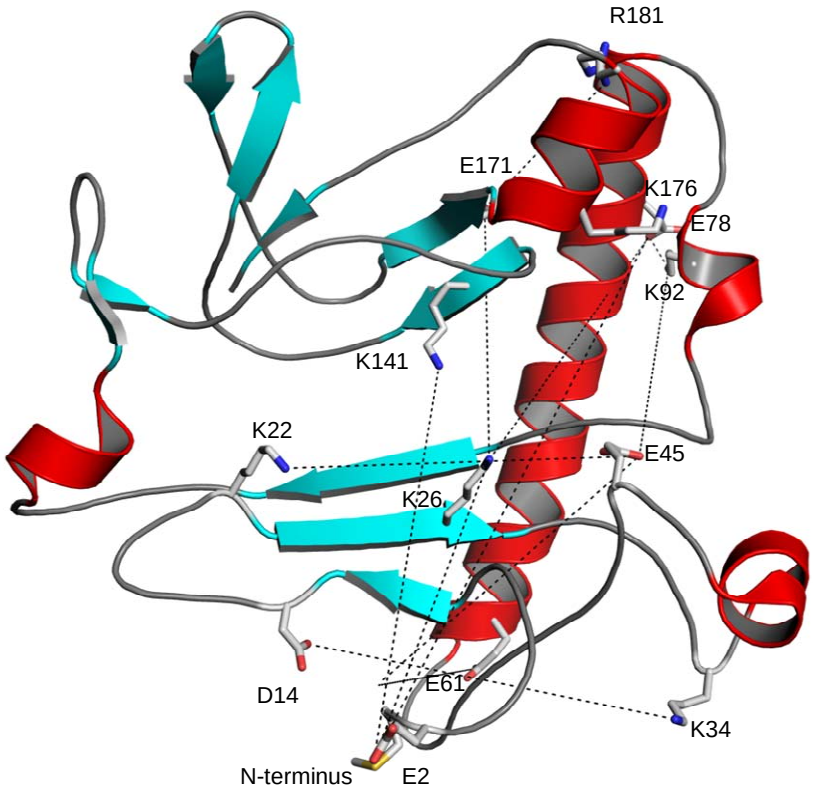

Cross-link Residue	Cross-link Residue	Distance (Angstroms)
Termini	E45	20.39
Termini	D61	21.58
E2	K26	21.29
E2	K141	20.41
E2	K176	35.87
D14	K34	21.77
K22	E45	20.41
K26	D78	24.96
K26	E171	20.20
E45	K92	20.84
D78	K92	2.95
E171	K181	12.18

Figure 1.2: Predictions of HIV-1 Vif Structure. (A.) Homology model of HIV-1 Vif based on comparisons with VHL and NarL (Lv, 2007). (B.) Homology model of HIV-1 Vif based on a comparison to isopenicillin N synthase (Balaji, 2006). (C.) Secondary structure prediction of HIV-1 Vif and the HIV-1 Vif sequence (Jones, 1999; Bryson, 2005). (D.) Intra-molecular cross-links from Chapter III mapped onto the homology model from (A.). Distances between residues are listed in the table. A distance is not listed for the E171-K181 cross-link because the C-terminus was absent from the model. (E). Intra-molecular cross-links from Chapter III mapped onto the homology model from (B.). Distances between residues are listed in the table. The pdb contained 2 extra residues at position 64 and 65, therefore residues involved in cross-links after these residues are shifted 2 amino acids towards the C-terminus. In addition, the sequence used to generate the model is different from the HXB2 sequence I used, so some residues are different amino acids than seen in my cross-linking data. For example, R181 shown here is equivalent to K181 in the HXB2 sequence.

Mutational Analysis

HIV-1 Vif residues critical for viral infectivity were identified throughout the viral protein by in-depth mutational analysis (Simon, 1999). For example, infectivity was reduced by greater than 85% due to mutations in the HIV-1 Vif N-terminus, including residues 38-40 and 43-44, which are adjacent to the APO3G-binding domain (Russell, 2007). Viral infectivity was also reduced by greater than 85% when both cysteines (residues 114 and 133), shown to be important for Cul5 binding, were mutated to serine (Kobayashi, 2005; Luo, 2005; Mehle, 2006; Xiao, 2006; Xiao, 2007a; Xiao, 2007b). Similarly, infectivity was decreased by greater than 85% after mutating the SOCS-box residues 144-146, shown to be important for Elongin C binding (Mehle, 2004; Yu, 2004; Kobayashi, 2005). Finally, infectivity fell by greater than 85% in the HIV-1 Vif triple mutant, at residues 161-163, which have been shown to be important for oligomerization (Yang, 2001; Yang, 2003; Zennou, 2006). The diverse nature of these residues indicates that multiple domains are necessary for HIV-1 Vif's function and viral infectivity. The domains highlighted by these mutational analyses, taken together with other biochemical and structural data, suggest that they could be used as targets to facilitate drug design (Simon, 1999). Therefore, these domains may be worth cloning and trying to express as soluble HIV-1 Vif protein.

Multimerization

The function of HIV-1 Vif has been implicated both *in vitro* and *in vivo* with homo-oligomerization as dimers, trimers, and tetramers (Yang, 2001; Yang, 2003). The proline-rich region in the C-terminus, residues 151-164, has been identified as the

putative oligomerization domain. A HIV-1 Vif deletion mutant of the putative oligomerization domain failed to rescue the infectivity of HIV-1 Vif-defective viruses (Yang, 2001). In addition, a peptide containing HIV-1 Vif residues 155-166 reduced both the number of HIV-1 Vif oligomers observed and HIV-1 replication in nonpermissive T-cells. The number of oligomers and HIV-1 replication was also reduced by other non-HIV-1 Vif peptides containing a PPXP domain, identified via phage display (Yang, 2003). Therefore, the key residues in HIV-1 Vif oligomerization are ^{161}PPLP^{164} (Yang, 2003). Thus, disrupting HIV-1 Vif oligomerization may inhibit HIV-1 Vif function and create noninfectious virus.

Phosphorylation

HIV-1 Vif phosphorylation on serines and threonines has been shown to be important for Vif function (Yang, 1996; Yang, 1998). The three phosphorylation sites originally identified were Ser144, Thr155, and Thr188 (Yang, 1996), followed by two more sites, Thr96 and Ser 165 (Yang, 1998). The kinase(s) responsible for phosphorylating residues 144, 155 and 188 are unknown, but p42/44 mitogen-activated protein kinase (MAPK) is responsible for phosphorylating residues 96 and 165 (Yang, 1998). Mutating both Ser144 and Thr96 resulted in loss of HIV-1 Vif activity and inhibition of HIV-1 replication, suggesting that they are important for both functions. HIV-1 Vif peptides containing the 96 and 165 phosphorylation sites were not phosphorylated, suggesting that structural determinants in HIV-1 Vif may be necessary for their phosphorylation (Yang, 1996; Yang, 1998). The infectivity of HIV-1 Vif-deficient cells was also enhanced by MAPK, suggesting that MAPK plays a role in HIV-

1 replication by both an HIV-1 Vif-dependent and an HIV-1 Vif-independent manner (Yang, 1999).

Phosphorylation of residues 96 and 165 was likely not observed with phosphorylation of 144, 155, and 188 because only low levels of MAPK were present in the original experiments (Yang, 1998). Therefore, other phosphorylation sites are possible, but not observed because the appropriate kinase is absent or in low abundance. The exact role of phosphorylation in HIV-1 Vif is unclear, but it may facilitate protein-protein interactions or regulate HIV-1 Vif activity. Therefore, disrupting phosphorylation of HIV-1 Vif may inhibit its function, yielding another potential drug target.

Macromolecular Interactions of HIV-1 Vif

The function of HIV-1 Vif has been implicated in its interactions with many host cell proteins, viral proteins, and nucleic acids. These interactions are crucial to HIV-1 Vif post-translational modification, packaging, and ability to target the endogenous antiviral protein APOBEC3G for proteosomal degradation. An important area of drug development will be developing novel drugs to inhibit any of these interactions.

Src proteins

HIV-1 Vif binds to two kinases from the Src family, Hck and Fyn, but does not appear to be phosphorylated by either kinase. Hck inhibits HIV-1 replication, and this inhibition is suppressed by HIV-1 Vif (Hassaine, 2001). In addition, Fyn and Hck have been shown to phosphorylate tyrosines in APO3G, which may regulate its function. HIV-1 Vif binding to Hck and Fyn inhibits their catalytic activity, likely inhibiting APO3G phosphorylation and affecting its function (Hassaine, 2001; Douaisi, 2005).

Furthermore, in the presence of Fyn and Hck and the absence of HIV-1 Vif, less APO3G is incorporated into virions, whereas more phosphorylated APO3G is encapsidated (Hassaine, 2001; Douaisi, 2005). Thus, Hck and Fyn may inhibit APO3G encapsidation by phosphorylating it in the absence of HIV-1 Vif (Douaisi, 2005). These results also suggest that HIV-1 Vif interacts with Src kinases (Fyn and Hck) and prevents them from inhibiting HIV-1 replication, presumably by blocking their kinase activity.

HIV-1 $Pr55^{Gag}$

In addition to binding to cellular proteins like the Src kinases, HIV-1 Vif has been shown to bind to the NC (nucleocapsid) p7 domain of HIV-1 $Pr55^{Gag}$ (Bouyac, 1997; Huvent, 1998). This interaction between HIV-1 Vif and $Pr55^{Gag}$ is prevented by deletion of the 22 C-terminal residues (171-192) and point mutations of basic residues (157-179) in the C-terminus of HIV-1 Vif, suggesting that the C-terminus is critical for its interaction with $Pr55^{Gag}$ (Bouyac, 1997). Furthermore, HIV-1 Vif packaging into virus-like particles of sf9 baculovirus cells was abrogated by HIV-1 Vif binding to the C-terminal domain of NC and by mutating or deleting NC. Therefore, the NC-Vif interaction may be crucial for HIV-1 Vif packaging into budding virions (Huvent, 1998). Finally, the interaction between Gag and HIV-1 Vif prevents the processing of $Pr55^{Gag}$ by the viral protease (Bardy, 2001). Although both HIV-1 Vif and HIV-1 Gag are basic proteins, I propose their interaction is specific because HIV-1 Vif packaging appears to depend on HIV-1 Gag. Therefore, blocking this interaction may affect viral budding and is an attractive drug target.

RNA

HIV-1 Vif has also been shown to bind RNA *in vitro* and viral genomic RNA *in vivo*, which likely helps regulate reverse transcription (Dettenhofer, 2000; Cancio, 2004; Henriet, 2005; Bernacchi, 2007; Henriet, 2007). In addition to regulating reverse transcription, HIV-1 Vif may be packaged into the virion through interactions with viral genomic RNA and nucleocapsid (Henriet, 2005). Deleting the first 43 amino acids in HIV-1 Vif prevents its binding to RNA, and deleting its last 56 amino acids prevents its ability to stimulate reverse transcription. The DNA synthesis activity of reverse transcriptase depends on RNA, and DNA is regulated by HIV-1 Vif (Cancio, 2004).

HIV-1 Vif binds viral genomic RNA fragments in the following regions: the 5'-untranslated region (5'-UTR), *gag*, and the 5' portion of *pol* with K_ds between 45 and 65nM. HIV-1 Vif appears to bind cooperatively to the 5'-UTR and *gag*, and some of the approximately 7-24 HIV-1 Vif molecules that bind to RNA do so in a cooperative fashion. Viral genomic RNA binding occurs in a hierarchical fashion, primarily at the TAR apical loop, poly(A) stem-loop, and a short region in *gag,* with K_ds between 9.5 and14nM (Henriet, 2005; Bernacchi, 2007). In addition to binding the viral RNA, HIV-1 Vif can bind the corresponding DNA and its complement at similar affinities (Bernacchi, 2007). HIV-1 Vif's ability to bind RNA could have evolved for two reasons: (1) HIV-1 Vif aids in RNA packaging and reverse transcription, and (2) HIV-1 Vif could protect the viral genomic RNA from APO3G deamination (Henriet, 2005; Bernacchi, 2007).

In addition to binding RNA, HIV-1 Vif can act as an RNA chaperone by helping to anneal $tRNA_3^{lys}$ to the viral RNA, thus initiating reverse transcription and facilitating

the first strand transfer (Henriet, 2007). HIV-1 Vif also stimulates weak HIV-1 genomic RNA dimers. HIV-1 Vif inhibits the formation of NCp-mediated RNA dimer formation and $tRNA_3^{lys}$ hybridization. Therefore, HIV-1 Vif may inhibit the early stages of reverse transcription and RNA dimer formation. However, this inhibition is likely overcome due to the low copy number of encapsidated HIV-1 Vif (Henriet, 2007).

APO3G and the Cullin-RING Ligase complex

Arguably the most important interactions of HIV-1 Vif are with Elongin B and C, Cullin 5, and the APOBEC3 family of proteins, including APO3G and APO3F. HIV-1 Vif binds APO3G, a cytidine deaminase, and targets it for proteosomal degradation through direct interaction with Cullin5, Elongin B, and Elongin C in a Cullin-RING ligase complex. HIV-1 Vif oligomerization may be necessary to neutralize APO3G; therefore strategies to block HIV-1 Vif oligomerization could prevent the neutralization of APO3G. However, since the importance of HIV-1 Vif oligomerization in the APO3G interaction is still being investigated, the interaction between HIV-1 Vif and APO3G is a more promising area for drug development because of APO3G's antiviral properties.

Apolipoprotein B mRNA Editing Enzyme, Catalytic Polypeptide-like 3G (APOBEC3G)

Identification: Nonpermissive and Permissive Cells

The production of infectious virus requires the presence of HIV-1 Vif in specific cell types (Sodroski, 1986; Strebel, 1987; Madani, 1998). Permissive cells include 293T, SupT1, and CEM-SS cells, whereas nonpermissive cells include peripheral blood

lymphocytes, CEM, H9 and Hut78 cells. In permissive cells the virus is infectious in the presence or absence of HIV-1 Vif, whereas in nonpermissive cells the virus is only infectious in the presence of HIV-1 Vif (Gabuzda, 1992; vonSchwedler, 1993; Sheehy, 2002; Ehrlich, 2006).

To examine what was responsible for loss of HIV-1 infectivity in nonpermissive cells, heterokaryon experiments were conducted in which a nonpermissive cell was fused with a permissive cell (Simon, 1998). If the permissive cell phenotype were dominant, then the fused cell would contain a cellular protein with a function similar to that of HIV-1 Vif, and if the nonpermissive phenotype were dominant, then the fused cell would likely have a factor that led to the loss of infectivity, which could be counteracted by HIV-1 Vif. In these experiments, when permissive 293T cells were fused with nonpermissive Hut78 cells, virions without HIV-1 Vif were 10-fold less infectious than virions produced from 293T cells alone. These results suggest that a factor in nonpermissive cells is the reason for this antiviral activity and that HIV-1 Vif likely counteracts its activity (Simon, 1998). This same result was supported by another heterokaryon experiment, in which nonpermissive H9 cells were fused with HeLa cells (Madani, 1998). A subtractive hybridization screen revealed the antiviral factor to be APO3G (Sheehy, 2002).

APO3G is a member of the APOBEC family of proteins which includes activation-induced cytidine deaminase (AID) and APOBEC1-APOBEC4. Many of the APOBEC family members have antiretroviral activity. For example, along with APO3G, APOBEC3F can inhibit HIV-1 in a Vif-dependent manner (Bishop, 2004; Liddament,

2004; Wiegand, 2004; Zheng, 2004; Holmes, 2007). In addition, APOBEC proteins from other species can inhibit HIV-1, suggesting the antiviral activity of APOBEC proteins is widespread and conserved throughout evolution (Mariani, 2003; Bishop, 2004; Bishop, 2004; Kobayashi, 2004; Wiegand, 2004; Cullen, 2006; Holmes, 2007).

Cytidine Deamination and Hypermutation

APOBEC3G (APO3G) is an endogenous cytidine deaminase that deaminates G-to-A in the plus strand of HIV-1 DNA reverse transcripts. In the presence of APO3G, the nascent HIV-1 reverse transcripts contain a large number of mutations, which may explain the lower accumulation of HIV-1 reverse transcripts (Harris, 2003; Lecossier, 2003; Mangeat, 2003; Sheehy, 2003; Zhang, 2003; Bishop, 2004; Harris, 2004; Liddament, 2004; Wiegand, 2004; Zheng, 2004; Doehle, 2005; Holmes, 2007). These mutations in the HIV-1 cDNA may create nonfunctional, mutant proteins or may inactivate the viral RNA, making the virus noninfectious.

In addition to deaminating HIV-1 reverse transcripts, APO3G represses replication of murine leukemia virus (MLV) (Harris, 2003; Mangeat, 2003; Bishop, 2004; Harris, 2004; Kobayashi, 2004; Holmes, 2007), foamy virus (Lochelt, 2005; Russell, 2005; Delebecque, 2006; Holmes, 2007), and equine infectious anemia virus (EIAV) (Mangeat, 2003; Holmes, 2007). Both MLV and EIAV lack a HIV-1 Vif-like protein/gene, but their repression by APO3G can be blocked by introducing HIV-1 Vif, indicating it can function without the presence of other HIV-1 factors (Mangeat, 2003).

Retrotransposition

Hypermutation has been shown to be one potential mechanism by which APO3G inhibits viral replication. However, other possible mechanisms have been described, including the ability of APO3G to inhibit retrotransposons in a deamination-dependent or deamination-independent fashion (Dutko, 2005; Esnault, 2005; Schumacher, 2005; Chiu, 2006; Ehrlich, 2006; Esnault, 2006; Holmes, 2007; Hulme, 2007; Niewiadomska, 2007). Retrotransposons are mobile genetic elements that can be classified into two general classes: (1) long interspersed nuclear elements (LINE) and (2) long terminal repeats (LTR). LTRs, also known as endogenous retroviruses, are related to infectious retroviruses (Esnault, 2006). APO3G can prevent the retrotransposition of IAP (intracisternal A-particles) and musD, two endogenous mouse retroviruses, with the transposed copies containing G-to-A mutations (Esnault, 2005; Esnault, 2006; Holmes, 2007). APO3G was also shown to decrease the amount of transposed IAP and musD cDNA without affecting the RNA transcript intermediate (Esnault, 2006). Thus, APO3G may have a dual inhibitory effect: editing and reducing transposed cDNAs (Ehrlich, 2006). In addition to restricting mouse retrotransposons, APO3G can restrict Ty1, a yeast retrotransposon, by reducing the integration of Ty1 cDNA, and resulting in G-to-A hypermutations in the integrated element (Dutko, 2005; Schumacher, 2005; Holmes, 2007). APO3G also interacts with Ty1 Gag and is packaged into Ty1 virus-like particles by a mechanism similar to that for its entry into HIV-1 virions, suggesting that APO3G restricts Ty1 and HIV-1 by similar mechanisms (Dutko, 2005).

In addition to its effects on LTR retrotransposons, APO3G may also influence LINE retrotransposons. APO3G was originally thought to have no effect on most LINE-1 retrotransposons (Esnault, 2005; Bogerd, 2006; Chen, 2006; Muckenfuss, 2006; Stenglein, 2006; Holmes, 2007; Hulme, 2007), but these findings are contradicted by a recent report that APO3G may affect LINE-1 retrotransposition in 293T cells (Niewiadomska, 2007). Regardless, APO3G appeared to inhibit Alu elements, short interspersed nuclear elements, or L1-mediated retrotransposons (Chiu, 2006; Hulme, 2007). Since this inhibition of Alu elements was independent of APO3G catalytic activity, G-to-A hypermutations were not present. The ability of APO3G to inhibit Alu elements was likely due to a catalytically inactive high molecular mass form of APO3G (Chiu, 2006).

APO3G complexes and Multimerization

APO3G exists in two forms: a high molecular-mass (HMM) form and low molecular-mass (LMM) form. The HMM ribonucleoprotein complex of APO3G is catalytically inactive and predominant in activated CD4+ T cells, but after RNase treatment, it is converted to the enzymatically active LMM form. The LMM form of APO3G is predominant in resting CD4+ T cells where HIV-1 replication is blocked and reverse transcription is impaired (Chiu, 2005). When resting CD4+ T cells are activated by mitogens and the cytokines interleukin-2, -7, and -15, LMM APO3G is recruited into HMM APO3G, which may be associated with the increased ability of these activated cells to be infected with HIV-1 (Chiu, 2005; Stopak, 2007). Therefore, the LMM form of APO3G acts as a post-entry restriction factor that protects resting CD4+ cells from HIV-1

infection (Chiu, 2005), whereas activated CD4+ cells containing catalytically inactive HMM complexes are susceptible to HIV-1 infection. HMM complexes were also found to include Staufen-containing RNA-transporting granules, Ro ribonucleoprotein complexes, and Alu and Y RNA retroelements. This finding indicates that Alu retroelements are sequestered in the HMM complex, thus preventing the nuclear L1 enzymatic machinery from retrotransposing] these elements (Chiu, 2006).

In addition to the HMM and LMM forms of APO3G, APO3G can form multimers (Opi, 2006; Wedekind, 2006; Opi, 2007), which are sensitive to RNase treatment (Opi, 2006; Opi, 2007). Monomeric APO3G is packaged into virions, is catalytically active, and has antiviral activity (Opi, 2006). A multimerization-defective mutant of APO3G, C97A, can form HMM complexes, suggesting that multimerization and HMM complex formation are two unrelated, RNA-dependent processes. This mutant is resistant to HIV-1 Vif-induced degradation, even though the two proteins still interact in immunoprecipitation experiments (Opi, 2007). Although resistant to degradation, C97A can be incorporated into virions and its antiviral activity is inhibited by HIV-1 Vif, suggesting that HIV-1 Vif's ability to target APO3G to the proteosome and prevent its incorporation into virions are two unique functions (Opi, 2006; Opi, 2007).

APO3G complexes and Multimerization

APO3G exists in two forms: a high molecular-mass (HMM) form and low molecular-mass (LMM) form. The HMM ribonucleoprotein complex of APO3G is catalytically inactive and predominant in activated CD4+ T cells, but after RNase treatment, it is converted to the enzymatically active LMM form. The LMM form of

APO3G is predominant in resting CD4+ T cells where HIV-1 replication is blocked and reverse transcription is impaired (Chiu, 2005). When resting CD4+ T cells are activated by mitogens and the cytokines interleukin-2, -7, and -15, LMM APO3G is recruited into HMM APO3G, which may be associated with the increased ability of these activated cells to be infected with HIV-1 (Chiu, 2005; Stopak, 2007). Therefore, the LMM form of APO3G acts as a post-entry restriction factor that protects resting CD4+ cells from HIV-1 infection (Chiu, 2005), whereas activated CD4+ cells containing catalytically inactive HMM complexes are susceptible to HIV-1 infection. HMM complexes were also found to include Staufen-containing RNA-transporting granules, Ro ribonucleoprotein complexes, and Alu and Y RNA retroelements. This finding indicates that Alu retroelements are sequestered in the HMM complex, thus preventing the nuclear L1 enzymatic machinery from retrotransposing] these elements (Chiu, 2006).

In addition to the HMM and LMM forms of APO3G, APO3G can form multimers (Opi, 2006; Wedekind, 2006; Opi, 2007), which are sensitive to RNase treatment (Opi, 2006; Opi, 2007). Monomeric APO3G is packaged into virions, is catalytically active, and has antiviral activity (Opi, 2006). A multimerization-defective mutant of APO3G, C97A, can form HMM complexes, suggesting that multimerization and HMM complex formation are two unrelated, RNA-dependent processes. This mutant is resistant to HIV-1 Vif-induced degradation, even though the two proteins still interact in immunoprecipitation experiments (Opi, 2007). Although resistant to degradation, C97A can be incorporated into virions and its antiviral activity is inhibited by HIV-1 Vif,

suggesting that HIV-1 Vif's ability to target APO3G to the proteosome and prevent its incorporation into virions are two unique functions (Opi, 2006; Opi, 2007).

Structural Insights into APO3G

As for HIV-1 Vif, no high-resolution structure is available for APO3G. However, homology models (Huthoff, 2005) and low-resolution structures (Wedekind, 2006) of the LMM and HMM species have been generated using small-angle x-ray scattering (SAXS) and advanced shape-recognition methods. The low-resolution structure of the LMM species shows an extended shape with tail-to-tail dimerization, and shape analysis of LMM and HMM species indicates that their association in dimers would lead to only minimal HMM complexes (Wedekind, 2006). These results suggest that other proteins or macromolecules (e.g., RNA) are needed to form the HMM complex.

In addition to the low-resolution structural models, the secondary structure arrangement of APO3G was predicted to be similar to those of other cytidine deaminases, except for an additional third alpha-helix exposing D128, the residue involved in species specificity (Huthoff, 2005). Finally, a model structure of APO3G was created based on the crystal structure of APOBEC2 (Figure 1.3; (Zhang, 2007). This model predicts that two residues important for packaging APO3G into the virion, R122 and W127, are on the surface of the protein. In addition to R122 and W127, and in agreement with the secondary structure analysis, D128 is on the surface of the protein with a negative electrostatic potential (Zhang, 2007). This structural information can be used in conjunction with other biochemical data to identify surfaces on APO3G where protein-

Figure 1.3

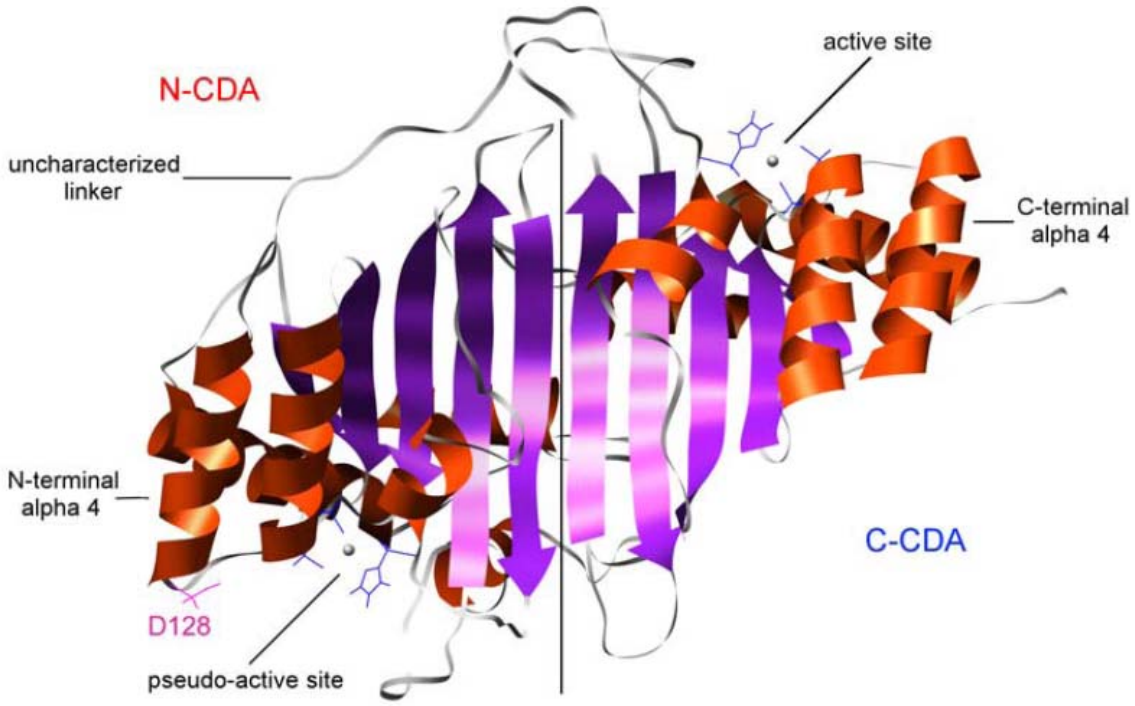

Zhang, K. B. *et al.* (2007) Model Structure of Human APOBEC3G. *PLoS One* 2(4): e378.

Figure 1.3: APOBEC3G structural model. Homology model of APO3G based on the APOBEC2 structure (Zhang, 2007).

protein interactions may occur, suggesting good target regions for drugs.

Species Specificity

HIV-1 Vif appears to form a complex with APO3G in a species-specific manner. HIV-1 Vif does not form a complex with murine APO3G (Mariani, 2003; Bogerd, 2004; Mangeat, 2004; Schrofelbauer, 2004), and African green monkey (AGM) Vif blocks the antiviral activity of AGM but not human APO3G (Mariani, 2003; Bogerd, 2004; Mangeat, 2004; Schrofelbauer, 2004). In addition, HIV-1 Vif reduced the amount of human APO3G packaged into the budding virion, but did not affect the packaging of murine or African green monkey APO3G. This species specificity in APO3G was due to one amino acid at position 128, an aspartic acid in humans, and a lysine in AGM (Mariani, 2003; Bogerd, 2004; Mangeat, 2004; Schrofelbauer, 2004). The species-specific sensitivity of human APO3G was changed by a D128K mutant from human Vif to simian immunodeficiency virus $(SIV)_{AGM}$ Vif, and a K128D mutant in AGM APO3G changed its specificity from SIV_{AGM} Vif to HIV-1 Vif (Mariani, 2003; Bogerd, 2004; Mangeat, 2004; Schrofelbauer, 2004).

Conservation of D128 indicates that this region in APO3G may be an ideal drug target. The conserved nature implies that drugs targeting this region would be specific for the HIV-1 Vif-APO3G interaction. Since only one residue is necessary, the surface required for inhibition may not be large. In addition, changing the species specificity disrupted the interaction between HIV-1 Vif and human APO3G, preventing the degradation of APO3G. If this interaction could be disrupted by a drug, the antiviral effects of APO3G would be sufficient to reduce viral infectivity.

RNA, HIV-1 Gag binding, and Virion Incorporation

HIV-1 Vif binds APO3G and prevents its incorporation into budding virions, with both HIV-1 Gag and RNA playing roles in APO3G packaging. Whether these interactions are direct and necessary for virion incorporation are unclear due to conflicting reports, but both Gag and RNA clearly play a role (Alce, 2004; Cen, 2004; Luo, 2004; Svarovskaia, 2004). A direct interaction between APO3G and the HIV-1 Gag polypeptide, in particular the nucleocapsid, is sufficient for APO3G packaging into Gag virus-like particles (Alce, 2004; Cen, 2004), even in the absence of viral genomic RNA (Luo, 2004). The N-terminus of nucleocapsid, NCp7, is the most critical region in facilitating the Gag-APO3G interaction, and incorporating APO3G into budding virions (Alce, 2004; Luo, 2004; Burnett, 2007). In addition, this interaction between NCp7 and APO3G allows APO3G to be close to the reverse transcriptase complex in the virion (Alce, 2004). Therefore, the APO3G-NCp7 interaction is not only important for APO3G incorporation, but also inhibits $tRNA_3^{Lys}$ (the primer tRNA for reverse transcription) annealing to viral RNA, which may lead to inhibition of reverse transcription initiation (Guo, 2007).

APO3G and Gag have been reported to interact both directly (Cen, 2004) and indirectly via an RNA-mediated mechanism (Svarovskaia, 2004). However, the packaging of APO3G is enhanced by but does not depend on viral genomic RNA (Luo, 2004; Svarovskaia, 2004). APO3G co-immunoprecipitates with HIV-1 RNA, mRNAs, and other RNA-binding proteins, but many of these RNAs and other APO3G-binding proteins are excluded from budding virions, suggesting that APO3G is packaged into

virions based on its affinity for HIV-1 RNA. Interestingly, almost all APO3G-associated proteins were released with ribonuclease treatment, but HIV-1 Vif remained bound (Kozak, 2006), suggesting that RNA is not needed to mediate the APO3G-Vif interaction. In a conflicting report, APO3G associates with HIV-1 nucleoprotein complexes through viral RNA, where an interaction with the 5'-UTR of HIV-1 RNA is necessary and sufficient for APO3G incorporation into budding virions (Khan, 2005).

APO3G incorporated into budding virions is found in a large complex with viral RNA (vRNA), which differs from the HMM form of APO3G (Burnett, 2007; Soros, 2007). This complex with viral RNA also includes APO3G multimers, formed in an RNA-dependent fashion, and recruited to the plasma membrane via HIV-1 Gag (Burnett, 2007). The vRNA in the APO3G-vRNA complex blocks the enzymatic activity of APO3G, which is restored during reverse transcription by RNase H. Therefore, RNase H appears not only to degrade the vRNA bound to APO3G, allowing APO3G to act on its viral minus-strand DNA substrate, but also to produce the APO3G DNA substrate (Soros, 2007).

In addition to being important for budding, the interaction of APO3G with RNA may give insights into its function in other cellular processes. For example, APO3G has been shown to localize to mRNA processing bodies (P-bodies) (Wichroski, 2006; Gallois-Montbrun, 2007). APO3G has also been shown to interact with Pol-III derived RNAs such as Y3 and 7SL RNAs (Wang, 2007). The packaging of 7SL into virions is mediated by its interaction with both APO3G and the RNA-binding domain of

nucleocapsid. This interaction with 7SL suggests a cellular role for APO3G (Wang, 2007).

HIV-1 Vif, APO3G, and the Cullin-RING Ligase Complex

APO3G Degradation

HIV-1 Vif binds directly to APO3G, preventing APO3G packaging and drastically reducing the amount of APO3G in the cell. This reduction of endogenous APO3G is caused by HIV-1 Vif weakening the translational efficiency of APO3G mRNA and targeting APO3G for degradation via the 26S proteosome (Marin, 2003; Sheehy, 2003; Stopak, 2003). HIV-1 Vif alone is sufficient to degrade APO3G; when HIV-1 Vif is expressed in the absence of other viral proteins, APO3G is still degraded (Stopak, 2003). HIV-1 Vif stimulates ubiquitination of APO3G, thus targeting it for degradation via the proteosome (Sheehy, 2003). In addition, HIV-1 Vif function was suggested to involve two domains; the first domain contained residues SLQ(Y/F)LA that were involved in degrading APO3G, and the second domain was implicated in binding to APO3G (Marin, 2003).

Although this APO3G-binding domain had been proposed, the HIV-1 Vif residues involved in binding to APO3G were only recently identified. A potential APO3G-binding domain in HIV-1 Vif was identified in studies of the D128K-APO3G mutant, which is unable to bind HIV-1 Vif or be degraded, as residues ^{14}DRMR^{17}, but other likely binding sites could not be ruled out (Schrofelbauer, 2006). In fact, the HIV-1 Vif residues ^{40}YRHHY^{44} are important for APO3G binding, and residues ^{14}DRMR^{17} are

important for APO3F binding (Russell, 2007). In addition, mutating the APO3G-binding site increased HIV-1 Vif's ability to hinder APO3F (Russell, 2007).

Proteosomal Degradation

HIV-1 Vif targets APO3G for proteosomal degradation through an interaction with Cullin5 (Cul5), Elongin B, Elongin C and Rbx1 (Figure 1.4). This interaction forms a Skp1-Cullin-F-box (SCF)-like complex, or a Cul5-EloB/C E3 ubiquitin-ligase complex, which facilities the ubiquitination and degradation of proteins, such as APO3G, via the proteosome. It is interesting to note that APO3G and HIV-1 Vif are both ubiquitinated and degraded, HIV-1 Vif to a lesser extent. A HIV-1 Vif mutant unable to interact with the Cul5 complex also could not facilitate the degradation of APO3G. In addition, this Vif-Cul5-EloB/C complex could ubiquitinate APO3G but not APO3G-D128K, an APO3G mutant unable to bind HIV-1 Vif (Yu, 2003; Mehle, 2004; Yu, 2004; Kobayashi, 2005; Luo, 2005).

HIV-1 Vif binds Elongin C through an interaction with its BC-box motif (the SLQ(Y/F)LA domain) in the SOCS (suppressor of cytokine signaling)-box (Mehle, 2004; Yu, 2004). Serine phosphorylation in the SOCS-box of HIV-1 Vif inhibited Elongin C binding (Mehle, 2004), and the SLQ/AAA mutant was unable to form the Cul5 complex and degrade APO3G (Kobayashi, 2005). Although the SOCS-box motif is necessary for assembly of the Cul5-EloB/C complex, it is not sufficient because two cysteines outside the SOCS-box are required for Cul5 binding. Therefore, HIV-1 Vif appears to act as a substrate receptor in the Cul5-EloB/C complex (Yu, 2004; Luo, 2005; Mehle, 2006; Xiao, 2006; Xiao, 2007a; Xiao, 2007b).

Figure 1.4

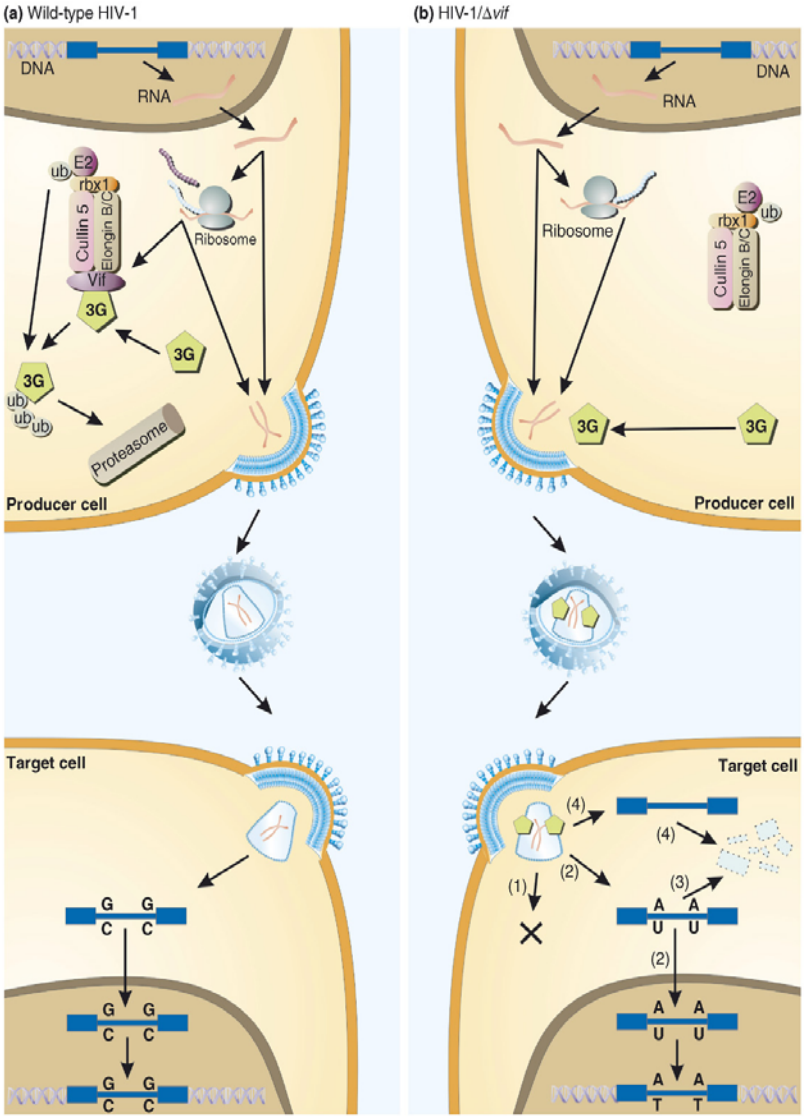

Reprinted from Trends in Biochemical Sciences, 32(3), Holmes, R., M. Malim, and K. Bishop, APOBEC-mediated viral restriction: not simply editing, 118-28, 2007, with permission from Elsevier.

Figure 1.4: Role of HIV-1 Vif in Proteosomal Degradation of APO3G in Nonpermissive Cells. In cells infected with wild-type virus, HIV-1 Vif binds to APO3G and targets it for proteosomal degradation through an interaction with a Cullin-RING ligase complex. The Cullin-RING ligase complex includes Cul5, Elongin B & C, and rbx1. In the absence of HIV-1 Vif, APO3G is not degraded and is packaged into the budding virion. APO3G is then released with the viral core into the host cell cytoplasm, where it causes G-to-A mutations of the plus-strand viral cDNA. These mutations inactivate the virus and prevent further infection (Holmes, 2007).

HIV-1 Vif binding to Cul5 involves Vif residues 100-142. In particular, residues $H^{108}C^{114}C^{133}H^{139}$ in HIV-1 Vif are required to form the Vif-Cul5-EloB/C E3 ligase complex. This HCCH motif is part of a larger motif, $Hx_5Cx_{17-18}Cx_{3-5}H$, which coordinates one zinc molecule and is necessary for assembling the Vif-Cul5-EloB/C complex through an interaction with Cul5 (Kobayashi, 2005; Luo, 2005; Mehle, 2006; Xiao, 2006; Xiao, 2007a; Xiao, 2007b). Also important in coordinating the zinc molecule, binding to Cul5, and degradation of APO3G are the hydrophobic HIV-1 Vif residues, Ile120, Ala123, and Leu124 (Mehle, 2006). HIV-1 Vif proteins lacking this HCCH motif or with mutations at these residues bound less strongly to Cul5, zinc, and degraded APO3G less than wild-type proteins (Kobayashi, 2005; Luo, 2005; Mehle, 2006; Xiao, 2007b). HIV-1 Vif binding to Cul5 is mediated through the N-terminus of the first Cullin repeat in Cul5 (Mehle, 2006; Xiao, 2006). HIV-1 Vif function was inhibited by chelating the zinc in the Vif-Cul5-EloB/C complex, but chelation did not affect cellular Cul5-SOCS3 E3 ligase assembly, suggesting that the zinc requirement for assembly may be unique to HIV-1 Vif and that the Vif-Cul5-EloB/C complex would be a good candidate for a drug target (Xiao, 2007a).

On the other hand, formation of the Vif-Cul5-EloB/C complex and degradation of APO3G do not appear to be unique to APO3G or HIV. Other APOBEC3 proteins are degraded by mechanisms similar to those for APO3G (Shirakawa, 2006) and an adenovirus protein, E4orf6, has been shown to contain a Vif-like BC-box essential for complex formation and p53 degradation, but no zinc is required (Luo, 2007). Thus, other viruses can apparently hijack the Cul5-EloB/C E3 ligase complex to degrade cellular

proteins, but the requirement for zinc is unique to HIV-1 Vif. Therefore, targeting the recruitment of viral proteins to this complex is a potential drug target, and the requirement for zinc gives a more specific target in the HIV-1 Vif-Cul5 interaction.

Summary

Obtaining structural information for HIV-1 Vif would give insights into the molecular mechanisms of its protein-protein interactions with other cellular and viral partners (Figure 1.5). This information would thus advance knowledge about HIV-1 Vif and suggest other likely functions.

HIV-1 Vif is an attractive target for structure-based drug design because it acts on the endogenous antiviral protein, APO3G, targeting it for proteosomal degradation. In the absence of HIV-1 Vif, APO3G is packaged into budding virions where it deaminates G-to-A in the plus strand of the viral cDNA, preventing further rounds of infection. Inhibiting the HIV-1 Vif-mediated degradation of APO3G would allow this host cell protein to perform its natural function as an antiviral agent, making HIV-1 Vif a good drug target. To date no structural data are available for HIV-1 Vif due to the difficulty in acquiring large quantities of soluble protein for X-ray crystallographic and NMR studies. Therefore, information on the structure of HIV-1 Vif from cross-linking and mass spectrometric studies will reveal the regions important for HIV-1 Vif function, thus signaling likely new drug targets. In addition, the cross-linking data will be confirmed by peptide-competition experiments, whose results may give insight into new peptidomimetics and molecules that can be used to disrupt the function of HIV-1 Vif.

Figure 1.5

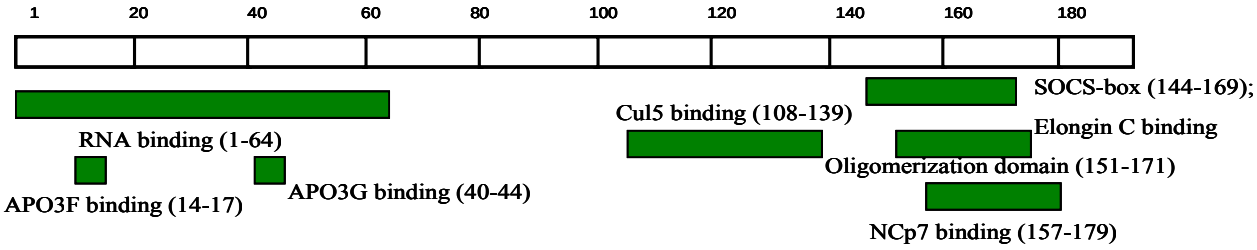
1
20
40
60
80
100
120
140
160
180
SOCS-box (144-169);
Cul5 binding (108-139)
Elongin C binding
RNA binding (1-64)
Oligomerization domain (151-171)
APO3F binding (14-17)
APO3G binding (40-44)
NCp7 binding (157-179)

Figure 1.5: HIV-1 Vif Binding Domains. The sequence of HIV-1 Vif is mapped with its binding domains as previously described (Bouyac, 1997; Huvent, 1998; Bardy, 2001; Yang, 2001; Yang, 2003; Cancio, 2004; Mehle, 2004; Yu, 2004; Kobayashi, 2005; Luo, 2005; Mehle, 2006; Schrofelbauer, 2006; Xiao, 2006; Auclair, 2007; Mehle, 2007; Russell, 2007; Xiao, 2007a; Xiao, 2007b).

References

Alce, T. M. and W. Popik (2004). "APOBEC3G Is Incorporated into Virus-like Particles by a Direct Interaction with HIV-1 Gag Nucleocapsid Protein." Journal of Biological Chemistry **279**(33): 34083.

Auclair, J., K. Green, S. Shandilya, J. Evans, M. Somasundaran and C. Schiffer (2007). "Mass spectrometry analysis of HIV-1 Vif reveals an increase in ordered structure upon oligomerization in regions necessary for viral infectivity." PROTEINS: Structure, Function, and Genetics **69**(2): 270-84.

Balaji, S., R. Kalpana and P. Shapshak (2006). "Paradigm development: Comparative and predictive 3D modeling of HIV-1 Virion Infectivity Factor (Vif)." Bioinformation **1**(8): 290-309.

Barbaro, G., A. Scozzafava, A. Mastrolorenzo and C. T. Supuran (2005). "Highly active antiretroviral therapy: current state of the art, new agents and their pharmacological interactions useful for improving therapeutic outcome." Curr Pharm Des. **11**(14): 1805-1843.

Bardy, M., B. Gay, S. Pebernard, N. Chazal, M. Courcoul, R. Vigne, E. Decroly and P. Boulanger (2001). "Interaction of human immunodeficiency virus type 1 Vif with Gag and Gag-Pol precursors: co-encapsidation and interference with viral protease-mediated Gag processing." Journal of General Virology **82**: 2719-2733.

Bernacchi, S., S. Henriet, P. Dumas, J. Paillart and R. Marquet (2007). "RNA and DNA binding properties of HIV-1 Vif protein: a fluorescence study." Journal of Biological Chemistry **282**(36): 26361-8.

Bishop, K. N., R. K. Holmes, A. M. Sheehy, N. O. Davidson, S.-J. Cho and M. H. Malim (2004). "Cytidine Deamination of Retroviral DNA by Diverse APOBEC Proteins." Current Biology **14**: 1392-1396.

Bishop, K. N., R. K. Holmes, A. M. Sheehy and M. H. Malim (2004). "APOBEC-mediated editing of viral RNA." Science **305**(5684): 645.

Bogerd, H. P., B. P. Doehle, H. L. Wiegand and B. R. Cullen (2004). "A single amino acid difference in the host APOBEC3G protein controls the primate species specificity of HIV type 1 virion infectivity factor." Proc. Natl. Acad. Sci USA **101**(11): 3770-3774.

Bogerd, H. P., H. L. Wiegand, B. P. Doehle, K. K. Lueders and B. R. Cullen (2006). "APOBEC3A and APOBEC3B are potent inhibitors of LTR-retrotransposon function in human cells." Nucleic Acids Research **34**(1): 89-95.

Bouyac, M., M. Courcoul, G. Bertoia, Y. Baudat, D. Gabuzda, D. Blanc, N. Chazal, P. Boulanger, J. Sire, R. Vigne and B. Spire (1997). "Human Immunodeficiency Virus Type 1 Vif Protein Binds to the Pr55Gag Precursor." Journal of Virology **71**(12): 9358-9365.

Bryson, K., L. McGuffin, R. Marsden, J. Ward, J. Sudhi and D. Jones (2005). "Protein structure prediction servers at University College London. ." Nucleic Acids Residues **33(Web server issue)**: W36-38.

Burnett, A. and P. Spearman (2007). "APOBEC3G multimers are recruited to the plasma membrane for packaging into HIV-1 virus-like particles in an RNA-dependent process requiring the NC basic linker." Journal of Virology **81**(10): 5000-13.

Cancio, R., S. Spadari and G. Maga (2004). "Vif is an auxiliary factor of the HIV-1 reverse transcriptase and facilitates abasic site bypass." Journal of Biochemistry **383**(3): 475-482.

Castro, H. C., N.I.V.Loureiro, M. Pujol-Luz, A. M. T. Souza, M. G. Albuquerque, D. O. Santos, L. M. Cabral, I. C. Frugulhetti and C. R. Rodrigues (2006). "HIV-1 Reverse Transcriptase: A Therapeutical Target in the Spotlight." Current Medical Chemistry **13**(313-324).

Cen, S., F. Guo, M. Niu, J. Saadatmand, J. Deflassieux and L. Kleiman (2004). "The Interaction between HIV-1 Gag and APOBEC3G." Journal of Biological Chemistry **279**(32): 33177-33184.

Chen, H., C. E. Lilley, Q. Yu, D. V. Lee, J. Chou, I. Narvaiza, N. R. Landau and M. D. Weitzman (2006). "APOBEC3A Is a Potent Inhibitor of Adeno-Associated Virus and Retrotransposons." Current Biology **16**(480-485).

Chiu, Y.-L., V. B. Soros, J. F. Kreisberg, K. Stopak, W. Yonemoto and W. C. Greene (2005). "Cellular APOBEC3G restricts HIV-1 infection in resting CD4+ T cells." Nature **435**(7038): 108-14.

Chiu, Y., H. Witkowska, S. Hall, M. Santiago, V. Soros, C. Esnault, T. Heidmann and W. Greene (2006). "High-molecular-mass APOBEC3G complexes restrict Alu retrotransposition." Proc. Natl. Acad. Sci USA **103**(42): 15588-93.

Cochrane, A. (2004). "Controlling HIV-1 Rev function." Current Drug Targets Immune Endocrine Metabol Disord. **4**(4): 287-95.

Coffin, J. M. (1995). "HIV Population Dynamics in Vivo: Implications for Genetic Variation, Pathogenesis, and Therapy." Science **267**: 483-489.

Cullen, B. R. (2006). "Role and Mechanism of Action of the APOBEC3 Family of Antiretroviral Resistance Factors." Journal of Virology **80**(3): 1067-1076.

Delebecque, F., R. Suspene, S. Calattini, N. Casartelli, A. Saib, A. Froment, S. Wain-Hobson, A. Gessain, J.-P. Vartanian and O. Schwartz (2006). "Restriction of Foamy Viruses by APOBEC Cytidine Deaminases." Journal of Virology **80**(2): 605-614.

Dettenhofer, M., S. Cen, B. A. Carlson, L. Kleiman and X.-F. Yu (2000). "Association of Human Immunodeficiency Virus Type 1 Vif with RNA and Its Role in Reverse Transcription." Journal of Virology **74**(19): 8938-8945.

Doehle, B. P., A. Schafer and B. R. Cullen (2005). "Human APOBEC3B is a potent inhibitor of HIV-1 infectivity and is resistant to HIV-1 Vif." Virology **339**(2): 281-8.

Doehle, B. P., A. Schafer, H. L. Wiegand, H. P. Bogerd and B. R. Cullen (2005). "Differential Sensitivity of Murine Leukemia Virus to APOBEC3-Mediated Inhibition Is Governed by Virion Exclusion." Journal Of Virology **79**(13): 8201-8207.

Douaisi, M., S. Dussart, M. Courcoul, G. Bessou, E. C. Lerner, E. Decroly and R. Vigne (2005). "The tyrosine kinases Fyn and Hck favor the recruitment of tyrosine-

phosphorylated APOBEC3G into vif-defective HIV-1 particles." Biochemical and Biophysical Research Communications **329**: 917-924.

Dutko, J. A., A. Schafer, A. E. Kenny, B. R. Cullen and M. J. Curcio (2005). "Inhibition of a Yeast LTR Retrotransposon by Human APOBEC3 Cytidine Deaminases." Current Biology **15**: 661-666.

Ehrlich, E. and X. Yu (2006). "Lentiviral vif: viral hijacker of the ubiquitin-proteasome system." International Journal of Hematology **83**(3): 208-212.

Esnault, C., O. Heidmann, F. Delebecque, M. Dewannieux, D. Ribet, A. J. Hance, T. Heidmann and O. Schwartz (2005). "APOBEC3G cytidine deaminase inhibits retrotransposition of endogenous retroviruses." Nature **433**: 430-433.

Esnault, C., J. Millet, O. Schwartz and T. Heidmann (2006). "Dual inhibitory effects of APOBEC family proteins on retrotransposition of mammalian endogenous retroviruses." Nucleic Acids Research **34**(5): 1522-1531.

Federico, M. (2004). "Targeting the Nef induced increase of HIV infectivity." Current Drug Targets Immune Endocrine Metabol Disord. **4**(4): 321-6.

Flexner, C. (2007). "HIV drug development: the next 25 years." Nature Reviews Drug Discovery **6**(12): 959-66.

Frankel, A. D. and J. A. T. Young (1998). "HIV-1 Fifteen Proteins and an RNA." Annu. Rev. Biochem. **67**: 1-25.

Gabuzda, D. H., K. Lawrence, E. Langhoff, E. Terwilliger, T. Dorfman, W. A. Haseltine and J. Sodroski (1992). "Role of vif in replication of human immunodeficiency virus type 1 in CD4+ T lymphocytes." Jounal of Virology **66**: 6489-6495.

Gallois-Montbrun, S., B. Kramer, C. M. Swansom, H. Byers, S. Lynham, M. Ward and M. H. Malim (2007). "Antiviral Protein APOBEC3G Localizes to Ribonucleoprotein Complexes Found in P Bodies and Stress Granules." Journal of Virology **81**(5): 2165-2178.

Gruttola, V. D., C. Flexner, J. Schapiro, M. Hughes, M. V. d. Laan and D. R. Kuritzkes (2006). "Drug Development Strategies for Salvage Therapy: Conflicts and Solutions." AIDS Research and Human Retroviruses **22**(11): 1106-1109.

Guo, F., S. Cen, M. Niu, Y. Yang, R. J. Gorelick and L. Kleiman (2007). "The Interaction of APOBEC3G with Human Immunodeficiency Virus Type 1 Nucleocapsid Inhibits tRNA3 Lys Annealing to Viral RNA." Journal of Virology **81**(20): 11322-11331.

Harrich, D., N. McMillan, L. Munoz, A. Apolloni and L. Meredith (2006). "Will diverse Tat interactions lead to novel antiretroviral drug targets?" Current Drug Targets **7**(12): 1595-606.

Harris, R. S., K. N. Bishop, A. M. Sheehy, H. M. Craig, S. K. Petersen-Mahrt, I. N. Watt, M. S. Neuberger and M. H. Malim (2003). "DNA Deamination Mediates Innate Immunity to Retroviral Infection." Cell **113**(6): 803-809.

Harris, R. S. and M. T. Liddament (2004). "Retroviral Restriction By APOBEC Proteins." Nature Reviews Immunology **4**: 868-877.

Hassaine, G., M. Courcoul, G. Bessou, Y. Barthalay, C. Picard, D. Olive, Y. Collette, R. Vigne and E. Decroly (2001). "The Tyrosine Kinase Hck Is an Inhibitor of HIV-1

Replication Counteracted by the Viral Vif Protein." Journal of Biological Chemistry **276**(20): 16885-16893.

Haubrich, R., C. Flexner, M. Lederman, M. Hirsch, C. Pettinelli, R. Ginsberg, P. Lietman, F. Hamzeh, S. Spector and D. Richman (1995). "A randomized trial of the activity and safety of Ro 24-7429 (Tat antagonist) versus nucleoside for human immunodeficiency virus infection. The AIDS Clinical Trials Group 213 Team." Journal of Infectious Disease **172**(5): 1246-52.

Henriet, S., D. Richer, S. Bernacchi, E. Decroly, R. Vigne, B. Ehresmann, C. Ehresmann, J.-C. Paillart and R. Marquet (2005). "Cooperative and Specific Binding of Vif to the 5' Region of HIV-1 Genomic RNA." Journal of Molecular Biology **354**: 55-72.

Henriet, S., L. Sinck, G. Bec, R. Gorelick, R. Marquet and J. Paillart (2007). "Vif is a RNA chaperone that could temporally regulate RNA dimerization and the early steps of HIV-1 reverse transcription." Nucleic Acids Research **35**(15): 5141-53.

Holmes, R., M. Malim and K. Bishop (2007). "APOBEC-mediated viral restriction: not simply editing?" Trends Biochem Sci **32**(3): 118-28.

Hulme, A., H. Bogerd, B. Cullen and J. Moran (2007). "Selective inhibition of Alu retrotransposition by APOBEC3G." Gene **390**(1-2): 199-205.

Huthoff, H. and M. H. Malim (2005). "Cytidine deamination and resistance to retroviral infection: Towards a structural understanding of the APOBEC proteins." Virology **334**(2): 147-53.

Huvent, I., S. S. Hong, C. Fournier, B. Gay, J. Tournier, C. Carriere, M. Courcoul, R. Vigne, B. Spire and P. Boulanger (1998). "Interaction and co-encapsidation of human immunodeficiency virus type 1 Gag and Vif recombinant proteins." Journal of General Virology **79**: 1069-1081

Jacks, T., M. D. Power, F. R. Masiarz, P. A. Luciw, P. J. Barr and H. E. Varmus (1988). "Characterization of ribosomal frameshifting in HIV-1 gag-pol expression." Nature **331**(21): 280-283.

Jones, D. (1999). "Protein secondary structure prediction based on position-specific scoring matrices." Journal of Molecular Biology **292**: 195-202.

Kalkhof, S., C. Ihling, K. Mechtler and A. Sinz (2005). "Chemical Cross-linking and High-Performance Fourier Transform Ion Cyclotron Resonance Mass Spectrometry for Protein Interaction Analysis: Application to a Calmodulin/Target Peptide Complex." Analytical Chemistry **77**(2): 495-503.

Kan, N. C., G. Franchini, F. Wong-Staal, G. C. DuBois, W. G. Robey, J. A. Lautenberger and T. S. Papas (1986). "Identification of HTLV-IIII/LAV sor Gene Product and Detection of Antibodies in Human Sera." Science **231**: 1553-1555.

Khan, M. A., S. Kao, E. Miyagi, H. Takeuchi, R. Goila-Gaur, S. Opi, C. L. Gipson, T. G. Parslow, H. Ly and K. Strebel (2005). "Viral RNA Is Required for the Association of APOBEC3G with Human Immunodeficiency Virus Type 1 Nucleoprotein Complexes." Journal of Virology **79**(9): 5870-5874.

Kobayashi, M., A. Takaori-Kondo, Y. Miyauchi, K. Iwai and T. Uchiyama (2005). "Ubiquitination of APOBEC3G by an HIV-1 Vif-Cullin5-ElonginB-ElonginC

complex is essential for Vif function." Journal of Biological Chemistry **280**(19): 18573-8.

Kobayashi, M., A. Takaori-Kondo, K. Shindo, A. Abudu, K. Fukunaga and T. Uchiyama (2004). "APOBEC3G Targets Specific Virus Species." Journal of Virology **78**(15): 8238-8244.

Kozak, S., M. Marin, K. Rose, C. Bystrom and D. Kabat (2006). "The anti-HIV-1 editing enzyme APOBEC3G binds HIV-1 RNA and messenger RNAs that shuttle between polysomes and stress granules." Journal of Biological Chemistry **281**(39): 29105-19.

Lecossier, D., F. Bouchonnet, F. Clavel and A. J. Hance (2003). "Hypermutation of HIV-1 DNA in the Absence of the Vif Protein." Science **300**(5622): 1112.

Lee, T.-H., J. E. Coligan, J. S. Allan, M. F. McLane, J. E. Groopman and M. Essex (1986). "A New HTLV-III/LAV Protein Encoded by a Gene Found in Cytopathic Retroviruses." Science **231**: 1546-1549.

Liddament, M. T., W. L. Brown, A. J. Schumacher and R. S. Harris (2004). "APOBEC3F Properties and Hypermutation Preferences Indicate Activity against HIV-1 in Vivo." Current Biology **14**: 1385-1391.

Lindwasser, O., R. Chaudhuri and J. Bonifacino (2007). "Mechanism of CD4 downregulation by the Nef and Vpu proteins of primate immunodeficiency viruses." Current Molecular Medicine **7**(2): 171-84.

Lochelt, M., F. Romen, P. Bastone, H. Muckenfuss, N. Kirchner, Y.-B. Kim, U. Truyen, U. Rosler, M. Battenberg, A. Saib, E. Flory, K. Cichutek and C. Munk (2005). "The antiretroviral activity of APOBEC3 is inhibited by the foamy virus accessory Bet protein." PNAS **102**(22): 7982-7987.

Luo, K., E. Ehrlich, Z. Xiao, W. Zhang, G. Ketner and X. Yu (2007). "Adenovirus E4orf6 assembles with Cullin5-ElonginB-ElonginC E3 ubiquitin ligase through an HIV/SIV Vif-like BC-box to regulate p53." FASEB J **21**(8): 1742-50.

Luo, K., B. Liu, Z. Xiao, Y. Yu, X. Yu, R. Gorelick and X.-F. Yu (2004). "Amino-Terminal Region of the Human Immunodeficiency Virus Type 1 Nucleocapsid Is Required for Human APOBEC3G Packaging." Journal of Virology **78**(21): 11841-11852.

Luo, K., Z. Xiao, E. Ehrlich, Y. Yu, B. Liu, S. Zheng and X.-F. Yu (2005). "Primate lentiviral virion infectivity factors are substrate receptors that assemble with cullin 5-E3 ligase through a HCCH motif to suppress APOBEC3G." Proc. Natl. Acad. Sci USA **102**(32): 11444-11449.

Lv, W., Z. Liu, H. Jin, X. Yu, L. Zhang and L. Zhange (2007). "Three-dimensional structure of HIV-1 VIF constructed by comparative modeling and the function characterization analyzed by molecular dynamics simulations." Organic and Biomolecular Chemistry **5**: 617-626.

Madani, N. and D. Kabat (1998). "An endogenous inhibitor of human immunodeficiency virus in human lymphocytes is overcome by the viral Vif protein." Journal of Virology **72**: 10251-10255.

Mangeat, B., P. Turelli, S. Liao and D. Trono (2004). "A single amino acid determination governs the species-specific sensitivity of APOBEC3G to Vif action." Journal of Biological Chemistry **279**(15): 14481-14483.

Mangeat, B., P. Turelll, G. Caron, M. Friedll, L. Perrin and D. Trono (2003). "Broad antiretroviral defence by human APOBEC3G through lethal editing of nascent reverse transcripts." Nature **424**(6944): 99-103.

Mariani, R., D. Chen, B. Schrofelbauger, F. Navarro, R. Konig, B. Bollman, C. Munk, H. Nymark-McMahon and N. R. Landau (2003). "Species-Specific Exlusion of APOBEC3G from HIV-1 Virions by Vif." Cell **114**(1): 21-31.

Marin, M., K. M. Rose, S. L. Kozak and D. Kabat (2003). "HIV-1 Vif Protein binds the editing enzyme APOBEC3G and induces its degradation." Nature Medicine **9**(11): 1398-1403.

Mehle, A., J. Goncalves, M. Santa-Marta, M. McPike and D. Gabuzda (2004). "Phosphorylation of a novel SOCS-box regulates assembly of the HIV-1 Vif-Cul5 complex that promotes APOBEC3G degradation." Genes & Development **18**(23): 2861-2866.

Mehle, A., B. Strack, P. Ancuta, C. Zhang, M. McPike and D. Gabuzda (2004). "Vif Overcomes the Innate Antiviral Activity of APOBEC3G by Promoting Its Degradation in the Ubiquitin-Proteasome Pathway." Journal of Biological Chemistry **279**(9): 7792-7798.

Mehle, A., E. R. Thomas, K. S. Rajendran and D. Gabuzda (2006). "A zinc-binding region in Vif binds Cul5 and determines Cullin selection." Journal of Biological Chemistry **281**(25): 17259-65.

Mehle, A., H. Wilson, C. Zhang, A. Brazier, M. McPike, E. Pery and D. Gabuzda (2007). "Identification of an APOBEC3G Binding Site in HIV-1 Vif and Inhibitors of Vif-APOBEC3G Binding." Journal of Virology **81**(23): 13235-41.

Muckenfuss, H., M. Hamdorf, U. Held, M. Perkovic, J. Lower, K. Cichutek, E. Flory, G. G. Schumann and C. Munk (2006). "APOBEC3 proteins inhibit human LINE-1 retrotransposition." Journal of Biological Chemistry **281**(31): 22161-72.

Nekhai, S. and K. Jeang (2006). "Transcriptional and post-transcriptional regulation of HIV-1 gene expression: role of cellular factors for Tat and Rev." Future Microbiology **1**: 417-26.

Niewiadomska, A., C. Tian, L. Tan, T. Wang, T. Nguyen, P. Sarkis and X. Yu (2007). "Differential inhibition of long interspersed element 1 by APOBEC3 does not correlate with high-molecular-mass-complex formation or P-body association." Journal of Virology **81**(17): 9577-83.

Opi, S., S. Kao, R. Goila-Gaur, M. Khan, E. Miyagi, H. Takeuchi and K. Strebel (2007). "Human immunodeficiency virus type 1 Vif inhibits packaging and antiviral activity of a degradation-resistant APOBEC3G variant." Journal of VIrology **81**(15): 8236-46.

Opi, S., H. Takeuchi, S. Kao, M. A. Khan, E. Miyagi, R. Goila-Gaur, Y. Iwatani, J. G. Levin and K. Strebel (2006). "Monomeric APOBEC3G Is Catalytically Active and Has Antiviral Activity." Journal of Virology **80**(10): 4673-4682.

Para, M., J. Schouten, S. Rosenkrantz and e. al. (2006). "A5200, phase II trial of the anti-HIV activity of mifepristone (MIF) in HIV infected subjects." in Program and Abstracts of the 46th Interscience Conference on Antimicrobial Agents and Chemotherapy. **Abstract H-256**: ASM Press, Herndon, Virginia, 2006.

Paxton, Y. H. W. A., S. M. Wolinsky, A. U. Neumann, L. Zhang, T. He, S. Kang, D. Ceradini, Z. Jin, K. Yazdanbakhsh, K. Kunstman, D. Erickson, E. Dragon, N. R. Landau, J. Phair, D. D. Ho and R. A. Koup (1996). "The role of a mutant CCR5 allele in HIV-1 transmission and disease progression." Nature Medicine **2**: 1240-1243.

Prabu-Jeyabalan, M., E. Nalivaika and C. Schiffer (2002). "Substrate shape determines specificity of recognition for HIV-1 protease: analysis of crystal structures of six substrate complexes." Structure **10**(3): 369-81.

Reeves, J. and A. Piefer (2005). "Emerging drug targets for antiretroviral therapy." Drugs **65**(13): 1747-66.

Rouzic, E. L. and S. Benichou (2005). "The Vpr protein from HIV-1: distinct roles along the viral life cycle." Retrovirology **2**: 11.

Russell, R. A. and V. K. Pathak (2007). "Identification of Two Distinct Human Immunodeficiency Virus Type 1 Vif Determinants Critical for Interactions with Human APOBEC3G and APOBEC3F." Journal of Virology **81**(15): 8201-8210.

Russell, R. A., H. L. Wiegand, M. D. Moore, A. Schafer, M. O. McClure and B. R. Cullen (2005). "Foamy Virus Bet Proteins Function as Novel Inhibitors of the APOBEC3 Family of Innate Antiretroviral Defense Factors." Journal Of Virology **79**(14): 8724-8731.

Schrofelbauer, B., D. Chen and N. R. Landau (2004). "A single amino acid of APOBEC3G controls its species-specific interaction with virion infectivity factor (Vif)." Proc. Natl. Acad. Sci USA **101**(11): 3927-3932.

Schrofelbauer, B., T. Senger, G. Manning and N. R. Landau (2006). "Mutational Alteration of Human Immunodeficiency Virus Type 1 Vif Allows for Functional Interaction with Nonhuman Primate APOBEC3G." Journal of Virology **80**(12): 5984-5991.

Schumacher, A. J., D. V. Nissley and R. S. Harris (2005). "APOBEC3G hypermutates genomic DNA and inhibits Ty1 retrotransposition in yeast." PNAS **102**(28): 9854-9859.

Sheehy, A. M., N. C. Gaddis, J. D. Choi and M. H. Malim (2002). "Isolation of a human gene that inhibits HIV-1 infection and is suppressed by the viral Vif protein." Nature **418**(6898): 646-650.

Sheehy, A. M., N. C. Gaddis and M. H. Malim (2003). "The Antiretroviral enzyme APOBEC3G is degraded by the proteasome in response to HIV-1 Vif." Nature Medicine **9**(11): 1404-1407.

Shirakawa, K., A. Takaori-Kondo, M. Kobayashi, M. Tomonaga, T. Izumi, K. Fukunaga, A. Sasada, A. Abudu, Y. Miyauchi, H. Akari, K. Iwai and T. Uchiyama (2006). "Ubiquitination of APOBEC3 proteins by the Vif-Cullin5-ElonginB-ElonginC complex." Virology **344**(2): 263-266.

Simon, J., N. Gaddis, R. Fouchier and M. Malim (1998). "Evidence for a newly discovered cellular anti-HIV-1 phenotype." Nature Medicine **4**(12): 1397-1400.

Simon, J. H. M., A. M. Sheehy, E. A. Carpenter, R. A. M. Fouchier and M. H. Malim (1999). "Mutational Analysis of the Human Immunodeficiency Virus Type 1 Vif Protein." Journal of Virology **73**(4): 2675-2681.

Sodroski, J., W. C. Goh, C. Rosen, A. Tartar, D. Portetelle, A. Burny and W. Haseltine (1986). "Replicative and Cytopathic Potential of HTLV-III/LAV with sor Gene Deletions." Science **231**: 1549-1553.

Soros, V., W. Yonemoto and W. Greene (2007). "Newly Synthesized APOBEC3G Is Incorporated into HIV virions, Inhibited by HIV RNA, and Subsequently Activated by RNase H." PLOS Pathogens **9**(3): e15.

Stebbins, C. E., W. G. Kaelin and N. P. Pavletich (1999). "Structure of the VHL-ElonginC-ElonginB Complex: Implications for VHL Tumor Suppressor Function." Science **284**: 455-61.

Stenglein, M. D. and R. S. Harris (2006). "APOBEC3B and APOBEC3F inhibit L1 retrotransposition by a DNA deamination-independent mechanism." Journal of Biological Chemistry **281**(25): 16837-41.

Stopak, K., Y. Chiu, J. Kropp, R. Grant and W. Greene (2007). "Distinct patterns of cytokine regulation of APOBEC3G expression and activity in primary lymphocytes, macrophages, and dendritic cells." Journal of Biological Chemistry **282**(6): 3539-46.

Stopak, K., C. d. Noronha, W. Yonemoto and W. C. Greene (2003). "HIV-1 Vif Blocks the Antiviral Activity of APOBEC3G by Impairing Both Its Translation and Intracellular Stability." Molecular Cell **12**(3): 591-601.

Strebel, K., D. Daugherty, K. Clouse, D. Cohen, T. Folks and M. A. Martin (1987). "The HIV 'A' (sor) gene product is essential for virus infectivity." Nature **328**: 728-730.

Svarovskaia, E. S., H. Xu, J. L. Mbisa, R. Barr, R. J. Gorelick, A. Ono, E. O. Freed, W.-S. Hu and V. K. Pathak (2004). "Human apolipoprotein B mRNA-editing enzyme-catalytic polypeptide-like 3G (APOBEC3G) is incorporated into HIV-1 virions through interactions with viral and nonviral RNAs." Journal of Biological Chemistry **279**(24): 35822-35828.

vonSchwedler, U., J. Song, C. Aiken and D. Trono (1993). "Vif is crucial for human immunodeficiency virus type 1 proviral DNA synthesis in infected cells." Journal of Virology **67**: 4945-4955.

Wang, T., C. Tian, W. Zhang, K. Luo, P. Thi, N. Sarkis, L. Yu, B. Liu, Y. Yu and X. Yu (2007). "7SL RNA mediates virion packaging of the antiviral cytidine deaminase APOBEC3G." Journal of Virology **in press**.

Wedekind, J. E., R. Gillilan, A. Janda, J. Krucinska, J. D. Salter, R. P. Bennett, J. Raina and H. C. Smith (2006). "Nanostructures of APOBEC3G support a hierarchical assembly model of high molecular mass ribonucleoprotein particles from dimeric subunits." Journal of Biological Chemistry **281**(50): 38122-6.

Wichroski, M. J., G. B. Robb and T. M. Rana (2006). "Human Retroviral Host Restriction Factors APOBEC3G and APOBEC3F Localize to mRNA Processing Bodies." PLOS Pathogens **2**(5): e41.

Wiegand, H. L., B. P. Doehle, H. P. Bogerd and B. R. Cullen (2004). "A second human antiretroviral factor, APOBEC3F, is suppressed by the HIV-1 and HIV-2 Vif proteins." The Embo Journal **23**(12): 2451-2458.

Xiao, Z., E. Ehrlich, K. Luo, Y. Xiong and X. Yu (2007a). "Zinc chelation inhibits HIV Vif activity and liberates antiviral function of the cytidine deaminase APOBEC3G." FASEB J **21**(1): 217-22.

Xiao, Z., E. Ehrlich, Y. Yu, K. Luo, T. Wang, C. Tian and X.-F. Yu (2006). "Assembly of HIV-1 Vif-Cul5 E3 ubiquitin ligase through a novel zinc-binding domain-stabilized hydrophobic interface in Vif." Virology **349**(2): 290-9.

Xiao, Z., Y. Xiong, W. Zhang, L. Tan, E. Ehrlich, D. Guo and X. Yu (2007b). "Characterization of a Novel Cullin5 Binding Domain in HIV-1 Vif." Journal of Molecular Biology **373**(3): 541-50.

Yang, B., L. Li, Z. Lu, X. Fan, C. A. Patel, R. J. Pomerantz, G. C. DuBois and H. Zhang (2003). "Potent Suppression of Viral Infectivity by the Peptides That Inhibit Multimerization of Human Immunodeficiency Virus Type 1 (HIV-1) Vif Proteins." The Journal of Biological Chemistry **278**(8): 6596-6602.

Yang, S., Y. Sun and H. Zhang (2001). "The Multimerization of Human Immunodeficiency Virus Type 1 Vif Protein." The Journal of Biological Chemistry **276**(7): 4889-4893.

Yang, X. and D. Gabuzda (1998). "Mitogen-activated Protein Kinase Phosphorylates and Regulates the HIV-1 Vif Protein." The Journal of Biological Chemistry **273**(45): 29879-29887.

Yang, X. and D. Gabuzda (1999). "Regulation of Human Immunodeficiency Virus Type 1 Infectivity by the ERK Mitogen-Activated Protein Kinase Signaling Pathway." Journal of Virology **73**(4): 3460-3466.

Yang, X., J. Goncalves and D. Gabuzda (1996). "Phosphorylation of Vif and Its Role in HIV-1 Replication." The Journal of Biological Chemistry **271**(17): 10121-10129.

Yu, X., M. Lichterfeld, M. Addo and M. Altfeld (2005). "Regulatory and accessory HIV-1 proteins: potential targets for HIV-1 vaccines." Current Medical Chemistry **12**(6): 741-7.

Yu, X., Y. Yu, B. Liu, K. Luo, W. Kong, P. Mao and X.-F. Yu (2003). "Induction of APOBEC3G Ubiquitination and degradation by an HIV-1 Vif-Cul5-SCF Complex." Science **302**(5647): 1056-1060.

Yu, Y., Z. Xiao, E. S. Ehrlich, X. Yu and X.-F. Yu (2004). "Selective assembly of HIV-1 vif-Cul5 ElonginB-ElonginC E3 ubiquitin ligase complex through a novel SOCS box and upstream cysteines." Genes & Development **18**: 2867-2872.

Zennou, V. and P. D. Bieniasz (2006). "Comparative analysis of the antiretroviral activity of APOBEC3G and APOBEC3F from primates." Virology **349**(1): 31-40.

Zhang, H., B. Yang, R. J. Pomerantz, C. Zhang, S. Arunachalam and L. Gao (2003). "The cytidine deaminase CEM15 induces hypermutation in newly synthesized HIV-1 DNA." Nature **424**(6944): 94-98.

Zhang, K., B. Mangeat, M. Ortiz, V. Zoete, D. Trono, A. Telenti and O. Michielin (2007). "Model Structure of Human APOBEC3G." PLOS One **2**(4): e378.

Zhao, L. and H. Zhu (2004). "Structure and function of HIV-1 auxiliary regulatory protein Vpr: novel clues to drug design." Current Drug Targets Immune Endocrine Metabol Disord. **4**(4): 265-75.

Zheng, Y.-H., D. Irwin, T. Kurosu, K. Tokunaga, T. Sata and B. M. Peterlin (2004). "Human APOBEC3F Is Another Host Factor That Blocks Human Immunodeficiency Virus Type 1 Replication." Journal of Virology **78**(11): 6073-6076.

CHAPTER II

METHODOLOGY

In this chapter I outline my experimental design and some of the techniques used to investigate the structural topology of HIV-1 Vif. Since HIV-1 Vif is an ideal candidate for structure-based drug design, my first goal was to obtain soluble protein for crystallographic studies. Therefore, I first discuss in detail the techniques used for protein expression, then those used in cross-linking and mass spectrometry to obtain structural information. Then I describe at length the techniques used to characterize the HIV-1 Vif/APOBEC3G (APO3G) interaction, including surface plasmon resonance, size-exclusion chromatography and laser light scattering (SEC-LS), and peptide-competition experiments. Finally, I will describe intrinsically disordered proteins.

Protein Expression

Structure-based strategies to design drugs that target HIV-1 Vif and APO3G have not been possible to date due to the lack of three-dimensional structures for these proteins. Only limited structural or biochemical information is available for these proteins because they could not be obtained in large quantities of soluble protein needed for conventional structural analyses such as X-ray crystallography or nuclear magnetic resonance (NMR). Large quantities of protein are generally obtained by bacterial expression systems that yield soluble and insoluble fractions (Appendix I). Proteins expressed in the soluble fraction are generally believed to be in a native conformation that retains their normal physiological functions, whereas proteins found in the insoluble fraction are unfolded and thus in a nonnative form. Thus, expressing milligram quantities of soluble protein, Vif and/or APO3G, in its native form is necessary to pursue structure-

based therapeutic strategies. Moreover, large quantities of these proteins will allow their use in conventional biophysical techniques to decipher their function(s).

To this end, I sought to obtain milligram quantities of both soluble HIV-1 Vif and APO3G for X-ray crystallographic studies by optimizing expression conditions. In my initial expression experiments, I varied (1) isopropyl β-D-1-thiogalactopyranoside (IPTG) concentration to induce protein expression, (2) temperature of induction and expression, and (3) type of induction/expression media. Lower concentrations of IPTG would slow the rate of protein (HIV-1 Vif and APO3G) induction and expression and decrease the accumulation of protein per cell. These conditions would prevent host *E. coli* cells from being overwhelmed by high levels of a foreign protein that they would sense as toxic and shuttle to inclusion bodies (insoluble fraction). Lower temperatures for induction and expression are used to slow the rates of natural host cell processes, thus preventing HIV-1 Vif and APO3G from being considered toxic by *E. coli*. Different media such as terrific broth (TB) and Luria broth (LB) are recommended for induction/expression because media with high nutrient contents promote robust growth of *E. coli* thus increasing the amount of HIV-1 Vif and APO3G produced.

Another technique I used to increase the yield of soluble protein was expressing HIV-1 Vif and APO3G with a tag known to be soluble. This technique has been reported to enhance the expression of toxic proteins in the soluble fraction by masking their toxic characteristics. I, therefore, tested expression constructs of HIV-1 Vif and APO3G as fusion proteins with maltose binding protein (MBP), glutathione S-transferase (GST), and NusA, all known to increase solubility of the expressed fusion proteins (Terpe, 2003).

To further increase the yield of soluble protein, I used four other strategies: codon optimized cells, baculovirus expression, recovery of protein from the insoluble fraction, and different HIV-1 Vif variants. First, I used codon optimized *E. coli* cells. The gene for HIV-1 Vif contains several codons for arginine, isoleucine, and leucine, which correspond to rare tRNAs in *E. coli.* To enhance synthesis of these rare tRNAs in *E. coli*, I used BL21CodonPlus(DE3)-RIL*E. coli* cells which have plasmids that produce these rare amino acids. Second, I tried to increase the yield of soluble APO3G and HIV-1 Vif by using baculovirus vectors to express the proteins in insect cells that have post-translational machinery. Post-translational modification may be crucial for folding of the respective proteins, as well as their functions. APO3G and HIV-1 Vif are reported to be phosphorylated (Yang, 1996; Yang, 1998; Yang, 1999; Douaisi, 2005). Third, I tried to recover HIV-1 Vif and APO3G from the insoluble fraction by using 8M urea or 6M guanidine hydrochloride, which denatures proteins, and then refolded to obtain native protein. A fourth approach was to use different Vif variants and species since the naturally occurring differences in amino acids might increase the solubility of a particular Vif protein. For example, the different amino acid sequence of SIV Vif might be more efficiently expressed as soluble protein than that of HIV-1 Vif.

Finally, I tried to increase the yield of soluble proteins by co-expressing HIV-1 Vif with APO3G. This strategy was based on the possibility that the complex would be more stable, thus more soluble, than each individual protein. All these strategies were used to reach the goal of obtaining soluble HIV-1 Vif and APO3G proteins for crystallographic studies that would provide data for use in structure-based drug design.

Mass Spectrometry: Methods for Chapter III

As described above, my first goal was to obtain soluble HIV-1 Vif and APO3G proteins for crystallographic studies of the structures for HIV-1 Vif, APO3G, and their complex. However, the strategies described in the previous section failed to produce soluble protein (Appendix I). Therefore, I sought low-resolution structural information by alternative strategies such as cross-linking and mass spectrometry (Figure 2.1).

Mass spectrometry has traditionally been used to identify proteins, but over the last few decades it has been increasingly used to probe protein-protein and protein-ligand interactions. In particular, when traditional structural methods such as X-ray crystallography or NMR cannot be used, mass spectrometry is useful because it can probe structural characteristics using small quantities (nM range) of protein in a relatively short amount of time (Farmer, 1998; Back, 2003; Trester-Zedlitz, 2003). In addition, cross-linking and mass spectrometry analysis can be used to validate the structural predictions of molecular simulations (Back, 2003; Trester-Zedlitz, 2003; Sinz, 2006).

Structural information about protein-protein and protein-ligand interactions can be obtained by matrix-assisted laser desorption/ionization-mass spectrometry (MALDI/MS). Most non-covalent protein complexes dissociate when subjected to MALDI/MS analysis, but these interactions can be kept intact by four main measures. First, specific matrix and protein concentrations can be used to favor the protein complex (Farmer, 1998). Second, "first shot" laser analysis can be utilized, in which each spot on the MALDI plate is only irradiated once at the threshold irradiance, and all the "first shots" are summed to prevent

Figure 2.1

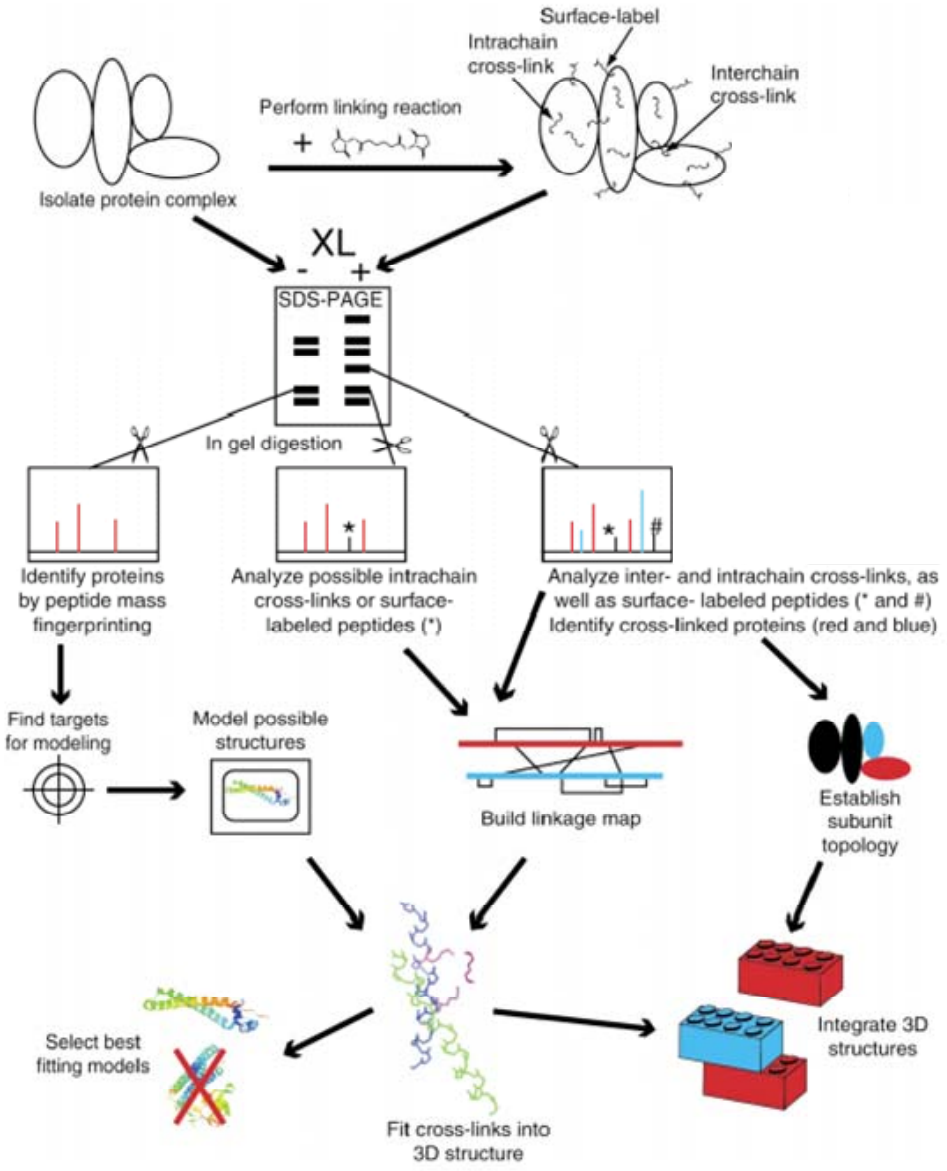

Reprinted from *Journal of Molecular Biology*, 331, Back, J.W., L.D. Jong, O. Muijsers, and C. G. de Koster, Chemical Cross-linking and Mass Spectrometry for Protein Structural Modeling, 303-313, 2003, with permission from Elsevier.

Figure 2.1: Cross-linking and Mass Spectrometry Analysis. A protein complex is cross-linked and resolved on a denaturing gel with a noncross-linked control. The noncross-linked control and cross-linked samples are in-gel digested and analyzed by mass spectrometry. The noncross-linked sample determines peptide coverage, the cross-linked monomer determines intra-molecular cross-links, and the cross-linked samples contain inter-molecular cross-links. Cross-linking data can be used as distance constraints to build three-dimensional models (Back, 2003).

radiation damage from disrupting the protein complex. Third, the pH of the sample and matrix can be adjusted to favor the protein complex. However, concerns that these techniques may not keep a complex intact have led to a fourth way to detect protein complexes: chemical cross-linking. MALDI/MS analysis of a complex prior to cross-linking allows the molecular masses of individual subunits to be determined, and after cross-linking this analysis allows the stoichiometry of the complex to be determined. Therefore, MALDI/MS can give insights into the composition of a protein-protein complex, the mass of its subunits, and the stoichiometry of the complex (Farmer, 1998).

Cross-linking and mass spectrometry analysis become particularly useful for investigating limited quantities of proteins as in the case of HIV-1 Vif. These techniques can be used to determine neighboring amino acids in three-dimensional space, when these relationships are not apparent from the primary sequence, thus allowing potential topology models to be built. Cross-linkers of different lengths and reactivities can be used to validate observed cross-links and to determine unique distant constraints for residues. Cross-linking conditions should be as near physiological as possible to ensure that the protein structure is not disturbed; chemical cross-linkers are typically not destructive since cross-linked enzymes generally retain their activity. The complexity of mass spectrometric analysis can be reduced by using gel separation and in-gel digestion to separate unique protein species (Back, 2003; Sinz, 2003; Sinz, 2006).

Cross-links have been identified by three mass spectrometric techniques: MALDI/MS, electrospray ionization (ESI)-MS/MS, and Fourier transform ion cyclotron resonance (FT-ICR). MALDI/MS and ESI can be used to identify cross-links based on

molecular weights. In addition, ESI-MS/MS can give sequence data about cross-links, which aids in their identification. The identification of cross-links has been advanced by the development of FT-ICR mass spectrometry. FT-ICR has great mass accuracy, more than 2 ppm, which reduces the number of cross-link candidates and increases the accuracy of identification (Back, 2003; Sinz, 2003; Sinz, 2006).

Looking for cross-links in mass spectrometry data is a daunting task. To aid in identifying cross-links, researchers have used many different techniques, including isotope labeling, fluorescence labeling, affinity cross-links, and ^{18}O labeling of peptides (Sinz, 2003; Trester-Zedlitz, 2003; Sinz, 2006). For example, protein samples can be divided, and half can be in-gel trypsin digested in the presence of ^{16}O and the other half in the presence of ^{18}O water. After digestion, the two samples are mixed and analyzed. Since oxygen molecules are incorporated into the C-terminus of tryptically cleaved peptides, cross-linked peptides have an 8-mass-unit shift and uncross-linked peptides have a 4-mass-unit shift (Yao, 2001; Back, 2002).

Cross-linking and mass spectrometry have been increasingly applied over the last several years to identify the structural characteristics of proteins, particularly as an alternative approach to obtaining structural information when large quantities of proteins and complexes cannot be isolated. For example, cross-linking and mass spectrometry analysis of apolipoprotein(apo)A-I cross-linked to high density lipoprotein (HDL) particles has given insight into the spatial orientation of apoA-I on HDL particles and supported two of three structural models (Davidson, 2003). In addition, calmodulin cross-linking to a small peptide, melittin, has been used to determine interacting regions

within the calmodulin-melittin complex (Schulz, 2004). These data have helped determine the orientation in which melittin binds calmodulin and have been used to create a novel three-dimensional model of the complex (Schulz, 2004). In addition to confirming structural models (Davidson, 2003) and creating new structural insights into peptide binding (Schulz, 2004), cross-linking and mass spectrometry analysis can be used to confirm data from crystallography and NMR. For example, the technique has been used to confirm NMR data on the interactions between calmodulin and a short skeletal muscle, myosin light-chain kinase peptide (M13) (Kalkhof, 2005).

Therefore, in the absence of milligram quantities of protein necessary for crystallography, mass spectrometric and cross-linking techniques are a valuable approach to obtaining structural information for protein-protein and protein-peptide interactions. Using cross-linkers with different reactivities and distance constraints can give insight into which residues are three-dimensionally adjacent and aid in constructing a three-dimensional model. Structural mapping via mass spectrometry can be used when crystallography and NMR are not available to create novel structural data, to confirm models, or to confirm experimentally collected structural data. These structural data can be used with other biochemical data to aid in drug design.

Surface Plasmon Resonance

A technique used to analyze protein-protein, protein-small molecule, and protein-nucleic acid interactions is surface plasmon resonance (SPR), which I used to obtain binding data for the HIV-1 Vif/APO3G interaction (Appendix II). SPR can measure

protein-protein interactions in real time and produces an on-rate (k_{on}) and an off-rate (k_{off}) that can be used to calculate a dissociation constant (K_d). The SPR machine (Biacore) measures binding in terms of response units (RUs), where 1000 RUs equals 1ng of mass per mm^2 (Fivash, 1998) www.biacore.com).

A sensor chip docked into the SPR machine is the surface on which proteins interact. Sensor chips are composed of carboxy-methylated dextran surfaces that allow ligand binding by multiple chemistries. The chemistry most commonly used in immobilization is amine coupling, but nickel and streptavidin affinity are also used. A ligand is immobilized onto the sensor chip surface by a covalent interaction, which allows the surface to be regenerated and reused. After the ligand is immobilized, an analyte is injected into the machine, and the ligand-analyte interaction is measured (Fivash, 1998) www.biacore.com).

This ligand-analyte e.g. protein-protein interaction is measured as the change in response units determined by the angle of light at an optical detection unit. The unit measures light refracted by molecular interactions on the sensor surface inside a flow cell, on which a polarized light beam is focused (www.biacore.com).

Size-exclusion Chromatography and Laser Light Scattering

Size-exclusion chromatography and laser light scattering (SEC-LS) are used to determine the molecular weights of proteins and protein-protein complexes. Therefore, I used this approach to determine the molecular weight of HIV-1 Vif and APO3G oligomers in solution as well as the molecular weight of the HIV-1 Vif-APO3G complex

(Appendix II). The goal of determining the exact molecular weight of the HIV-1-Vif APO3G complex was to give insight into its stoichiometry.

In SEC-LS experiments, proteins are first separated on a size-exclusion column and analyzed by laser light scattering. The amount of scattered light is related to the molecular weight of a protein or protein complex; therefore, the absolute mass (molecular weight [MW]) and size (radius of gyration) of macromolecules can be determined. Using SEC-LS has numerous advantages: (1) macromolecules are studied in solution, (2) experiments can be conducted faster (in hours) than other techniques (in days), and (3) the MW determination is accurate to within 7% error. In addition, SEC-LS can directly measure MW, whereas dynamic light scattering indirectly calculates the MW of a sample by measuring its polydiversity and other parameters (Yale Keck Facility website, www.keck.med.yale.edu).

Peptides: Methods for Chapter IV

Since high-resolution structural data could not be obtained for the HIV-1 VIf-APO3G interaction, I confirmed my low-resolution structural data and identified potential inhibitors of a specific protein-protein interaction by using peptide-competition experiments. In addition, the peptides used in the peptide competition experiments can be tagged with antennapedia for cellular uptake to correlate my low resolution structural data with viral infectivity (Yang, 2003). In the case of HIV-1 Vif, peptides could be isolated to block either oligomerization or the Vif-APO3G interaction. These peptides

could be used to block HIV-1 Vif's function, thus allowing APO3G to perform its role as an antiretroviral agent.

In a similar manner to my peptide competition experiments, Phage display has been used to develop peptides that bind to HIV-1 Vif and prevent its ability to self-associate (Yang, 2003). These peptides contain a PXP motif that is consistent with the ^{161}PPLP^{164} motif observed in HIV-1 Vif's proposed oligomerization domain. Indeed, when peptides containing the PPLP domain were identified via phage display and tagged with antennapedia, they inhibited HIV-1 replication *in vivo* (Yang, 2003). The antennapedia-tag acts as a cellular uptake signal, and HIV-1 replication is inhibited, presumably by peptide-mediated inhibition of HIV-1 Vif oligomerization (Yang, 2003). The same PPLP-containing peptides have recently been tagged to the TAT-uptake signal and shown to inhibit viral infectivity (Miller, 2007). These peptides were also shown to reduce the number of HIV-1 Vif multimers, thus increasing the amount of APO3G and reducing infectivity (Miller, 2007).

The function of HIV-1 Vif can be disrupted not only by blocking its oligomerization (the Vif-Vif interaction), but also by disrupting the Vif-APO3G interaction. The HIV-1-APO3G interaction has been shown to be strongly inhibited by N-terminal HIV-1 Vif peptides in peptide-competition assays where the most potent peptide contained residues 57-71 (Mehle, 2007). This peptide reduced the amount of Vif-APO3G binding to almost background levels. This result not only gives insight into potential therapeutics, but also implicates the N-terminal region of HIV-1 Vif in APO3G binding (Mehle, 2007).

Intrinsic Disorder

The techniques described above can also give insight into potentially disordered regions in HIV-1 Vif. A central theme in structural biology is that structure and function are correlated; therefore, protein function has been assumed to depend on a well-defined structure. However, a class of proteins was recently discovered to function without a defined structure; these proteins are known as intrinsically disordered (Dyson, 2005; Fink, 2005). Intrinsically disordered proteins have three main characteristics: (1) lack of a specific tertiary structure but a defined secondary structure, (2) low overall hydrophobicity, and (3) high net charge. Therefore, these characteristics allow the proteins to sample an ensemble of conformations (Dyson, 2005; Fink, 2005).

Lack of order is determined by a protein's underlying amino acid sequence (Dyson, 2005; Fink, 2005). Based on sequence, disordered proteins fall into two groups, those without any structure at all and those with disordered domains. These disordered proteins or regions have few bulky hydrophobic amino acids such as Val, Leu, Ile, Met, Phe, Trp, and Tyr, whereas they have more polar and charged amino acids such as Gln, Ser, Pro, Glu, Lys, Gly, and Ala. These patterns have been used to develop programs that predict disorder in proteins based on their sequence (Dyson, 2005; Fink, 2005).

Intrinsic disorder provides a unique functional advantage to proteins; it allows them to bind a large diverse set of ligands. Upon ligand binding, the disordered region undergoes a disorder-to-order transition, suggesting that folding and binding are coupled in these proteins. Many of these proteins are involved in molecular regulation; therefore, they are abundant in cell cycle control, transcriptional and translational regulation, and

have been linked to cancer. On a similar note, hub proteins in large protein networks are often intrinsically disordered. This disorder allows these proteins to bind the large and diverse set of ligands involved in the network (Iakoucheva, 2002; Dunker, 2005; Dyson, 2005; Fink, 2005). Therefore, intrinsic disorder plays an important functional role, but more research is needed to identify the importance of intrinsic disorder in other processes, including viral infection.

References

Back, J., V. Notenboom, L. de Koning, A. Muijsers, T. Sixma, C. de Koster and L. de Long (2002). "Identification of cross-linked peptides for protein interaction studies using mass spectrometry and 18O labeling." Anal Chem. **74**(17): 4417-22.

Back, J. W., L. d. Jong, A. O. Muijsers and C. G. d. Koster (2003). "Chemical Cross-linking and Mass Spectrometry for Protein Structural Modeling." Journal Molecular Biology **331**: 303-313.

Davidson, W. S. and G. M. Hilliard (2003). "The Spatial Organization of Apolipoprotein A-I on the Edge of Discoidal High Density Lipoprotein Particles." The Journal of Biological Chemistry **278**(29): 27199-27207.

Douaisi, M., S. Dussart, M. Courcoul, G. Bessou, E. C. Lerner, E. Decroly and R. Vigne (2005). "The tyrosine kinases Fyn and Hck favor the recruitment of tyrosine-phosphorylated APOBEC3G into vif-defective HIV-1 particles." Biochemical and Biophysical Research Communications **329**: 917-924.

Dunker, A., M. Cortese, P. Romero, L. Iakoucheva and V. Uversky (2005). "Flexible nets. The roles of intrinisic disorder in protein interaction networks." FEBS **272**(20): 5129-48.

Dyson, H. J. and P. E. Wright (2005). "Intrinsically Unstructured Proteins and Their Functions." Nature Reviews Molecular Cell Biology **6**: 197-208.

Farmer, T. B. and R. M. Caprioli (1998). "Determination of Protein-Protein Interactions by Matrix-assisted Laser Desorption/Ionization Mass Spectrometry." Journal of Mass Spectrometry **33**: 697-704.

Fink, A. L. (2005). "Natively unfolded proteins." Current Opinion in Structural Biology **15**: 35-41.

Fivash, M., E. M. Towler and R. J. Fisher (1998). "BIAcore for macromolecular interaction." Current Opinion in Biotechnology **9**: 97-101.

Iakoucheva, L. M., C. J. Brown, J. D. Lawson, Z. Obradovic and A. K. Dunker (2002). "Intrinsic Disorder in Cell-signaling and Cancer-associated Proteins." Journal of Molecular Biology **323**: 573-584.

Kalkhof, S., C. Ihling, K. Mechtler and A. Sinz (2005). "Chemical Cross-linking and High-Performance Fourier Transform Ion Cyclotron Resonance Mass Spectrometry for Protein Interaction Analysis: Application to a Calmodulin/Target Peptide Complex." Analytical Chemistry **77**(2): 495-503.

Mehle, A., H. Wilson, C. Zhang, A. Brazier, M. McPike, E. Pery and D. Gabuzda (2007). "Identification of an APOBEC3G Binding Site in HIV-1 Vif and Inhibitors of Vif-APOBEC3G Binding." Journal of Virology **81**(23): 13235-41.

Miller, J., V. Presnyak and H. Smith (2007). "The dimerization domain of HIV-1 viral infectivity factor Vif is required to block APOBEC3G incorporation with virions." Retrovirology **4**(1): 81.

Schulz, D. M., C. Ihling, G. M. Clore and A. Sinz (2004). "Mapping the Topology and Determination of a Low-Resolution Three Dimensional Structure of the Calmodulin-Melittin Complex by Chemical Cross-linking and High-Resolution

FTICRMS: Direct Demonstration of Multiple Binding Modes." Biochemistry **43**: 4703-4715.

Sinz, A. (2003). "Chemical Cross-linking and mass spectrometry for mapping three-dimensional structures of proteins and protein complexes." Journal of Mass Spectrometery **38**: 1225-1237.

Sinz, A. (2006). "CHEMICAL CROSS-LINKING AND MASS SPECTROMETRY TO MAP THREE-DIMENSIONAL PROTEIN STRUCTURES AND PROTEIN–PROTEIN INTERACTIONS." Mass Spectrometry Reviews **25**: 663-682.

Terpe, K. (2003). "Overview of tag protein fusions: from molecular and biochemical fundamentals to commercial systems." Appl Microbiol Biotechnol **60**: 523-533.

Trester-Zedlitz, M., K. Kamada, S. K. Burley, D. Fenyo, B. T. Chait and T. W. Muir (2003). "A Modular Cross-Linking Approach for Exploring Protein Interactions." Journal of American Chemical Society **125**: 2416-2425.

Yang, B., L. Li, Z. Lu, X. Fan, C. A. Patel, R. J. Pomerantz, G. C. DuBois and H. Zhang (2003). "Potent Suppression of Viral Infectivity by the Peptides That Inhibit Multimerization of Human Immunodeficiency Virus Type 1 (HIV-1) Vif Proteins." The Journal of Biological Chemistry **278**(8): 6596-6602.

Yang, X. and D. Gabuzda (1998). "Mitogen-activated Protein Kinase Phosphorylates and Regulates the HIV-1 Vif Protein." The Journal of Biological Chemistry **273**(45): 29879-29887.

Yang, X. and D. Gabuzda (1999). "Regulation of Human Immunodeficiency Virus Type 1 Infectivity by the ERK Mitogen-Activated Protein Kinase Signaling Pathway." Journal of Virology **73**(4): 3460-3466.

Yang, X., J. Goncalves and D. Gabuzda (1996). "Phosphorylation of Vif and Its Role in HIV-1 Replication." The Journal of Biological Chemistry **271**(17): 10121-10129.

Yao, X., A. Freas, J. Ramirez, P. Demirev and C. Fenselau (2001). "Proteolytic 18O labeling for comparative proteomics: model studies with two serotypes of adenovirus." Anal Chem. **73**(13): 2836-42.

CHAPTER III

MASS SPECTROMETRY ANALYSIS OF HIV-1 VIF REVEALS AN INCREASE IN ORDERED STRUCTURE UPON OLIGOMERIZATION IN REGIONS NECESSARY FOR VIRAL INFECTIVITY

ABSTRACT

HIV-1 Vif, an accessory protein in the viral genome, performs an important role in viral pathogenesis by facilitating the degradation of APOBEC3G (APO3G), an endogenous cellular inhibitor of HIV-1 replication. In this study, intrinsically disordered regions in HIV-1 Vif were predicted using sequence-based algorithms. This disorder may explain why traditional methods to determine the structure of HIV-1 Vif have been unsuccessful, making structure-based drug design impossible. To characterize HIV-1 Vif's structural topology and to map its oligomerization domains, I used chemical cross-linking, proteolysis and mass spectrometry. Cross-linking showed evidence of monomer, dimer, and trimer species via denaturing gel analysis and an additional tetramer via western blot analysis. Among the noncross-linked monomer, and cross-linked monomer, dimer, and trimer samples, I identified 47 unique linear peptides and 24 (13 intramolecular, 11 intermolecular) noncontiguous cross-linked peptides. In all samples analyzed, I found almost complete peptide coverage of the N-terminus, but reduced peptide coverage in the C-terminal region of the dimer and trimer samples. These differences in peptide coverage or "protections" between dimers and trimers indicate specific differences in packing between the 2 oligomeric forms. Intramolecular cross-links within the monomer suggest that the N-terminus is folded into a compact domain, while the C-terminus remains intrinsically disordered. The intermolecular cross-link data also show that upon oligomerization, the C-terminus of one Vif protein becomes ordered by wrapping back on the N-terminal domain of another monomer. In addition, the majority of intramolecular cross-links maps to regions previously reported to be

necessary for viral infectivity. Thus, my data suggest that HIV-1 Vif is in a dynamic equilibrium among its various oligomers, potentially allowing it to interact with other binding partners.

INTRODUCTION

The human immunodeficiency virus type-1 (HIV-1) accessory protein, viral infectivity factor or Vif, is a 23 kDa highly basic protein (pI 10.7) present in all lentiviruses except equine anemia infectious virus. Over the last several years, the function and interactions of HIV-1 Vif have been extensively investigated (Lake, 2003; Baraz, 2004; Navarro, 2004; Rose, 2004). HIV-1 Vif potentially interacts with many viral and cellular macromolecules: APOBEC3G (APO3G), an endogenous cytidine deaminase (Madani, 2000; Sheehy, 2002), and its family members such as APOBEC3F (Wiegand, 2004; Liu, 2005), HIV-1 Gag (Bardy, 2001), HIV-1 protease (Hutoran, 2004), viral RNA (Cancio, 2004; Henriet, 2005), and 2 proteins in a cullin-RING ligase complex: Cullin5 (Luo, 2005; Mehle, 2006; Xiao, 2006) and elongin C (Yu, 2003; Mehle, 2004; Yu, 2004).

When HIV-1 Vif is absent or nonfunctional, post-infection viral replication and viral production are dramatically reduced in "nonpermissive" primary CD4 T-cells. This reduced viral production is likely due to the irreversible effects of the cellular enzyme APO3G found in nonpermissive cells, which inhibits viral replication possibly through its deaminase activity or by preventing the build-up of reverse transcripts (Gabuzda, 1992; Sakai, 1993; Sova, 1993; vonSchwedler, 1993; Sheehy, 2002; Bishop, 2006). HIV-1 Vif binds APO3G and targets it for proteosomal degradation through a cullin-RING ligase complex, which includes interactions with elongin C and Cullin5 in the Cullin5-elongin BC complex and may also block APO3G's translation (Marin, 2003; Sheehy, 2003; Stopak, 2003; Mehle, 2004; Kobayashi, 2005; Luo, 2005; Mehle, 2006; Shirakawa,

2006). Specifically, HIV-1 Vif interacts with elongin C through HIV-1 Vif's SOCS box motif (Yu, 2003; Mehle, 2004; Yu, 2004), and HIV-1 Vif binds Cullin5 via an HCCH zinc-binding motif in HIV-1 Vif (Luo, 2005; Mehle, 2006; Xiao, 2006). Therefore, it is likely that HIV-1 Vif's interactions with other macromolecules are important to its function in suppressing the effects of APO3G.

The lack of or slowing of disease progression to AIDS in HIV-1-infected patients has been correlated with mutations in the HIV-1 Vif gene (Hassaine, 2000; Sakurai, 2004; Farrow, 2005). Therefore, the spread of HIV-1 infection might be prevented by blocking HIV-1 Vif's ability to inhibit APO3G, thus allowing the full action of its antiviral effects. Inhibiting HIV-1 Vif function might therefore suppress viral replication. Thus, HIV-1 Vif is considered a viable therapeutic target either for structure-based inhibitors or as a potential vaccine candidate.

To develop HIV-1 Vif into a viable therapeutic target, the molecular mechanisms need to be clearly understood for HIV-1 Vif function, including its oligomerization and interactions with putative functional partners. To date, little biochemical data are available on HIV-1 Vif, and more importantly, no structural data. This lack of data is partially due to an inability to express high levels of soluble recombinant protein using either prokaryotic or baculovirus expression systems. However, as I will show, regions of HIV-1 Vif are highly likely to be intrinsically disordered. Intrinsically disordered proteins have extensive regions that lack a fixed tertiary structure (Romero, 2006) and are characterized by a high net charge and low overall hydrophobicity (Dyson, 2005; Fink, 2005). In addition, proteins with regions known to be disordered tend to bind a large and

diverse set of proteins and nucleic acids (Dunker, 2005; Fink, 2005). These properties of intrinsically disordered proteins are also known characteristics of HIV-1 Vif.

Although little structural or biochemical data are available for HIV-1 Vif, homo-oligomerization has been implicated in its function. A putative oligomerization domain has been found to map to amino acid residues 151-164 (Yang, 2001). Indeed, if this region is deleted or mutated, HIV-1 Vif function is significantly reduced. More specifically, residues 161-164, which map to the PPLP domain of HIV-1 Vif, were shown to be necessary for HIV-1 Vif oligomerization (Yang, 2003). In addition, peptides corresponding to the region 153-171 drastically reduced the number of HIV-1 Vif oligomers observed. Adding these short peptides also inhibited HIV-1 replication in nonpermissive cells, presumably by competing with the functionally necessary step of oligomerization in HIV-1 Vif (Yang, 2003). Taken together, these data suggest that the oligomerization domain in HIV-1 Vif is residues 151-171 (AALITPKKIKPPLPSVTKLTE).

In this study, sequence-based algorithms were used to predict intrinsically disordered regions of HIV-1 Vif. These regions may explain why traditional methods to determine the structure of HIV-1 Vif, and thus structure-based drug design, have been elusive. For proteins like HIV-1 Vif, which are difficult to express in large quantities, an ideal method to obtain structural information at the level of individual amino acids is mass spectrometry (MS). MS uses only nanogram amounts of protein, as opposed to milligrams for other biophysical and structural techniques (Farmer, 1998; Back, 2003; Sinz, 2003; Trester-Zedlitz, 2003; Eyles, 2004; Schulz, 2004; Kalkhof, 2005). Using a

novel approach involving short covalent chemical cross-linkers to stabilize the protein-protein complex, proteolysis and various forms of MS techniques, I identified HIV-1 Vif oligomer (protein-protein) interactions. By determining a series of these interactions, I also obtained a low-resolution structural map of HIV-1 Vif. Here I report for the first time data on the structural topology of HIV-1 Vif, the domains involved in HIV-1 Vif oligomerization, and a mechanism by which Vif may bind other proteins.

MATERIALS AND METHODS

HIV-1 Vif: This protein, which had been expressed and purified by Immunodiagnostics, Inc., Woburn, MA, was obtained from the AIDS Research and Reagent Program or directly from Immunodiagnostics, Inc. According to the manufacturer's product sheet, the HIV-1 Vif protein was from strain HXB2, expressed in *Escherichia coli* with a 6X His tag that is cleaved under native conditions, stored in 50 mM Tris, pH 8.0, 150 mM sodium chloride, and was >99% pure. Several lots of HIV-1 Vif protein were obtained and all gave consistent results.

The purity of the HIV-1 Vif protein from Immunodiagnostics was analyzed by SDS PAGE (Figure 3.1B). The predominant band corresponded to monomeric HIV-1 Vif protein with a molecular weight of 23 KDa and was approximately 95% pure as determined by densometric analysis of the SDS PAGE. However, along with the 23 KDa band, multiple lower molecular weight bands were observed. These bands are likely degradation products of the HIV-1 Vif protein, suggesting the protein may be unstable. Further analysis of these smaller products are needed because they may be more soluble

forms of HIV-1 Vif that can be used in further structural and biochemical analysis. In addition, the HIV-1 Vif protein became insoluble when I tried to concentrate it. Thus, even if the expression of this protein could be scaled up, larger amounts of protein would likely be unobtainable Lastly, when HIV-1 Vif cross-links were analyzed by MS, the proteins were sequenced by MALDI-TOF and peptides from the entire protein were identified, confirming the full-length HXB2 Vif protein sequence (Table 3.2).

APO3G: This protein, which had been expressed and purified by Immunodiagnostics, Inc., Woburn, MA, was obtained from the AIDS Research and Reagent Program. According to the manufacturer's product sheet, the protein was expressed in *E. coli* or baculovirus. When expressed in *E. coli*, APO3G was 6X His-tagged, purified to >95% purity via preparative SDS-PAGE, and stored in PBS, 30% glycerol, 0.1% sarcosyl; when expressed in baculovirus, APO3G was a T-tag fusion protein, purified to >95% purity using $(NH_4)_2SO_4$ fractionation and immunoaffinity chromatography, and stored in 20 mM Tris, pH 8.0, 0.1 M sodium chloride, 0.01% sarcosyl.

Co-Immunoprecipitation: HIV-1 Vif was captured by immunoprecipitation on an EZview^{TM} Red Protein A Affinity gel (Sigma) using an anti-Vif antibody (TG001 obtained from the NIH AIDS Research and Reagent Program). The affinity gel with immobilized HIV-1 Vif was washed with 20 mM Tris, pH 8.0, 0.5 M sodium chloride buffer, and incubated with APO3G overnight at 4°C. After APO3G incubation, the gel beads were washed, and the HIV-1 Vif-APO3G complex was eluted by boiling. The samples were then analyzed by 16% Tris-Glycine SDS PAGE and western blotted using an antibody for APO3G. The same protocol was followed for APO3G, with APO3G

captured by immunoprecipitation on the Protein A Affinity gel using an anti-APO3G antibody and western blotted using a HIV-1 Vif antibody (TG001).

Cross-linking of HIV-1 Vif: The "zero length" cross-linking agent, EDC (1-ethyl-3-[3-dimethylaminopropyl] carbodiamide; Pierce), and sulfo-NHS (N-hydroxysuccinimide; Pierce) were prepared freshly as 0.1 M stock solutions in deionized water. The cross-linking reaction was performed in solution as described (Grabarek, 1990). HIV-1 Vif protein (5 mg/ml) was diluted in 50 µl activation buffer (0.1 M MES, pH 6.0, 0.5 M NaCl) to 29 µM, 1 µl of EDC stock solution was added to give a final EDC concentration of 2 mM, and 2.5 µl of sulfo-NHS stock solution was added to give a final concentration of 5 mM. Cross-linking reactions were also performed at 4 µM, 1 µM, and 0.63 µM HIV-1 Vif. Other HIV proteins such as HIV-1 Vpr are found intracellular at 5 nM at viral entry and up to 43 nM in later stages of viral replication (Popov, 1998). Although the 1 µM and 0.63 µM HIV-1 Vif concentrations are likely above the intracellular concentration of HIV-1 Vif, they are likely more closely related to the intracellular concentration of HIV-1 Vif than the original 29 µM concentration used for cross-linking. These low-concentration HIV-1 Vif solutions were used because they are dilute, therefore avoiding random protein-protein interactions. Preliminary experiments determined that the minimal time required for optimal cross-linking in solution was 15 minutes. Thus, the cross-linking reaction was conducted at room temperature for 15 minutes and quenched by adding SDS PAGE gel-loading dye with 2-mercaptoethanol. The resulting mixture of HIV-1 Vif oligomers was resolved by 16% SDS-PAGE with a noncross-linked HIV-1 Vif protein, allowing each species to be individually proteolyzed. Similar

cross-linking results were obtained using multiple lots of HIV-1 Vif protein. The density of the Coomassie blue-stained gel bands was determined using UVP Bio-imaging System EPI Chemi II Dark Room and LabWorks 4.0 software. Cross-linking experiments using purified proteins can only be performed *in vitro*.

HIV-1 Vif-specific oligomers were identified by western blot analysis using a monoclonal antibody to HIV-1 Vif (TG001) obtained from the NIH AIDS Research and Reagent program. Proteins were transferred from a SDS polyacrylamide gel to nitrocellulose membrane at 200 mAMPS for 2 hours at 4°C. After transfer, the membrane was treated with blocking buffer (10 mM Tris-HCl, pH 8.0, 0.3 M NaCl, 0.25% Tween, and 5% milk) for approximately 4 hours at room temperature. After blocking, the membrane was incubated overnight at 4°C with a 1:20,000 dilution of the HIV-1 Vif monoclonal antibody in blocking buffer. The membrane was then washed 6 times with blocking buffer without milk and incubated at room temperature for 1 hour with goat anti-mouse secondary antibody (1:40,000). The membrane was then washed 6 times and developed using the Pierce Supersignal ECL kit and a Kodak X-Omat machine.

Preparation of Samples for Mass Spectrometry (MS): Four samples of HIV-1 Vif (the noncross-linked monomer band, and the cross-linked monomer, dimer, and trimer bands) were in-gel digested in preparation for MALDI-TOF MS, LC-ion trap-MS, and LC-QTof-MS analyses in the presence or absence of heavy water (^{18}O) (Yao, 2001; Back, 2002). Heavy water (^{18}O) was used to label peptides and cross-links. Therefore, peptides digested in ^{18}O water were 4 mass units larger than those digested in ^{16}O water and cross-linked peptides were 8 mass units larger. Gel bands were in-gel digested with trypsin or

chymotrypsin using the Calbiochem ProteoExtract™ All-in-one Trypsin Digestion Kit according to the manufacturer's protocol or as described (Soskic, 2001). Briefly, gel bands containing each oligomer were excised and cut into small pieces. One-half was digested in an Eppendorf tube in ^{16}O water, and the other half was digested in an Eppendorf tube in ^{18}O water. The gel pieces were washed 2 times with wash buffer (50 mM ammonium bicarbonate in 50% ethanol) at room temperature. Gel slices were shrunk in 100% ethanol, and incubated for 1 hour at 56°C with 50 mM ammonium bicarbonate containing DTT. After cooling to room temperature, gel slices were incubated for 30 min with iodoacetamide at room temperature in the dark, washed, shrunk, and dried. Dried gel slices were digested overnight with trypsin (1 µl of 8 ng/µl) at 37°C with either ^{16}O or ^{18}O water. Peptides were extracted using 50 mM ammonium bicarbonate and 50% N,N-dimethyl formamide and evaporated to dryness using a SpeedVac. Dried peptides were dissolved in 2% acetonitrile, 0.1% TFA. Finally, peptides digested in ^{16}O water were added to their corresponding half sample digested in ^{18}O water.

Peptide Analysis using Reflectron MALDI-TOF MS: HIV-1 Vif noncross-linked and cross-linked peptides extracted from gel bands were purified using an Omix C18 ZipTip reverse-phase cleanup pipette tip. The ZipTip was prewashed with 50% acetonitrile and equilibrated with 0.1% trifluoroacetic acid (TFA). Peptides were bound to the ZipTip by aspirating them 5 times through the ZipTip. The ZipTip was then washed by repeated aspiration of 10 µl of 0.1% TFA, and peptides were eluted by repeated aspiration of 5 µl of 50% acetonitrile containing 0.1% TFA. The eluate (1 µl) was spotted onto a MALDI-

TOF MS target plate with 1 µl of 10 mg/ml α-cyano-4-hydroxycinnamic acid matrix (α-cyano) in 50% acetonitrile, 0.1% TFA, and air dried. Samples were analyzed using a Waters MALDI L/R MALDI-TOF mass spectrometer in the reflectron mode to acquire spectra from m/z 400 - 6000. Each spectrum was the sum of 500 laser shots and was lock-mass calibrated using a mixture of synthetic peptides in the lock-mass well. MALDI-TOF heavy water experiments were repeated in triplicate.

Liquid Chromatography Mass Spectrometry (LC-ion trap-MS) of Peptide Fragments: The HIV-1 Vif digests of the noncross-linked and cross-linked gel bands were analyzed by capillary HPLC nanoelectrospray (NESI) MS and data-dependent MS/MS using a ThermoFinnigan LTQ linear quadrupole ion trap MS equipped with a Finnigan Surveyor HPLC pumping system. Samples (1-5 µl) were injected into a 35 µl/min flow of 2% acetonitrile in 0.1% formic acid onto a 300 µm X 5 mm C-18 Pepmap trapping column (LC Packings) using a manual NanoPeak injection valve (UpChurch Scientific). A 30-min solvent gradient from 5 to 50% acetonitrile in 0.1% formic acid was then passed in the reverse direction at 200 nl/min through the trapping column. The trapping column eluate was passed through a 75 µm ID X 10 cm ProteoPrep II packed PicoFrit HPLC column/electrospray emitter (New Objectives, Inc.) installed in the NESI source of the mass spectrometer. Positive ion ESI MS spectra were acquired during the elution with one full scan MS, followed by data-dependent MS/MS product ion spectra (35% normalized collision energy) of the 10 most intense ions from the full-scan MS spectrum. The NESI source was operated with the source at 1.8 kV and capillary at 250^{o}C.

LC-QTof-MS Mass Spectrometry of Peptide Fragments (Q-Tof): The HIV-1 Vif noncross-linked and cross-linked peptide digests were analyzed by capillary nanoelectrospray (NESI) MS and data-dependent MS/MS using a Waters Q-Tof Premier Mass Spectrometer equipped with a Waters CapLC HPLC pumping system. Samples (1-5 µl) were injected by a manual NanoPeak injection valve onto a CAPTRAP (Michrome Bioresources, Inc.) trapping column at 12 µl/min flow of 2% acetonitrile in 0.1% formic acid. A 30-min solvent gradient from 2 to 98% acetonitrile in 0.1% formic acid was then passed through the trapping column in the reverse direction at 200 nl/min. The trapping column eluate was passed through a 75 µm ID X 10 cm ProteoPrep II-packed PicoFrit column/electrospray emitter (New Objectives, Inc.) installed in the NESI source of the mass spectrometer. Data-dependent positive ion NESI MS spectra were acquired during the elution with one full-scan MS spectrum followed by MS/MS product ion spectra of the 4 most intense ions from the full-scan MS lock-mass spectrum. The NESI source was operated with the source at 2.7 kV and capillary at 200^{o}C.

Data Analysis: HIV-1 Vif noncross-linked and cross-linked peptides were identified from molecular weight and MS/MS sequence data using SEQUEST and analyzed using PAWS (Protein Analysis Worksheet), GPMAW (General Protein Mass Analysis for Windows), and MassLynx software tools (Sinz, 2003). PAWS was used to match peptide MH^{+} ions observed in the MALDI-TOF MS data to sequences from HIV-1 Vif, and GPMAW was used to similarly match sequences from both normal peptides and cross-linked peptides observed in MALDI-TOF MS and LCMS (ion trap and QTof) analyses. MassLynx was used to analyze MALDI-TOF spectra and to identify ^{16}O and ^{18}O ion

pairs from linear and cross-linked peptides. The mass (molecular weight) of a cross-linked peptide was assigned only if the cross-link met the following criteria: 1) its cleavage was trypsin specific (R or K), 2) the cross-linked peptide must contain at least one Lys residue in one peptide and at least one Glu or Asp residue in the other, 3) ions present in the cross-linked sample must be absent in the noncross-linked control, 4) intramolecular cross-linked peptides were identified by their presence in the monomer cross-linked sample, 5) intermolecular cross-links were inferred when they were seen only in the cross-linked dimer or cross-linked trimer and not in the monomer (Davidson, 2003), 6) the cross-link was present in at least 2 out of 3 experiments, and 7) linear peptides showed a mass shift of +4 Da, and cross-linked peptides showed a mass shift of +8 Da. Criterion 2 reflects that cross-linking reactions form amide bonds between lysine side-chain amine groups and glutamic acid or aspartic acid side-chain carboxyl groups. Criterion 7 reflects that trypsin cleavage in heavy water led to 2 atoms of ^{18}O being incorporated into the carboxy terminus of each peptide, resulting in a mass shift of +4 Da for a linear peptide and +8 Da for a cross-linked peptide (Yao, 2001; Back, 2002).

Although high molecular weight cross-links are prone to less accurate mass matches, due to a higher signal-to-noise ratio, particular care was taken to ensure the accuracy of identifying cross-linked peptides (Table 3.3). These cross-links were only identified if they were reproduced in more than one sample and had the appropriate heavy water label. The majority of the data is within an acceptable parts-per-million (ppm) range; however, the few values that diverge slightly meet the other criteria for being cross-linked and are still less than one Dalton different from the theoretical mass.

Structure Predictions: Intrinsically disordered regions of HIV-1 Vif were predicted from PONDR®, Predictors of Natural Disordered Regions, which utilizes sequence-based algorithms (Romero, 2001; Vucetic, 2005). Access to PONDR® was provided by Molecular Kinetics (6201 Las Pas Trail-Ste 160, Indianapolis, IN 46268; 317-280-8737; E-mail: main@molecularkinetics.com). VL-XT is copyright©1999 by the WSU Research Foundation, all rights reserved. PONDR® is copyright©2004 by Molecular Kinetics, all rights reserved. In addition to the prediction of intrinsic disorder, a consensus secondary-structure prediction was obtained from the Pole BioInformatique Lyonnais website using Network Protein Sequence Analysis (Combet, 2000).

RESULTS

HIV-1 Vif co-immunoprecipitates with APO3G

The HIV-1 Vif protein from Immunodiagnostics was determined to be biologically functional by co-immunoprecipitating it with its known binding partner, APO3G. HIV-1 Vif bound to immobilized APO3G expressed in either *E. coli* or baculovirus, and APO3G bound to immobilized HIV-1 Vif (Figure 3.1A). These results suggest that the HIV-1 Vif protein obtained was in a biologically relevant form, thus folded and functional.

HIV-1 Vif forms higher order oligomers *in vitro*

To isolate oligomeric forms of HIV-1 Vif, chemical cross-linking experiments were performed. Higher order oligomers of HIV-1 Vif were observed *in vitro* using the

hetero-bifunctional zero-length cross-linker, EDC. EDC first reacts with the carboxylic group of an aspartic or glutamic acid, forming an amine-reactive *O*-acylisourea intermediate. This intermediate is stabilized by adding sulfo-NHS to create an amine-active ester with an extended half-life. Extending the amine-active ester's half-life facilitates its interaction with the amine group of lysine, thus forming a peptide bond. Peptide bond formation results in loss of a water molecule, decreasing the mass of each cross-linked peptide by 18.011 mass units (Schulz, 2004; Kalkhof, 2005). Cross-links are formed between acidic residues and lysines with distances $\leq$ 5 Å, based on the length of the EDC molecule itself (Kalkhof, 2005) (Figure 3.1).

Analysis of cross-linked HIV-1 Vif protein by denaturing PAGE showed three oligomeric forms: cross-linked monomer (24 kDa), cross-linked dimer (48 kDa), and cross-linked trimer (72 kDa) (Figure 3.2B, lane 3). The presence of oligomers of HIV-1 Vif was confirmed by western blotting, which showed not only the monomer, dimer, and trimer forms, but also a cross-linked tetramer (Figure 3.2C, lane 2). The oligomers on the Coomassie-stained gel were quantified by densitometric analysis, which suggested that approximately 46% of the reaction product is cross-linked monomer, 39% is cross-linked dimer, and 15% is cross-linked trimer (Figure 3.2B, lane 3). A noncross-linked sample of HIV-1 Vif, run as a control, showed a band consistent with a HIV-1 Vif monomer (Figure 3.2B, lane 2). The western blot of the noncross-linked monomer (Figure 3.2C, lane 1) shows a small amount of HIV-1 Vif dimer, which is sometimes observed for oligomeric proteins under reducing and denaturing conditions (Figure 3.2C, lane 1). If the HIV-1 Vif dimer in the noncross-linked monomer sample is due to disulfide bonding,

Figure 3.1

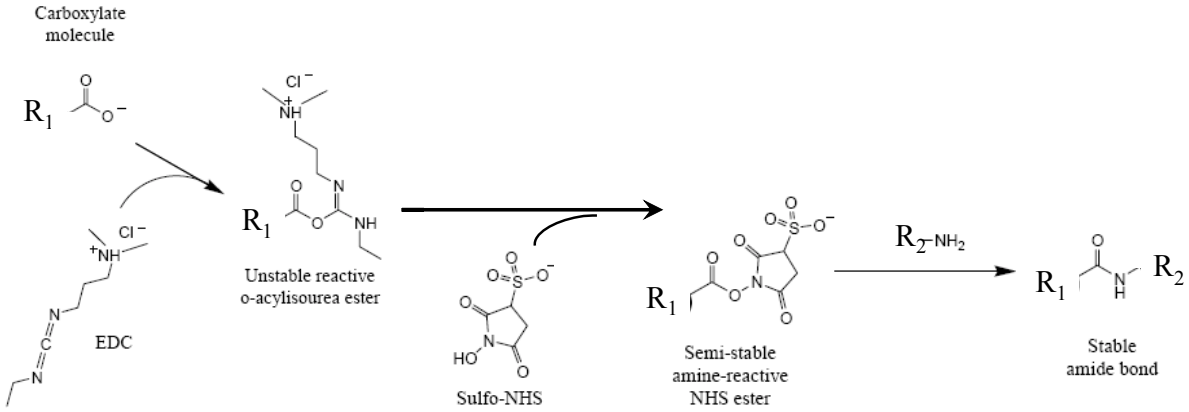
Carboxylate molecule
EDC
Unstable reactive o-acylisourea ester
Sulfo-NHS
Semi-stable amine-reactive NHS ester
Stable amide bond

Figure 3.1: Cross-linking reaction using EDC (1-ethyl-3-[3-dimethylaminopropyl] carbodiamide) (modified from Pierce website; www.piercenet.com)

Figure 3.2

A.

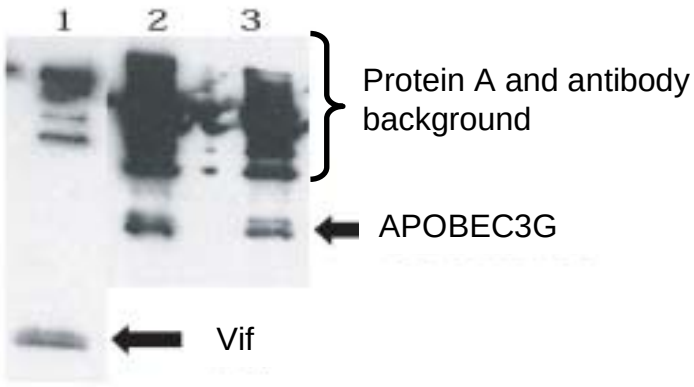

B.

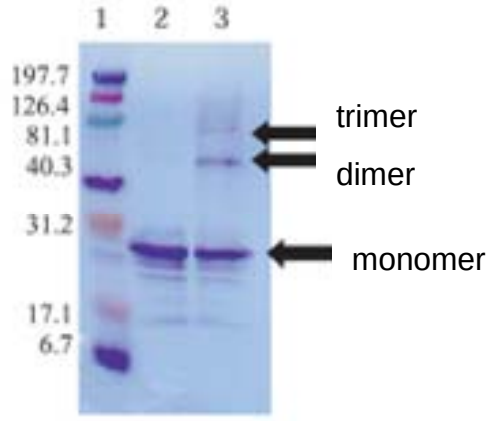

C.

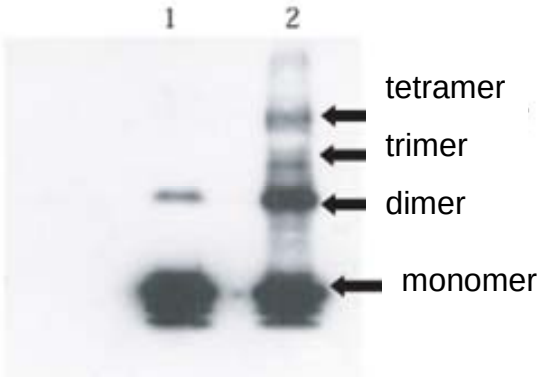

Figure 3.2: HIV-1 Vif is functional and can form higher order oligomers. (A) HIV-1 Vif co-immunoprecipitates with APO3G. Vif (APO3G) was immobilized on Protein A affinity beads, incubated overnight with APO3G (Vif), and eluted via boiling. *Lane 1:* Immobilized APO3G interacts with HIV-1 Vif. *Lane 2:* Immobilized HIV-1 Vif interacts with baculovirus-expressed APO3G. *Lane 3:* Immobilized HIV-1 Vif interacts with *E. coli*-expressed APO3G. The higher molecular weight bands are the result of heavy chains, light chains, and Protein A background routinely observed in immunoprecipitation experiments. **(B)** SDS PAGE analysis of HIV-1 Vif cross-links. *Lane 1:* Molecular weight markers (kDa). *Lane 2*: Noncross-linked HIV-1 Vif control predominantly as a monomer (23 kDa). *Lane 3:* EDC cross-linked HIV-1 Vif, with evidence for a dimer (46 kDa) and trimer (69 kDa). **(C)** Western blot of HIV-1 Vif cross-links. *Lane 1:* A noncross-linked HIV-1 Vif control that is predominantly monomeric, with a small amount of dimer. The presence of dimer is likely due to unreduced the hydrophobic effect. *Lane 2:* EDC cross-linked HIV-1 Vif, with evidence for dimer, trimer, and tetramer forms.

The band distances in the Coomassie-stained gel (B) appear smaller than those in the western blot (C), however the distances are similar suggesting the bands in the SDS PAGE are the same as in the western blot. I measured the total lane distance from well to dye front and labeled that Z, then I measured the respective distances from the dye front to each oligomeric state and labeled them A (monomer), B (dimer), and C (trimer). Next I calculated the ratio R_f, which is A/Z (monomer), B/Z (dimer), and C/Z (trimer), in both

the SDS PAGE and western blot. The $R_{f,\ monomer}$ is 0.73 for SDS PAGE and 0.72 for the western blot, the $R_{f,\ dimer}$ is 0.65 versus 0.69, and the $R_{f,\ trimer}$ is 0.42 versus 0.44.

treatment with 2-mercaptoethanol or iodacetamide should reduce the band, thus shifting the dimer to monomer. The HIV-1 Vif noncross-linked sample was treated with 50 mM and 100 mM 2-mercaptoethanol as well as 55 mM iodacetamide (Grabarek, 1990) and the HIV-1 Vif dimer band remained. Therefore, this residual HIV-1 Vif dimer is likely not due to disulfide bonding but to other effects such as the hydrophobic effect (Tsai, 1997).

Before analyzing the cross-linked monomer and oligomers to gain insight into the topology of HIV-1 Vif and to map its oligomerization domains, I examined HIV-1 Vif for its predicted regions of intrinsic disorder and secondary structure. Understanding the regions of disorder in HIV-1 Vif would give a better understanding of the protein may be folded.

Structure Predictions

HIV-1 Vif was examined for regions of intrinsic disorder by submitting the HXB2 HIV-1 Vif sequence to PONDR®, Predictors of Natural Disordered Regions, which uses a sequence-based algorithm with four predictor algorithms or routines to predict regions of disorder. PONDR® predictors are feedforward neural networks of 21 amino acids per window and have been trained on a specific set of ordered and disordered sequences. The information obtained is smoothed over a 9-amino acid sliding window, and residues above 0.5 are considered disordered (Romero, 2001; Vucetic, 2005). Of the four predictor routines used by PONDR®, only one, VL-XT, predicted that the N-terminus of HIV-1 Vif is disordered, and two, VL-XT and XL1-XT, predicted that two short regions

(possibly extended loops) between residues 50-63 and 87-100 are disordered. However, all four predictors unanimously predicted that the C-terminus is disordered (Figure 3.3). These predictions suggest that the C-terminus of HIV-1 Vif is intrinsically disordered.

Since intrinsically disordered proteins often do not have defined secondary structure (Figure 3.7A) (Combet, 2000), the secondary structure of HIV-1 Vif was predicted using the Pole BioInformatique Lyonnais Network Protein Sequence Analysis (NPS) secondary-structure consensus prediction program. The majority of HIV-1 Vif's secondary structure is predicted to be random coil, but its predicted secondary structure also included an ordered N-terminus consisting of mostly beta-sheets and one alpha helix as well as a disordered C-terminus consisting of mostly alpha helices.

Identification of Noncross-linked Linear Peptides

As mentioned above, analysis of the cross-linked monomer and oligomers will give insight into the topology of HIV-1 and help to map its oligomerization domains. To that end, the regions of HIV-1 Vif that were protected from protease digestion upon folding and oligomerization were elucidated by detailed examination of the linear peptides (Strochlic, 2001). Because the cross-linking reaction is not 100% efficient, some peptides may be observed with diminished intensity in regions that are important for oligomerization. Noncross-linked HIV-1 Vif, cross-linked monomer, cross-linked dimer, and cross-linked trimer were excised from gels, trypsin digested separately in ^{16}O and ^{18}O water, and analyzed by reflectron MALDI-TOF MS, LC-ion trap-MS, and LC-QTof-MS. Gel bands were digested in ^{18}O water to label peptides and cross-links for

Figure 3.3

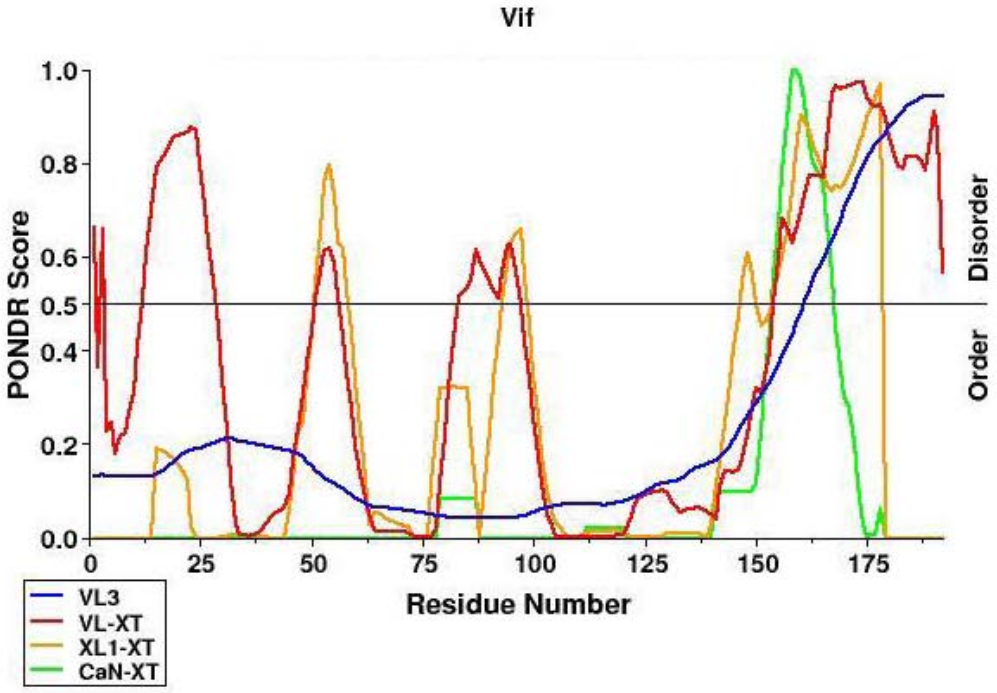
Vif
PONDR Score
1.0
0.8
0.6
0.5
0.4
0.2
0.0
Disorder
Order
0
25
50
75
100
125
150
175
Residue Number
VL3
VL-XT
XL1-XT
CaN-XT

Figure 3.3: Predicted regions of intrinsic disorder for HIV-1 Vif. Regions of disorder were predicted using PONDR®, Predictors of Natural Disordered Regions (Romero, 2001; Vucetic, 2005). Each color indicates a separate predictor algorithm: blue, VL3; red, VL-XT; yellow, XL1-XT; and green, CaN-XT.

identification. During trypsin cleavage, two oxygen atoms are added to the C-terminus of each peptide, so that peptides digested in ^{18}O water will be 4 mass units larger than peptides digested in ^{16}O water and cross-links will be 8 mass units larger than their unlabelled counterparts. For example, Figure 3.4 shows a region of the MALDI-TOF spectrum for a peptide where the first peak (with mass-to-charge [m/z] of 728.351]) represents the unlabelled peptide (^{16}O), and the fifth peak is 4 Da higher ([m/z 732.367]) represents the labeled peptide (^{18}O). The ion at m/z 728.351 corresponds to a theoretical mass of 728.351 for the peptide 37-41. All experimental peptides identified via MALDI-TOF were analyzed as above, and their parts per million (ppm) and mass difference from the theoretical mass are shown in Table 3.1.

All three mass spectrometry techniques mentioned above and both trypsin and chymotrypsin digests were used to identify peptides that provide 100% sequence coverage for the noncross-linked sample, 99% coverage for the cross-linked monomer, 95% for the dimer, and 83% for the trimer (Figure 3.6 and 3.7). The difference in coverage (particularly in the C-terminus) between monomer, dimer, and trimer suggests that the dimer and trimer samples have more protected areas, indicating conformational change due to oligomerization. However, just because a particular peptide is not observed does not mean it no longer exists. For example, the loss of coverage in the high molecular weight samples could correspond to modification of lysines by EDC, thus preventing trypsin cleavage.

Analysis of the MALDI-TOF MS, LC-ion trap-MS, and LC-QTof-MS data shows complete peptide sequence coverage for all samples analyzed from residues 1 to 91. The

Figure 3.4

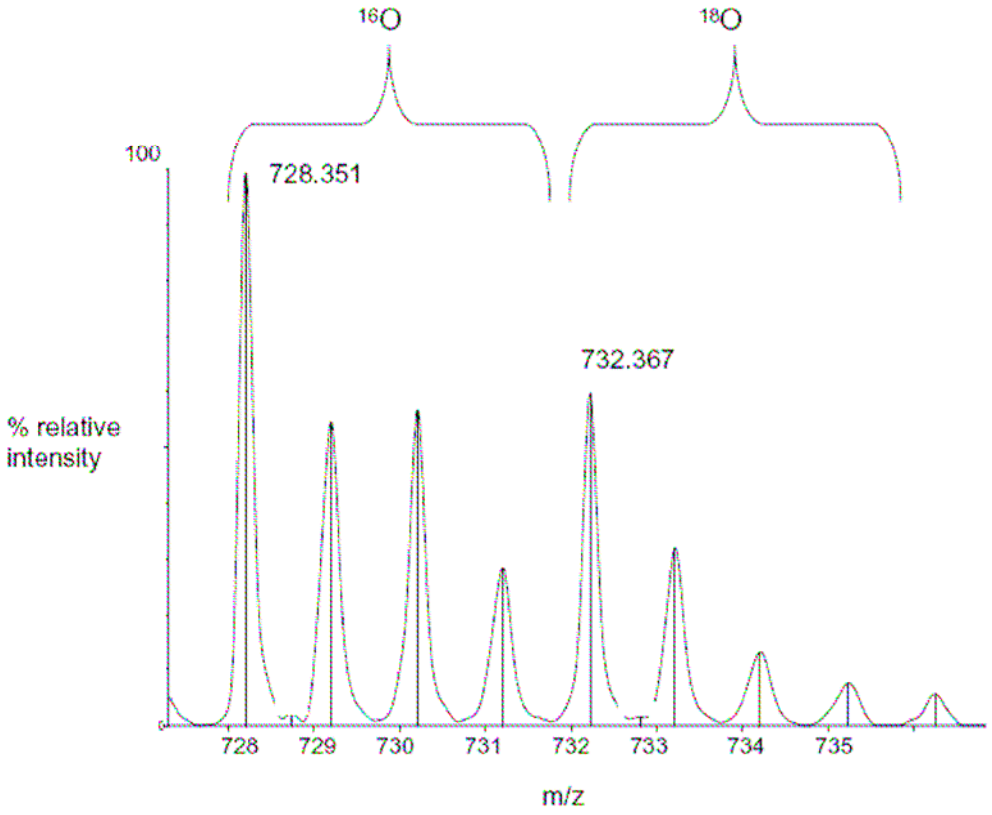
16O
18O
100
728.351
732.367
% relative intensity
0
728
729
730
731
732
733
734
735
m/z

Figure 3.4: Analysis of an HIV-1 Vif peptide using reflectron MALDI-TOF-MS. The mass spectrometry data presented here represent an example of a peptide spectrum. The mass-to-charge ratio (m/z) shown for a singly charged molecular ion, MH+, represents the molecular weight of a peptide. This spectrum shows an unlabelled peptide at m/z 728.351 and its labeled (^{18}O) counterpart (4Da larger) at m/z 732.367. This peptide corresponds to residues 37-41 in HIV-1 Vif.

Table 3.1

Peptide	Theoretical MW	Noncross-linked	ppm	Mass difference	Monomer	ppm	Mass difference	Dimer	ppm	Mass difference	Trimer	ppm	Mass difference
1-15	2021.968	2021.919	24.2	0.049	2021.893	37.1	0.075	2021.925	21.3	0.043	2021.893	37.1	0.075
16-22	1006.561	1006.528	32.8	0.033				1006.507	53.7	0.054	1006.485	75.5	0.076
23-26	446.297	446.062	526.9	0.235	446.018	625.6	0.279	446.048	558.3	0.249	446.033	591.9	0.264
23-36	1612.874	1612.980	65.8	0.106	1612.872	1.2	0.002	1612.870	2.5	0.004	1612.924	31.0	0.050
27-41	1910.923	1910.976	27.7	0.053									
35-41	955.490	955.510	20.9	0.020	955.447	45.0	0.043	955.489	1.0	0.001	955.447	45.0	0.043
37-41	728.351	728.351	0.0	0.000	728.351	0.0	0.000	728.301	68.7	0.050	728.351	0.0	0.00
42-50	1159.539	1159.603	55.2	0.064	1159.509	25.9	0.030	1159.509	25.9	0.030	1159.532	6.0	0.007
42-63	2534.265	2534.310	17.8	0.045	2534.352	34.3	0.087	2534.345	31.6	0.080	2534.275	3.9	0.010
51-63	1393.743	1393.788	32.3	0.045	1393.710	23.7	0.033	1393.736	5.0	0.007	1393.710	23.7	0.033
64-77	1645.870	1645.875	3.0	0.005	1645.819	31.0	0.051	1645.848	13.4	0.022	1645.764	64.4	0.106
78-90	1582.776	1582.816	25.3	0.040	1582.733	27.2	0.043	1582.788	7.6	0.012	1582.733	27.2	0.043
78-91	1710.871	1710.884	7.6	0.013	1710.884	7.6	0.013				1710.969	57.3	0.098
123-132	1062.642	1062.667	23.5	0.025	1062.600	39.5	0.042	1062.645	2.8	0.003	1062.600	39.5	0.042
174-184	1379.765	1379.679	62.4	0.086	1379.628	99.3	0.137	1379.654	80.5	0.111	1379.628	99.3	0.137
185-192	840.342	840.476	159.5	0.134	840.376	40.5	0.034	840.436	111.9	0.094	840.416	88.1	0.074

Table 3.1: Peptides Identified by MALDI-TOF MS. A noncross-linked sample and cross-linked monomer, dimer, and trimer samples were excised from an SDS polyacrylamide gel, in-gel trypsin digested, and peptides were identified by MALDI-TOF MS. Experimental molecular weights for identified peptides are listed with their ppm and mass difference from the theoretical molecular weight of the peptide. The values in this table represent three experiments.

monomer, dimer, and trimer samples have an area of protection around residues 92-94 (KKR), which may be due to a conformational change or possibly due to trypsin cleavage at each site, creating single-residue peptides. The trimer sample, but not the monomer or dimer sample, has an area of protection from residues 107-121 (IHLYYFDCFDSAIR), suggesting that these residues may be involved in trimerization. This region in the trimer is also well conserved, contains several aromatic residues, and includes one of the 2 cysteines in the protein, suggesting that this trimer region is a functional domain. From residues 122 to 147, there is almost complete peptide coverage in all samples analyzed. Peptide coverage is reduced in the C-terminal domain of the dimer and trimer. In other words, "protection" is increased in this region, suggesting that it is involved in HIV-1 Vif oligomerization, consistent with a previous report that the oligomerization domain is from residues 151-171 (Yang, 2001; Yang, 2003).

For example, the trimer sample shows an area of protection in residues 148-157 (LALAALITPK), and the dimer and trimer samples show a region of protection in 169-173 (LTEDR). In addition, the sample digested with chymotrypsin contains a peptide in the noncross-linked and cross-linked monomers, corresponding to residues 151-174. This peptide is lost in the dimer and trimer, supporting the importance of this region for oligomerization. The different areas of protection observed between the dimer and trimer samples suggest changes in the details of interactions as the protein's oligomeric state transitions from dimer to trimer (Figure 3.6 and Table 3.2). Finally, the "protection" observed in the C-terminus of the dimer and trimer sample are consistent with these regions becoming more ordered upon oligomerization.

Table 3.2

UnX-T	UnX-T-MS	UnX-C	Mono-T	Mono-T-MS	Mono-C	Dimer-T	Dimer-T-MS	Dimer-C	Trimer-T	Trimer-T-MS	Trimer-C
1–15			1–15			1–15			1–15		
				5–19			5–19			*5–19*	
		12–21			12–21						
16–22						16–22			16–22		
23–26			23–26			23–26			23–26		
					22–30			22–30			22–30
	23–34										
23–36			23–36			23–36			23–36		
27–41											
		30–39									
		31–39			31–39						
					31–40			31–40			
35–41			35–41			35–41			35–41		
37–41	*37–41*		37–41	*37–41*		37–41	*37–41*		37–41	**37–41**	
		39–44			39–44			39–44			39–44
42–50	*42–50*		42–50	*42–50*		42–50	*42–50*		42–50		
42–63			42–63			42–63			42–63		
51–63	**51–63**		51–63	**51–63**		51–63	**51–63**		51–63	**51–63**	
64–77	64–77		64–77	64–77		64–77	64–77		64–77	64–77	
		70–79			70–79			70–79			70–79
		70–89									
		71–79			71–79						71–79
78–90	**78–90**		78–90	**78–90**		78–90	**78–90**		78–90	78–90	
78–91	**78–91**		78–91						78–91		
	78–92										
	93–122										
	94–121			94–121			94–121				
	94–122			94–122			94–122				
								95–106			95–106
					112–115						
	122–132			**122–132**						122–132	
123–132	**123–132**		123–132	**123–132**		123–132	**123–132**		123–132	**123–132**	
								126–135			126–135
	133–157										
		136–147			136–147			136–147			136–147
	142–157			**142–157**			**142–157**				
		148–174									
		151–174			151–174						
	158–168			*158–168*			*158–168*			**158–168**	
	159–168			*159–168*			*159–168*			**159–168**	
	159–173										
	161–168									161–168	
	161–173										
174–184	*174–184*		174–184	*174–184*		174–184			174–184		
					175–192			175–192			
	182–192										
185–192			185–192			185–192			185–192		

Table 3.2: Peptide Analysis of HIV-1 Vif. Peptides were identified by mass spectrometry (MS) of HIV-1 Vif fragments that were uncross-linked (UnX), cross-linked monomer (Mono), dimer, or trimer and digested with either trypsin (T) or chymotrypsin (C). Identification by LC-QTof-MS is indicated by italics, and identification by both LC-QTof-MS and LC-ion trap-MS is indicated by bold.

Identification of Cross-linked Peptides

In addition to the linear peptides, cross-linked peptides were observed by reflectron MALDI-TOF MS labeled with heavy water (^{18}O). These cross-linked peptides were identified by the presence of peaks not seen in the noncross-linked sample and a +8 Da mass shift due to the incorporation of four ^{18}Os in the two cross-linked peptides. For example, a region of the MALDI-TOF spectrum from an intermolecular cross-link seen only in the dimer and trimer (Figure 3.5) shows an ion (m/z 3068.305) in the trimer sample for the unlabelled (^{16}O) cross-link, and 8 mass units higher an ion (m/z 3076.720) is seen for the labeled (^{18}O) cross-link. For this high molecular-weight range, the m/z ion at 3068.305 is well correlated, to within less than half a Dalton, with a theoretical m/z ion of 3068.710 for the cross-linked peptides residues 51-63 linked to residues 159-173. All experimental cross-links identified via MALDI-TOF MS, with their parts per million and mass difference from the theoretical mass, are shown in Table 3.3.

In all cross-linked samples but not in the noncross-linked control, I identified 13 intramolecular cross-links (Table 3.4), of which two map to the same residue, thus appearing only once in Figure 3.7B (E45 to K92). This core of intramolecular cross-links seen in all 3 oligomeric forms are between distinct and distant residues separated in 2-dimensional sequence, indicating that HIV-1 Vif is compactly folded in 3-dimensional space. In addition, one cross-linked peptide, residues 23-34 linked to residues 159-172, is specific to the monomer sample, suggesting a possible conformational change upon oligomerization (Table 3.4 and Figure 3.7B).

Figure 3.5

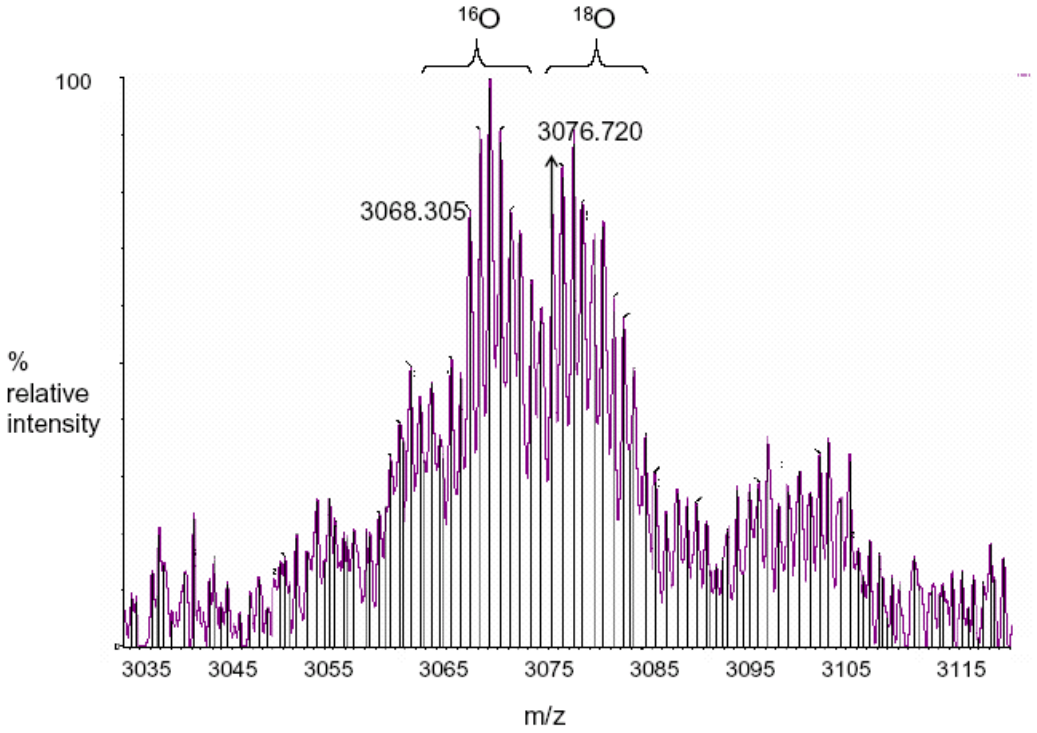
16O
18O
100
3076.720
3068.305
% relative intensity
3035
3045
3055
3065
3075
3085
3095
3105
3115
m/z

Figure 3.5: Analysis of an HIV-1 Vif Cross-link Using Reflectron MALDI-TOF-MS. These mass spectrometry data represent a sample spectrum of a cross-linked HIV-1 Vif peptide. The mass-to-charge ratio (m/z) shown for a singly charged molecular ion, MH+, represents the molecular weight of a peptide. This spectrum shows an unlabelled intermolecular cross-linked peptide at m/z 3068.305 and its labeled (^{18}O) counterpart, 8Da larger, at m/z 3076.720. This region corresponds to a cross-link between peptides residues 51-63 and residues 159-173 and is only seen in the dimer and trimer. The beginning of the +8 Da ion series is indicated by an arrow.

Table 3.3

Cross-link	Theoretical	Monomer	ppm	Mass difference	Dimer	ppm	Mass difference	Trimer	ppm	Mass difference
23-34; 159-173	3076.698	3076.880	59.2	0.182						
1-4; 42-50	1705.761				1705.909	86.8	0.148	1705.906	85.0	0.145
1-15; 42-50	3162.490	3162.110	120.2	0.380						
1-4; 64-77	2192.092	2192.154	28.3	0.062	2192.283	87.1	0.191	2192.316	102.2	0.224
1-4; 23-36	2175.091	2175.003	40.5	0.088	2175.081	4.6	0.010	2175.016	34.5	0.075
1-4; 133-141	1594.661	1594.762	63.4	0.101	1594.776	72.1	0.115	1594.762	63.4	0.101
1-4; 174-181	1575.806	1575.724	52.1	0.082	1575.799	4.4	0.007	1575.724	52.1	0.082
5-17; 23-34	3161.596	3161.412	58.2	0.184	3161.526	22.1	0.070	3161.606	3.2	0.010
20-26; 42-50	2002.041	2002.014	13.5	0.027	2002.970	464.0	0.929	2002.137	48.0	0.096
23-34; 78-91	3093.584	3093.779	63.0	0.195	3093.335	80.5	0.249	3093.387	63.7	0.197
37-50; 91-93	2281.164	2281.060	45.6	0.104	2281.093	31.1	0.071	2281.093	31.1	0.071
37-50; 92-93	2153.069	2153.150	37.6	0.081	2153.018	23.7	0.051	2153.241	79.9	0.172
78-90; 91-93	1995.067	1995.030	18.5	0.037	1995.112	22.6	0.045	1995.112	22.6	0.045
169-181; 180-192	3060.529	3060.326	66.3	0.203	3060.333	64.1	0.196	3060.565	11.8	0.036
27-36; 133-141	2231.011				2231.285	122.8	0.274	2231.876	387.7	0.865
42-50; 174-179	1940.963				1940.902	31.4	0.061	1940.871	47.4	0.092
51-63; 159-173	3068.710				3068.926	70.4	0.216	3068.305	132.0	0.405
92-93; 169-181	1928.082				1927.959	63.8	0.123	1928.836	391.1	0.754
5-17; 158-168	2967.642							2967.777	45.5	0.135
27-36; 185-192	2038.908							2038.883	12.3	0.025
158-168; 169-173	1822.080							1822.058	12.1	0.022
158-168; 182-192	2395.278							2395.438	66.8	0.160
159-173; 182-192	2881.485							2881.978	171.1	0.493
159-179; 185-192	3312.727							3312.766	11.8	0.039
169-173; 180-184	1212.644							1212.746	84.2	0.102

Table 3.3: Cross-links Identified by MALDI-TOF MS. A noncross-linked sample and cross-linked monomer, dimer, and trimer samples were excised from an SDS polyacrylamide gel, in-gel trypsin digested, and analyzed by MALDI-TOF MS to identify cross-links. Cross-linked peptides were identified, as shown, by their experimental molecular weight and mass difference from their theoretical molecular weight, in ppm. Values are the best representatives of three experiments.

Intermolecular cross-links were observed in the cross-linked dimer and trimer samples (Table 3.4 and Figure 3.7C, D). These intermolecular cross-links were identified by their presence in the dimer and/or trimer sample but not in the noncross-linked or cross-linked monomer samples, and by the presence of a +8 Da mass unit shift. Also identified were 7 cross-links specific to the trimer, and 4 in both the dimer and trimer. The majority of cross-links observed in the cross-linked dimer and trimer mapped to the N- and C-termini of HIV-1 Vif. The trimer also contained a set of cross-links that mapped to the C-terminus of each respective monomer, suggesting not only an N- to C-terminus interaction in the trimer, but also a C- to C-terminus interaction.

Overall, cross-link sequence coverage was observed in 62.5% of the monomer, 69.3% of the dimer, and 69.8% of the trimer. Complete cross-link sequence coverage is not expected since cross-linked fragments are likely in digested dimers and trimers above 4000 Da. Given the current technology, peptides with molecular weights greater than 4000 are difficult to uniquely identify. These differences in levels of coverage between cross-links in the monomer and those in the dimer and trimer suggest a conformational change that allows the C-terminus to become more accessible to cross-linking, implying that the region becomes more ordered upon higher-order oligomerization. The redundancy in intermolecular cross-links indicates that oligomerization occurs in a unique, specific manner that is likely functionally significant and not due to nonspecific aggregation. The identified intramolecular cross-links give insight into the tertiary fold of the HIV-1 Vif protein, whereas the intermolecular cross-links give insight into the quaternary fold of the homo-oligomer (Figure 3.7, Figure 3.8, and Table 3.4).

Table 3.4

Monomer		Dimer		Trimer	
K26, K34	**E171**, D172				
Termini	**E45**	**Termini**	**E45**	**Termini**	E45
Termini	**D61**, E76	**Termini**	**D61**, E76	**Termini**	**D61**, E76
E2	***K26****, K34*	***E2***	***K26****, K34*	***E2***	***K26****, K34*
E54, D61	*K176, K179*	*E54, D61*	*K176, K179*	*E54, D61*	*K176, K179*
E2	**K141**	**E2**	**K141**	**E2**	**K141**
E2	**K176**, K179, K181	**E2**	**K176**, K179, K181	**E2**	**K176**, K179, K181
D14	K26, **K34**	**D14**	K26, **K34**	**D14**	K26, **K34**
K22, K26	**E45**	**K22**, K26	**E45**	**K22**, K26	**E45**
K26, K34	**D78**, E88	**K26**, K34	**D78**, E88	**K26**, K34	**D78**, E88
E45	K91, **K92**	**E45**	K91, **K92**	**E45**	K91, **K92**
E45	**K92**	**E45**	**K92**	**E45**	**K92**
D78, E88	K91, **K92**	**D78**, E88	K91, **K92**	**D78**, E88	K91, **K92**
E171, D172	**K181**	**E171**, D172	**K181**	**E171**, D172	**K181**
		K34	**E134**	**K34**	**E134**
		E45	**K176**, K179	**E45**	**K176**, K179
		D61	**K160**, K168	**D61**	**K160**, K168
		K92	**E171**, D172	**K92**	**E171**, D172
				D14	**K158**, K160, K168
				K34	**Termini**
				K158, K160, K168	**E171**, D172
				K158, K160, K168	**Termini**
				K160, K168, E171, D172	**Termini**
				K160, K168, E171, D172, K176, K179	**Termini**
				E171, D172	**K181**

Table 3.4: Cross-links of HIV-1 Vif. Cross-linked residues were identified by MALDI-TOF-MS and heavy water labeling of trypsin-digested monomeric, dimeric, or trimeric forms of HIV-1 Vif. The cross-linking agent EDC specifically links lysine (K) to either aspartic acid (D) or glutamic acid (E). If more than one lysine or acidic residue is within an identified fragment, all are listed. Linking residues are listed sequentially. Cross-linked residues in bold appear in Figure 3.7. Italics indicate that experimental molecular weights were consistent with theoretical molecular weights of both cross-links.

Figure 3.6A

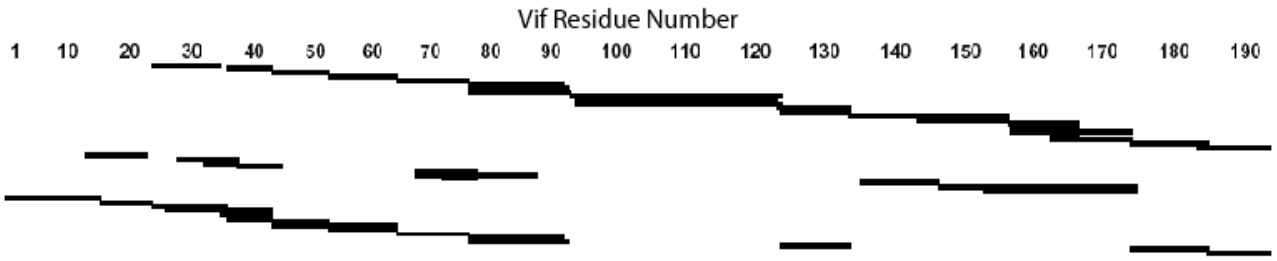

Figure 3.6B

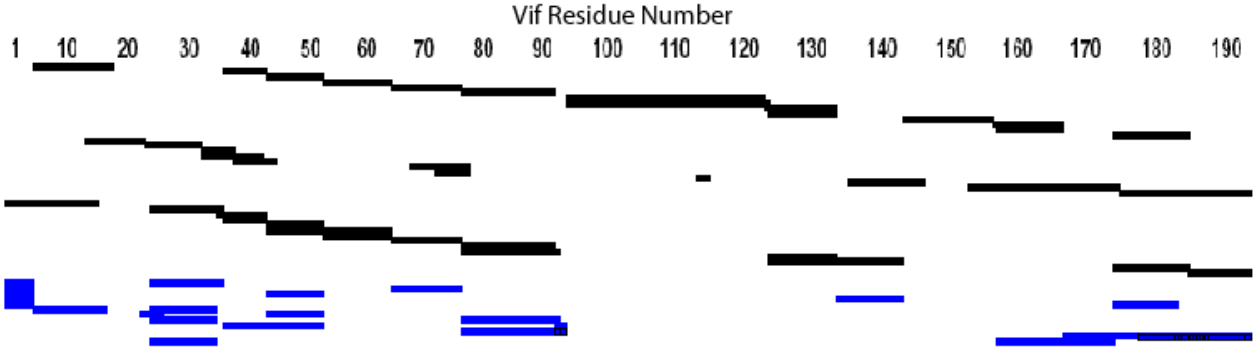

Figure 3.6C

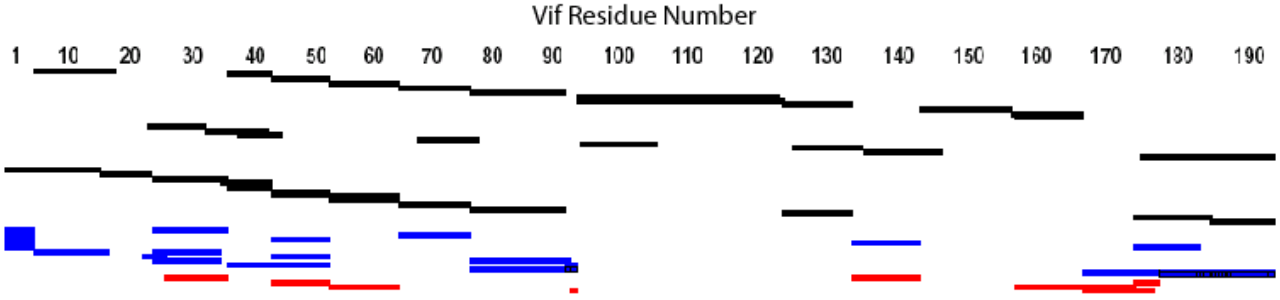

Figure 3.6D

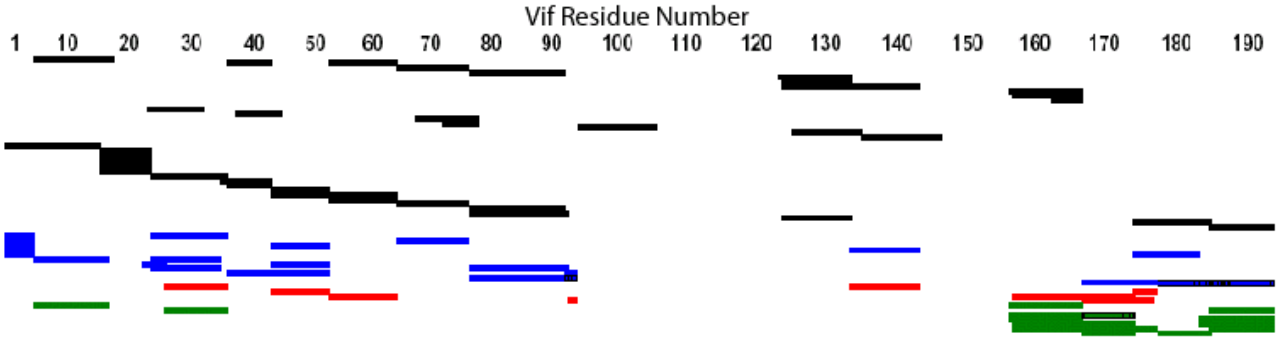
Vif Residue Number
1
10
20
30
40
50
60
70
80
90
100
110
120
130
140
150
160
170
180
190

Figure 3.6: HIV-1 Vif Peptide-Sequence Coverage Map. Coverage maps of peptides created by tryptic and chymotryptic digestion of HIV-1 Vif and identified by MALDI-TOF, LC-ion trap-MS, and LC-QTof-MS, and of cross-linked peptides created by tryptic digestion and identified from MALDI-TOF. Peptides and cross-links were identified by comparing their experimental molecular weights with a list of theoretical molecular weights calculated from ProteinProspector or GPMAW. In addition, identification of peptide or cross-link ions was confirmed by the heavy water label; a corresponding ion 4 Da larger for a peptide and 8 Da larger for a cross-link. **(A)** Noncross-linked. **(B)** Monomers. **(C)** Dimers. **(D)** Trimers. Identified regions are those that are cross-linked to each other and those that are protected. Black: peptides; blue: intramolecular cross-links; red: cross-links in the dimer and trimer; green: trimer cross-links.

Figure 3.7A

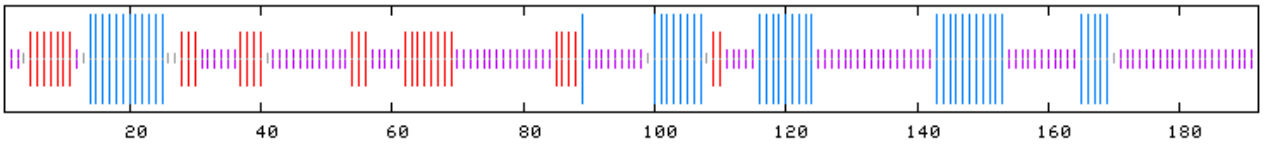

Figure 3.7B

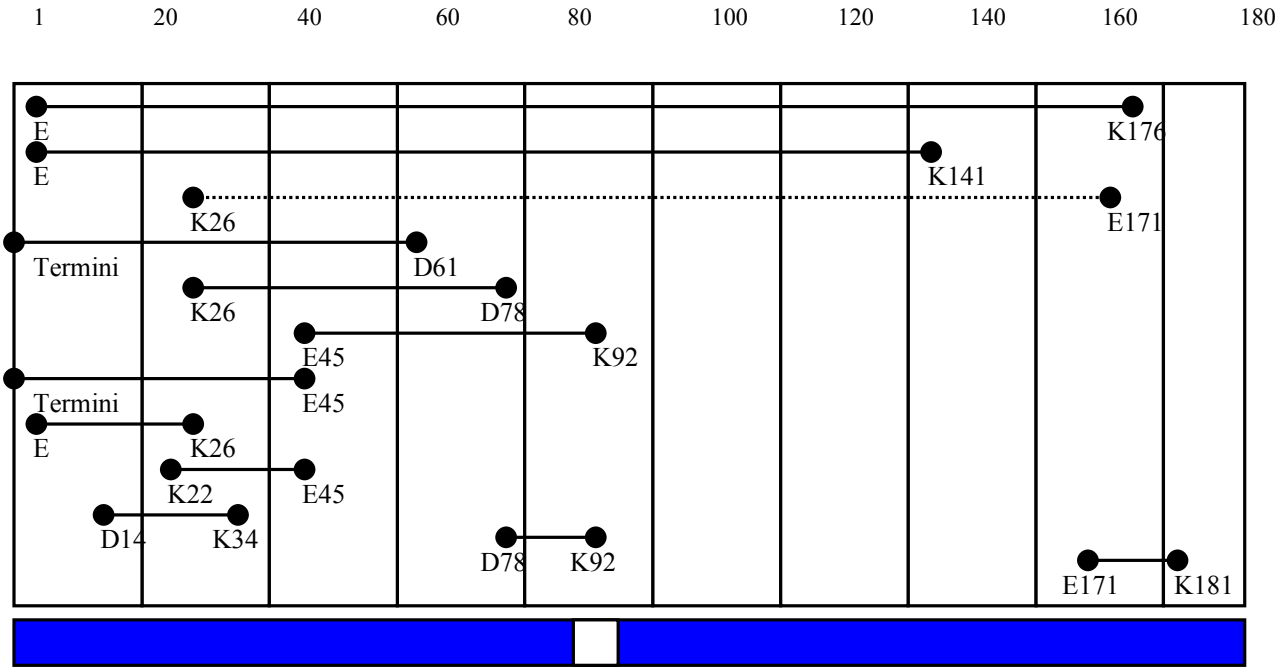

Figure 3.7C

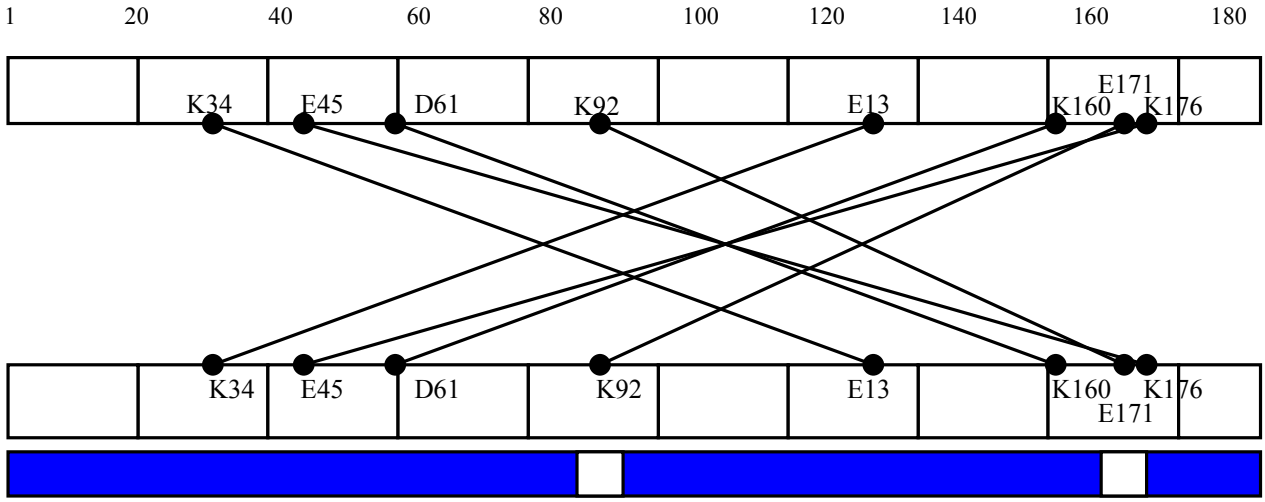
1
20
40
60
80
100
120
140
160
180
K34
E45
D61
K92
E13
E171
K160
K176
K34
E45
D61
K92
E13
K160
K176
E171

Figure 3.7D

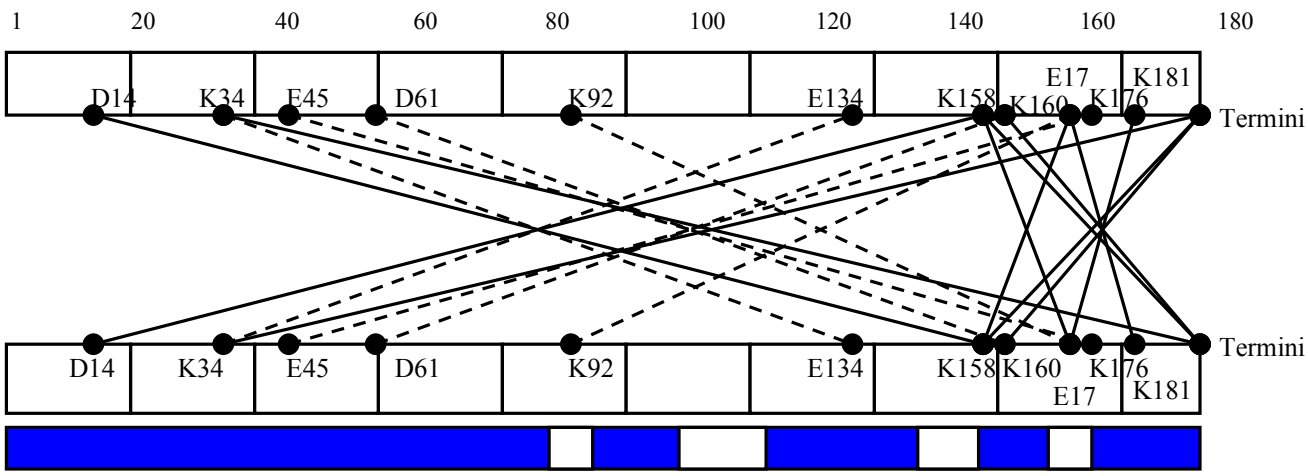
1
20
40
60
80
100
120
140
160
180
D14
K34
E45
D61
K92
E134
K158
E17
K160
K176
K181
Termini
D14
K34
E45
D61
K92
E134
K158
K160
K176
E17
K181
Termini

Figure 3.7: Cross-links of HIV-1 Vif. Schematic diagram of cross-links observed in different oligomeric states of HIV-1 Vif as analyzed by MALDI-TOF and heavy water labeling. **(A)** Consensus secondary structure predicted for HIV-1 Vif (Combet, 2000). Red: beta-sheet. Blue: alpha-helix. Purple: random coil **(B)** Cross-links observed in the monomer sample. **(C)** Cross-links observed in the dimer sample, shown from the N- to C-terminal and from the C- to N-terminal directions. **(D)** Cross-links observed in the trimer, shown from the N- to C-terminal and from the C- to N-terminal directions. *Cross-linking:* Dotted lines indicate that cross-links appeared in both the dimer and trimer samples. The blue bars represent peptide coverage for each oligomeric state.

DISCUSSION

Here, I report novel data on the topology and oligomerization of HIV-1 Vif. These data were obtained using techniques that require small amounts of protein, specifically cross-linking, proteolysis, and state-of-the-art mass spectrometry (LC-QTof-MS, LC-ion trap-MS and MALDI-TOF MS) (Farmer, 1998; Yao, 2001; Back, 2002; Back, 2003; Sinz, 2003).

My analyses of HIV-1 Vif elucidated a variety of its oligomeric states: monomeric, dimeric, and trimeric. Linear peptides identified by my analyses covered the entire protein for both the noncross-linked and cross-linked monomers of HIV-1 Vif. In the dimer and trimer, however, certain regions of the oligomers were not observed, indicating that cross-linking "protected" them from proteolysis. Such protected linear peptides were observed in the dimer and trimer at residues 169-173 and in the trimer alone at 107-121 and 148-157. The difference in protection between the dimer and trimer indicates specific differences in packing between the two oligomers, likely reflecting increased order upon oligomerization.

In addition to linear peptides, 24 specific intra- and intermolecular cross-links were identified in the various oligomeric states (Figure 3.7). These observed cross-links are not due to nonspecific aggregation since they involved only a limited number of lysine and aspartic/glutamic acid residues in HIV-1 Vif. In fact, only 9 of 14 (64%) lysines and 7 of 16 (44%) acidic residues are involved in cross-links, whereas 224 cross-links are possible if all lysines randomly interacted with all possible acids. Since the

"zero-length" cross-linking agent, EDC, only links groups that are within 5 Å (Kalkhof, 2005), the observed cross-links are specific and not due to nonspecific aggregation.

Multiple, essentially redundant cross-links, were also observed between similar regions of the protein particularly in the N-terminus, indicating a specific fold. Thirteen cross-links were observed in the cross-linked monomer, dimer, and trimer, and are therefore intramolecular. Of these 13 intramolecular cross-links, 10 are within the amino-terminal half of HIV-1 Vif, indicating that this region is likely folded into a compact domain. Only one cross-link was observed between residues 171 and 181 in the carboxy-terminal half of HIV-1 Vif, suggesting that this region is less ordered in the monomer. This intramolecular cross-link in the C-terminus may be due to C-terminal disorder, making it mobile and able to interact with nearby residues. Another possibility is that this region has some defined secondary structure, with adjacent helix or sheet residues that can form a cross-link. The HIV-1 Vif region between the two termini has only three cross-links (between residues 2 and 141, 2 and 176, and 26 and 171) and none in the last 16 residues of the protein (Figure 3.7B), indicating minimal interactions between N- and C-terminal regions within the monomer.

The cross-linking data show that one residue can form a heterogeneous mixture of cross-links (Table 3.3, Table 3.4, Figure 3.6, and Figure 3.7). For example, E2 cross-links with residues K26, K34; K141, and/or K176, K179, or K181. Although the N-terminal domain of HIV-1 Vif is likely folded into a compact globular domain, I propose that this domain is unlikely to be a fixed structure, but dynamic and mobile. This motion would allow residues such as E2 to contact multiple amino acids. Another explanation

for one residue being involved in multiple cross-links is the less than 100% efficiency of the cross-linking reaction.

The heterogeneity of cross-links may also be due to heterogeneity in the mass spectrometry analysis. Cross-links with same theoretical molecular weight cannot be distinguished without MS/MS (sequence) information for the cross-links. For example, the theoretical molecular weight for the cross-link between E2 and K26 is identical to that for the cross-link between E54 and K176. Without sequence information, one cannot determine which cross-link is related to the theoretical molecular weight.

Heterogeneity in cross-linking specificity has also been observed by other groups for other proteins. For example, EDC cross-linking data showed intermolecular cross-links between peptides 1-7 in melittin and 1-13 in calmodulin as well as between 1-7 in melittin and 127-148 in calmodulin (Schulz, 2004). Heterogeneity was also observed for a sDST (disulfosuccinimidyl tartrate) cross-linking reaction between annexin A2 and the S100A10 protein, p11. Annexin A2 residues 33-50 showed intermolecular cross-linking to p11 residues 52-58 as well as between annexin A2 residues 109-124 and p11 residues 52-56. In this latter example, analysis of the known crystal structures of both proteins indicates that the observed cross-linking heterogeneity is between noncontiguous residues in the structures (Schulz, 2007).

Another explanation for heterogeneity in cross-linking specificity may be that EDC reacts only with acidic residues in the monomer and not lysines, leaving an EDC molecule on the end of a given residue. Thus, EDC might only interact with acidic residues in the monomer, but in the higher order oligomers it might actually form cross-

links. The high heterogeneity in my cross-liked samples may also be due the large number of cross-links observed, which was more than that observed by most other groups performing similar experiments (Schulz, 2004; Kalkhof, 2005; Schulz, 2007). Furthermore, intramolecular cross-links appear concentration dependent, suggesting that analyzing cross-linking reactions at different concentrations would give insight into heterogeneity and which cross-links are most robust.

Additional specific intermolecular cross-links were observed in the dimer and trimer of HIV-1 Vif. Four cross-links in the dimer were also observed in the trimer, where they link residues in the amino half of the protein, between 34 and 92, with residues in the carboxyl half of the protein, between 134 and 176. An additional 6 cross-links were observed in the trimer. Of these intermolecular cross-links, 2 involve extensive interactions between the two termini of the protein, and the remaining 4 occur within the carboxy quarter of the protein, between residues 158 to 192. This observation suggests that, the carboxy-terminal domain, which is disordered in the structure of the monomer, becomes more ordered upon dimerization and trimerization. To determine which intermolecular cross-links are lost, future experiments could include an HIV-1 Vif construct defective for oligomerization. The results of such experiments would support the presence of intermolecular cross-links and may help identify any nonspecific cross-links. In addition, my cross-linking and peptide mass spectrometry data could be used to validate any homology models or theoretical structures generated.

In fact, some of the intermolecular cross-links I observed could be new intramolecular cross-links that occur upon conformational changes due to higher-order

oligomerization. Although I can't rule out this possibility, I don't think it's likely for all the observed intermolecular cross-links because a dimer and trimer species are present in SDS polyacrylamide gels of cross-linked samples suggesting intermolecular cross-links exist in these species. Even if some of these intermolecular cross-links are intramolecular, they are still important because they give insight into the structure of HIV-1 Vif as well as its possible dynamic motions upon oligomerization. Whether some of the intermolecular cross-links are new intramolecular cross-links could be resolved by more in-depth analyses. Multiple cross-linking agents could be used and sequence information could be obtained for the cross-links to determine whether peptides from two unique monomers were involved in the cross-link.

Proteins that contain regions of intrinsic disorder are characterized when studied in isolation by regions with poorly defined tertiary structure. These proteins become more ordered when they oligomerize with or bind to other biological macromolecules (Dunker, 2005; Romero, 2006). In addition, intrinsically disordered proteins have high net charge and low overall hydrophobicity (Dyson, 2005; Fink, 2005). Interestingly, both characteristics are attributable to HIV-1 Vif. The propensity for intrinsic disorder can be successfully predicted from a protein's sequence by programs such as PONDR® (Romero, 2001; Vucetic, 2005). For example, PONDR VL-XT successfully predicted regions of intrinsic disorder in p53 and Mdm2 (Iakoucheva, 2002). In p53, the middle portion of the protein is ordered, whereas both the N- and C-termini are predominantly disordered, as experimentally confirmed by NMR. "Disorder-to-order transitions" were also observed in p53 upon tetramerization and binding to other proteins. Similarly, the

p53-binding domain in Mdm2 was predicted and confirmed to be ordered, with other regions confirmed to undergo "disorder-to-order transitions" (Iakoucheva, 2002). Interestingly, Mdm2 targets p53 for proteosomal degradation in an analogous fashion to HIV-1 Vif and APO3G.

When the HIV-1 Vif_{HXB2} sequence was submitted to PONDR® (Vucetic, 2005), all four predictor algorithms scored the C-terminus as highly disordered (Figure 3.3). Only one of the four predictors suggests that the N-terminus might also be disordered. This weak prediction for N-terminal disorder is consistent with my mass spectrometry data, with 10 internal cross-links within the N-terminus strongly supporting that it is predominantly ordered, in contrast to the C-terminus, where only one internal cross-link was observed (Figure 3.7B). Thus, the C-terminus of monomeric HIV-1 Vif is likely intrinsically disordered and may become more ordered upon oligomerization. This model is supported by our cross-linking data, since 4 new cross-links (Figure 3.7C) and another 6 cross-links (Figure 3.7D) were obtained in the C-terminus for the dimer and trimer, respectively. A 2-dimensional schematic (Figure 3.8) shows how HIV-1 Vif may homo-oligomerize based on observed areas of protection and cross-links from the mass spectrometry analysis, with the carboxy termini becoming more structured as oligomerization occurs. This schematic, where the twists and turns correspond to areas predicted to be random coils, is consistent with the secondary structure prediction (Figure 3.7A). The ordering of HIV-1 Vif upon oligomerization is consistent with the behavior of other intrinsically disordered proteins that become more ordered upon binding to other biological macromolecules (Dunker, 2005; Romero, 2006).

Figure 3.8A

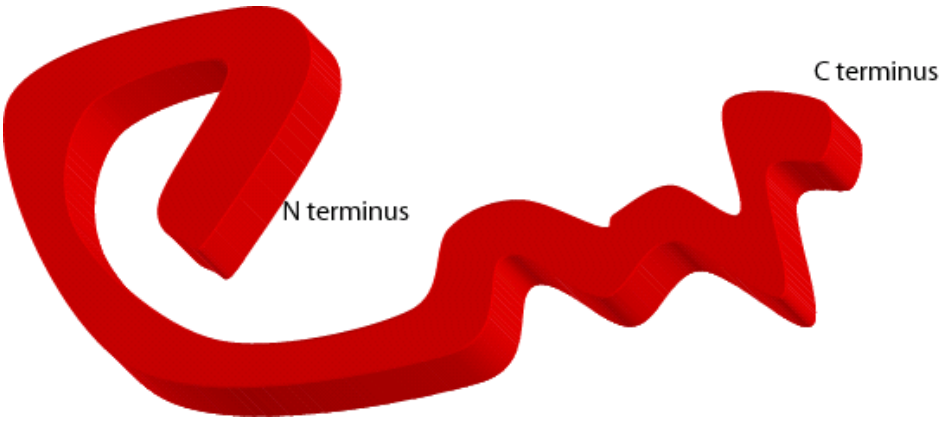

Figure 3.8B

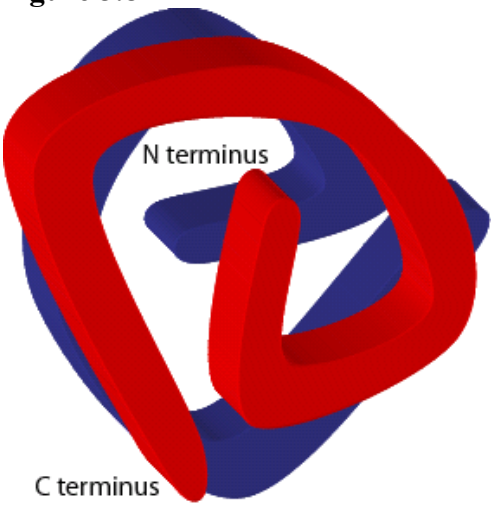

Figure 3.8C

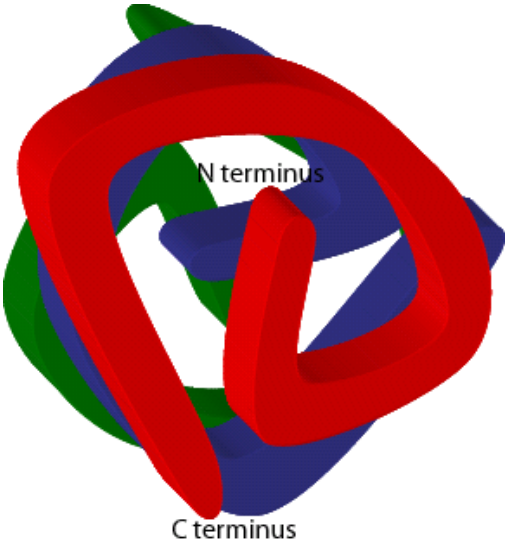

Figure 3.8D

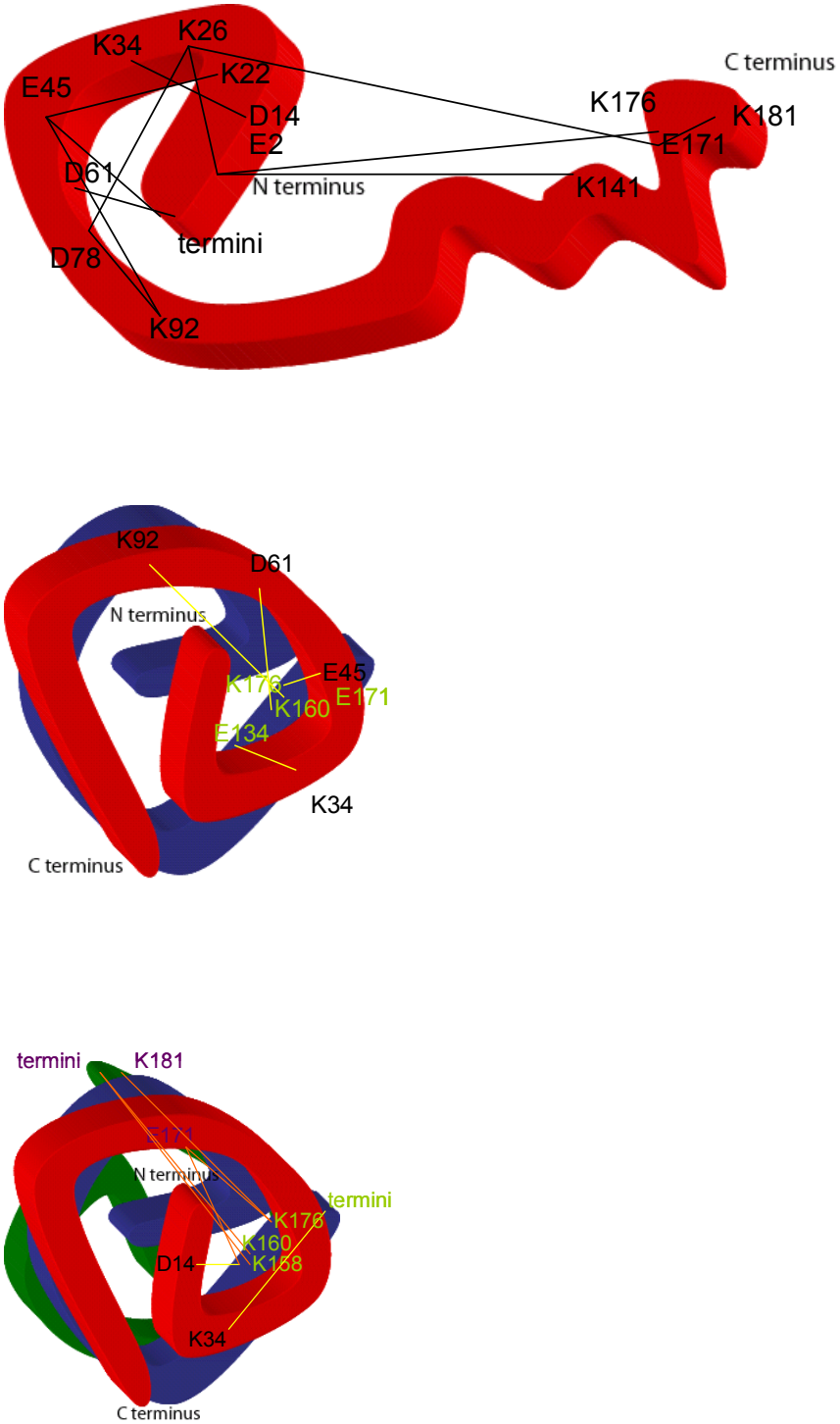
K34
K26
K22
E45
D14
E2
D61
N terminus
termini
D78
K92
C terminus
K176
K181
E171
K141
K92
D61
N terminus
K176
E45
K160
E171
E134
K34
C terminus
termini
K181
E171
N terminus
termini
K176
K160
D14
K158
K34
C terminus

Figure 3.8: Model for Topology and Multimerization of HIV-1 Vif: (A) Intramolecular cross-links suggest that the N-terminus is folded into a compact domain and the C-terminus is less structured. The HIV-1 Vif monomer is globular in shape**. (B** and **C)** Schematic of how the HIV-1 Vif dimer and trimer may fold. The carboxyl terminus becomes more ordered upon oligomerization. **(D)** Intra-molecular cross-links from Figure 3.7A mapped onto the model. **(E)** Inter-molecular cross-links specific to the dimer from Figure 3.7B mapped onto the model. **(F)** Inter-molecular cross-links sfrom Figure 3.7C pecific to the trimer mapped onto the model.

Intrinsic disorder can also be used to address two potential models for protein and substrate binding: an induced fit model, and a structure-capture or "lock and key" model. In the induced fit model, amino acids undergo conformational changes to form specific shapes that allow them to interact with their substrates. In addition, in the induced fit model a protein binds with higher affinity to a reactions transition state than to either its substrates or products. In the structure-capture or "lock and key" model, substrates bind to a fixed protein structure. Therefore, the disorder-to-order transition observed for HIV-1 Vif upon oligomerization suggests that it interacts with its binding partners through neither induced fit nor structure-capture but through induced folding (personal communication Sean Ryder). The C-terminal domain of HIV-1 Vif can be shaped into the respective structure to bind a particular substrate, and multiple conformations can be sampled to allow binding to different substrates.

Thus, in the absence of high-resolution structural data, I have successfully defined the oligomeric states and molecular topology of HIV-1 Vif. These data, obtained from identification of both peptide-protection areas and specific cross-links, complement and expand previous reports on the identification of important HIV-1 Vif residues and regions required for HIV-1 infectivity. For example, HIV-1 infectivity was reduced by more than 85% when 20 HIV-1 Vif residues were mutated individually or in combination, and infectivity was reduced more than 50% by mutating another 9 residues (Simon, 1999). Of these 29 residues, 27 were identified by my mass spectrometry analysis as important for infectivity. Three HIV-1 variants [(Q105A, L106A, I107V), (Y111A, F112A), (C114S)] containing 6 of the 27 sites of mutation (Simon, 1999) overlap directly with a

protected peptide I observed in the trimer (107-121). This protected peptide contains H108, C114 and I120, which are important in Cullin5 binding (Luo, 2005; Mehle, 2006; Xiao, 2006). Thus, protection of the region 107-121 in the trimer suggests that trimerization is essential for HIV-1 Vif activity, perhaps by facilitating Cullin5 binding through a mechanism that displaces one or more HIV-1 Vif monomers.

Among these important residues, the remaining 21 map near two separate cross-links that occur only when a dimer and trimer are formed. Of these 21 residues, 5 are in three variants [(P161A, P162A, L163A), (P164A), (S165A)] and map adjacent to a cross-link of K160 to D61. The remaining 16 residues map to the region contiguous with K34 cross-linking to E134. In this region, 4 variants [(W38A, F39A, Y40A), (H43A, Y44A), (C133S), (S144A, L145A, Q146A)] affect infectivity by greater than 85%, and 3 variants [(M29A, Y30A, I31V), (Y135A, Q136A), (N140A, K141A)] affect infectivity by greater than 50% (Simon, 1999). My cross-linking data for K34 linking to E134 indicate that these essential regions, 29-44 and 133-146, are close together in 3-dimensional space. These data suggest that in the dimer and trimer, these regions come together to form a single molecular surface creating a "hot spot" for biological activity and possibly facilitating Cullin5 binding through C133 of the HCCH zinc-binding motif (Figure 3.9) (Luo, 2005; Mehle, 2006; Xiao, 2006). Such a "hot spot" in HIV-1 Vif is supported by the HIV-1 viral RNA-binding site, residues 1-64, since it overlaps with "hot spot" residues 29-44. Indeed, RNA binding activity was significantly reduced by mutating the HIV-1 Vif residues W11A, Y30A, and Y40A (Zhang, 2000), and Y30A and Y40A are adjacent to the proposed "hotspot" for biological activity. Furthermore, HIV-1 Vif

Figure 3.9

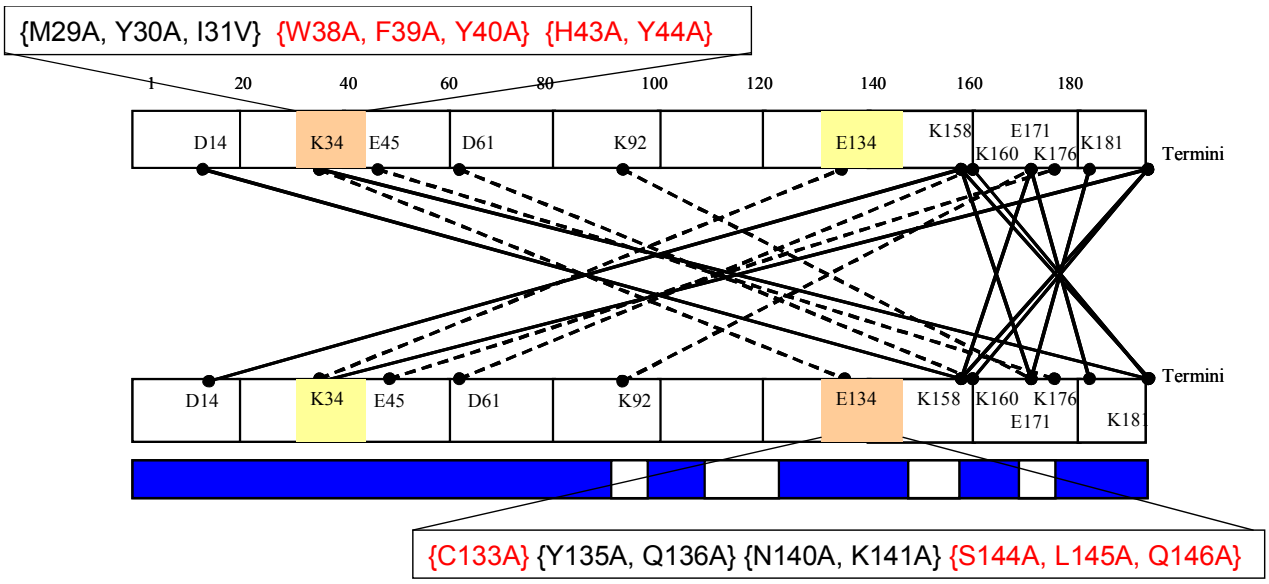
{M29A, Y30A, I31V} {W38A, F39A, Y40A} {H43A, Y44A}
1
20
40
60
80
100
120
140
160
180
D14
K34
E45
D61
K92
E134
K158
E171
K160
K176
K181
Termini
D14
K34
E45
D61
K92
E134
K158
K160
K176
E171
K18
Termini
{C133A} {Y135A, Q136A} {N140A, K141A} {S144A, L145A, Q146A}

Figure 3.9: Residues K34 and E134 form a "hot spot" for biological activity. When residues surrounding K34 and E134 come together in 3-dimensional space, they appear to form a "hot spot" for biological activity, consistent with mutations near these residues decreasing the amount of infectious virions produced (Simon, 1999).

appears to bind cooperatively to viral RNA due to HIV-1 Vif multimers binding to the viral RNA (Henriet, 2005).

Peptide-protection data in the dimer and/or trimer of residues 148-157 and 169-173, and cross-links at residues 158, 160, and 170 are also consistent with the previously identified oligomerization domain, 151-171 (Yang, 2001; Yang, 2003). In fact, 148-157 overlaps with the SOCS box, residues 145-169, where HIV-1 Vif interacts with elongin C in the elongin BC complex. This overlap is similar to the trimer-specific peptide protection of residues 107-121 corresponding with Cullin5 binding. In addition, the oligomerization domain is also adjacent to and overlaps the putative HIV-1 NCp7 (Gag)-binding site, residues 157-179 (Bouyac, 1997). Therefore, not only are our protection and cross-linking data consistent with the previously reported oligomerization domain, but the overlap of this region with the NCp7 (Gag) binding site also suggests that Gag is important for HIV-1 Vif function. A possible molecular mechanism is that the Cullin5-elonginBC complex displaces one (or more) of the HIV-1 Vif monomers, thereby inducing a conformational change that may also facilitate the binding and targeting of APO3G for degradation. Therefore, the structurally important HIV-1 Vif regions identified in my mass spectrometry analysis likely undergo a "disorder-to-order" transition upon oligomerization or binding to other macromolecules such as Cullin5, elongin C, viral RNA, and HIV-1 NCp7 (Gag) (Figure 3.10). Although the sequence of HIV-1 Vif is not highly conserved among other lentiviral Vifs, the majority of cross-links and peptide-protection regions observed in this study occur at residues that are conserved among HIV-1 subtypes. Among those cross-linked residues, E2, D14, K22, K26, and

Figure 3.10

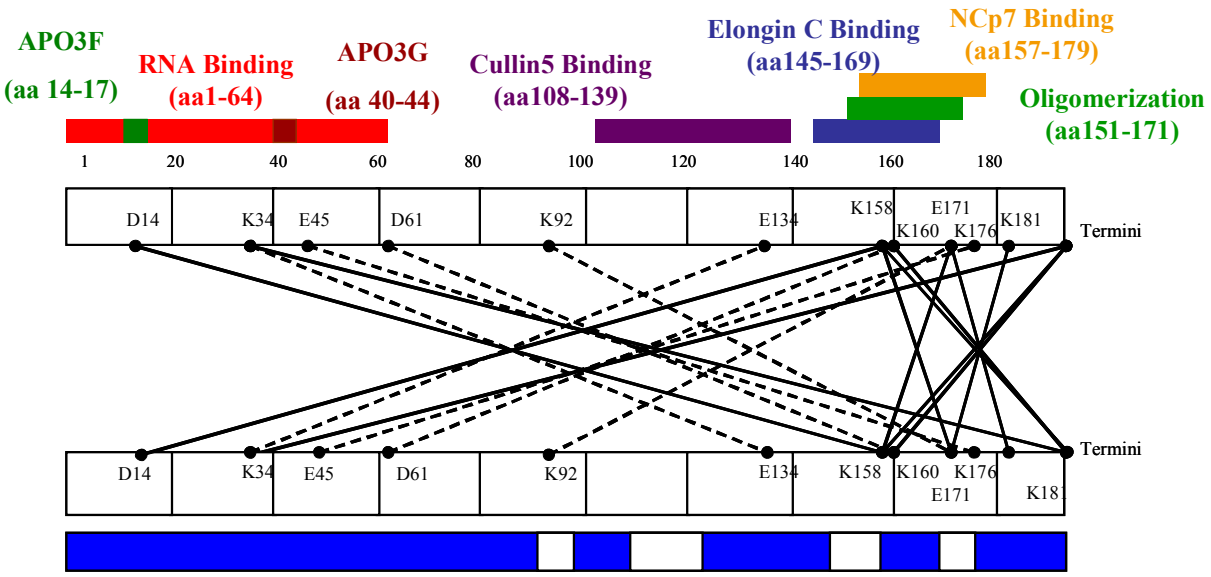
APO3F
(aa 14-17)
RNA Binding
(aa1-64)
APO3G
(aa 40-44)
Cullin5 Binding
(aa108-139)
Elongin C Binding
(aa145-169)
NCp7 Binding
(aa157-179)
Oligomerization
(aa151-171)
1
20
40
60
80
100
120
140
160
180
D14
K34
E45
D61
K92
E134
K158
E171
K160
K176
K181
Termini
D14
K34
E45
D61
K92
E134
K158
K160
K176
E171
K18
Termini

Figure 3.10: HIV-1 Vif binding domains map onto a diagram of observed intermolecular cross-links. The majority of observed cross-links mapped to regions of HIV-1 Vif involved in protein-protein interactions. Cross-links in the N-terminal domain mapped to the RNA-, APO3G-, and APO3F-binding domains, whereas the C-terminal cross-links mapped to the Elongin C-, NCp7-, and oligomerization-binding domains. No cross-links were observed in the Cul5-binding domain, but that region has an area of protection, suggesting that it may be involved in cross-links that are too large to be detected. All these results taken together suggest that the regions observed in cross-linking are structurally and functionally important domains.

E34 in the N-terminus and E134, K141, K158, K160, K171, and K176 in the C-terminus cluster as two regions of high-sequence conservation. Conservation of these residues and cross-linking data are consistent with residues 29-44 and 133-146 being a "hotspot" for HIV-1 Vif's biological activity. As for HIV-1 Vif, PONDR® predicts that the C-termini of HIV-2 and SIV Vif are both disordered. Therefore, these lentiviral Vifs may undergo a similar "disorder-to-order" transition upon oligomerization and binding of other macromolecules, similar to the one proposed for HIV-1 Vif.

This first evidence for HIV-1 Vif's molecular structure supports the following hypothesis: HIV-1 Vif monomers are likely in dynamic equilibrium between various homo-oligomers (dimer and trimer), Cullin5-elonginBC complex, APO3G, and possibly other biological macromolecules such as HIV-1 NCp7 (Gag) and HIV-1 viral RNA. The HIV-1 Vif monomer is likely only transient, with a structurally defined N-terminal region and an intrinsically disordered C-terminus. This disorder may facilitate the dynamic equilibrium of the various complexes. Upon HIV-1 Vif binding to other macromolecules, the structure of its monomeric C-terminus becomes more defined, as observed in the C-terminal region upon formation of HIV-1 Vif dimers and trimers (Figures 3.7 and 3.8). Specifically, this increase in structure, or "disorder-to-order" transition, is likely to be critical to HIV-1 Vif's function in viral infectivity, as regions with specific cross-links and protected peptides correspond to previously identified regions critical to viral infectivity. In addition, this disorder in the HIV-1 Vif C- terminus will likely make it impossible to obtain a full-length high-resolution structure of HIV-1 Vif. However, obtaining structural information may be possible for HIV-1 Vif truncation

mutants or HIV-1 Vif in complex with one of its binding partners. Regardless, the structure and biochemical properties of these complexes need to be determined to better elucidate the specifics of HIV-1 Vif interactions, as disrupting one or more of these interactions critical for HIV-1 Vif function will be involved in future inhibitor design.

Acknowledgements: We thank Jinal Patel (UMass Proteomics Mass Spectrometry Facility) for help with collecting and analyzing the mass spectrometry data; Jennifer Saporita for help with determining the complete density of gel bands; Melissa Grabowski for critically reading the manuscript; Mary Munson, William Kobertz, and C. Robert Matthews for helpful discussions; the NIH AIDS Research and Reference Reagent Program, Division of AIDS, NIAID, NIH and Dr. Opendra Sharma. This work was supported by a grant from the NIH (R21 AI056935 and R21 AI067021) and a UMass CFAR grant (5P3O AI42845).

REFERENCES

Back, J., V. Notenboom, L. de Koning, A. Muijsers, T. Sixma, C. de Koster and L. de Long (2002). "Identification of cross-linked peptides for protein interaction studies using mass spectrometry and 18O labeling." Anal Chem. **74**(17): 4417-22.

Back, J. W., L. d. Jong, A. O. Muijsers and C. G. d. Koster (2003). "Chemical Cross-linking and Mass Spectrometry for Protein Structural Modeling." Journal Molecular Biology **331**: 303-313.

Baraz, L. and M. Kotler (2004). "The Vif protein of human immunodeficiency virus type 1 (HIV-1): enigmas and solutions." Current Medical Chemistry **11**: 221-231.

Bardy, M., B. Gay, S. Pebernard, N. Chazal, M. Courcoul, R. Vigne, E. Decroly and P. Boulanger (2001). "Interaction of human immunodeficiency virus type 1 Vif with Gag and Gag-Pol precursors: co-encapsidation and interference with viral protease-mediated Gag processing." Journal of General Virology **82**: 2719-2733.

Bishop, K. N., R. K. Holmes and M. H. Malim (2006). "Antiviral Potency of APOBEC Proteins Does Not Correlate with Cytidine Deamination." Journal of Virology **80**(17): 8450-8458.

Bouyac, M., M. Courcoul, G. Bertoia, Y. Baudat, D. Gabuzda, D. Blanc, N. Chazal, P. Boulanger, J. Sire, R. Vigne and B. Spire (1997). "Human Immunodeficiency Virus Type 1 Vif Protein Binds to the Pr55Gag Precursor." Journal of Virology **71**(12): 9358-9365.

Cancio, R., S. Spadari and G. Maga (2004). "Vif is an auxiliary factor of the HIV-1 reverse transcriptase and facilitates abasic site bypass." Journal of Biochemistry **383**(3): 475-482.

Combet, C., C. Blanchet, C. Geourjon and G. Deleage (2000). "NPS@: Network Protein Sequence Analysis." TIBS **25**(3): 147-150.

Davidson, W. S. and G. M. Hilliard (2003). "The Spatial Organization of Apolipoprotein A-I on the Edge of Discoidal High Density Lipoprotein Particles." The Journal of Biological Chemistry **278**(29): 27199-27207.

Dunker, A., M. Cortese, P. Romero, L. Iakoucheva and V. Uversky (2005). "Flexible nets. The roles of intrinisic disorder in protein interaction networks." FEBS **272**(20): 5129-48.

Dyson, H. J. and P. E. Wright (2005). "Intrinsically Unstructured Proteins and Their Functions." Nature Reviews Molecular Cell Biology **6**: 197-208.

Eyles, S. J. and I. A. Kaltashov (2004). "Methods to study protein dynamics and folding by mass spectrometry." Methods **34**: 88-99.

Farmer, T. B. and R. M. Caprioli (1998). "Determination of Protein-Protein Interactions by Matrix-assisted Laser Desorption/Ionization Mass Spectrometry." Journal of Mass Spectrometry **33**: 697-704.

Farrow, M. A., M. Somasundaran, C. Zhang, D. Gabuzda, J. L. Sullivan and T. C. Greenough (2005). "Nuclear Localization of HIV Type 1 Vif Isolated from a Long-Term Asymptomatic Individual and Potential Role in Virus Attenuation." AIDS Res Hum Retroviruses **21**(6): 565-574.

Fink, A. L. (2005). "Natively unfolded proteins." Current Opinion in Structural Biology **15**: 35-41.

Gabuzda, D. H., K. Lawrence, E. Langhoff, E. Terwilliger, T. Dorfman, W. A. Haseltine and J. Sodroski (1992). "Role of vif in replication of human immunodeficiency virus type 1 in CD4+ T lymphocytes." Jounal of Virology **66**: 6489-6495.

Grabarek, Z. and J. Gergely (1990). "Zero-length crosslinking procedure with the use of active esters." Analytical Biochemistry **185**: 131-135.

Hassaine, G., I. Agostini, D. Candotti, G. Bessou, M. Caballero, H. Agut, B. Autran, Y. Barthalay, t. F. A. S. Group and R. Vigne (2000). "Characterization of Human Immunodeficiency Virus Type 1 vif Gene in Long-Term Asymptomatic Individuals." Virology **276**: 169-180.

Henriet, S., D. Richer, S. Bernacchi, E. Decroly, R. Vigne, B. Ehresmann, C. Ehresmann, J.-C. Paillart and R. Marquet (2005). "Cooperative and Specific Binding of Vif to the 5' Region of HIV-1 Genomic RNA." Journal of Molecular Biology **354**: 55-72.

Hutoran, M., E. Britan, L. Baraz, I. Blumenzweig, M. Steinitz and M. Kotler (2004). "Abrogation of Vif function by peptide derived from the N-terminal region of the human immunodeficiency virus type 1 (HIV-1) protease." Virology **330**: 261-270.

Iakoucheva, L. M., C. J. Brown, J. D. Lawson, Z. Obradovic and A. K. Dunker (2002). "Intrinsic Disorder in Cell-signaling and Cancer-associated Proteins." Journal of Molecular Biology **323**: 573-584.

Kalkhof, S., C. Ihling, K. Mechtler and A. Sinz (2005). "Chemical Cross-linking and High-Performance Fourier Transform Ion Cyclotron Resonance Mass Spectrometry for Protein Interaction Analysis: Application to a Calmodulin/Target Peptide Complex." Analytical Chemistry **77**(2): 495-503.

Kobayashi, M., A. Takaori-Kondo, Y. Miyauchi, K. Iwai and T. Uchiyama (2005). "Ubiquitination of APOBEC3G by an HIV-1 Vif-Cullin5-ElonginB-ElonginC complex is essential for Vif function." Journal of Biological Chemistry **280**(19): 18573-8.

Lake, J.-a., J. Carr, F. Feng, L. Mundy, C. Burrell and P. Li (2003). "The role of Vif during HIV-1 infection: interaction with novel host cellular factors." Journal of Clinical Virology **26**: 143-152.

Liu, B., P. T. N. Sarkis, K. Luo, Y. Yu and X.-F. Yu (2005). "Regulation of Apobec3F and Human Immunodeficiency Virus Type 1 Vif by Vif-Cul5-ElonB/C E3 Ubiquitin Ligase." Journal of Virology **79**(15): 9579-9587.

Luo, K., Z. Xiao, E. Ehrlich, Y. Yu, B. Liu, S. Zheng and X.-F. Yu (2005). "Primate lentiviral virion infectivity factors are substrate receptors that assemble with cullin 5-E3 ligase through a HCCH motif to suppress APOBEC3G." Proc. Natl. Acad. Sci USA **102**(32): 11444-11449.

Madani, N. and D. Kabat (2000). "Cellular and viral specificities of human immunodeficiency virus type 1 vif protein." Journal of Virology **74**: 5982-5987.

Marin, M., K. M. Rose, S. L. Kozak and D. Kabat (2003). "HIV-1 Vif Protein binds the editing enzyme APOBEC3G and induces its degradation." Nature Medicine **9**(11): 1398-1403.

Mehle, A., J. Goncalves, M. Santa-Marta, M. McPike and D. Gabuzda (2004). "Phosphorylation of a novel SOCS-box regulates assembly of the HIV-1 Vif-Cul5 complex that promotes APOBEC3G degradation." Genes & Development **18**(23): 2861-2866.

Mehle, A., E. R. Thomas, K. S. Rajendran and D. Gabuzda (2006). "A zinc-binding region in Vif binds Cul5 and determines Cullin selection." Journal of Biological Chemistry **281**(25): 17259-65.

Navarro, F. and N. R. Landau (2004). "Recent insights into HIV-1 Vif." Current Opinion in Immunology **16**: 477-482.

Popov, S., M. Rexach, G. Zybarth, N. Reiling, M.-A. Lee, L. Ratner, C. M. Lane, M. S. Moore, G. Blobel and M. Bukrinsky (1998). "Viral protein R regulates nuclear import of the HIV-1 pre-integration complex." The EMBO Journal **17**(4): 909-917.

Romero, P., Z. Obradovic, X. Li, E. C. Garner, C. J. Brown and A. K. Dunker (2001). "Sequence Complexity of Disordered Protein." PROTEINS: Structure, Function, and Genetics **42**: 38-48.

Romero, P. R., S. Zaida, Y. Y. Fang, V. N. Uversky, P. Radivojac, C. J. Oldfield, M. S. Cortese, M. Sickmeier, T. LeGall, Z. Obradovic and A. K. Dunker (2006). "Alternative splicing in concert with protein intrinsic disorder enables increased functional diversity in multicellular organisms." PNAS **103**(22): 8390-8395.

Rose, K. M., M. Marin, S. L. Kozak and D. Kabat (2004). "The viral Infectivity factor (Vif) of HIV-1 unveiled." TRENDS in Molecular Medicine **10**(6): 291-297.

Sakai, H., R. Shibata, J. Sakuragi, S. Sakuragi, M. Kawamura and A. Adachi (1993). "Cell-dependent requirement of human immunodeficiency virus type 1 Vif protein for maturation of virus particles." Journal of Virology **67**(3): 1663-1666.

Sakurai, A., A. Jere, A. Yoshido, T. Yamada, A. Iwamoto, A. Adachi and M. Fujita (2004). "Functional analysis of HIV-1 vif genes derived from Japanese long-term nonprogressors and progressors for AIDS." Microbes and Infection **6**(9): 799-805.

Schulz, D., S. Kalkhouf, A. Schmidt, C. Ihling, C. Stingl, K. Mechtler, O. Zschornig and A. Sinz (2007). "Annexin A2/P11 interaction: New insights into annexin A2 tetramer structure by chemical cross-linking, high resolution mass spectrometry, and computational modeling." Proteins: Structure, Function, Bioinformatics **69**: 254-269.

Schulz, D. M., C. Ihling, G. M. Clore and A. Sinz (2004). "Mapping the Topology and Determination of a Low-Resolution Three Dimensional Structure of the Calmodulin-Melittin Complex by Chemical Cross-linking and High-Resolution FTICRMS: Direct Demonstration of Multiple Binding Modes." Biochemistry **43**: 4703-4715.

Sheehy, A. M., N. C. Gaddis, J. D. Choi and M. H. Malim (2002). "Isolation of a human gene that inhibits HIV-1 infection and is suppressed by the viral Vif protein." Nature **418**(6898): 646-650.

Sheehy, A. M., N. C. Gaddis and M. H. Malim (2003). "The Antiretroviral enzyme APOBEC3G is degraded by the proteasome in response to HIV-1 Vif." Nature Medicine **9**(11): 1404-1407.

Shirakawa, K., A. Takaori-Kondo, M. Kobayashi, M. Tomonaga, T. Izumi, K. Fukunaga, A. Sasada, A. Abudu, Y. Miyauchi, H. Akari, K. Iwai and T. Uchiyama (2006). "Ubiquitination of APOBEC3 proteins by the Vif-Cullin5-ElonginB-ElonginC complex." Virology **344**(2): 263-266.

Simon, J. H. M., A. M. Sheehy, E. A. Carpenter, R. A. M. Fouchier and M. H. Malim (1999). "Mutational Analysis of the Human Immunodeficiency Virus Type 1 Vif Protein." Journal of Virology **73**(4): 2675-2681.

Sinz, A. (2003). "Chemical Cross-linking and mass spectrometry for mapping three-dimensional structures of proteins and protein complexes." Journal of Mass Spectrometery **38**: 1225-1237.

Soskic, V. and J. Godovac-Zimmerman (2001). "Improvement of an in-gel tryptic digestion method for matrix-assisted laser desorption/ionization-time of flight mass spectrometry peptide mapping by use of volatile solubilizing agents." Proteomics **1**(11): 1364-1367.

Sova, P. and D. J. Volsky (1993). "Efficiency of viral DNA synthesis during infection of permissive and nonpermissive cells with vif-negative human immunodeficiency virus type 1." Journal of Virolgoy **67**: 6322-6326.

Stopak, K., C. d. Noronha, W. Yonemoto and W. C. Greene (2003). "HIV-1 Vif Blocks the Antiviral Activity of APOBEC3G by Impairing Both Its Translation and Intracellular Stability." Molecular Cell **12**(3): 591-601.

Strochlic, L., A. Cartaud, V. Labas, W. Hoch, J. Rossier and J. Cartaud (2001). "MAGI-1C: A Synaptic MAGUK Interacting with MuSK at the Vertebrate Neuromuscular Junction." Journal of Cell Biology **153**(5): 1127-1132.

Trester-Zedlitz, M., K. Kamada, S. K. Burley, D. Fenyo, B. T. Chait and T. W. Muir (2003). "A Modular Cross-Linking Approach for Exploring Protein Interactions." Journal of American Chemical Society **125**: 2416-2425.

Tsai, C. J., S. L. Lin, H. J. Wolfson and R. Nussinov (1997). "Studies of protein-protein interfaces: A statistical analysis of the hydrophobic effect." Protein Science **6**: 53-64.

vonSchwedler, U., J. Song, C. Aiken and D. Trono (1993). "Vif is crucial for human immunodeficiency virus type 1 proviral DNA synthesis in infected cells." Journal of Virology **67**: 4945-4955.

Vucetic, S., Z. Obradovic, V. Vacic, P. Radivojac, K. Peng, L. Iakoucheva, M. Cortese, J. Lawson, C. Brown, J. Sikes, C. Newton and A. Dunker (2005). "DisProt: A Database of Protein Disorder." Bioinformatics **21**: 137-140.

Wiegand, H. L., B. P. Doehle, H. P. Bogerd and B. R. Cullen (2004). "A second human antiretroviral factor, APOBEC3F, is suppressed by the HIV-1 and HIV-2 Vif proteins." The Embo Journal **23**(12): 2451-2458.

Xiao, Z., E. Ehrlich, Y. Yu, K. Luo, T. Wang, C. Tian and X.-F. Yu (2006). "Assembly of HIV-1 Vif-Cul5 E3 ubiquitin ligase through a novel zinc-binding domain-stabilized hydrophobic interface in Vif." Virology **349**(2): 290-9.

Yang, B., L. Li, Z. Lu, X. Fan, C. A. Patel, R. J. Pomerantz, G. C. DuBois and H. Zhang (2003). "Potent Suppression of Viral Infectivity by the Peptides That Inhibit

Multimerization of Human Immunodeficiency Virus Type 1 (HIV-1) Vif Proteins." The Journal of Biological Chemistry **278**(8): 6596-6602.

Yang, S., Y. Sun and H. Zhang (2001). "The Multimerization of Human Immunodeficiency Virus Type 1 Vif Protein." The Journal of Biological Chemistry **276**(7): 4889-4893.

Yao, X., A. Freas, J. Ramirez, P. Demirev and C. Fenselau (2001). "Proteolytic 18O labeling for comparative proteomics: model studies with two serotypes of adenovirus." Anal Chem. **73**(13): 2836-42.

Yu, X., Y. Yu, B. Liu, K. Luo, W. Kong, P. Mao and X.-F. Yu (2003). "Induction of APOBEC3G Ubiquitination and degradation by an HIV-1 Vif-Cul5-SCF Complex." Science **302**(5647): 1056-1060.

Yu, Y., Z. Xiao, E. S. Ehrlich, X. Yu and X.-F. Yu (2004). "Selective assembly of HIV-1 vif-Cul5 ElonginB-ElonginC E3 ubiquitin ligase complex through a novel SOCS box and upstream cysteines." Genes & Development **18**: 2867-2872.

Zhang, H., R. J. Pomerantz, G. Dornadula and Y. Sun (2000). "Human Immunodeficiency Virus Type 1 Vif Protein Is an Integral Component of an mRNP Complex of Viral RNA and Could Be Involved in the Viral RNA Folding and Packaging Process." The Journal of Virology **74**(18): 8252-8261.

Footnotes

[†]authors contributed equally to this work

Abbreviations used are APO3G, APOBEC3Gl; EDC, 1-ethyl-3-(3-dimethylaminopropyl) carbodiamide; HIV-1, human immunodeficiency virus type 1; Vif, virion infectivity factor; MALDI-TOF, matrix-assisted laser desorption/ionization-time of flight; LC-ion trap-MS, ion-trap liquid-chromatography mass spectrometry; LC-QTof-MS, quadrupole time of flight liquid-chromatography mass spectrometry; m/z, mass-to-charge ratio; ppm, parts per million.

CHAPTER IV

PEPTIDE-COMPETITION RESULTS CORROBORATE LOW-RESOLUTION STRUCTURAL ANALYSIS AND SUGGEST NEW DRUG SCAFFOLDS FOR HIV-1 VIF

INTRODUCTION

The human immunodeficiency virus type-1 (HIV-1) encodes a highly basic (pI 10.7) 23-kDa accessory protein, viral infectivity factor (Vif). Vif is conserved in all lentiviruses, except equine anemia infectious virus (EAIV) (Kan, 1986; Lee, 1986; Sodroski, 1986). If HIV-1 Vif is absent or nonfunctional in nonpermissive primary CD4 T-cells, post-infection viral replication and viral production are dramatically reduced, likely due to a family of cellular cytidine deaminases, APOBEC3 proteins (Gabuzda, 1992; vonSchwedler, 1993; Sheehy, 2002). Two such APOBEC3 proteins, APOBEC3G (APO3G) and APOBEC3F, likely prevent viral infection by causing a G-to-A hypermutation in the plus strand of the viral cDNA or by preventing the buildup of reverse transcripts (Lecossier, 2003; Mangeat, 2003; Zhang, 2003; Bishop, 2004; Bishop, 2004; Harris, 2004; Liddament, 2004; Wiegand, 2004; Zheng, 2004; Doehle, 2005; Holmes, 2007). HIV-1 Vif may overcome the antiviral activity of APO3G or APOBEC3F by binding and targeting it for proteosomal degradation through a Cullin-RING ligase complex (Yu, 2003; Mehle, 2004; Yu, 2004; Kobayashi, 2005; Luo, 2005).

Therefore, blocking the interaction between HIV-1 Vif and APO3G or APOBEC3F may allow these antiviral proteins to function normally, thus preventing the spread of HIV-1 infection. However, biochemical data on HIV-1 Vif have been difficult to obtain because of an inability to express high concentrations of soluble protein. Nevertheless, the function of HIV-1 Vif has been linked to a putative C-terminal homo-oligomerization domain, PPLP (161-164), which maps to residues 151-164 (Yang, 2001;

Yang, 2003). HIV-1 Vif was also shown by our lab to homo-oligomerize in an N- to C-terminal fashion requiring both the N- and C-termini (Auclair, 2007).

In addition to evidence linking the function of HIV-1 Vif to its homo-oligomerization, two distinct HIV-1 Vif domains have been shown to interact with APO3G and APOBEC3F. APO3G interacts with HIV-1 Vif at residues 40-44 (YRHHY), and APOBEC3F interacts with HIV-1 Vif at residues 14-17 (DRMR) (Russell, 2007). These results have been supported by the identification of other N-terminal domains of HIV-1 Vif important for its interaction with APO3G (Schrofelbauer, 2006; Mehle, 2007).

In addition to limited biochemical data on HIV-1 Vif, traditional structure-based drug design to target this protein has proven difficult because of the inability to obtain milligram quantities of soluble protein. One potential reason for this insolubility lies in the intrinsically disordered characteristics of HIV-1 Vif. Indeed, I have shown that the C-terminus of HIV-1 Vif may be intrinsically disordered and have identified two structurally important regions in HIV-1 Vif (Auclair, 2007). Those studies suggest that the C-terminus of HIV-1 Vif undergoes a disorder-to-order transition upon oligomerization bringing an N-terminal region surrounding Lys34 in proximity to a C-terminal region surrounding Glu134 creating one molecular surface as a potential "hot spot" for biological activity and protein binding, which is in agreement with a mutation analysis done by Simon *et al* (Simon, 1999; Auclair, 2007).

In the current study, we have identified HIV-1 Vif peptides adjacent to and including Lys34 and Glu134 that disrupt oligomerization and impact HIV-1 Vif, APO3G,

and/or the Vif-APO3G interaction. These peptides map to the proposed "hot spot" for biological activity, which supports our previous structural analysis. Therefore, these HIV-1 Vif peptides may be useful in designing novel drugs targeting HIV-1 Vif or APO3G.

MATERIALS AND METHODS

Proteins: Both HIV-1 Vif and APO3G were expressed and purified by Immunodiagnostics, Woburn, MA as described in Chapter III (Auclair, 2007).

Monoclonal Antibodies: The HIV-1 Vif antibody (319) was obtained through the AIDS Research and Reagent Program, Division of AIDS, NIAID, NIH: HIV-1 Vif Monoclonal Antibody (#319) from Dr. Michael Malim. The immunogen used to generate this antibody was a 6XHis-Vif fusion protein overexpressed in BL21(DE3)pLysS *Escherichia coli* and purified under denaturing conditions. Purified HIV-1 Vif protein from the pIIIB strain was used to immunize BALB/c mice. The spleen of one immunized mouse was recovered to generate hybridomas with the mouse plasmacytoma cell line SP2/0Ag. The antibody did not show any cross-reactivity with non-HIV-1 Vif proteins (Simon, 1995).

The APO3G antibody was originally obtained through the AIDS Research and Reagent Program, Division of AIDS, NIAID, NIH: APO3G antibody from Immunodiagnostics, Inc., Woburn, MA. Subsequently the antibody was obtained directly from Immunodiagnostics, Inc. Woburn, MA. Due to the company's proprietary information, the immunogen and methods used to generate this antibody are unavailable.

The information provided by antibody manufacturers was supplemented by performing a wavescan from 200 nm to 350 nm (data not shown) to analyze antibody purity. Antibodies were first diluted 1/100 in PBS (92 mM sodium phosphate dibasic, 16 mM sodium phosphate monobasic, 1.5 M NaCl, pH 7.2) and mixed via pipette. A spectrum of PBS alone showed a straight line across all wavelengths. The spectrum for the HIV-1 Vif monoclonal antibody (#319) showed a large peak at approximately 215-220 nm, representing peptide bonds, and a smaller peak at 280 nm, representing aromatic residues. No peaks or noise were seen above the 300 nm (where DNA contamination can be detected), suggesting little or no DNA contamination. The spectrum for the APO3G monoclonal antibody was similar to that of the HIV-1 Vif monoclonal antibody (#319). A large peak was seen at 215-220 nm, representing peptide bonds, and a much smaller peak at 280 nm, representing aromatic residues. Some residual noise was seen at wavelengths above 300 nm, suggesting nucleotide contamination.

Concentration Dependence of Oligomerization: The "zero-length" cross-linking agent, EDC (1-ethyl-3-[3-dimethylaminopropyl] carbodiamide; Pierce), and sulfo-NHS (N-hydroxysuccinimide; Pierce) were prepared freshly as 0.1 M stock solutions in 0.1 M MES, pH 6.0, 0.5 M NaCl (cross-linking buffer). Cross-linking reactions were set-up with 4 µg of HIV-1 Vif, 2.5 µl of 0.1 M NHS, 1 µl 0.1 M EDC, and varying volumes of cross-linking buffer from 25 µl to 275 µl (in 25 µl increments). Therefore, all amounts (µg) of HIV-1 Vif and cross-linkers were kept constant, and the volume of the reaction was varied to change the final concentration of HIV-1 Vif per reaction: 6.96 µM, 3.48 µM, 2.32 µM, 1.74 µM, 1.39 µM, 1.16 µM, 0.99 µM, 0.87µM, 0.79 µM, 0.70 µM, and

0.63 μM. Cross-linking reactions were carried out for 30 min at room temperature. After cross-linking, an equal volume of 20% v/v TCA (trichloroacetic acid) was added to each reaction and incubated on ice for 10 min. Reaction tubes were centrifuged at 14000 rpm, supernatants were removed, and pellets were washed and resuspended in 10 μl ddH_2O plus 10 μl 2% v/v Novex loading dye. The reactions were analyzed by 16% Tris glycine SDS PAGE and transferred to nitrocellulose membrane at 50 mA for 12 h. The nitrocellulose membranes were blocked for approximately 6 h in 10 mM Tris, pH 8.0, 0.3 M NaCl, 0.25% v/v Tween 20 and 5% w/v non-fat dry milk. After blocking, membranes were incubated overnight with 1:20,000 anti-Vif (319) antibody in blocking buffer plus 5% milk. The membranes were washed, incubated with 1:40,000 goat anti-mouse secondary antibody, washed again, and developed using Pierce Supersignal ECL kit a Fuji LAS-3000. This assay was repeated 3 times.

Peptide-competition experiments: Oligomerization: The cross-linking agent, EDC, and sulfo-NHS were prepared freshly as 0.1 M stock solutions in cross-linking buffer (0.1 M MES, pH 6.0, 0.5 M NaCl). The HIV-1 Vif protein (43.48 μM) was diluted in 50 μl cross-linking buffer to a final concentration of 1 μM. The HIV-1 Vif protein was then incubated for 30 minutes on ice in the presence or absence of 1mM or 500 μM HIV-1 Vif peptides (Figure 4.1): Vif(25-39), Vif (29-43), Vif(69-83), Vif(125-139), Vif(129-143), Vif(145-159), and Vif(157-171). These peptides were obtained from the NIH AIDS Research and Reagent Program and selected because they are from HIV-1 Vif regions that have been implicated in protein-protein interactions and/or have structural importance in creating a "hot spot" for biological activity (Figure 4.1) (Bouyac, 1997;

Huvent, 1998; Bardy, 2001; Yang, 2001; Yang, 2003; Cancio, 2004; Mehle, 2004; Yu, 2004; Kobayashi, 2005; Luo, 2005; Mehle, 2006; Schrofelbauer, 2006; Xiao, 2006; Auclair, 2007; Mehle, 2007; Russell, 2007; Xiao, 2007a; Xiao, 2007b). After incubation, reaction mixtures were cross-linked for 30 min at room temperature, in solution as described above. Cross-linking reactions were quenched by precipitating with 20% v/v TCA and adding SDS PAGE-gel loading dye with 2-mercaptoethanol. TCA precipitation allowed the total sample supernatant with equal amounts of protein to be loaded into each lane of the SDS polyacrylamide gel. The resulting mixture of HIV-1 Vif oligomers was resolved by 16% Tris glycine SDS PAGE and confirmed by western blot analysis using a monoclonal antibody to HIV-1 Vif, 319, obtained from the NIH AIDS Research and Reagent program as described above. The membrane was developed using the Pierce Supersignal ECL kit and a Fuji LAS-3000. The bands were quantitated using multigage and plotted on a semi-log plot as oligomer band intensity divided by whole lane intensity versus HIV-1 Vif concentration. This competition experiment was repeated three times.

Co-immunoprecipitation and Peptide-Competition Experiments: HIV-1 Vif/APO3G Binding: EZview^{TM} Red Protein A Affinity gel (Sigma) was conjugated with an APO3G antibody (Immunodiagnostics) by incubating overnight at 4ºC with end-over-end shaking. Both HIV-1 Vif protein (43.48 µM) and APO3G protein (21.74 µM) were diluted in 50 µl Tris buffer (20 mM Tris, pH 8.0, 0.5 M NaCl) to a final concentration of 1 µM and mixed gently. The 1:1 molar ratio Vif/APO3G solution was then incubated for 30 min in the presence or absence of 1mM HIV-1 Vif peptides on ice. Stock peptides were diluted in DMSO such that the final DMSO concentration in reactions was

Figure 4.1

Peptide	Sequence
Vif(25-39)	VKHHMYISGKAKGWF
Vif(29-43)	MYISGKAKGWFYRHH
Vif(69-83)	YWGLHTGERDWHLGQ
Vif(125-139)	LGHIVSPRCEYQAGH
Vif(129-143)	VSPRCEYQAGHNKVG
Vif(145-159)	LQYLALAALITPKKI
Vif(157-171)	KKIKPPLPSVTKLTE

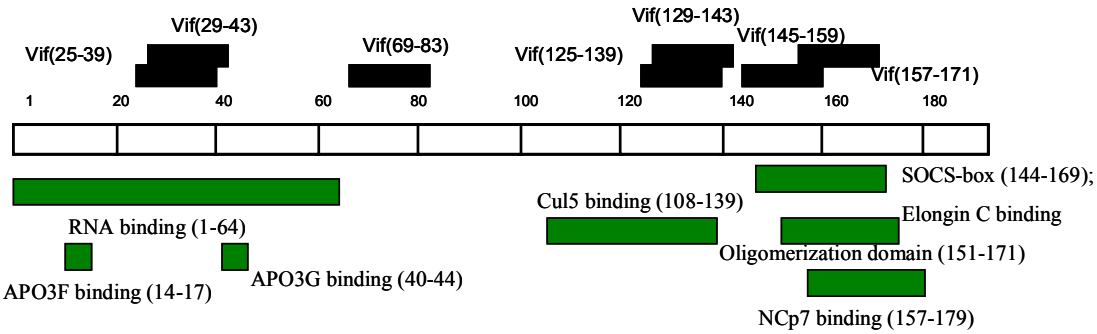

Figure 4.1: HIV-1 Vif Peptides and Schematic of Peptide Coverage. The seven HIV-1 Vif peptides used in the peptide-competition experiments were obtained from the NIH AIDS Research and Reagents Program. The two N-terminal peptides, Vif(29-43) and Vif(25-39), along with the C-terminal peptides, Vif(125-139) and Vif(129-143), were selected because they have been shown to be important for HIV-1 Vif structure These amino acid domains are involved in K34-E134 cross-linking creating a putative "hot spot" for biological activity (Auclair, 2007). The C-terminal peptides, Vif(145-159) and Vif(157-171), were selected because they overlap the proposed HIV-1 Vif oligomerization domain, 151-171 (Yang, 2001; Yang, 2003). The peptide Vif(69-83) was chosen as a control for which no specific oligomerization and APO3G binding have been reported. The peptides used in peptide-competition experiments are mapped as black boxes above the sectioned rectangle representing the HIV-1 Vif sequence, and below are HIV-1 Vif-binding domains (Bouyac, 1997; Huvent, 1998; Bardy, 2001; Yang, 2001; Yang, 2003; Cancio, 2004; Mehle, 2004; Yu, 2004; Kobayashi, 2005; Luo, 2005; Mehle, 2006; Schrofelbauer, 2006; Xiao, 2006; Auclair, 2007; Mehle, 2007; Russell, 2007; Xiao, 2007a; Xiao, 2007b).

approximately 4%. The no-peptide control sample contained an equivalent amount of DMSO. These experiments used the same peptides as in the peptide-competition experiments described above, with the addition of a β-endorphin peptide shown to have no effect on HIV-1 Vif (Potash, 1998). While the proteins and peptides were incubating, the anti-APO3G-conjugated Protein A Affinity resin was washed with Tris buffer and incubated on ice. After incubation, HIV-1 Vif-APO3G-peptide reactions were incubated for 3-5 h with the washed anti-APO3G-conjugated Protein A Affinity resin at 4°C with end-over-end mixing. After this 5-h incubation, the Protein A Affinity beads with captured Vif-APO3G complex were washed with 20 mM Tris, pH 8.0, 0.5 M NaCl buffer and eluted from the gel via boiling. Equal volumes of the samples were resolved by 16% Tris-glycine SDS PAGE and western blotted. After transfer nitrocellulose membrane, the membranes were cut along the 38 KDa marker. The top half of the membrane was probed with an antibody to APO3G, and the bottom half was probed with an antibody to HIV-1 Vif (319). This Co-IP experiment was repeated three times.

Serial dilution (2/3) experiments for peptides Vif(25-39), Vif(29-43), Vif(69-83), and Vif(125-139) were carried out in a similar fashion, except instead of using different peptides a range of peptide concentrations were used from 1 mM to 0.30 μM. Stock peptides were diluted in 100% DMSO, and the initial 1 mM dilution contained approximately 4% DMSO. The same amount of DMSO was not added to each dilution in the series; thus, the no-peptide control contained the highest amount of DMSO used. Band intensities were quantitated using the LAS-3000 and Fujifilm Multigage software. The HIV-1 Vif band intensities were divided by the APO3G band intensities and these

normalized band intensities were plotted versus peptide concentration on a semi-log scale. These experiments were also repeated three times.

In these peptide-competition experiments, 1 μM HIV-1 Vif was incubated with 1 μM APO3G for 30 min before adding each respective peptide, and incubations were continued for 3-5 h. Preliminary binding information suggested that the interaction between HIV-1 Vif and APO3G is weak (Appendix II); therefore, I expected that the peptides would disrupt the protein-protein interaction. However, if HIV-1 Vif and APO3G bound tightly, their interaction would not be efficiently inhibited by the peptides. To address these two possibilities, the order of adding components could be altered in peptide-competition experiments. For example, HIV-1 Vif could be incubated with the respective peptides before adding APO3G, which could allow the peptides to bind to either HIV-1 Vif or APO3G preventing the other respective protein binding instead of the peptide competing for binding with the other respective protein.

In-vitro HIV-1 Vif-peptide uptake experiments: 293T cells were transfected with a plasmid containing the full-length infectious NL4-3 strain of HIV-1. Cell supernatants containing virions were collected, quantified for HIV-1 p24 amounts, and used to infect nonpermissive CEM cells at a m.o.i. of 0.1. An aliquot of CEM T-cells were mock-infected and served as a negative control for infection. After 2 hr of initial infection, the cells were washed and then split into aliquots. An aliquot was cultured in the absence of any peptide and served as the positive control for infection. The other aliquots were cultured in the presence of one of the following antennapedia (RQIKIWFQNRRMKWKK)-tagged HIV-1 Vif peptides: Vif(29-43), Vif(69-83),

Vif(125-139) (see Figure 4.1 for sequences of the previous 3 peptides), Vif(155-166) [KPKQIKPPLPSV], and a scrambled protein kinase C (PKC) control [KCVHVGAKQKQIAHLHRR]. Infected cultures were maintained in the presence or absence of these peptides for 15 days, with periodic replenishing of the peptides and after day 15 post-infection they were cultured in the absence of any peptide. Aliquots of infected culture supernatants were sampled during the infection period to monitor viral replication using a HIV-1 p24 antigen-capture ELISA assay to detect the amount of p24 protein present in the supernatant. These experiments were repeated in duplicate.

RESULTS

The relationship between the rate of oligomerization and HIV-1 Vif concentration were examined by measuring the concentration dependence of oligomerization. To confirm the low-resolution structural data obtained in Chapter III and to determine potential peptides that could be used in drug design, competition was examined between HIV-1 Vif and various HIV-1 Vif peptides. Both the disruption of oligomerization and the Vif-APO3G interaction were investigated.

Oligomerization of HIV-1 Vif depends on its concentration

To determine the the relationship between rate of oligomerization and HIV-1 Vif concentration, oligomerization products were measured at various HIV-1 Vif concentrations. Oligomerization was measured in cross-linking reactions with constant amounts of HIV-1 Vif protein and cross-linker in varying volumes, thus varying only the protein concentration. Each reaction was TCA precipitated based on its total reaction volume (see Methods) before SDS PAGE analysis; therefore, the same amount of HIV-1

Vif (4 μM) was added to each lane. As the volume of the cross-linking reaction was increased, thus decreasing the protein concentration, the amount of cross-linked products, dimer and trimer, also decreased. The amount of monomer increases as the amount of dimer and trimer decreases (Figure 4.2A). These experiments were repeated three times, with similar results in each case.

To obtain a K_d of dimerization, the band intensity for the dimer was normalized to that for the whole lane and plotted versus HIV-1 Vif protein concentration (Figure 4.2B). These normalized intensities did not change significantly over the concentrations investigated, making it impossible to determine a K_d of dimerization. To determine a K_d, further experiments are needed with a wider range of protein concentrations.

HIV-1 Vif Peptides Block Oligomerization

To determine if HIV-1 Vif peptides could inhibit HIV-1 Vif oligomerization, peptide-competition experiments were performed. The peptides were selected from HIV-1 Vif regions shown to be important for oligomerization, other protein-protein interactions, and/or structurally important for Vif function (Figure 4.1; (Bouyac, 1997; Huvent, 1998; Bardy, 2001; Yang, 2001; Yang, 2003; Cancio, 2004; Mehle, 2004; Yu, 2004; Kobayashi, 2005; Luo, 2005; Mehle, 2006; Schrofelbauer, 2006; Xiao, 2006; Auclair, 2007; Mehle, 2007; Russell, 2007; Xiao, 2007a; Xiao, 2007b). Peptide-competition experiments were conducted with a 500-fold or 1000-fold excess of peptide such that 1μM HIV-1 Vif was cross-linked in the presence or absence of 1mM or 500μM HIV-1 peptides and analyzed via western blotting. A no-peptide control sample shows the presence of monomeric and dimeric HIV-1 Vif (Figure 4.3A, lane 1). Peptides

Figure 4.2A

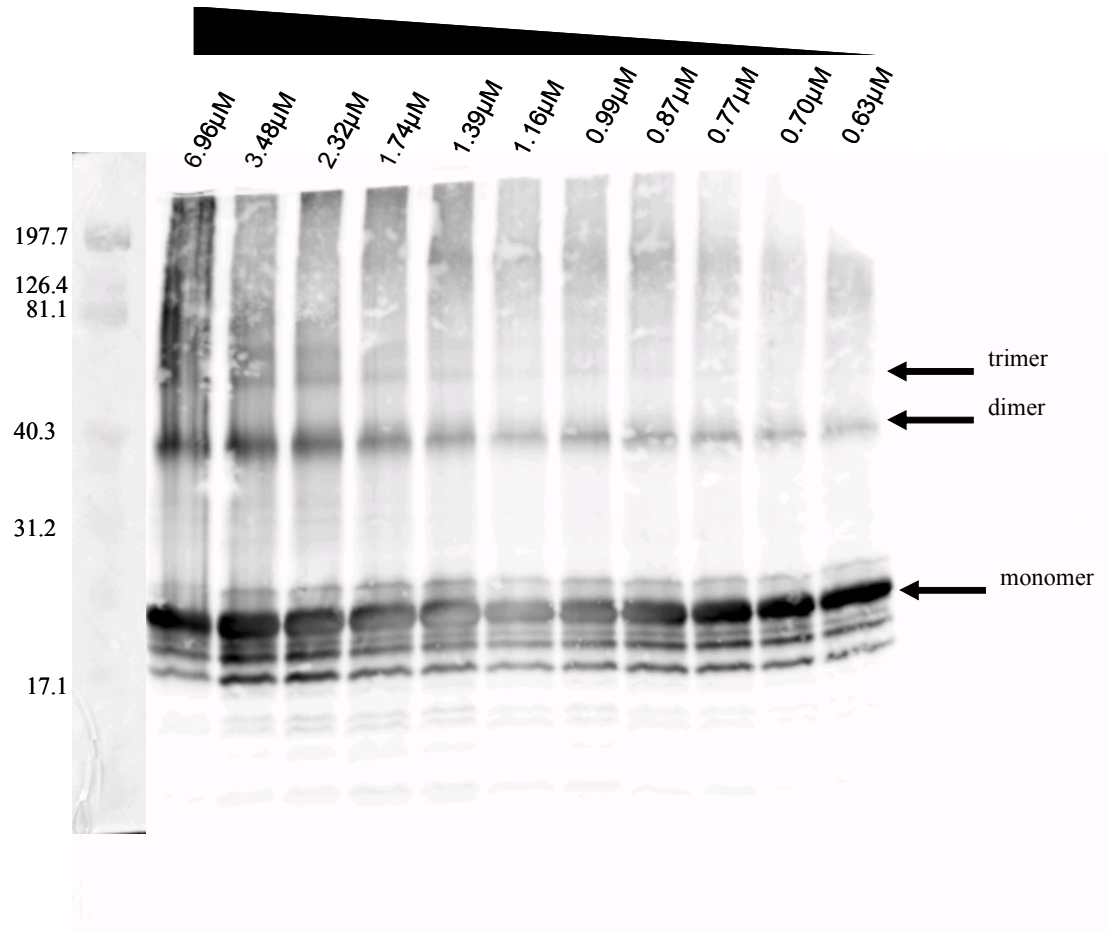
6.96µM
3.48µM
2.32µM
1.74µM
1.39µM
1.16µM
0.99µM
0.87µM
0.77µM
0.70µM
0.63µM
197.7
126.4
81.1
40.3
31.2
17.1
trimer
dimer
monomer

Figure 4.2B

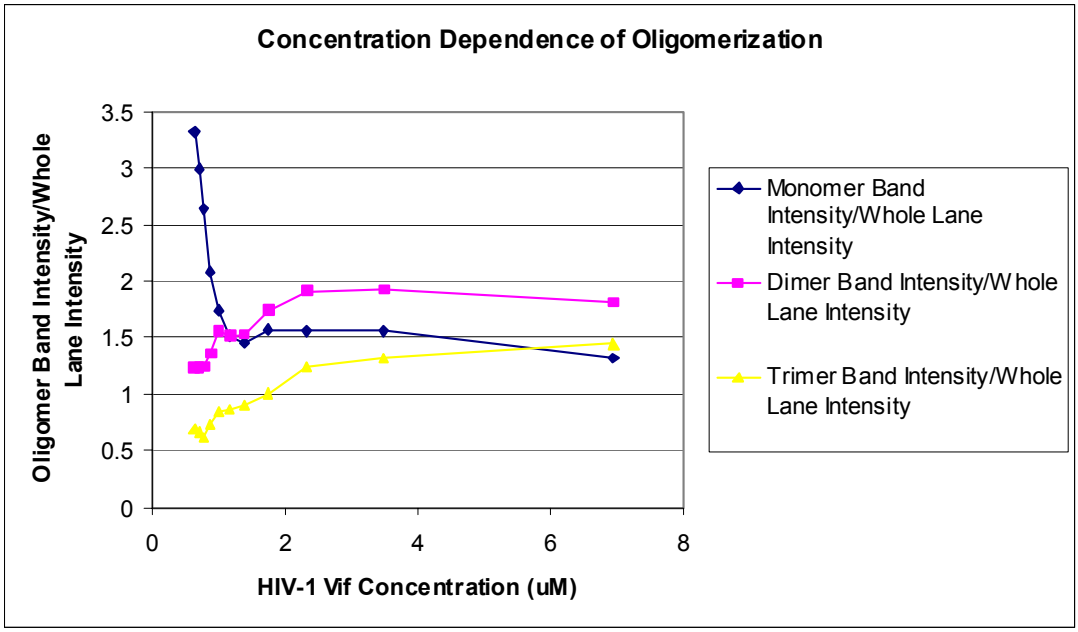
Concentration Dependence of Oligomerization
Oligomer Band Intensity/Whole Lane Intensity
3.5
3
2.5
2
1.5
1
0.5
0
0
2
4
6
8
HIV-1 Vif Concentration (uM)
Monomer Band Intensity/Whole Lane Intensity
Dimer Band Intensity/Whole Lane Intensity
Trimer Band Intensity/Whole Lane Intensity

Figure 4.2: HIV-1 Vif Oligomerization Depends on HIV-1 Vif Concentration. **(A.)** HIV-1 Vif was cross-linked in the presence of equal amounts of protein and cross-linking agent, but volumes were changed to vary final protein concentrations. Cross-linking reaction products were analyzed by SDS PAGE and western blot using an antibody against HIV-1 Vif. The molecular weight marker is in kilodaltons (kDa). The protein concentration for each lane is listed above the respective lane. As reaction volume increased and the protein concentration thus decreased, the amount of dimer and trimer decreased. The amount of monomer increased as the amount of dimer and trimer decreased. **(B.)** The amount of monomer, dimer, and trimer product was quantitated and normalized by dividing each respective oligomeric state band intensity by the intensity of the whole lane and plotting versus protein concentration on a semi-log scale. The monomer data was normalized to 2 to put it on the same scale as the dimer and trimer samples.

Vif(25-39) and Vif(69-83) do not appear to affect HIV-1 Vif oligomerization as similar levels of oligomer products are observed as in the no-peptide control (Figure 4.3A, lanes 2 and 4). In addition, peptides Vif(129-143), Vif(145-159), and Vif(157-171) appear to have little or no effect on the amount of oligomers formed (Figure 4.3A, lanes 6-8), but peptides Vif(29-43) and Vif(125-139) dramatically reduced the amount of HIV-1 Vif oligomer products (Figure 4.3A, lanes 3 and 5). These two peptides, Vif(29-43) and Vif(125-139), map to the region previously identified as a "hot spot" for binding to proteins important for HIV-1 Vif function (Auclair, 2007).

The apparent failure of peptides Vif(129-143) and Vif(157-171) to inhibit oligomerization is noteworthy because they were shown by my cross-linking data (Chapter III) to be involved in oligomerization. Similarly, Vif(157-171) has been reported to lie within the HIV-1 Vif oligomerization domain (Yang, 2001; Yang, 2003). A possible explanation for why these peptides did not inhibit oligomerization is that higher concentrations of peptide are needed or other cell factors (proteins) are involved. These experiments were repeated in triplicate, with similar results in each case.

Both N-terminal and C-terminal regions in HIV-1 Vif interact with APO3G

To determine if HIV-1 Vif peptides could disrupt the HIV-1 Vif-APO3G interaction, the same peptides as above were used in co-immunoprecipitation (co-IP) and peptide-competition experiments. In co-IP experiments, mixtures of 1 μM HIV-1 Vif and 1μM APO3G were incubated for 0.5 h with and without 1000-fold excess peptide (1 mM) before adding APO3G antibody-conjugated beads and incubating 3 to 5 h longer. HIV-1 Vif-APO3G complexes were eluted from beads and analyzed via western blot

Figure 4.3A

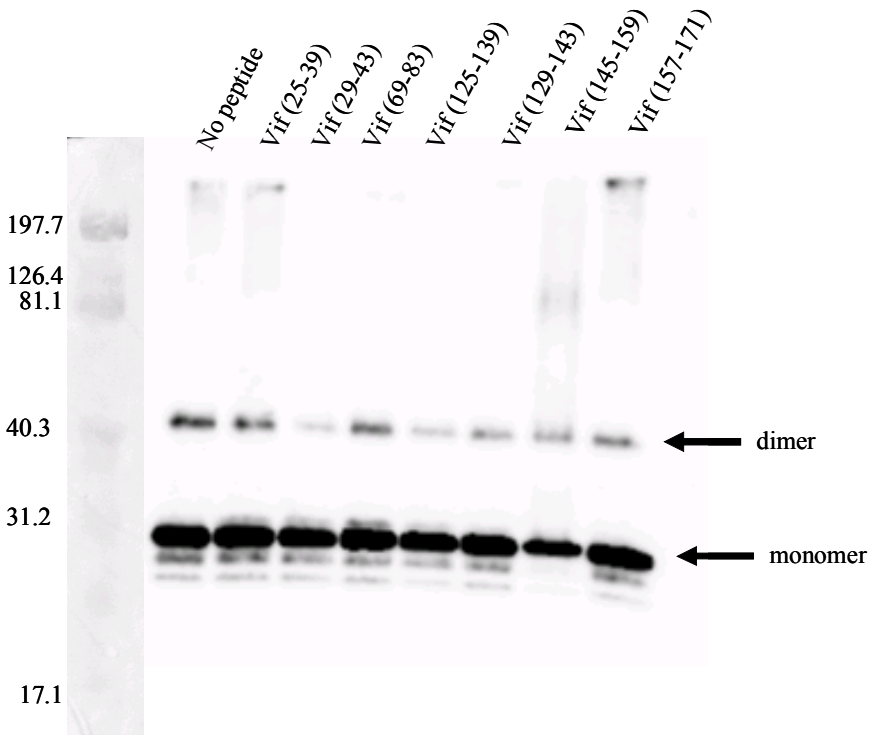
No peptide
Vif (25-39)
Vif (29-43)
Vif (69-83)
Vif (125-139)
Vif (129-143)
Vif (145-159)
Vif (157-171)
197.7
126.4
81.1
40.3
31.2
17.1
dimer
monomer

Figure 4.3A: HIV-1 Vif Peptides Block Oligomerization. To determine if HIV-1 Vif 15-mer peptides inhibited HIV-1 Vif oligomerization, HIV-1 Vif was incubated in the presence or absence of peptides and cross-linked. Reaction products were analyzed by SDS PAGE and western blotted using an antibody against HIV-1 Vif. The peptides were selected based on their involvement in Vif-Vif interactions as previously observed (Auclair, 2007). *Lane 1*: No peptide. *Lane 2*: HIV-1 Vif(25-39). *Lane 3*: HIV-1 Vif(29-43). *Lane 4*: HIV-1 Vif(69-83). *Lane 5*: HIV-1 Vif(125-139). *Lane 6*: HIV-1 Vif(129-143). *Lane 7*: HIV-1 Vif(145-159). *Lane 8*: HIV-1 Vif(157-171). Peptides Vif(29-43) and Vif(125-139) appeared to have the greatest ability to inhibit dimerization, whereas peptides Vif(129-143), Vif(145-159), and Vif(157-171) appeared to have a minor effect on inhibiting dimerization, and peptides Vif(25-39) and Vif(69-83) appeared to have no effect on HIV-1 Vif dimerization. The molecular weight marker is in kDa.

with anti-HIV-1 Vif and APO3G antibodies. Peptides Vif(125-139), Vif(129-143), Vif(145-159), and Vif(157-171) had little effect on the amount of HIV-1 Vif observed (Figure 4.3B, lanes 5-8), whereas peptides Vif(25-39) and Vif(29-43) displaced HIV-1 Vif (Figure 4.3B, lanes 2 and 3). In addition, Vif(69-83) appeared to have levels of HIV-1 Vif that were consistent with the no-peptide control (Figure 4.3B, lane 4). As a control peptide, I used β-endorphin (YGGFMTSEKSQTPLVTLFKNAIIKNAYKKGE), which has been shown to have no effect on HIV-1 Vif, (Potash, 1998), but in my hands β-endorphin appeared to displace the amount of HIV-1 Vif that interacted with APO3G (Figure 4.3B, lane 9).

In addition to probing the co-immunoprecipitated complexes for HIV-1 Vif, I probed for APO3G to determine how much APO3G was immobilized on the Protein A affinity beads. The peptides Vif(69-83), Vif(125-139), Vif(129-143), and Vif(157-171) appear to have immobilized a similar amount of APO3G as the no-peptide control (Figure 4.3B, lanes 4-6 and lane 8). Vif(145-159) appears to have immobilized half as much APO3G as the control, and peptides Vif(25-39) and Vif(29-43) appear to have immobilized almost no APO3G (Figure 4.3B, lane 7 and lanes 2-3). A control peptide which has been shown to have no effect on HIV-1 Vif, β-endorphin, (Potash, 1998) appeared to reduce the amount of APO3G in the putative HIV-1 Vif-APO3G complex (Figure 4.3B, lane 9).

The detection of reduced APO3G is surprising since one would expect to always detect APO3G after using an anti-APO3G antibody to isolate APO3G on the Protein A beads in order to isolate the putative HIV-1 Vif-APO3G complex. Thus, further

Figure 4.3B

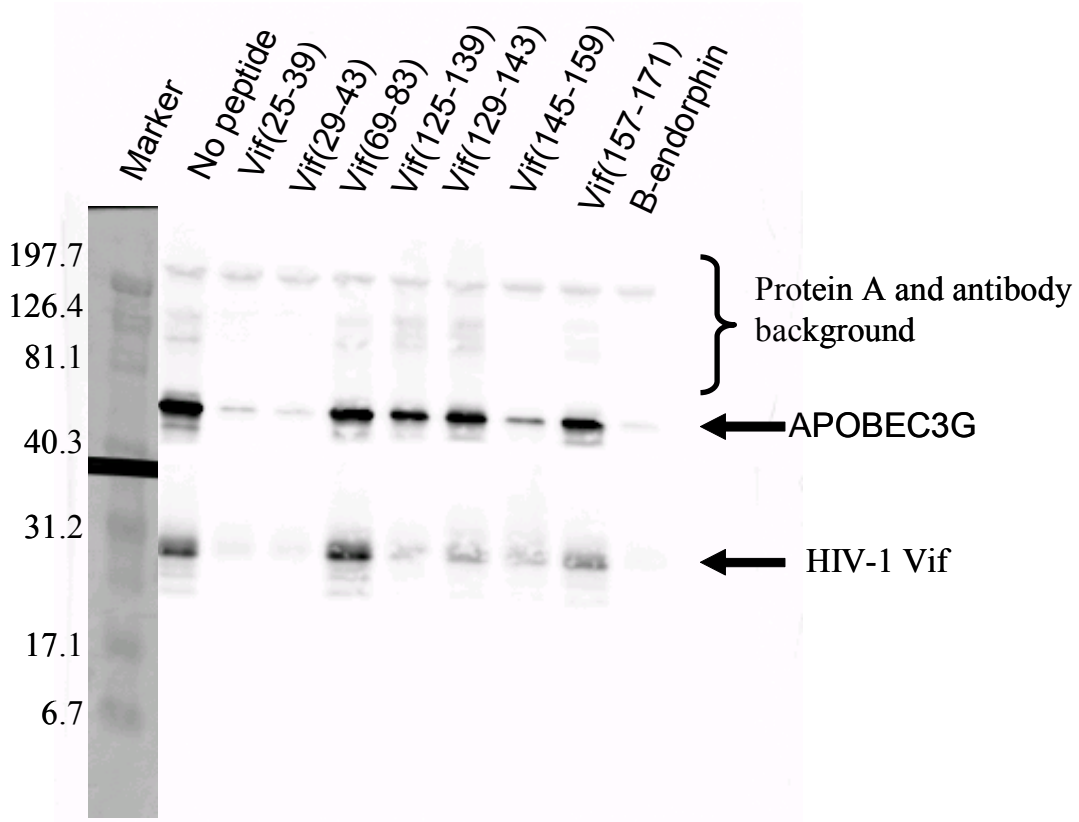
Marker
No peptide
Vif(25-39)
Vif(29-43)
Vif(69-83)
Vif(125-139)
Vif(129-143)
Vif(145-159)
Vif(157-171)
B-endorphin
197.7
126.4
81.1
40.3
31.2
17.1
6.7
Protein A and antibody background
APOBEC3G
HIV-1 Vif

Figure 4.3B: Both N-terminal and C-terminal regions in HIV-1 Vif interact with APO3G. HIV-1 Vif was co-immunoprecipitated with APO3G in the presence or absence of HIV-1 Vif 15-mer peptides and analyzed via western blotting using both HIV-1 Vif and APO3G antibodies. The peptides were selected based on their involvement in Vif-Vif interactions (Auclair, 2007)**.** *Lane 1*: No peptide. *Lane 2*: Vif(25-39). *Lane 3*: Vif(29-43). *Lane 4*: Vif(69-83). *Lane 5*: Vif(125-139). *Lane 6*: Vif(129-143). *Lane 7*: Vif(145-159). *Lane 8*: Vif(157-171). N-terminal peptides, Vif(25-39) and Vif(29-43), reduced the amount of both Vif and APO3G, whereas peptides Vif(125-139), Vif(129-143) and Vif(157-171) had little effect on Vif and APO3G levels. Peptide Vif(145-159) seemed to reduce the amount of APO3G, but the level of HIV-1 Vif was only minimally reduced. Peptide Vif(69-83) appeared to have levels of APO3G and HIV-1 Vif consistent with the no-peptide control. β-endorphin was selected as a control because it was shown to have no effect on HIV-1 Vif (Potash, 1998), but in this case it reduced both the amount of HIV-1 Vif and APO3G observed. To determine if the same amount of protein was loaded in each lane I could compare the amount of APO3G immobilized on the beads, however I incubated APO3G with HIV-1 Vif and peptide and then immobilized on the beads. Because of this, I am unable to determine if the same amount of protein is loaded in each lane. To correct for this in future experiments I would immobilize APO3G on the beads and then incubated with HIV-1 Vif and peptides. The molecular weight marker is in kDa.

investigation is warranted into why APO3G detection was reduced by some of these peptides. One possibility is that the APO3G or HIV-1 Vif sample was contaminated by RNA thus blocking the antibody binding site and, reducing the protein observed. This possibility could be examined by repeating these experiments in the presence of RNase A. These experiments were repeated three times, with similar results in each case.

Another unexpected result was that the β-endorphin control reduced the amounts of both HIV-1 Vif and APO3G observed. β-endorphin has been used in cellular uptake experiments, where it did not reduce the amount of HIV-1 antigen p24, indicating no effect on viral replication (Potash, 1998). In those experiments, however, β-endorphin was monitored for its ability to inhibit viral replication in cells, not its ability to interact with APO3G or HIV-1 Vif. In those experiments β-endorphin was added to a cell culture system, whereas I added it to purified proteins that are known to be unstable. The peptide may be causing HIV-1 Vif and APO3G to aggregate or may affect the purified proteins by an unknown mechanism. In addition, I cannot rule out the possibility that the β-endorphin peptide is contaminated with proteases, however it is unlikely since other HIV-1 Vif peptides I tested reduced the amount of HIV-1 Vif and APO3G.

In addition to the β-endorphin control, another interesting control to consider would be determining the effect of mutant HIV-1 Vif peptides on viral replication. This would help to elucidate the potential role wild type peptides may have on the Vif-APO3G interaction. If a mutant peptide had no effect particular residues could be identified as playing a crucial role in the interaction.

HIV-1 Vif(25-39) and HIV-1 Vif(29-43) Disrupt the HIV-1 Vif-APO3G Interaction

To determine the concentration range necessary to disrupt the HIV-1 Vif-APO3G interaction, I used serial dilutions (2/3) of HIV-1 Vif peptides and co-immunoprecipitation. HIV-1 Vif (1 μM) was incubated with APO3G (1 μM) and either Vif(25-39), Vif(29-43), Vif(69-83), or Vif(125-139) from 1mM to 0.30 μM. Reactions were analyzed for Vif-APO3G complexes as for the previous Vif-APO3G co-immunoprecipitation experiments. Band intensities for HIV-1 Vif-APO3G complexes on western blots were quantitated, normalized, and plotted versus peptide concentration. The amount of APO3G or HIV-1 Vif was not affected by Vif(69-83) and Vif(125-139) compared to the no-peptide control (Figure 4.4C and 4.4D). Vif(25-39) and Vif(29-43) reduced the amounts of HIV-1 Vif and APO3G to levels comparable to the no-peptide control. Vif(25-39) at concentrations above 88μM and Vif(29-43) above 17 μM appeared to reduce the amount of APO3G observed (Figure 4.4A and 4.4B, respectively). Below these two concentrations, the peptides appear to have no effect on HIV-1 Vif binding to APO3G. These experiments were repeated in duplicate, with similar results in each case.

HIV-1 Vif peptides inhibit viral replication *in vitro*

To determine if HIV-1 Vif peptides could disrupt viral replication nonpermissive CEM T-cells were infected with infectious HIV-1 $_{NL4-3}$ virus and the cells were maintained in culture with or without antennapedia-tagged HIV-1 Vif peptides for 21 days. Antennapedia-tag is a tag that allows for cellular uptake of peptides. As a positive

control, cells were treated with no peptide and infected with HIV-1 virions collected from the supernatant of infected 293T cells. HIV-1 replication, shown by the amount of its p24 antigen in cell supernatants, increased to a maximum at 11 days post-infection, after which the amount decreased because of the cytopathic effects of HIV-1 (Figure 4.5, red squares). Two negative controls were used: uninfected cells and infected cells treated with PKC-scrambled peptide. In uninfected controls no p24 was produced (Figure 4.5, cyan diamonds), and in cells treated with the PKC-scrambled peptide, p24 levels did not differ from those of infected positive controls, suggesting that there was no non-specific inhibitory effect on spread of infection in culture in the presence of antennapedia peptides (Figure 4.5, yellow triangles).

When HIV-1-infected CEM T-cells were treated with the HIV-1 Vif peptides, Vif(29-43), Vif(69-83), and Vif(125-139), the amount of p24 production decreased by approximately an order of magnitude (Figure 4.5, blue asterisks, green X, orange circles). Removing the peptides after day 15 led to a rebound in viral p24 production (Figure 4.5, blue asterisks, green X, orange circles). The peptide Vif(155-166), which has been shown to reduce viral replication (Yang, 2003), also reduced p24 production and thus viral replication (Figure 4.5, purple plus signs), but not to the same extent as the other HIV-1 Vif peptides tested.

DISCUSSION

Here I report novel data on concentration dependence of HIV-1 Vif oligomerization, HIV-1 Vif peptides that can disrupt HIV-1 Vif Oligomerization, HIV-1

Figure 4.4A

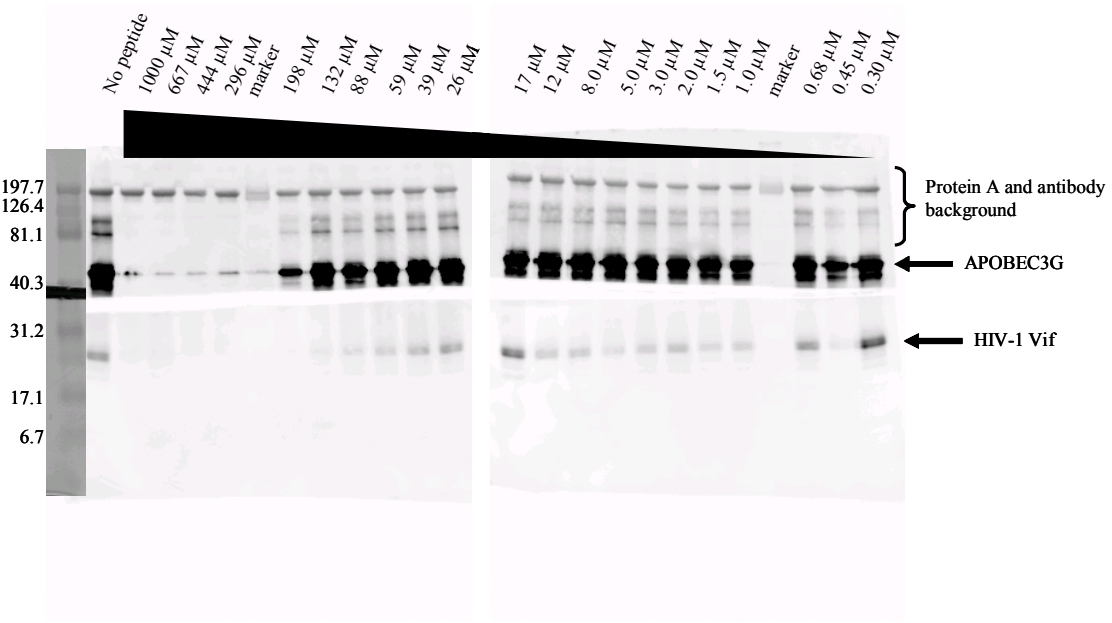
No peptide
1000 μM
667 μM
444 μM
296 μM
marker
198 μM
132 μM
88 μM
59 μM
39 μM
26 μM
17 μM
12 μM
8.0 μM
5.0 μM
3.0 μM
2.0 μM
1.5 μM
1.0 μM
marker
0.68 μM
0.45 μM
0.30 μM
197.7
126.4
81.1
40.3
31.2
17.1
6.7
Protein A and antibody background
APOBEC3G
HIV-1 Vif

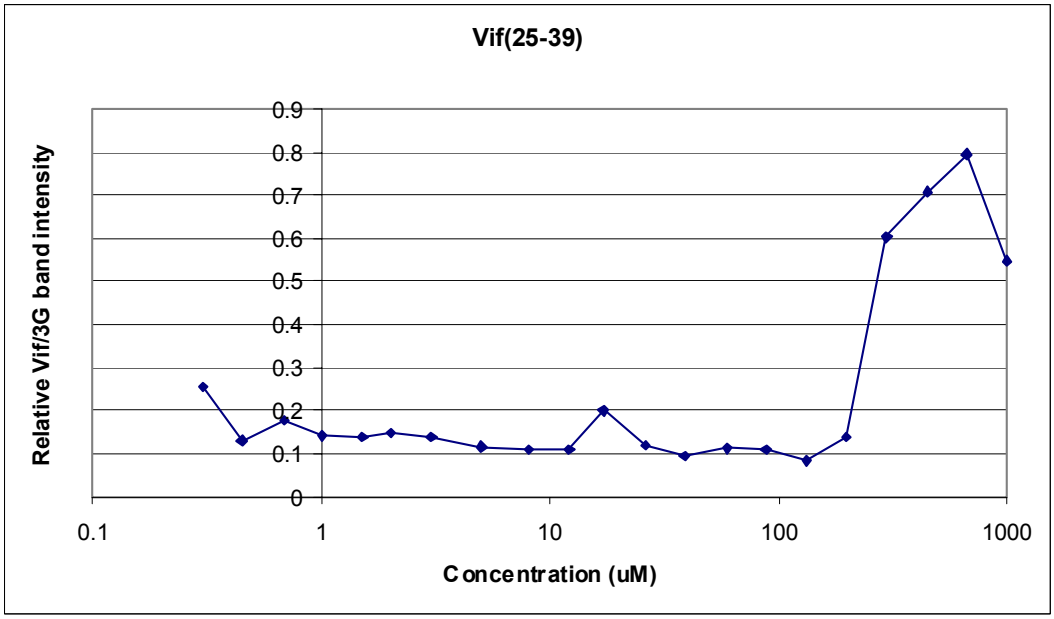
Vif(25-39)
Relative Vif/3G band intensity
0.9
0.8
0.7
0.6
0.5
0.4
0.3
0.2
0.1
0
0.1
1
10
100
1000
Concentration (uM)

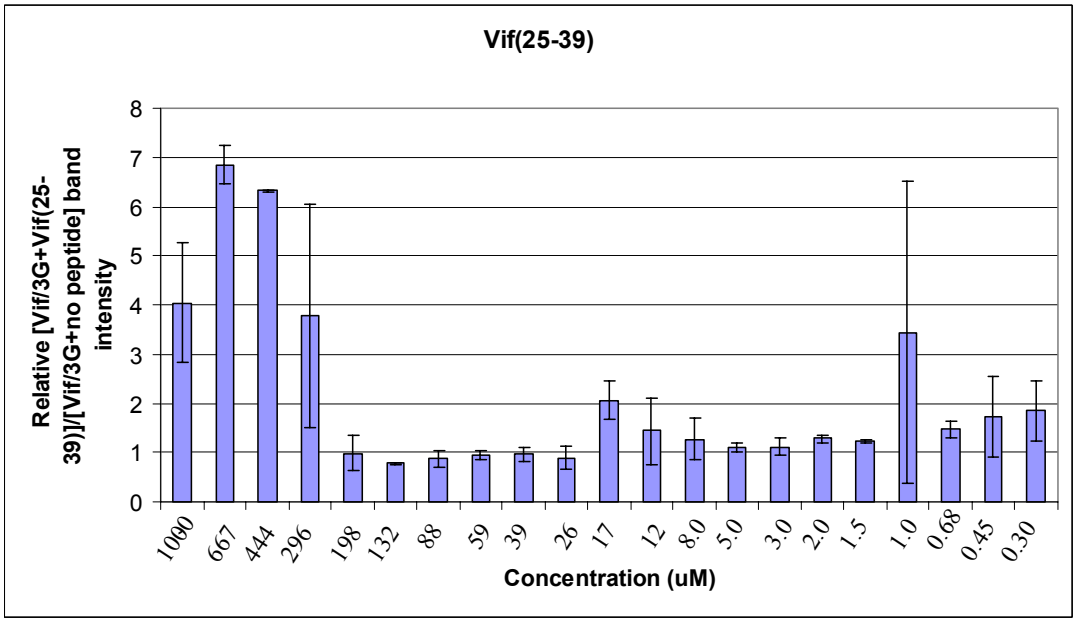
Vif(25-39)
Relative [Vif/3G+Vif(25-39)]/[Vif/3G+no peptide] band intensity
0
1
2
3
4
5
6
7
8
1000
667
444
296
198
132
88
59
39
26
17
12
8.0
5.0
3.0
2.0
1.5
1.0
0.68
0.45
0.30
Concentration (uM)

Figure 4.4B

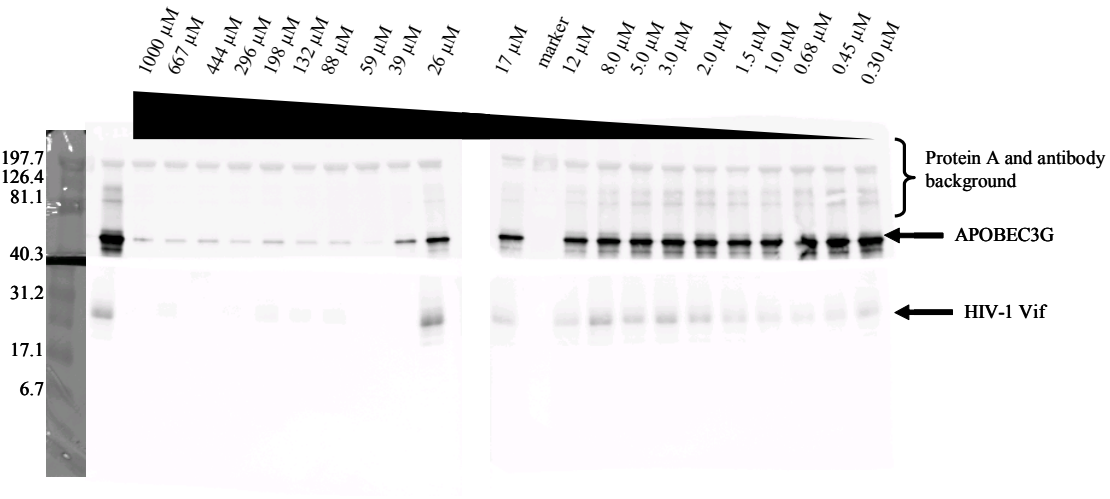
1000 µM
667 µM
444 µM
296 µM
198 µM
132 µM
88 µM
59 µM
39 µM
26 µM
17 µM
marker
12 µM
8.0 µM
5.0 µM
3.0 µM
2.0 µM
1.5 µM
1.0 µM
0.68 µM
0.45 µM
0.30 µM
197.7
126.4
81.1
40.3
31.2
17.1
6.7
Protein A and antibody background
APOBEC3G
HIV-1 Vif

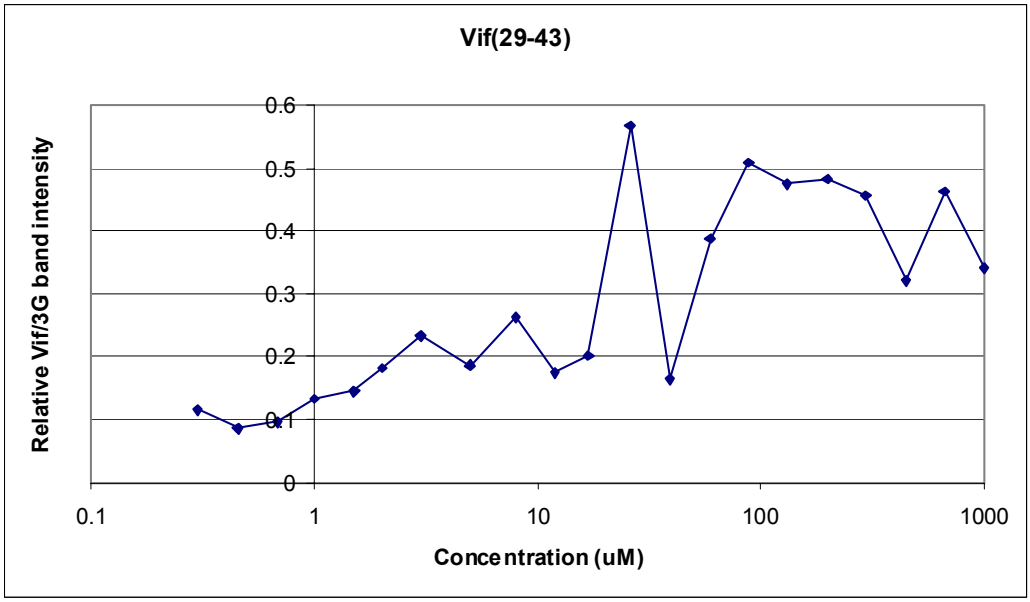
Vif(29-43)
Relative Vif/3G band intensity
0.6
0.5
0.4
0.3
0.2
0.1
0
0.1
1
10
100
1000
Concentration (uM)

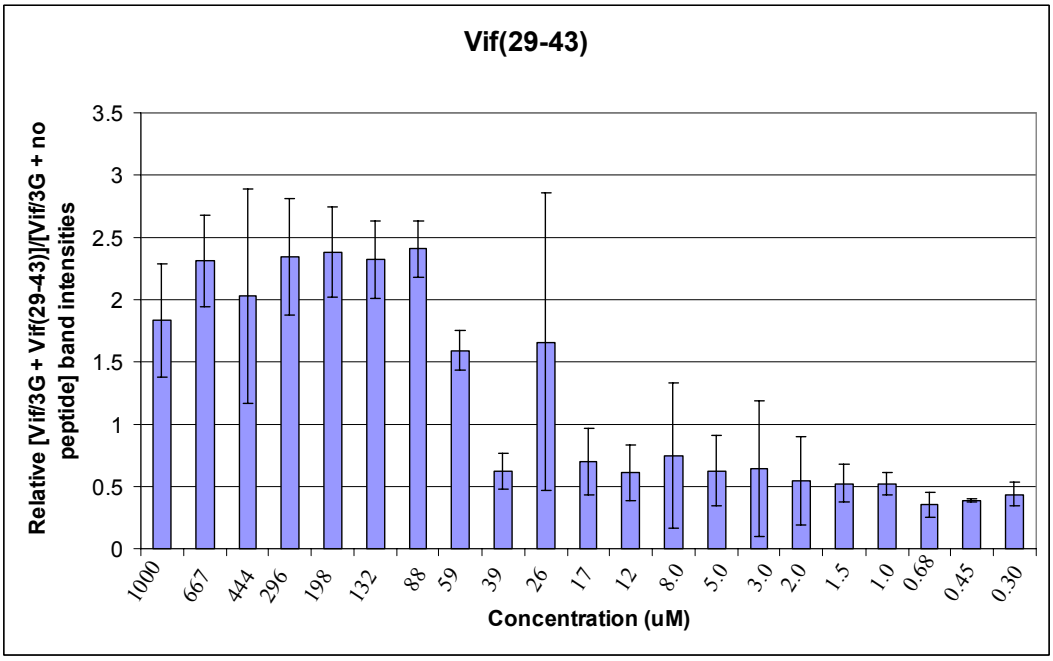
Vif(29-43)
Relative [Vif/3G + Vif(29-43)]/[Vif/3G + no peptide] band intensities
3.5
3
2.5
2
1.5
1
0.5
0
1000
667
444
296
198
132
88
59
39
26
17
12
8.0
5.0
3.0
2.0
1.5
1.0
0.68
0.45
0.30
Concentration (uM)

Figure 4.4C

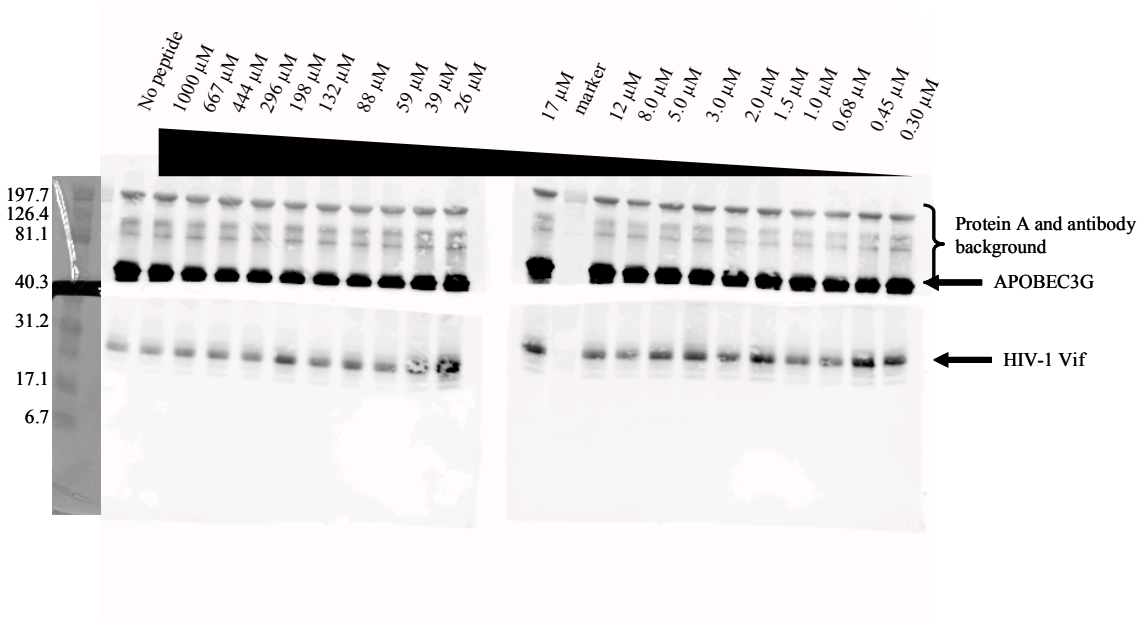
No peptide
1000 μM
667 μM
444 μM
296 μM
198 μM
132 μM
88 μM
59 μM
39 μM
26 μM
17 μM
marker
12 μM
8.0 μM
5.0 μM
3.0 μM
2.0 μM
1.5 μM
1.0 μM
0.68 μM
0.45 μM
0.30 μM
197.7
126.4
81.1
40.3
31.2
17.1
6.7
Protein A and antibody background
APOBEC3G
HIV-1 Vif

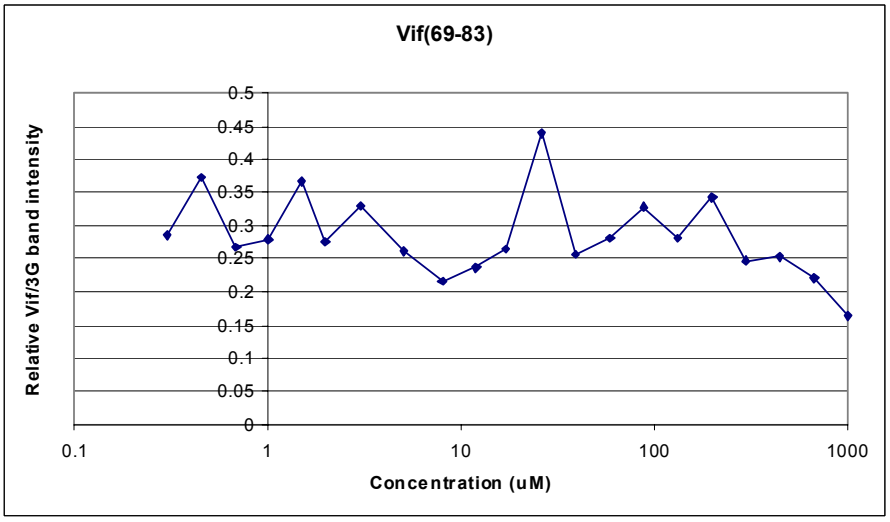
Vif(69-83)
Relative Vif/3G band intensity
0.5
0.45
0.4
0.35
0.3
0.25
0.2
0.15
0.1
0.05
0
0.1
1
10
100
1000
Concentration (uM)

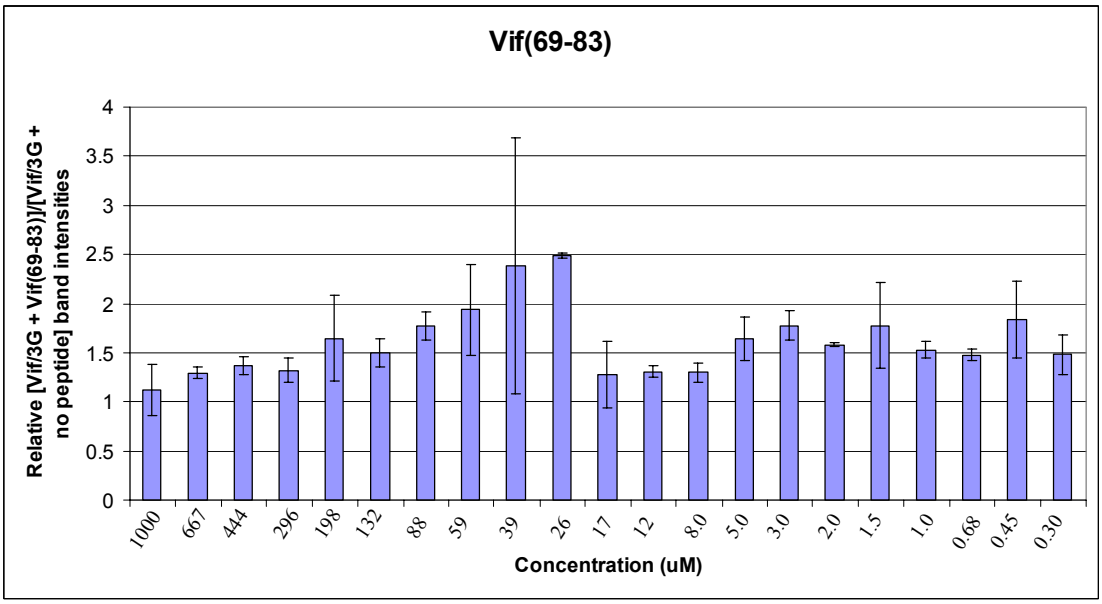
Vif(69-83)
Relative [Vif/3G + Vif(69-83)]/[Vif/3G + no peptide] band intensities
4
3.5
3
2.5
2
1.5
1
0.5
0
1000
667
444
296
198
132
88
59
39
26
17
12
8.0
5.0
3.0
2.0
1.5
1.0
0.68
0.45
0.30
Concentration (uM)

Figure 4.4D

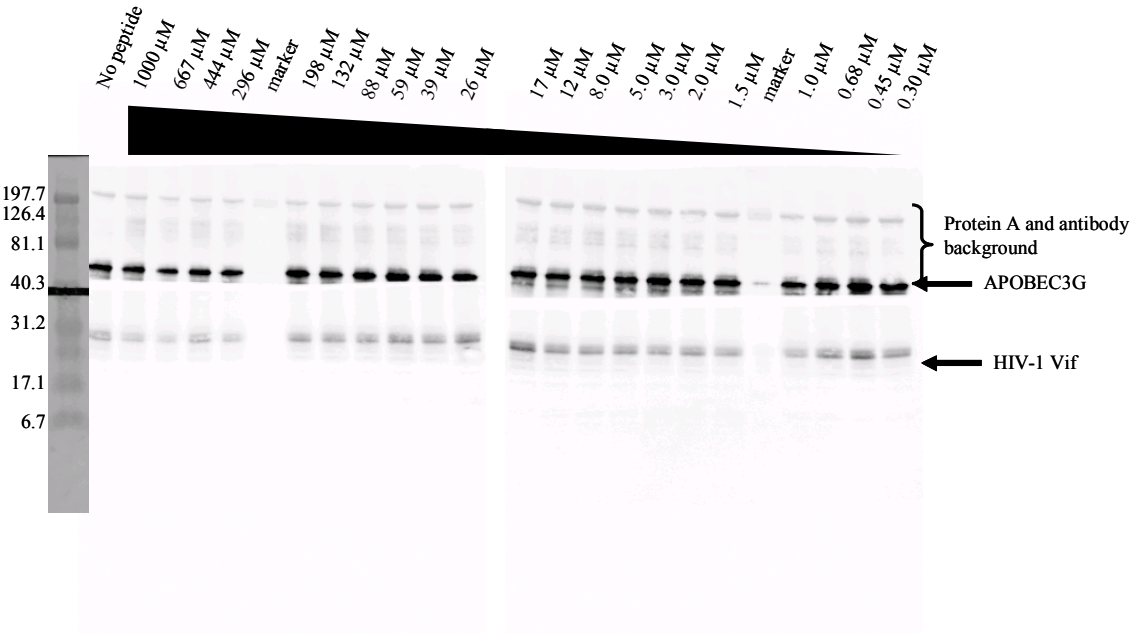
No peptide
1000 µM
667 µM
444 µM
296 µM
marker
198 µM
132 µM
88 µM
59 µM
39 µM
26 µM
17 µM
12 µM
8.0 µM
5.0 µM
3.0 µM
2.0 µM
1.5 µM
marker
1.0 µM
0.68 µM
0.45 µM
0.30 µM
197.7
126.4
81.1
40.3
31.2
17.1
6.7
Protein A and antibody background
APOBEC3G
HIV-1 Vif

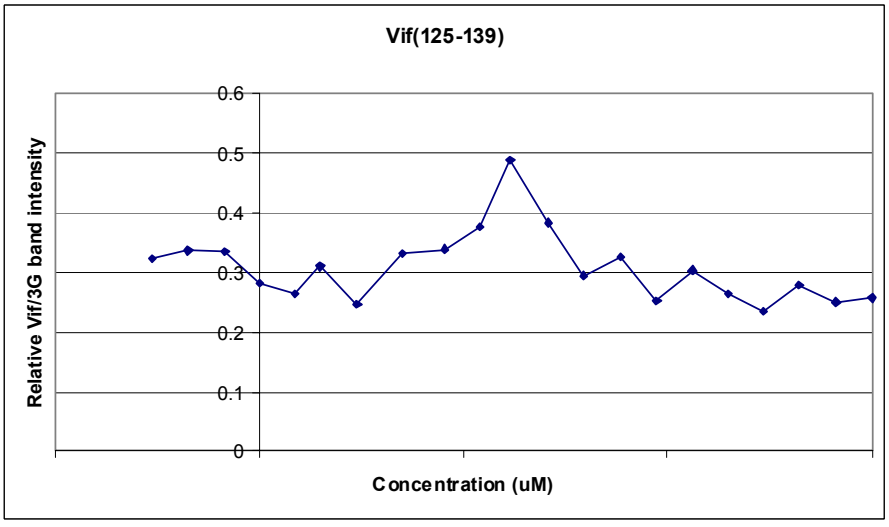
Vif(125-139)
Relative Vif/3G band intensity
0.6
0.5
0.4
0.3
0.2
0.1
0
Concentration (uM)

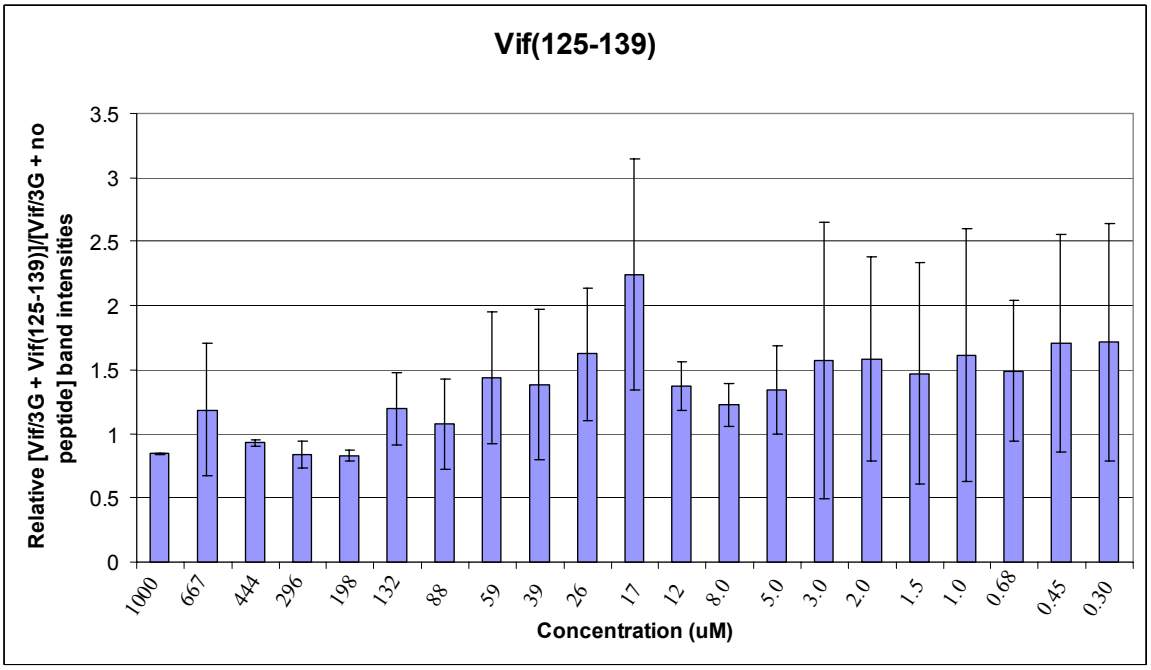
Vif(125-139)
Relative [Vif/3G + Vif(125-139)]/[Vif/3G + no peptide] band intensities
3.5
3
2.5
2
1.5
1
0.5
0
1000
667
444
296
198
132
88
59
39
26
17
12
8.0
5.0
3.0
2.0
1.5
1.0
0.68
0.45
0.30
Concentration (uM)

Figure 4.4: HIV-1 Vif(25-39) and HIV-1 Vif(29-43) Disrupt the HIV-1 Vif-APO3G interaction. The binding characteristics between HIV-1 Vif and APO3G were examined by co-immunoprecipitating 1 μM HIV-1 Vif with 1 μM APO3G in the presence or absence of serial dilutions of the following 15-mer peptides: Vif(25-39) (A), Vif(29-43) (B), Vif(69-83) (C), and Vif(125-139) (D). Interactions were analyzed via western blotting using both HIV-1 Vif and APO3G antibodies. **(A)** *Lane 1*: No peptide. *Lane 2-23:* 2/3 serial dilutions starting at 1 mM and ending at 0.30 μM; *lane 6 and 21* marker. **(B.)** *Lane 2*: No peptide. *Lane 3-23:* 2/3 serial dilutions starting at 1 mM and ending at 0.30 μM; *lane 1 and 14* marker. **(C.)** *Lane 2*: No peptide. *Lane 3-23:* 2/3 serial dilutions starting at 1 mM and ending at 0.30 μM; *lane 1 and 14* marker. **(D.)** *Lane 1*: No peptide. *Lane 2-23:* 2/3 serial dilutions starting at 1 mM and ending at 0.30 μM; *lane 6 and 20* marker. Along with the western blots for each peptide (A-D) a representative plot of relative Vif/APO3G band intensity versus concentration (μM) is shown plotted on a semi-log scale. In addition, for each peptide (A-D) a histogram is shown of relative [Vif/APO3G + respective peptide]/[Vif/APO3G + no peptide] at each concentration. These histograms are the average of two experiments and plotted along with the standard deviation for each concentration. Vif(25-39) and Vif(29-43) at concentrations above 88 μM and 17 μM, respectively, appear to disrupt the interaction between APO3G and HIV-1 Vif as compared with the no-peptide control. Below these peptide concentrations, Vif(69-83) and Vif(125-139) appeared to have no effect on APO3G or HIV-1 Vif. These experiments were repeated in duplicate, with similar results in each case.

Ideally the no peptide control lane would be the most intense band, thus giving the largest ratio of Vif/APO3G. In this case the histograms would not exceed 1 on the y-axis. However, in these experiments the no peptide control was not always the most intense band and the Vif/APO3G normalization of some lanes where neither HIV-1 Vif nor APO3G were readily detectable gave a normalized band intensity larger than the no peptide control, thus giving y-axis values above 1.

Figure 4.5

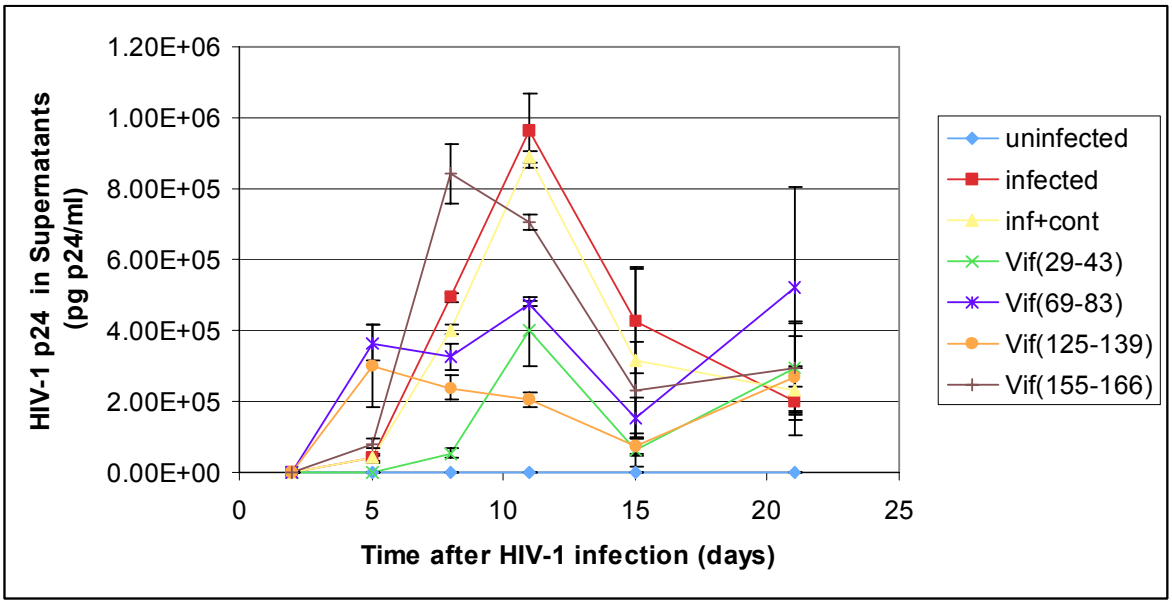
1.20E+06
1.00E+06
8.00E+05
6.00E+05
4.00E+05
2.00E+05
0.00E+00
HIV-1 p24 in Supernatants (pg p24/ml)
0
5
10
15
20
25
Time after HIV-1 infection (days)
uninfected
infected
inf+cont
Vif(29-43)
Vif(69-83)
Vif(125-139)
Vif(155-166)

Figure 4.5. HIV-1 Vif peptides inhibit viral replication *in vitro*. Cells were incubated in the presence of each respective peptide until day 15, after day 15 peptides were removed. No replication was observed in the uninfected control (blue diamonds). HIV-1 Vif peptides, Vif(29-43), Vif(69-83), and Vif(125-139), reduced the amount of p24 expressed in infected cells (green X Vif(29-43), blue asterisk Vif(69-83), and orange circle Vif(125-139)) as compared to the infected control (red squares). In addition, Vif(155-166) reduced the amount of p24 observed to a lesser extent then the other HIV-1 Vif peptides (purple plus sign). p24 levels for the PKC control did not differ from those of infected controls (yellow triangles versus red squares). Removing the peptides after day 15 led to a rebound in viral p24 production (blue asterisks, green X, orange circles). This experiment was repeated in duplicate and an average of both of these experiments is represented in the graph above plotted with standard deviation for each point.

Vif peptides that can disrupt the putative HIV-1 Vif-APO3G interaction, and HIV-1 Vif peptides that disrupt viral replication. These data were obtained using co-immunoprecipitation and peptide-competition experiments. Viral replication data was obtained using HIV-1 Vif peptides tagged with antennapedia, a cellular uptake signal.

This study shows that HIV-1 Vif oligomerization is concentration dependent. As the protein concentration decreases the number of oligomers, dimers and trimers, observed decreases. The amount of monomer appears to increase. This finding indicates that cross-linking is not due to nonspecific protein-protein interactions. Further analysis with a larger protein concentration range could lead to an approximate K_d for HIV-1 Vif dimerization.

The formation of HIV-1 Vif dimers was reduced by two HIV-1 Vif peptides, Vif(29-43) and Vif(125-139). This result suggests that both of these regions are important for HIV-1 Vif dimerization, consistent with my observation that the N-terminus of one HIV-1 Vif monomer cross-links with the C-terminus of another HIV-1 Vif monomer (Auclair, 2007). In particular, these two HIV-1 Vif peptides include either Lys34 or Glu134, which also comprise the proposed "hot spot" of biological activity (Auclair, 2007). These peptides could be used as scaffolds to design new drugs that disrupt oligomerization, thus potentially inhibiting HIV-1 Vif function.

The peptides used to examine their effect on HIV-1 oligomerization were also used to disrupt the Vif-APO3G interaction as assessed by co-immunoprecipitation. Two of these peptides, Vif(25-39) and Vif(29-43), appeared to decrease the amount of APO3G

immobilized on affinity beads and thus the amount of HIV-1 Vif co-immunoprecipitated. The action of these two peptides is interesting because they might be disrupting the APO3G-antibody interaction in the co-IP, aggregating APO3G, and/or disrupting the APO3G-Vif interaction.

To further elucidate the role of these peptides [Vif(25-39), Vif(29-43), Vif(69-83), and Vif(125-139)] in disrupting the HIV-1 Vif-APO3G interaction I performed serial dilution experiments and co-immunoprecipitations. In an ideal experimental condition I would use concentrations of APO3G 2-3-fold higher than the K_d, but to date there are no K_d values for the APO3G-Vif interaction [Preliminary surface plasmon resonance experiments suggest it may be on the order of 100 μM (Appendix 2)]. Due to protein instability the highest concentration of APO3G attainable is approximately 27 μM. Therefore, due to the limited amount of APO3G, serial dilution experiments were performed with an equimolar amount of HIV-1 Vif and APO3G (1μM). Vif(69-83) and Vif(125-139) appeared to have no effect on the amount of HIV-1 Vif or APO3G present in the serial dilution IPs (Figure 4C and 4D), but both Vif(25-39) and Vif(29-43) at concentrations above 88 μM and 17 μM, respectively, seemed to reduce the amount of Vif and APO3G. Below these two concentrations the peptides had no apparent effect on HIV-1 Vif binding to APO3G (Figure 4A and 4B).

The different concentration ranges in which these peptides affect APO3G suggest that one may more strongly inhibit the Vif-APO3G interaction than the other. The serial dilution experiments confirmed the single concentration experiments, suggesting that these two peptides may disrupt the APO3G-antibody interaction or the Vif-APO3G

interaction, or aggregate APO3G. The site at which these HIV-1 Vif peptides bind is unclear; they could bind to the APO3G antibody, to HIV-1 Vif, or to APO3G. In the last case, the peptide might change the protein conformation, thus preventing the protein-antibody interactions. However, the HIV-1 Vif peptide is unlikely to bind the APO3G antibody because the APO3G antibody binds strongly the APO3G protein. This issue might be addressed by varying the order in which components are added to the reaction. Another possibility is that the peptides trigger a conformational change in APO3G, thus releasing it from its antibody (Figure 4.6).

Although for these experiments I assume HIV-1 Vif and APO3G bind directly and the majority of evidence suggests that, it is possible that the HIV-1 Vif-APO3G interaction is mediated via another macromolecule. For example, both proteins are known to bind RNA, suggesting that their interaction could be mediated by RNA (Svarovskaia, 2004; Henriet, 2005). To rule out this possibility, further investigation is needed. A large-scale mutational analysis of HIV-1 Vif and APO3G in the presence of RNase A would help elucidate whether in fact their interaction was direct.

Whether the peptides bind to APO3G or HIV-1 VIf could be determined by direct ELISA in which peptides are immobilized. If the HIV-1 Vif peptides in fact aggregate APO3G, this finding would suggest a novel function for HIV-1 Vif, i.e., that it can aggregate APO3G prior to proteosomal degradation. Such a finding would be consistent with the suggestion that targeting APO3G to the proteosome and preventing its incorporation into virions are unique functions of HIV-1 Vif (Opi, 2006; Opi, 2007). Therefore, it is tempting to speculate that the decrease of APO3G I observe with Vif(25-

39) and Vif(29-43) may be a mechanism for HIV-1 Vif to inhibit incorporation of APO3G into virions.

Furthermore, the ability of Vif(25-39) and Vif(29-43) to disrupt the HIV-1 Vif-APO3G interaction was likely specific for four reasons. First, the no-peptide control cultures had the highest concentration of DMSO, which did not affect the proteins or their interaction. Second, peptides Vif(69-83) and Vif(125-139) did not affect APO3G, HIV-1 Vif, or their interaction, although the experiments were conducted under the same conditions as for Vif(25-39) and Vif(29-43). Third, the highest concentrations of DMSO used in HIV-1 Vif-APO3G experiments were also used in the peptide-competition experiment of oligomerization where they had no affect on the HIV-1 Vif protein. Fourth, the concentrations at which Vif(25-39) and Vif(29-43) disrupted the HIV-1 Vif-APO3G interaction, 88μM and 17μM respectively, were consistent among multiple experiments for each peptide.

Some of the same peptides used in the competition experiments were also used in preliminary in vitro cellular experiments to test whether they have an effect on viral replication. An antennapedia tag was used for cellular uptake of HIV-1 Vif peptides. These peptides, which correspond to the "hot spot" for biological activity, reduced the amount of p24 observed, and thus reduced the levels of viral replication. For example, HIV-1 Vif peptides Vif(29-43), Vif(69-83) and Vif(125-139) all reduced the amount of p24 observed in cell-free culture supernatants by approximately an order-of-magnitude compared to the infected positive control. While these experiments suggest inhibitory effects of the selected HIV-1 Vif peptides on spread of viral infection in the test-cultures,

Figure 4.6

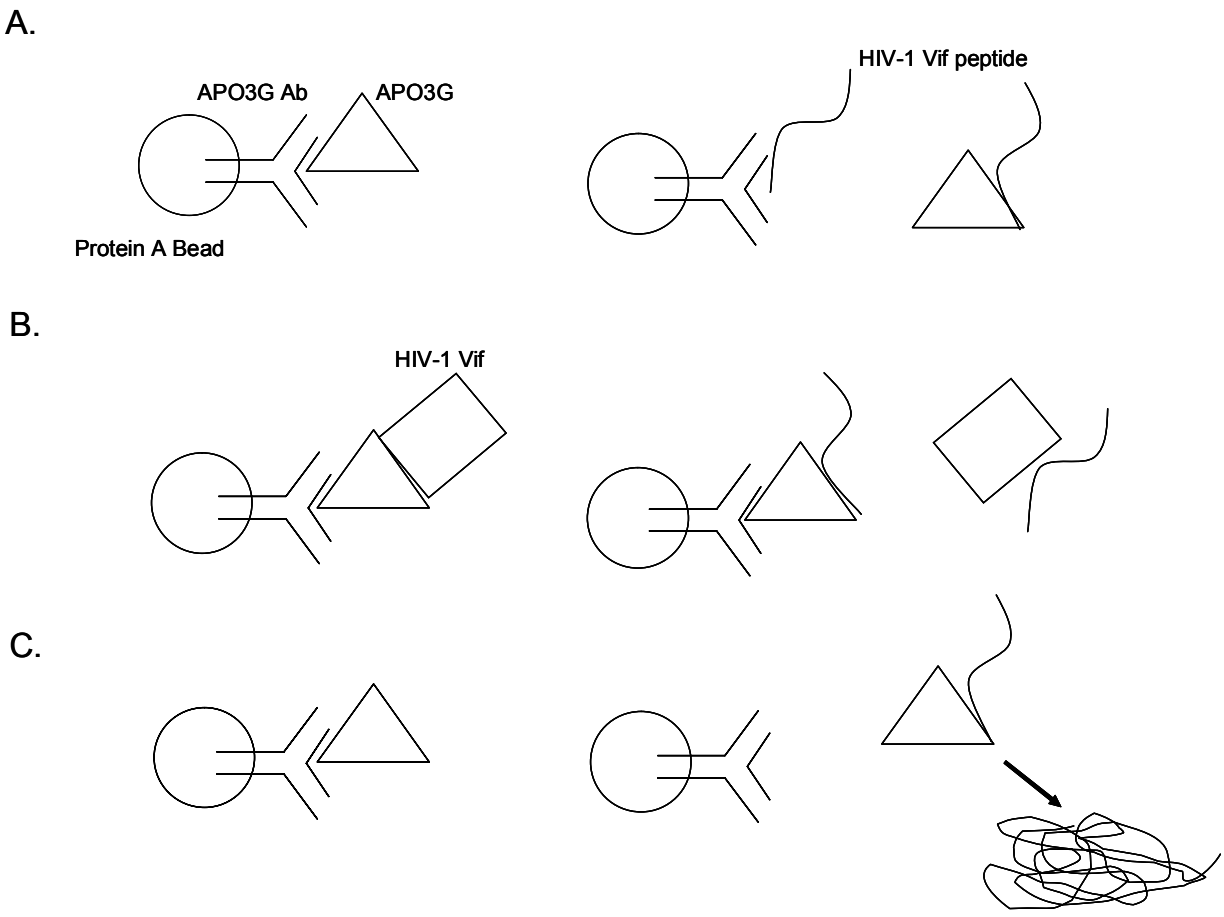

Figure 4.6: Proposed mechanisms for Vif(25-39) and Vif(29-43) inhibition of the HIV-1 Vif-APO3G interaction. (A.) Vif(25-39) and Vif(29-43) could inhibit the interaction between APO3G and its antibody, thus preventing its immobilization and co-immunoprecipitation with HIV-1 Vif. Another possibility is that the peptides could trigger a conformational change in APO3G, thus releasing it from its antibody **(B.)** Vif(25-39) and Vif 29-43) could inhibit the interaction between APO3G and HIV-1 Vif. For both (A.) and (B.), it is unclear to which protein the peptide binds, but in the case of (B.) a peptide interaction with APO3G might explain why it is not immobilized. Peptide binding could cause a conformational change in APO3G and prevent its binding to both HIV-1 Vif and the antibody. **(C.)** Vif(25-39) and Vif(29-43) could bind to APO3G and nucleate its aggregation.

it will be necessary to determine whether the virus in cell-free supernatant collected from the peptide-treated cultures retained infectivity-potential by using it in primary infections of permissive or nonpermissive cells. These experiments will delineate whether the HIV-1 Vif peptides blocked Vif-APO3G interaction leaving free APO3G to be packaged in the output virus. Further experiments are needed to elucidate the direct or indirect mechanism of the inhibitory effects of the peptides and to determine the exact role of APO3G. Experiments that would potentially allow us to obtain this information will be to perform similar in vitro experiments in permissive cells, where APO3G is absent, and experiments using HIV-1 with no functional Vif (Vif-deleted) and monitor viral replication.

Thus, the peptide-competition experiments suggest a role for the HIV-1 N-terminus in oligomerization and the Vif-APO3G interaction. These results are consistent with a previous report of HIV-Vif peptides disrupting the Vif-APO3G interaction (Mehle, 2007). In that study, N-terminal peptides disrupted the Vif-APO3G interaction with the most potent effect shown by Vif(57-71). This inhibition by Vif(57-71) was dose-dependent, and the Vif(57-71) mutant Y69A/W70A failed to inhibit the Vif-APO3G interaction, suggesting that the inhibition is specific and that Y69 and W70 are critical residues in the interaction. On the other hand, Vif(25-39) appeared to enhance the Vif-APO3G interaction in that study, whereas the same peptide appeared to reduce the HIV-1 Vif- APO3G interaction in mine. In both studies, Vif(125-139) did not affect Vif-APO3G binding. Although further experiments are necessary to conclusively understand the mechanism by which these peptides interfere with the HIV-1 Vif-APO3G interaction,

these data taken with those reported here demonstrate that N-terminal peptides impact the HIV-1 Vif-APO3G interaction (Mehle, 2007).

Here I show that HIV-1 Vif oligomerization is concentration dependent, thus not due to random protein-protein interactions from aggregation. HIV-1 Vif oligomerization was apparently blocked by HIV-1 Vif peptides, Vif(29-43) and Vif(125-139), consistent with my structural analysis implicating residues 34 and 134 in a "hot spot" for biological activity (Auclair, 2007). The results presented here also indicate that Vif(25-39) and Vif(29-43) reduce the co-IP of APO3G and HIV-1 Vif . In addition, I show that the two HIV-1 Vif peptides that disrupted oligomerization and one peptide that disrupted the HIV-1 Vif-APO3G interaction mapped to similar regions, suggesting that oligomerization and Vif-APO3G binding may use similar binding sites. All these data are consistent with a putative "hot spot" for biological activity at Lys34 and Glu134 in HIV-1 Vif (Auclair, 2007) and suggest they may also be important for the Vif-APO3G interaction. Finally, I showed that HIV-1 Vif peptides [Vif(29-43), Vif(69-83), and Vif(125-139)] tagged with antennapedia could reduce the amount of viral replication in nonpermissive cells. Thus, these residues could be targeted in the design of potential inhibitors to disrupt this interaction. Disrupting this interaction would prevent degradation of APO3G, allowing it to act against the viral cDNA and prevent infectivity. By identifying peptides that disrupt HIV-1 Vif oligomerization and affect HIV-1 Vif and/or APO3G, this study present novel agents that can be used as scaffolds in designing novel drugs for HIV-1/AIDS.

REFERENCES

Auclair, J., K. Green, S. Shandilya, J. Evans, M. Somasundaran and C. Schiffer (2007). "Mass spectrometry analysis of HIV-1 Vif reveals an increase in ordered structure upon oligomerization in regions necessary for viral infectivity." PROTEINS: Structure, Function, and Genetics **69**(2): 270-84.

Bardy, M., B. Gay, S. Pebernard, N. Chazal, M. Courcoul, R. Vigne, E. Decroly and P. Boulanger (2001). "Interaction of human immunodeficiency virus type 1 Vif with Gag and Gag-Pol precursors: co-encapsidation and interference with viral protease-mediated Gag processing." Journal of General Virology **82**: 2719-2733.

Bishop, K. N., R. K. Holmes, A. M. Sheehy, N. O. Davidson, S.-J. Cho and M. H. Malim (2004). "Cytidine Deamination of Retroviral DNA by Diverse APOBEC Proteins." Current Biology **14**: 1392-1396.

Bishop, K. N., R. K. Holmes, A. M. Sheehy and M. H. Malim (2004). "APOBEC-mediated editing of viral RNA." Science **305**(5684): 645.

Bouyac, M., M. Courcoul, G. Bertoia, Y. Baudat, D. Gabuzda, D. Blanc, N. Chazal, P. Boulanger, J. Sire, R. Vigne and B. Spire (1997). "Human Immunodeficiency Virus Type 1 Vif Protein Binds to the Pr55Gag Precursor." Journal of Virology **71**(12): 9358-9365.

Cancio, R., S. Spadari and G. Maga (2004). "Vif is an auxiliary factor of the HIV-1 reverse transcriptase and facilitates abasic site bypass." Journal of Biochemistry **383**(3): 475-482.

Doehle, B. P., A. Schafer, H. L. Wiegand, H. P. Bogerd and B. R. Cullen (2005). "Differential Sensitivity of Murine Leukemia Virus to APOBEC3-Mediated Inhibition Is Governed by Virion Exclusion." Journal Of Virology **79**(13): 8201-8207.

Gabuzda, D. H., K. Lawrence, E. Langhoff, E. Terwilliger, T. Dorfman, W. A. Haseltine and J. Sodroski (1992). "Role of vif in replication of human immunodeficiency virus type 1 in CD4+ T lymphocytes." Jounal of Virology **66**: 6489-6495.

Harris, R. S. and M. T. Liddament (2004). "Retroviral Restriction By APOBEC Proteins." Nature Reviews Immunology **4**: 868-877.

Henriet, S., D. Richer, S. Bernacchi, E. Decroly, R. Vigne, B. Ehresmann, C. Ehresmann, J.-C. Paillart and R. Marquet (2005). "Cooperative and Specific Binding of Vif to the 5' Region of HIV-1 Genomic RNA." Journal of Molecular Biology **354**: 55-72.

Holmes, R., M. Malim and K. Bishop (2007). "APOBEC-mediated viral restriction: not simply editing?" Trends Biochem Sci **32**(3): 118-28.

Huvent, I., S. S. Hong, C. Fournier, B. Gay, J. Tournier, C. Carriere, M. Courcoul, R. Vigne, B. Spire and P. Boulanger (1998). "Interaction and co-encapsidation of human immunodeficiency virus type 1 Gag and Vif recombinant proteins." Journal of General Virology **79**: 1069-1081

Kan, N. C., G. Franchini, F. Wong-Staal, G. C. DuBois, W. G. Robey, J. A. Lautenberger and T. S. Papas (1986). "Identification of HTLV-IIII/LAV sor Gene Product and Detection of Antibodies in Human Sera." Science **231**: 1553-1555.

Kobayashi, M., A. Takaori-Kondo, Y. Miyauchi, K. Iwai and T. Uchiyama (2005). "Ubiquitination of APOBEC3G by an HIV-1 Vif-Cullin5-ElonginB-ElonginC complex is essential for Vif function." Journal of Biological Chemistry **280**(19): 18573-8.

Lecossier, D., F. Bouchonnet, F. Clavel and A. J. Hance (2003). "Hypermutation of HIV-1 DNA in the Absence of the Vif Protein." Science **300**(5622): 1112.

Lee, T.-H., J. E. Coligan, J. S. Allan, M. F. McLane, J. E. Groopman and M. Esses (1986). "A New HTLV-III/LAV Protein Encoded by a Gene Found in Cytopathic Retroviruses." Science.

Liddament, M. T., W. L. Brown, A. J. Schumacher and R. S. Harris (2004). "APOBEC3F Properties and Hypermutation Preferences Indicate Activity against HIV-1 in Vivo." Current Biology **14**: 1385-1391.

Luo, K., Z. Xiao, E. Ehrlich, Y. Yu, B. Liu, S. Zheng and X.-F. Yu (2005). "Primate lentiviral virion infectivity factors are substrate receptors that assemble with cullin 5-E3 ligase through a HCCH motif to suppress APOBEC3G." Proc. Natl. Acad. Sci USA **102**(32): 11444-11449.

Mangeat, B., P. Turelll, G. Caron, M. Friedll, L. Perrin and D. Trono (2003). "Broad antiretroviral defence by human APOBEC3G through lethal editing of nascent reverse transcripts." Nature **424**(6944): 99-103.

Mehle, A., J. Goncalves, M. Santa-Marta, M. McPike and D. Gabuzda (2004). "Phosphorylation of a novel SOCS-box regulates assembly of the HIV-1 Vif-Cul5 complex that promotes APOBEC3G degradation." Genes & Development **18**(23): 2861-2866.

Mehle, A., B. Strack, P. Ancuta, C. Zhang, M. McPike and D. Gabuzda (2004). "Vif Overcomes the Innate Antiviral Activity of APOBEC3G by Promoting Its Degradation in the Ubiquitin-Proteasome Pathway." Journal of Biological Chemistry **279**(9): 7792-7798.

Mehle, A., E. R. Thomas, K. S. Rajendran and D. Gabuzda (2006). "A zinc-binding region in Vif binds Cul5 and determines Cullin selection." Journal of Biological Chemistry **281**(25): 17259-65.

Mehle, A., H. Wilson, C. Zhang, A. Brazier, M. McPike, E. Pery and D. Gabuzda (2007). "Identification of an APOBEC3G Binding Site in HIV-1 Vif and Inhibitors of Vif-APOBEC3G Binding." Journal of Virology **81**(23): 13235-41.

Opi, S., S. Kao, R. Goila-Gaur, M. Khan, E. Miyagi, H. Takeuchi and K. Strebel (2007). "Human immunodeficiency virus type 1 Vif inhibits packaging and antiviral activity of a degradation-resistant APOBEC3G variant." Journal of VIrology **81**(15): 8236-46.

Opi, S., H. Takeuchi, S. Kao, M. A. Khan, E. Miyagi, R. Goila-Gaur, Y. Iwatani, J. G. Levin and K. Strebel (2006). "Monomeric APOBEC3G Is Catalytically Active and Has Antiviral Activity." Journal of Virology **80**(10): 4673-4682.

Potash, M. J., G. Bentsman, T. Muir, C. Krachmarov and P. Sova (1998). "Peptide inhibitors of HIV-1 protease and viral infection of peripheral blood lymphocytes based on HIV-1 Vif." Proc. Natl. Acad. Sci USA **95**: 13865-13868.

Russell, R. A. and V. K. Pathak (2007). "Identification of Two Distinct Human Immunodeficiency Virus Type 1 Vif Determinants Critical for Interactions with Human APOBEC3G and APOBEC3F." Journal of Virology **81**(15): 8201-8210.

Schrofelbauer, B., T. Senger, G. Manning and N. R. Landau (2006). "Mutational Alteration of Human Immunodeficiency Virus Type 1 Vif Allows for Functional Interaction with Nonhuman Primate APOBEC3G." Journal of Virology **80**(12): 5984-5991.

Sheehy, A. M., N. C. Gaddis, J. D. Choi and M. H. Malim (2002). "Isolation of a human gene that inhibits HIV-1 infection and is suppressed by the viral Vif protein." Nature **418**(6898): 646-650.

Simon, J. H. M., A. M. Sheehy, E. A. Carpenter, R. A. M. Fouchier and M. H. Malim (1999). "Mutational Analysis of the Human Immunodeficiency Virus Type 1 Vif Protein." Journal of Virology **73**(4): 2675-2681.

Simon, J. H. M., T. E. Southerling, J. C. Peterson, b. E. Meyer and M. H. Malim (1995). "Complementation of vif-Defective Human Immunodeficiency Virus Type 1 by Primate, but Not Nonprimate, Lentivirus vif genes." Journal of Virology **69**(7): 4166-4172.

Sodroski, J., W. C. Goh, C. Rosen, A. Tartar, D. Portetelle, A. Burny and W. Haseltine (1986). "Replicative and Cytopathic Potential of HTLV-III/LAV with sor Gene Deletions." Science **231**: 1549-1553.

Svarovskaia, E. S., H. Xu, J. L. Mbisa, R. Barr, R. J. Gorelick, A. Ono, E. O. Freed, W.-S. Hu and V. K. Pathak (2004). "Human apolipoprotein B mRNA-editing enzyme-catalytic polypeptide-like 3G (APOBEC3G) is incorporated into HIV-1 virions through interactions with viral and nonviral RNAs." Journal of Biological Chemistry **279**(24): 35822-35828.

vonSchwedler, U., J. Song, C. Aiken and D. Trono (1993). "Vif is crucial for human immunodeficiency virus type 1 proviral DNA synthesis in infected cells." Journal of Virology **67**: 4945-4955.

Wiegand, H. L., B. P. Doehle, H. P. Bogerd and B. R. Cullen (2004). "A second human antiretroviral factor, APOBEC3F, is suppressed by the HIV-1 and HIV-2 Vif proteins." The Embo Journal **23**(12): 2451-2458.

Xiao, Z., E. Ehrlich, K. Luo, Y. Xiong and X. Yu (2007a). "Zinc chelation inhibits HIV Vif activity and liberates antiviral function of the cytidine deaminase APOBEC3G." FASEB J **21**(1): 217-22.

Xiao, Z., E. Ehrlich, Y. Yu, K. Luo, T. Wang, C. Tian and X.-F. Yu (2006). "Assembly of HIV-1 Vif-Cul5 E3 ubiquitin ligase through a novel zinc-binding domain-stabilized hydrophobic interface in Vif." Virology **349**(2): 290-9.

Xiao, Z., Y. Xiong, W. Zhang, L. Tan, E. Ehrlich, D. Guo and X. Yu (2007b). "Characterization of a Novel Cullin5 Binding Domain in HIV-1 Vif." Journal of Molecular Biology **373**(3): 541-50.

Yang, B., L. Li, Z. Lu, X. Fan, C. A. Patel, R. J. Pomerantz, G. C. DuBois and H. Zhang (2003). "Potent Suppression of Viral Infectivity by the Peptides That Inhibit Multimerization of Human Immunodeficiency Virus Type 1 (HIV-1) Vif Proteins." The Journal of Biological Chemistry **278**(8): 6596-6602.

Yang, S., Y. Sun and H. Zhang (2001). "The Multimerization of Human Immunodeficiency Virus Type 1 Vif Protein." The Journal of Biological Chemistry **276**(7): 4889-4893.

Yu, X., Y. Yu, B. Liu, K. Luo, W. Kong, P. Mao and X.-F. Yu (2003). "Induction of APOBEC3G Ubiquitination and degradation by an HIV-1 Vif-Cul5-SCF Complex." Science **302**(5647): 1056-1060.

Yu, Y., Z. Xiao, E. S. Ehrlich, X. Yu and X.-F. Yu (2004). "Selective assembly of HIV-1 vif-Cul5 ElonginB-ElonginC E3 ubiquitin ligase complex through a novel SOCS box and upstream cysteines." Genes & Development **18**: 2867-2872.

Zhang, H., B. Yang, R. J. Pomerantz, C. Zhang, S. Arunachalam and L. Gao (2003). "The cytidine deaminase CEM15 induces hypermutation in newly synthesized HIV-1 DNA." Nature **424**(6944): 94-98.

Zheng, Y.-H., D. Irwin, T. Kurosu, K. Tokunaga, T. Sata and B. M. Peterlin (2004). "Human APOBEC3F Is Another Host Factor That Blocks Human Immunodeficiency Virus Type 1 Replication." Journal of Virology **78**(11): 6073-6076.

CHAPTER V

DISCUSSION

Millions of people worldwide are infected with AIDS, and no cure is currently known. The greatest hope for controlling the expanding HIV epidemic is developing a preventive HIV vaccine. Despite almost 20 years of effort, the search for a beneficial HIV vaccine continues. The HIV vaccine field is a very active and challenging one that will continue to push forward understanding of basic immunology and drive the development of new vaccine technologies. However, in the absence of a vaccine HIV/AIDS has been successfully treated by current drug regimens, but these drugs are becoming less effective due to drug resistance. Drug resistance is a change in molecular recognition that allows viral proteins to evade current drugs, creating a need for novel drug targets. One such target is the interaction between HIV-1 Vif and the host cell antiviral protein, APOBEC3G (APO3G).

An effective approach to designing inhibitors to disrupt the HIV-1 Vif-APO3G interaction is based on target structure, but no structural information is currently available for either HIV-1 Vif or APO3G. Therefore, my dissertation research focused on collecting and analyzing structural data for possible use in targeting HIV-1 Vif and to elucidate mechanisms of HIV-1 Vif function.

Structural Analysis of HIV-1 Vif

At the time this dissertation was written, HIV-1 Vif was the only HIV-1 protein with no available structural data (crystallographic or NMR structure). Therefore, I made extensive attempts to express and purify soluble HIV-1 Vif and APO3G proteins for use in crystallographic studies (Appendix I). To that end, diverse strategies were employed, including using different strains of HIV-1 Vif, multiple fusion proteins known to increase

solubility, expressing Vif and APO3G in both *E. coli* and baculovirus, and co-expressing HIV-1 Vif with APO3G. One fusion-protein tag, NusA, did produce large quantities of soluble HIV-1 Vif protein that oligomerized (Appendix I) in a similar fashion to the untagged HIV-1 Vif protein (Chapter III). However, when the NusA tag was cleaved, the HIV-1 Vif protein was unstable and precipitated/aggregated. Since large quantities of soluble HIV-1 Vif and APO3G proteins were not obtainable, I used mass spectrometry and cross-linking to obtain low-resolution structural data on HIV-1 Vif (Yao, 2001; Back, 2002; Back, 2003; Sinz, 2003; Trester-Zedlitz, 2003; Sinz, 2006).

These studies gave insights into the tertiary and quaternary structures of HIV-1 Vif by identifying both intra- and inter-molecular cross-links (Chapter III). The majority of intra-molecular cross-links were found in the N-terminal region of the HIV-1 Vif monomer, whereas almost no intra-molecular cross-links were found in the C-terminus. Thus, the N-terminal domain of HIV-1 Vif is folded into a compact and globular structure, and the C-terminal domain may be disordered. The N-terminal region of HIV-1 Vif, which is responsible for binding to RNA (Dettenhofer, 2000; Cancio, 2004; Henriet, 2005; Bernacchi, 2007; Henriet, 2007), APO3G (Sheehy, 2002; Marin, 2003; Sheehy, 2003; Stopak, 2003; Russell, 2007), and APO3F (Bishop, 2004; Liddament, 2004; Wiegand, 2004; Zheng, 2004; Russell, 2007) might do so through a specific-binding interface, whereas the disorder in the C-terminus may facilitate binding of a diverse set of proteins such as Cullin5, elongin C, NcP7 Gag, and HIV-1 Vif itself.

The lack of intra-molecular cross-links in the C-terminus of monomeric HIV-1 Vif led me to hypothesize that the C-terminus was disordered. This hypothesis was

tested by submitting the HIV-1 Vif sequence to PONDR®, a program that predicts regions of disorder in proteins based on a series of sequence-prediction algorithms. The C-terminus of HIV-1 Vif was predicted to be disordered, as well as the C-termini of HIV-2 and simian immunodeficiency virus (SIV) Vif. In addition, I observed only a few cross-links in the HIV-1 Vif monomer suggesting the C-termini is disordered. New inter-molecular cross-links in the dimer and trimer species of HIV-1 Vif suggested a disorder-to-order transition in the C-termini (Chapter III). These inter-molecular cross-links were between the N-terminus of one HIV-1 Vif monomer and the C-terminus of another HIV-1 Vif monomer, suggesting that oligomerization occurs in a head-to-tail fashion. These new cross-links in the HIV-1 Vif C-terminus suggest that it undergoes a disorder-to-order transition during oligomerization. This mechanism of action may be general, applying to other HIV-1 Vif C-terminal binding partners such as elongin C, Cullin5, and NcP7, which may undergo a disorder-to-order transition during binding.

Drawing from my inter-molecular cross-linking results, I hypothesized that Lys34 and Glu134 come in proximity to each other in 3-dimensional space, forming a “hot spot” for biological activity. This possibility is consistent with evidence that mutating residues around 34 and 134 reduced viral infectivity by greater than 85% (Simon, 1999). Further support for my hypothesis for a “hot spot” of biological activity is that Lys34 is adjacent to the HIV-1 Vif binding domains for APO3G, APO3F, RNA (Dettenhofer, 2000; Sheehy, 2002; Marin, 2003; Sheehy, 2003; Stopak, 2003; Bishop, 2004; Cancio, 2004; Liddament, 2004; Wiegand, 2004; Zheng, 2004; Henriet, 2005; Bernacchi, 2007; Henriet, 2007; Russell, 2007) and Glu134 is near the binding domains for Cullin5, elongin C,

NcP7 Gag, and oligomerization (Bouyac, 1997; Huvent, 1998; Yang, 2001; Yang, 2003; Kobayashi, 2004; Mehle, 2004; Yu, 2004; Kobayashi, 2005; Luo, 2005; Mehle, 2006; Xiao, 2006; Auclair, 2007; Xiao, 2007a; Xiao, 2007b) domains.

This analysis of low-resolution structural data identified regions in HIV-1 Vif that may be ideal targets for small-molecule inhibitors. The analysis also elucidated a potential mechanism in which HIV-1 Vif undergoes a disorder-to-order transition to interact with a diverse set of proteins and nucleic acids. Disrupting this transition may also prove to be a useful target for future drug design. Therefore, the structural data collected provide a useful guide to future structural and functional studies of HIV-1 Vif.

Drug Design

Another strategy to confirm my low-resolution structural analysis and to identify potential scaffolds for novel drug design was to explore HIV-1 Vif peptides that competed with HIV-1 Vif oligomerization and the HIV-1 Vif-APO3G interaction (Chapter IV). I found that peptides HIV-1 Vif(29-43) and Vif(125-139) inhibited HIV-1 Vif oligomerization, specifically dimerization. This result confirmed my previous low-resolution structural analysis and identified two HIV-1 Vif peptides that could be used as scaffolds in drug design.

In addition to disrupting HIV-1 Vif oligomerization, I tested the same peptides in co-immunoprecipitation experiments to determine if they disrupted the HIV-1 Vif-APO3G interaction. Two HIV-1 Vif peptides, Vif(25-39) and Vif(29-43), decreased the amount of co-immunoprecipitated complex. Analysis of these complexes reveals that the peptides may have other effects besides disrupting the HIV-1 Vif-APO3G interaction.

The peptides might also be: (1) disrupting the APO3G-antibody interaction, (2) aggregating APO3G, and/or (3) exerting an unknown effect on HIV-1 Vif. Further investigation is needed into the mechanisms of action of these peptides, but they remain attractive therapeutic scaffolds because of their proximity to the potential "hot spot" for biological activity (Chapter III) and to a recently proposed APO3G-binding site (Russell, 2007).

In addition, I have done preliminary in vivo experiments using the cellular uptake, tag, antennapedia. I infected nonpermissive cells with a protein kinase C scrambled control peptide and three HIV-1 Vif peptides: HIV-1 Vif(29-43), HIV-1 Vif(69-83), and HIV-1 Vif(125-139). Two of the three peptides, HIV-1(29-43) and HIV-1 Vif(125-139) map to the proposed "hot spot" for biological activity (Chapter III). The PKC control peptide did not reduce the amount of p24 observed, whereas each HIV-1 Vif peptide reduced the amount of p24 by approximately an order of magnitude. These preliminary results suggest that these HIV-1 Vif peptides could be used as scaffolds for the design of novel drugs.

Future Research Directions

HIV-1 Vif plays significant roles in interacting with multiple proteins (Bouyac, 1997; Huvent, 1998; Yang, 2001; Yang, 2003; Kobayashi, 2004; Mehle, 2004; Yu, 2004; Kobayashi, 2005; Luo, 2005; Mehle, 2006; Xiao, 2006; Auclair, 2007; Xiao, 2007a; Xiao, 2007b) and RNA (Dettenhofer, 2000; Cancio, 2004; Henriet, 2005; Bernacchi, 2007; Henriet, 2007) , as well as in preventing the antiviral activity of APO3G (Sheehy, 2002; Marin, 2003; Sheehy, 2003; Stopak, 2003; Russell, 2007), making it an important

protein to characterize. However, the difficulties of working with full-length HIV-1 Vif protein in biochemical and biophysical studies have led to studying HIV-1 Vif by characterizing its protein fragments. An interesting fragment to consider in future studies would be a C-terminal mutant. Such studies could include further analysis of maltose binding protein (MBP)-Vif_{140} and MBP-Vif_{150} mutants with a truncated C-terminus (Appendix I). My prediction that the C-terminus is intrinsically disordered (Chapter III) suggests that removing it would make HIV-1 more stable and expressible, while maintaining functionality specific to its N-terminus. Thus, one could use such N-terminal fragments to elucidate specific interactions between HIV-1 Vif and APO3G, APO3F, and RNA.

The reciprocal approach could also be taken. C-terminal fragments could be generated, and if these proteins were expressible and stable, their interactions with HIV-1 Vif-binding partners could be studied. For example, a C-terminal Vif mutant containing the Cullin5-binding domain, residues 108-139, could be expressed and incubated with Cullin5 (Kobayashi, 2005; Luo, 2005; Mehle, 2006; Xiao, 2006; Xiao, 2007a; Xiao, 2007b). The resulting complex of Cullin5 with this C-terminal HIV-1 Vif fragment could be analyzed by x-ray crystallography to determine its structure, leading to an understanding of these two proteins at the atomic level. The HIV-1 Vif fragments for such studies could be elucidated by cross-linking and mass spectrometric analyses (Chapter III). Indeed, two HIV-1 Vif regions, residues 34-61 and 158-192, which were identified as involved in oligomerization (Chapter III), could be synthesized and studied with their respective binding partners. The HIV-1 Vif(34-61) fragment could help

elucidate interactions with both APO3G and RNA, whereas a fragment from 158-192 could help elucidate interactions with Elongin C, HIV-1 Gag, and oligomerization.

To obtain soluble HIV-1 Vif, mutants could be generated and screened for solubility. One approach would be to produce random mutations in GFP-tagged HIV-1 Vif, transform into bacterial cells ,and select for soluble mutant protein in green fluorescent colonies. Soluble HIV-1 Vif could be isolated from green colonies and sequenced for use in further structural and biochemical analysis. In addition to a mutagenesis screen for solubility, HIV-1 Vif mutants could be screened for failure to oligomerize, which might improve solubility; the monomeric form of HIV-1 Vif may be more soluble and easier to work with (Chapter III; Appendix I).

Another approach to identifying HIV-1 Vif fragments would be limited proteolysis. HIV-1 Vif could be incubated with different proteases, thus creating unique cleavage products. The HIV-1 Vif regions most accessible to proteases (unstructured domains) would likely be cleaved first, whereas those less accessible (compact domains) would likely not be cleaved. Therefore, limited proteolysis would likely identify compact globular domains that could be used to study HIV-1 Vif's binding characteristics. These domains might also be useful in obtaining soluble HIV-1 Vif constructs, which could be used to solve a three-dimensional structure of HIV-1 Vif. The results of limited proteolysis could also confirm my prediction that the HIV-1 Vif C-terminus is disordered. If my prediction is correct, the C-terminal fragment of HIV-1 Vif should be cleaved early and not remain in compact domains.

Based on my prediction that oligomerization of HIV-1 Vif would lead to a disorder-to-order transition of its C-terminal domain (Chapter III), I hypothesized that this transition is a general mechanism by which HIV-1 Vif binds to its diverse set of interaction partners. Therefore, it is important to further examine this transition using techniques such as NMR, which allows proteins to be studied in solution and to gain insights into their protein dynamics. Therefore, NMR data could be collected on HIV-1 Vif and compared to data on HIV-1 Vif in complex with one of its C-terminal-binding partners such as Elongin C. One would expect the NMR spectra to show a disordered HIV-1 Vif C-terminus, and the emergence of an ordered HIV-1 Vif C-terminus in the presence of Elongin C would support my hypothesis. Further support for this hypothesis could be gained by cross-linking and mass spectroscopic analysis of HIV-1 Vif and its binding partners such as APO3G. An increase in cross-links in the C-terminus of HIV-1 Vif upon binding to APO3G or HIV-1 Gag would support a general mechanism for protein-protein interactions being facilitated by a disorder-to-order transition.

In addition to *in vitro* characterization of the structural interactions between HIV-1 Vif and its binding partners, these interactions could be studied *in vivo* (cell culture). The HIV-1 Vif regions involved in oligomerization and in cross-links, 34-61 and 158-192, the region surrounding the proposed “hot spot” for biological activity (Chapter III), could be mutated and analyzed *in vivo* to elucidate their role in infectivity. If deleting or substituting these residues reduced viral infectivity, this finding would suggest that infectivity is related to protein-protein interactions. The importance of these regions in

HIV-1 Vif could be confirmed by cross-linking HIV-1 Vif to its binding partners such as APO3G.

Another approach to *in vivo* studies of HIV-1 Vif interactions would be to examine the effect of disrupting HIV-1 Vif oligomerization. Nonpermissive cells could be infected with NL4-3 HIV-1 and cultured in media spiked with antennapedia-tagged peptides (Vif[29-43] and Vif[125-139]; Chapter IV). Viral replication would be monitored by ELISA for production of p24 core protein in cell supernatants. If these regions are important for infectivity, disrupting them should reduce viral infectivity. Such differences in infectivity could be explored by dose-response studies to tease out the mechanism by which the peptides act.

My initial goal was to obtain large quantities of soluble HIV-1 Vif protein for crystallographic characterization of HIV-1 Vif and identification of functional domains that could be targeted for inhibition. Despite considerable efforts (Appendix I), I did not achieve my goal with full-length protein, but I did obtain low-resolution structural data that was confirmed in peptide-competition experiments. These analyses predicted that HIV-1 Vif contains a compact globular N-terminus and a disordered C-terminus. Analysis of cross-linked HIV-1 Vif oligomers led to the hypothesis that upon HIV-1 Vif oligomerization, its C-terminus undergoes a disorder-to-order transition. This transition may be a general mechanism that allows HIV-1 Vif to bind a large variety of macromolecules. In addition, my structural analysis identified HIV-1 Vif peptides, Vif(29-43) and Vif(125-139), that block oligomerization and can be used as scaffolds for future drug design. Therefore, in the absence of high-resolution structural data, my low-

resolution data advance existing knowledge on the structure and function of HIV-1 Vif by showing that its N-terminus is ordered and that its C-terminus undergoes a disorder-to-order transition upon oligomerization.

REFERENCES

Auclair, J., K. Green, S. Shandilya, J. Evans, M. Somasundaran and C. Schiffer (2007). "Mass spectrometry analysis of HIV-1 Vif reveals an increase in ordered structure upon oligomerization in regions necessary for viral infectivity." PROTEINS: Structure, Function, and Genetics **69**(2): 270-84.

Back, J., V. Notenboom, L. de Koning, A. Muijsers, T. Sixma, C. de Koster and L. de Long (2002). "Identification of cross-linked peptides for protein interaction studies using mass spectrometry and 18O labeling." Anal Chem. **74**(17): 4417-22.

Back, J. W., L. d. Jong, A. O. Muijsers and C. G. d. Koster (2003). "Chemical Cross-linking and Mass Spectrometry for Protein Structural Modeling." Journal Molecular Biology **331**: 303-313.

Bernacchi, S., S. Henriet, P. Dumas, J. Paillart and R. Marquet (2007). "RNA and DNA binding properties of HIV-1 Vif protein: a fluorescence study." Journal of Biological Chemistry **282**(36): 26361-8.

Bishop, K. N., R. K. Holmes, A. M. Sheehy, N. O. Davidson, S.-J. Cho and M. H. Malim (2004). "Cytidine Deamination of Retroviral DNA by Diverse APOBEC Proteins." Current Biology **14**: 1392-1396.

Bishop, K. N., R. K. Holmes, A. M. Sheehy and M. H. Malim (2004). "APOBEC-mediated editing of viral RNA." Science **305**(5684): 645.

Bouyac, M., M. Courcoul, G. Bertoia, Y. Baudat, D. Gabuzda, D. Blanc, N. Chazal, P. Boulanger, J. Sire, R. Vigne and B. Spire (1997). "Human Immunodeficiency Virus Type 1 Vif Protein Binds to the Pr55Gag Precursor." Journal of Virology **71**(12): 9358-9365.

Cancio, R., S. Spadari and G. Maga (2004). "Vif is an auxiliary factor of the HIV-1 reverse transcriptase and facilitates abasic site bypass." Journal of Biochemistry **383**(3): 475-482.

Dettenhofer, M., S. Cen, B. A. Carlson, L. Kleiman and X.-F. Yu (2000). "Association of Human Immunodeficiency Virus Type 1 Vif with RNA and Its Role in Reverse Transcription." Journal of Virology **74**(19): 8938-8945.

Henriet, S., D. Richer, S. Bernacchi, E. Decroly, R. Vigne, B. Ehresmann, C. Ehresmann, J.-C. Paillart and R. Marquet (2005). "Cooperative and Specific Binding of Vif to the 5' Region of HIV-1 Genomic RNA." Journal of Molecular Biology **354**: 55-72.

Henriet, S., L. Sinck, G. Bec, R. Gorelick, R. Marquet and J. Paillart (2007). "Vif is a RNA chaperone that could temporally regulate RNA dimerization and the early steps of HIV-1 reverse transcription." Nucleic Acids Research **35**(15): 5141-53.

Huvent, I., S. S. Hong, C. Fournier, B. Gay, J. Tournier, C. Carriere, M. Courcoul, R. Vigne, B. Spire and P. Boulanger (1998). "Interaction and co-encapsidation of human immunodeficiency virus type 1 Gag and Vif recombinant proteins." Journal of General Virology **79**: 1069-1081

Kobayashi, M., A. Takaori-Kondo, Y. Miyauchi, K. Iwai and T. Uchiyama (2005). "Ubiquitination of APOBEC3G by an HIV-1 Vif-Cullin5-ElonginB-ElonginC

complex is essential for Vif function." Journal of Biological Chemistry **280**(19): 18573-8.

Kobayashi, M., A. Takaori-Kondo, K. Shindo, A. Abudu, K. Fukunaga and T. Uchiyama (2004). "APOBEC3G Targets Specific Virus Species." Journal of Virology **78**(15): 8238-8244.

Liddament, M. T., W. L. Brown, A. J. Schumacher and R. S. Harris (2004). "APOBEC3F Properties and Hypermutation Preferences Indicate Activity against HIV-1 in Vivo." Current Biology **14**: 1385-1391.

Luo, K., Z. Xiao, E. Ehrlich, Y. Yu, B. Liu, S. Zheng and X.-F. Yu (2005). "Primate lentiviral virion infectivity factors are substrate receptors that assemble with cullin 5-E3 ligase through a HCCH motif to suppress APOBEC3G." Proc. Natl. Acad. Sci USA **102**(32): 11444-11449.

Marin, M., K. M. Rose, S. L. Kozak and D. Kabat (2003). "HIV-1 Vif Protein binds the editing enzyme APOBEC3G and induces its degradation." Nature Medicine **9**(11): 1398-1403.

Mehle, A., J. Goncalves, M. Santa-Marta, M. McPike and D. Gabuzda (2004). "Phosphorylation of a novel SOCS-box regulates assembly of the HIV-1 Vif-Cul5 complex that promotes APOBEC3G degradation." Genes & Development **18**(23): 2861-2866.

Mehle, A., E. R. Thomas, K. S. Rajendran and D. Gabuzda (2006). "A zinc-binding region in Vif binds Cul5 and determines Cullin selection." Journal of Biological Chemistry **281**(25): 17259-65.

Russell, R. A. and V. K. Pathak (2007). "Identification of Two Distinct Human Immunodeficiency Virus Type 1 Vif Determinants Critical for Interactions with Human APOBEC3G and APOBEC3F." Journal of Virology **81**(15): 8201-8210.

Sheehy, A. M., N. C. Gaddis, J. D. Choi and M. H. Malim (2002). "Isolation of a human gene that inhibits HIV-1 infection and is suppressed by the viral Vif protein." Nature **418**(6898): 646-650.

Sheehy, A. M., N. C. Gaddis and M. H. Malim (2003). "The Antiretroviral enzyme APOBEC3G is degraded by the proteasome in response to HIV-1 Vif." Nature Medicine **9**(11): 1404-1407.

Simon, J. H. M., A. M. Sheehy, E. A. Carpenter, R. A. M. Fouchier and M. H. Malim (1999). "Mutational Analysis of the Human Immunodeficiency Virus Type 1 Vif Protein." Journal of Virology **73**(4): 2675-2681.

Sinz, A. (2003). "Chemical Cross-linking and mass spectrometry for mapping three-dimensional structures of proteins and protein complexes." Journal of Mass Spectrometery **38**: 1225-1237.

Sinz, A. (2006). "CHEMICAL CROSS-LINKING AND MASS SPECTROMETRY TO MAP THREE-DIMENSIONAL PROTEIN STRUCTURES AND PROTEIN–PROTEIN INTERACTIONS." Mass Spectrometry Reviews **25**: 663-682.

Stopak, K., C. d. Noronha, W. Yonemoto and W. C. Greene (2003). "HIV-1 Vif Blocks the Antiviral Activity of APOBEC3G by Impairing Both Its Translation and Intracellular Stability." Molecular Cell **12**(3): 591-601.

Trester-Zedlitz, M., K. Kamada, S. K. Burley, D. Fenyo, B. T. Chait and T. W. Muir (2003). "A Modular Cross-Linking Approach for Exploring Protein Interactions." Journal of American Chemical Society **125**: 2416-2425.

Wiegand, H. L., B. P. Doehle, H. P. Bogerd and B. R. Cullen (2004). "A second human antiretroviral factor, APOBEC3F, is suppressed by the HIV-1 and HIV-2 Vif proteins." The Embo Journal **23**(12): 2451-2458.

Xiao, Z., E. Ehrlich, K. Luo, Y. Xiong and X. Yu (2007a). "Zinc chelation inhibits HIV Vif activity and liberates antiviral function of the cytidine deaminase APOBEC3G." FASEB J **21**(1): 217-22.

Xiao, Z., E. Ehrlich, Y. Yu, K. Luo, T. Wang, C. Tian and X.-F. Yu (2006). "Assembly of HIV-1 Vif-Cul5 E3 ubiquitin ligase through a novel zinc-binding domain-stabilized hydrophobic interface in Vif." Virology **349**(2): 290-9.

Xiao, Z., Y. Xiong, W. Zhang, L. Tan, E. Ehrlich, D. Guo and X. Yu (2007b). "Characterization of a Novel Cullin5 Binding Domain in HIV-1 Vif." Journal of Molecular Biology **373**(3): 541-50.

Yang, B., L. Li, Z. Lu, X. Fan, C. A. Patel, R. J. Pomerantz, G. C. DuBois and H. Zhang (2003). "Potent Suppression of Viral Infectivity by the Peptides That Inhibit Multimerization of Human Immunodeficiency Virus Type 1 (HIV-1) Vif Proteins." The Journal of Biological Chemistry **278**(8): 6596-6602.

Yang, S., Y. Sun and H. Zhang (2001). "The Multimerization of Human Immunodeficiency Virus Type 1 Vif Protein." The Journal of Biological Chemistry **276**(7): 4889-4893.

Yao, X., A. Freas, J. Ramirez, P. Demirev and C. Fenselau (2001). "Proteolytic 18O labeling for comparative proteomics: model studies with two serotypes of adenovirus." Anal Chem. **73**(13): 2836-42.

Yu, Y., Z. Xiao, E. S. Ehrlich, X. Yu and X.-F. Yu (2004). "Selective assembly of HIV-1 vif-Cul5 ElonginB-ElonginC E3 ubiquitin ligase complex through a novel SOCS box and upstream cysteines." Genes & Development **18**: 2867-2872.

Zheng, Y.-H., D. Irwin, T. Kurosu, K. Tokunaga, T. Sata and B. M. Peterlin (2004). "Human APOBEC3F Is Another Host Factor That Blocks Human Immunodeficiency Virus Type 1 Replication." Journal of Virology **78**(11): 6073-6076.

APPENDIX I

ATTEMPTS TO EXPRESS AND PURIFY HIV-1 VIF AND APOBEC3G

METHODS AND RESULTS

GST-Vif

The GST-Vif_{LAI} expression construct was obtained from Drs. Melissa Farrow and Mohan Somasundaran. HIV-1 Vif_{LAI} was cloned into the pGEX-3X expression vector, which contains the GST-fusion protein. Expression trials were performed at both 37°C and room temperature (approximately 25°C), in LB broth, at 1mM and 2 mM IPTG, and in BL21(DE3) and BL21(DE3)CodonPlus-RIL cells (Figure A1.1A) . The BL21(DE3)CodonPlus-RIL cells are enriched with plasmids that produce tRNAs for the rare *E. coli* codons, arginine, isoleucine, and leucine, and are supposed to aid in expressing proteins such as HIV-1 Vif with an abundance of these rare codons. Proteins were expressed for 4 hours at 37°C was carried out for 4 hours or at room temperature for 24 hours. For large-scale expression of HIV-1 Vif, one 37°C expression trial was conducted in a 10 L fermentor.

Cell samples were taken at various times during the overexpression experiments to monitor protein levels in both the soluble and insoluble fractions. Samples were centrifuged, the pellets were resuspended, and the suspension was sonicated. The samples were centrifuged again and collected as supernatants (soluble fraction) and pellets (insoluble fraction). The pellet was resuspended in acetic acid and analyzed with the supernatant by 16% SDS PAGE. Since the majority of GST-Vif_{LAI} protein was found in the inclusion bodies, they were collected from a 37°C experiment, solubilized in 8M urea, and dialyzed into PBS to refold the protein. After dialysis, the protein aggregated or did not refold, which may have been due to the slow protein refolding in dialysis.

Figure A1.1A

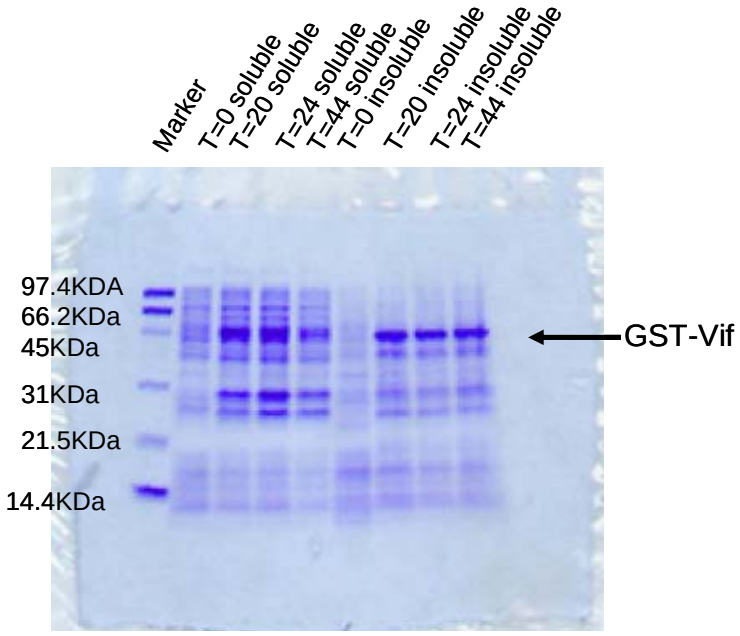
Marker
T=0 soluble
T=20 soluble
T=24 soluble
T=44 soluble
T=0 insoluble
T=20 insoluble
T=24 insoluble
T=44 insoluble
97.4KDA
66.2KDa
45KDa
31KDa
21.5KDa
14.4KDa
GST-Vif

Figure A1.1A: GST-Vif Expression. HIV-1 Vif was cloned into the pGEX-3X vector with a GST tag and expressed at room temperature in BL21CodonPlus(DE3)-RIL *E. coli* cells. Protein expression was induced by treating the cultures with 1mM IPTG in LB for 44 hours. Expression was analyzed by 16% SDS PAGE. The majority of the GST-Vif was expressed in the insoluble fraction.

Therefore, protein samples were subjected to drop-wise refolding into PBS, but the protein still aggregated. I next tried refolding protein samples drop-wise into a panel of 16 buffers known as the FoldIt Screen (Hampton Research). All refolding attempts resulted in protein aggregation.

HAT-Vif

The pHAT-Vif_{LAI} expression construct was obtained from Drs. Melissa Farrow and Mohan Somasundaran. HIV-1 Vif_{LAI} was cloned into a pHAT11 vector containing a HAT tag. The HAT tag (Clontech) is derived from chicken lactate dehydrogenase protein and contains 6 unevenly distributed histidines. This uneven distribution removes the excessive positive charge found in most 6X His tags, increasing solubility.

Expression trials were carried out for pHAT-Vif_{LAI} at 37°C, 28°C, 25°C (room temperature), 20°C, and 18°C. Both BL21(DE3)CodonPlus-RIL and BL21(DE3) cell lines were used as was LB and TB (terrific broth). TB is similar to LB, but it contains more nutrients that increase the yield of *E. coli* and thus the yield of target protein. In addition to varying temperature, media, and cell line, I varied IPTG concentration for induction (including 2 mM, 1 mM, and 0.33 mM) and time of expression (3 to 48 hours). Each expression trial was analyzed by 16% SDS PAGE, and in all cases HIV-1 Vif protein was found in the inclusion bodies or insoluble fraction (Figure A1.1B).

In addition to the pHAT-Vif_{LAI} construct, HIV-1 Vif_{HXB2} was cloned into the pHAT11 vector. I hypothesized that the HIV-1 Vif protein might be more soluble if expressed by naturally occurring different codons. This hypothesis was tested by using

Figure A1.1B

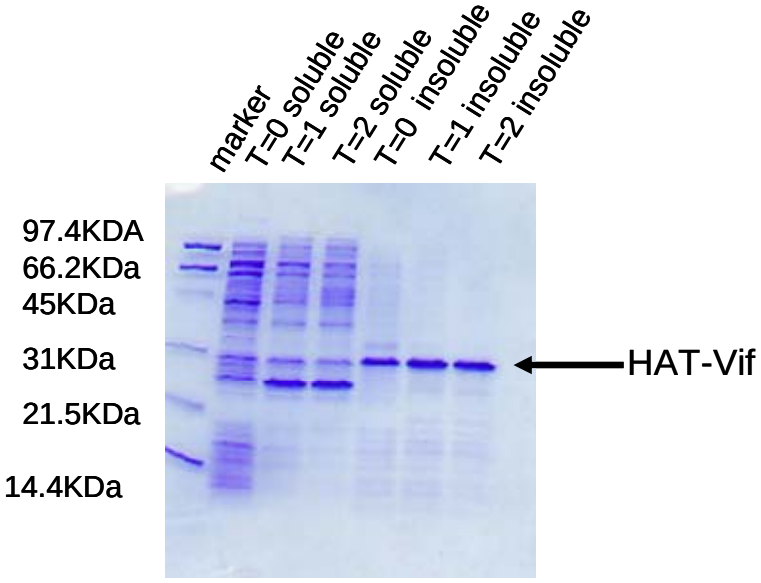
marker
T=0 soluble
T=1 soluble
T=2 soluble
T=0 insoluble
T=1 insoluble
T=2 insoluble
97.4KDA
66.2KDa
45KDa
31KDa
21.5KDa
14.4KDa
HAT-Vif

Figure A1.1B: HAT-Vif Expression. HIV-1 Vif was cloned into the pHAT11 vector with a modified His tag, HAT, and expressed at 28°C for 2 hours in BL21(DE3) cells. Protein expression was induced by treating cultures with 1 mM IPTG in TB and analyzed via 16% SDS PAGE. The HAT-Vif fusion protein was expressed in the insoluble fraction.

HXB2, another molecular clone of clade B HIV-1 with an amino acid sequence identical to that of LAI, but coded by different codons. Expression of pHAT-Vif_{HXB2} was induced for 4 hours by treating BL21(DE3) cells with 1mM IPTG in both TB and 2XYT media, respectively, at 28°C. Analysis of protein expression by denaturing gel electrophoresis consistently showed HIV-1 Vif_{HXB2} protein in the insoluble fraction. In this instance, the difference in codon used to determine the HIV-1 Vif amino acid sequence did not improve protein solubility. The inclusion bodies from the TB expression were pelleted and dissolved in 6 M guanidine hydrochloride, 0.1 M sodium phosphate, pH 8.0 and dialyzed into 50 mM MOPS, 150 mM sodium chloride, pH 6.5 with decreasing amounts of guanidine hydrochloride (Yang, 1996). The HIV-1 Vif protein was not refolded from the inclusion bodies by this method.

VIF140 and Vif150

The maltose binding protein (MBP)-Vif_{140} and MBP-Vif_{150} expression constructs for truncated HIV-1 Vif were obtained from Dr. Hui Zhang. Both HIV-1 Vif truncation mutants were cloned into the pMAL-2C expression vector containing the MBP fusion protein. The C-terminal region of Vif was truncated in order to remove the proposed oligomerization domain, which may facilitate in HIV-1 Vif solubility (Yang, 2001; Yang, 2003).

MBP-Vif_{140} was expressed at 37°C, 30°C, and room temperature (approximately 25°C) in BL21(DE3) cells and induced with 1 mM IPTG in LB for 3-5 hours. The MBP-Vif_{140} protein was expressed in the inclusion bodies in the 37°C expression; however in

the 30°C expression trials approximately 30-50% of the MBP-Vif_{140} protein expressed was in the soluble fraction.

To increase the yield of soluble truncated HIV-1 Vif protein, a greater number of expression conditions were tried for MBP-Vif_{150} compared to MBP-Vif_{140}. Expression trials were conducted at 37°C, 30°C, 28°C, 25°C (room temperature), and 20°C. Induction was conducted in BL21(DE3) cells with 1mM or 0.33mM IPTG in LB or TB for 4-24 hours. The expression experiments conducted at 37°C and 20°C yielded insoluble MBP-Vif_{150} protein (Figure A1.1C), but expression at 28°C in either 1 mM IPTG or 0.33 mM IPTG yielded soluble MBP-Vif_{150}. It appeared that 30-50% of the MBP-Vif_{150} protein expressed in these conditions was soluble (Figure A1.1D). However, the stability of the protein made it insufficient for structural analysis via X-ray crystallography and NMR.

In addition to cloning MBP-Vif_{140} and MBP-Vif_{150} into the pMAL-2c expression vector, they were also cloned into the pET43.1b (NusA expression vector). Expression of NusA-Vif_{140} and NusA-Vif_{150} was conducted in LB or TB at 28°C in BL21(DE3) cells induced with either 1 mM or 0.5mM IPTG for 4-24 hours. In some expression trials approximately 50% of the NusA-Vif_{140} or NusA-Vif_{150} was soluble, whereas in others it was completely insoluble. Further analysis via western blot of those trials with some soluble protein revealed that the quantity observed was considerably less than 50%.

The MBP fusion protein had aided in obtaining soluble Vif_{140} or Vif_{150}, where approximately 50% of the protein obtained in expression trials at 28°C was soluble as compared to all the protein yielded from expression trials at 37°C being insoluble. The

Figure A1.1C

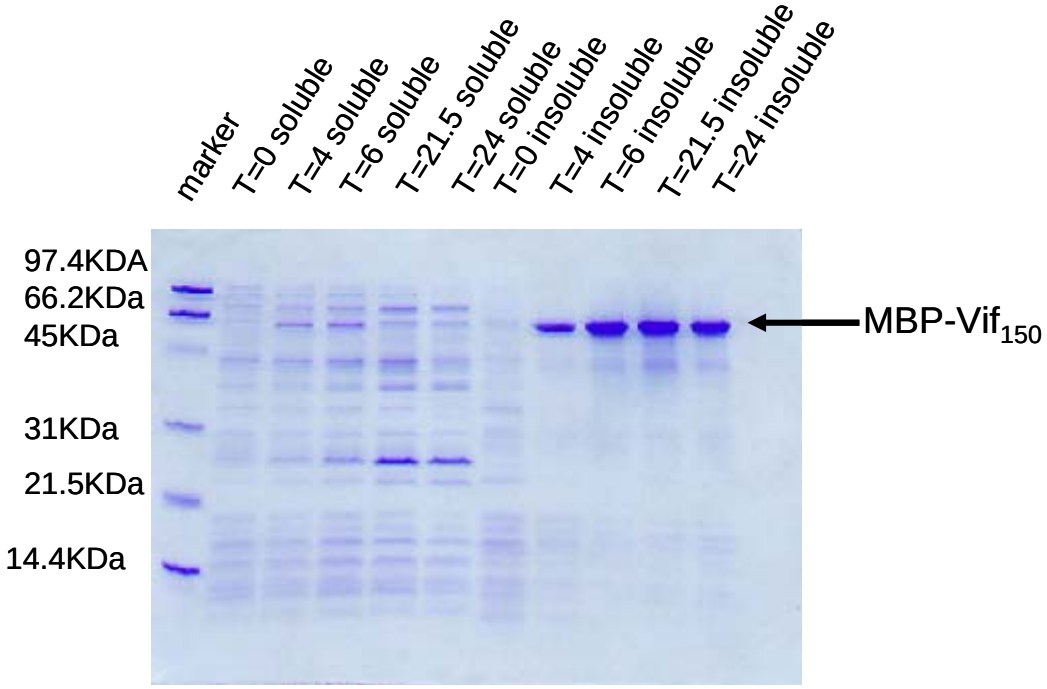
marker
T=0 soluble
T=4 soluble
T=6 soluble
T=21.5 soluble
T=24 soluble
T=0 insoluble
T=4 insoluble
T=6 insoluble
T=21.5 insoluble
T=24 insoluble
97.4KDA
66.2KDa
45KDa
31KDa
21.5KDa
14.4KDa
MBP-Vif150

Figure A1.1D

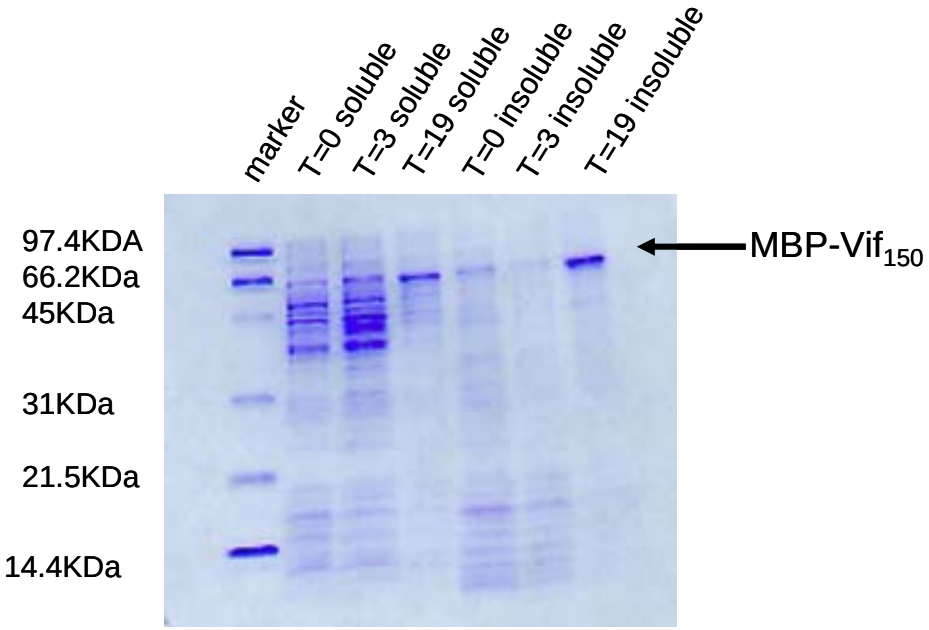
marker
T=0 soluble
T=3 soluble
T=19 soluble
T=0 insoluble
T=3 insoluble
T=19 insoluble
97.4KDA
66.2KDa
45KDa
31KDa
21.5KDa
14.4KDa
MBP-Vif150

Figure A1.1C and A1.1D: MBP-Vif$_{150}$ Expression. (C.) HIV-1 Vif$_{150}$ was cloned into the pMAL-2C vector containing an MBP tag. pMBP-Vif$_{150}$ is a truncation mutant of HIV-1 Vif were the C-terminus has been deleted. Expression was conducted using BL21(DE3) cells at 28°C in LB for 24 hours and induced with 1 mM IPTG. Expression was analyzed via 16% SDS PAGE. The majority of the MBP- Vif$_{150}$ was expressed in the insoluble fraction. (D.) The pMBP-Vif$_{150}$ construct was expressed using BL21(DE3) cells at 37°C for 3 hours and then 28°C overnight in LB and induced with 1mM IPTG. Expression was analyzed via 16% SDS PAGE. After overnight expression about 50% of the fusion protein produced is in the soluble fraction.

NusA fusion protein seemed to give less consistent results with the majority of the protein obtained being insoluble. Further optimization will be necessary to determine if MBP truncation mutants will provide milligram quantities of fusion-protein and whether the protein will remain soluble and folded when the tag is cleaved.

SIV-Vif

In addition to trying expression of different strains of HIV-1 Vif such as LAI and HXB2, we also tried to express SIV Vif. SIV Vif and HIV-1 Vif share a conserved function in there respective hosts (Bogerd, 2004; Mangeat, 2004; Schrofelbauer, 2004) and the naturally occurring sequence difference in SIV Vif would aid in producing soluble protein. As an alternative to mutagenizing HIV-1 Vif, it was determined whether trying to express SIV Vif might lead to the expression of soluble protein, albeit my goal for further analysis was to use HIV-1 Vif.

SIV_{239} Vif was cloned into the pHAT11 expression vector. It was expressed in 2XYT media in BL21(DE3) cells and induced with 1 mM IPTG at 28°C for 4 hours. The protein expression was analyzed by 16% SDS PAGE and found to be in the insoluble protein. SIV Vif expression was observed preinduction indicating expression was likely under the control of a leaky promoter (Figure A1.1E).

Baculovirus Expression (APO3G and Vif)

The Baculodirect™ Baculovirus expression system using Gateway technology (Invitrogen) was used to carry out expression of HIV-1 Vif_{LAI}, HIV-1 Vif_{HXB2}, and

Figure A1.1E

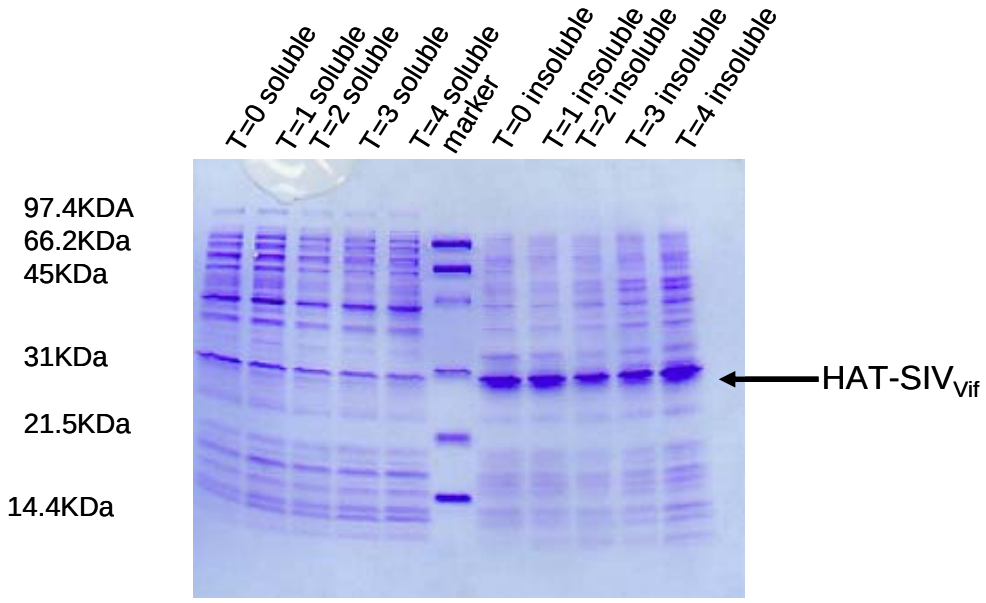
T=0 soluble
T=1 soluble
T=2 soluble
T=3 soluble
T=4 soluble
marker
T=0 insoluble
T=1 insoluble
T=2 insoluble
T=3 insoluble
T=4 insoluble
97.4KDA
66.2KDa
45KDa
31KDa
21.5KDa
14.4KDa
HAT-SIV$_{Vif}$

Figure A1.1E: SIV-Vif Expression. SIV Vif was cloned into the pHAT11 vector and expressed using BL21(DE3) cells in 2XYT at 28°C for 4 hours with 1mM IPTG induction and analyzed via 16% SDS PAGE. The pHAT-Vif_{SIV} protein produced is insoluble.

APOBEC3G (APO3G). HIV-1 Vif_{LAI}, HIV-1 Vif_{HXB2}, and APO3G were cloned into the pENTR Gateway entry vector either with or without a stop codon present. A stop codon was absent from some of the constructs in order to allow for a C-terminal tag, such as a V5 epitope or HA tag, to be added to the expressed protein for purification and/or detection. The Gateway entry vectors take advantage of the bacteriophage lambda site-specific recombination system, thus allowing genes cloned into the entry vector to be transferred to other vectors, such as the BaculoDirect™ Linear DNA.

The pENTR-Vif_{LAI}, pENTR-Vif_{HXB2}, and pENTR-APO3G constructs were incubated in the presence of BaculoDirect™ Linear DNA and LR Clonase™, which facilitates the transfer of the respective gene from the entry clone to the BaculoDirect™ Linear DNA. After the recombination event the BaculoDirect™ Linear DNA with the respective gene was incubated with Proteinase K and added to a cellfectin reagent and unsupplemented Grace's Insect Media mixture. This transfection mixture was added to sf9 insect cells and incubated at 22°C for 5 hours, after 5 hours it was removed and complete growth media was added, and then the cells were incubated at 27°C for 72 hours.

After the 3 day incubation the media (supernatant) was removed, stored as P1 viral stock, and used to infect new sf9 cells. The new cells infected with P1 viral stocks then produced P2 viral stocks which were used to infect new sf9 cells, and so on. The cells produced were centrifuged and checked for expression by 16% SDS PAGE and western blotting. Antibodies to HIV-1 Vif and APO3G were used in the western blots; and since a V5 epitope was expressed in fusion with the protein of interest, an antibody to

V5 was also used in western blots. Both HIV-1 Vif and APO3G expression were observed via western blot (Figure A1.2).

Infections were carried out using P1-P5 viral stocks and time points up to day 22. HIV-1 Vif_{HXB2} and HIV-1 Vif_{LAI} with no stop codon produced soluble Vif protein that was only observable in western blots and not in regular coomassie stained gels. In no samples was Vif protein observed in the SDS polyacrylamide gels, suggesting that only very small quantities were expressed. APO3G with no stop codon and with a stop codon were expressed and analyzed via SDS PAGE and western blotting. No APO3G protein could be detected in the SDS polyacrylamide gels, although protein was detected in the western blots. There was a larger amount of APO3G with no stop produced than that of APO3G with a stop codon (Figure A1.2). In addition, APO3G-HA was expressed as determined via western blot. However, as in the case of HIV-1 Vif no APO3G protein was detected in SDS polyacrylamide gels, suggesting that only small quantities of the proteins were being produced with the baculovirus expression system.

NusA-Vif

HIV-1 Vif_{LAI} was cloned into pET43.1 (Novagen), which encodes the NusA gene to express the NusA-fusion protein. NusA is an *E. coli* protein that has been shown to be highly soluble, thus the characteristics of NusA can help insoluble proteins be expressed in the soluble fraction. Based on our previous experience with HIV-1 Vif expression and the experience of others with expression of proteins with the NusA tag, we tried expression of NusA-Vif_{LAI} in BL21(DE3) cells in TB induced with 50 µM IPTG at 28°C

Figure A1.2

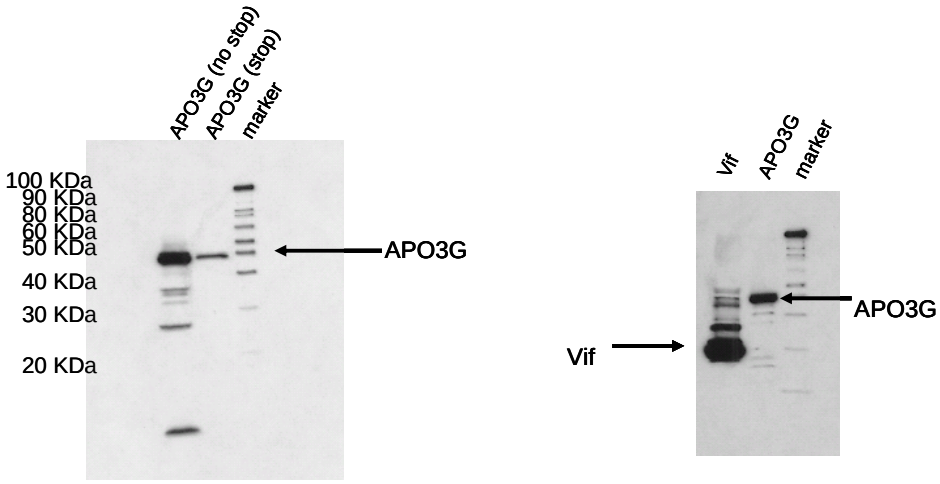
APO3G (no stop)
APO3G (stop)
marker
100 KDa
90 KDa
80 KDa
60 KDa
50 KDa
40 KDa
30 KDa
20 KDa
APO3G
Vif
APO3G
marker
Vif
APO3G

Figure A1.2: Baculovirus Expression of HIV-1 Vif and APO3G. Baculovirus expression of APO3G with a stop codon, APO3G with no stop codon, and HIV-1 Vif was performed and analyzed via western blotting. *Left panel*: Both APO3G with a stop codon and without a stop codon were expressed in sf9 insect cells and the day 9 sample was analyzed via western blot. More APO3G without a stop codon was produced than APO3G with a stop codon, but in each case no protein expression was observed by 16% SDS PAGE. *Right panel*: APO3G and HIV-1 Vif with no stop codons were expressed in sf9 insect cells and the day 22 sample was analyzed using a V5-antibody and western blotting. Both soluble APO3G and HIV-1 Vif expression were observed, but no expression was visible on a 16% SDS polyacrylamide gel.

for approximately 18 hours. The NusA-Vif_{LAI} expression was checked by 16% SDS PAGE where approximately 50% of the protein expressed was soluble. To further optimize protein expression similar conditions were used as mentioned above with varying concentrations of IPTG: 100 µM, 200 µM, 400 µM, 600 µM and 1 mM. The 100 µM IPTG induction yielded similar amounts of soluble protein as the 50 µM induction, the 200 µM and the 400 µM induction yielded a slightly lesser amount of soluble protein about 40%, and 600 µM and 1mM IPTG inductions yielded only 20% soluble protein. Therefore, the original expression conditions were determined to be optimal.

A similar strategy was undertaken for NusA-Vif_{LAI} purification as was described for NusA-APO3G purification above. First, NusA-Vif_{LAI} was purified using nickel affinity chromatography and the fractions were analyzed by 16% SDS PAGE. The majority of NusA-Vif_{LAI} copurified with free NusA, as was the case with the NusA-APO3G purification, but in the later fractions NusA-Vif_{LAI} was observed to be about 80% pure with no free NusA observed. The NusA-Vif_{LAI} protein purified from these samples was confirmed to be Vif_{LAI} by both western blotting and mass spectrometry. The NusA-Vif_{LAI} obtained from the nickel affinity purification was further purified using anion exchange chromatography (MonoQ 10/10). The SDS PAGE analysis of the MonoQ purified NusA-Vif_{LAI} revealed that it was purified away from the free NusA (Figure A1.3A). However, Size Exclusion Chromatography (SEC) purification using the Superdex 200 and S protein affinity purification (a second tag present in the NusA expression vector) were tried in an attempt to obtain pure NusA-Vif_{LAI} above 95%. The

Figure A1.3A

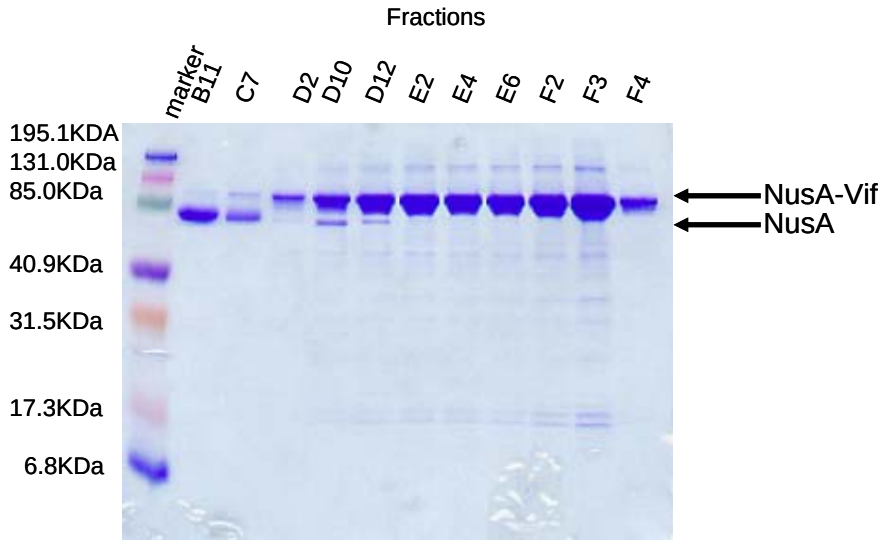
Fractions
marker
B11
C7
D2
D10
D12
E2
E4
E6
F2
F3
F4
195.1KDA
131.0KDa
85.0KDa
40.9KDa
31.5KDa
17.3KDa
6.8KDa
NusA-Vif
NusA

Figure A1.3A: NusA-Vif Purification. HIV-1 Vif was cloned into the pET43.1 vector containing the NusA fusion tag. pNusA-Vif was expressed in Bl21(DE3) cells overnight at 28°C in TB induced with 50μM IPTG. The majority of the pNusA-Vif protein expressed was soluble and further purified using nickel affinity chromatography and anion exchange chromatograpy and analyzed via 16% SDS PAGE.

NusA-Vif_{LAI} protein aggregated, and these step were eliminated from further purification protocols of NusA-$Vif_{LAI.}$

After purification of NusA-Vif_{LAI}, cleavage reactions were performed to obtain free $Vif_{LAI.}$ There are two possible protease cleavage sites between the NusA tag and HIV-1 Vif_{LAI}, i.e. enterokinase and thrombin. The original attempts to cleave the fusion protein were with enterokinase, but after attempts at optimizing cleavage using different enzyme concentrations of the protease it was determined that the enterokinase-cleavage reaction was relatively inefficient. Therefore, cleavage of the fusion protein was attempted with thrombin. Thrombin cleaved the NusA-Vif_{LAI} fusion protein, but about 97% of the free HIV-1 Vif_{LAI} precipitated leaving about 3% free HIV-1 Vif_{LAI}. Cleavage reaction with thrombin was optimized using various conditions: (1) using different thrombin concentration; (2) addition of glycerol to stabilize the protein; (3) using different sodium chloride concentrations up to 1 M; and (4) trying different times and temperatures for the cleavage reaction. However, the majority of the cleaved HIV-1 Vif_{LAI} aggregated in all cases. Even though the majority of the cleaved HIV-1 Vif_{LAI} protein aggregated, attempts were made to purify the soluble protein. First a negative purification approach was undertaken and the cleaved protein was run over the nickel affinity column again to obtain cleaved HIV-1 Vif_{LAI} protein in the flow through; however, all the protein was lost in this purification step. Size exclusion chromatography, both a Superdex 200 and Superdex G75 column, were used to purify the cleaved Vif_{LAI} but the aggregated protein eluted in the void volume. Further purification of the cleaved protein was attempted using a Superose 6 column for size exclusion

chromatography (SEC), as was a MonoQ (negative purification) and MonoS column (the pI of Vif is 10.7 thus it should bind to a cation exchanger like the MonoS). Interestingly the cleaved HIV-1 Vif_{LAI} protein from the MonoS and SEC columns produced no pure HIV-1 Vif protein, were as in the MonoQ purification instead of not binding and coming out in the flow through the HIV-1 Vif_{LAI} copurified with any remaining uncleaved NusA-Vif_{LAI} protein. This suggests that NusA-Vif_{LAI} is forming an oligomer with cleaved HIV-1 Vif_{LAI}.

Cleavage of the NusA-Vif_{LAI} fusion protein proved unsuccessful, but since there was very little biochemical data available for Vif we attempted to perform a few experiments using the NusA-Vif_{LAI} fusion protein. First, binding experiments were attempted: NusA-Vif_{LAI} and NusA-APO3G were incubated in the presence of zinc, cleaved HIV-1 Vif_{LAI} and NusA-APO3G in the presence of zinc, NusA-Vif_{LAI} and NusA-APO3G in the absence of zinc, and cleaved HIV-1 Vif_{LAI} and NusA-APO3G in the absence of zinc. The binding of HIV-1 Vif_{LAI} with APO3G might potentially induce conformational changes in the proteins that make them more stable, thus giving us soluble protein to work with. In addition, zinc could help stabilize the proteins since HIV-1 Vif has been shown to be a zinc binding protein (Kobayashi, 2005; Luo, 2005; Mehle, 2006; Xiao, 2006; Xiao, 2007a; Xiao, 2007b). Each individual protein and the binding reactions were analyzed by size exclusion chromatography using a Superose 6 column. Unfortunately, each protein and the complex eluted in the void volume suggesting they were aggregated. In addition to trying to stabilize the proteins using Zinc

post purification, the purification was tried using magnesium chloride to try to stabilize the proteins. This also did not aid in obtaining soluble protein.

The purified NusA-Vif_{LAI} fusion protein was used in crystallization screens. NusA-Vif_{LAI} at concentrations between 4 mg/ml and 7 mg/ml were used to set crystal trays using the Hampton I & II, the Wizard I & II, and the Wizard PEG-8000 crystallization kits. Since none of these conditions yielded crystals, therefore an expanded screen was attempted. Purified NusA-Vif_{LAI} was sent to the Hauptman-Woodward Medical Research Institute where 1536 unique crystallization conditions were screened using a high-throughput screen. Several conditions produced crystalline-like objects; the most promising conditions contained lithium chloride, Tris, pH 8.0, ammonium sulfate, magnesium hydrate and ammonium sulfate or chloride. Further optimization was performed using these conditions; despite all these attempts no defractable crystals were produced.

Finally, cross-linking experiments similar to those described in chapter III were performed. NusA and NusA-Vif_{LAI} (0.66 mg/ml each) were cross-linked using 2 mM EDC and 5 mM sulfo-NHS for 15 and 30 minutes at room temperature. Cross-linking assays were also performed under similar conditions in the absence of NHS. The reaction mixtures were analyzed via 10% SDS PAGE and western blotting. In the case of NusA no cross-links were observed, and in the case of NusA-Vif_{LAI} cross-links corresponding to dimers and trimers were observed. The cross-links observed for NusA-Vif_{LAI} were consistent with those observed from cross-linking of HIV-1 Vif in chapter III (Figure A1.3B).

Figure A1.3B

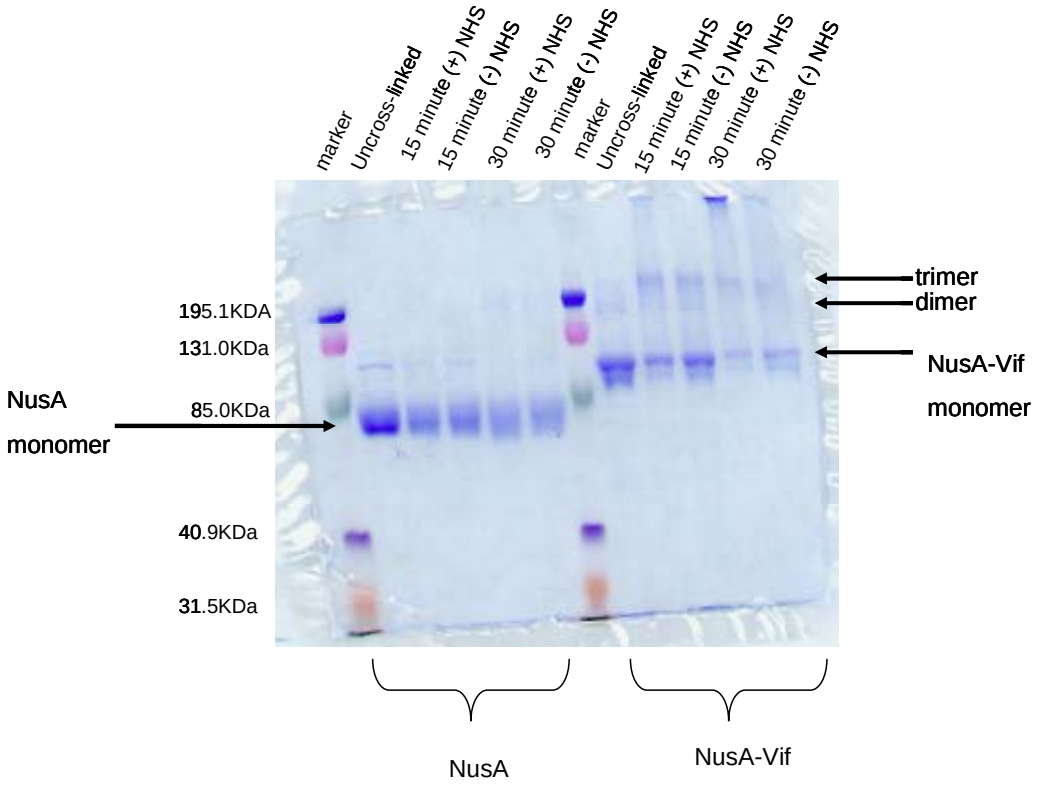
marker
Uncross-linked
15 minute (+) NHS
15 minute (-) NHS
30 minute (+) NHS
30 minute (-) NHS
marker
Uncross-linked
15 minute (+) NHS
15 minute (-) NHS
30 minute (+) NHS
30 minute (-) NHS
195.1KDA
131.0KDa
85.0KDa
40.9KDa
31.5KDa
NusA
monomer
trimer
dimer
NusA-Vif
monomer
NusA
NusA-Vif

Figure A1.3B: Cross-linking of NusA-Vif. pNusA and pNusA-Vif were cross-linked using 2 mM EDC and (+/-) 5mM sulfo-NHS for 15 or 30 minutes and analyzed by 10% SDS PAGE. No cross-links were observed for NusA alone and cross-links consistent with NusA-Vif dimers and trimers were observed for pNusA-Vif cross-linking, which is consistent with the cross-linking of HIV-1 Vif observed in Chapter III.

NusA-APO3G

As outlined above, the majority of my efforts were on expressing and purifying HIV-1 Vif. However attempts were also made to express and purify soluble APO3G. APO3G was cloned into pET43.1 (Novagen), which encodes the NusA fusion protein. pNusA-APO3G was used in expression trials to try to obtain soluble APO3G protein.

pNusA-APO3G was expressed in BL21(DE3) cells at 18°C, 28°C, and 37°C in TB or LB and induced with either 1 mM, 0.5 mM, or 50 μM IPTG for 4-18 hours. Expression conducted at 37°C yielded no visible protein whereas expression at both 18°C and 28°C yielded low levels of expression, albeit, it was mostly soluble. Therefore the ideal expression condition for NusA-APO3G were determined to be in BL21 (DE3) cells in TB and induced with 50 μM IPTG at 28°C for 16 hours. NusA-APO3G expressed using these conditions produced soluble protein as determined by both 16% SDS PAGE and western blotting.

After expressing the NusA-APO3G protein, purification of the protein was attempted. The NusA tag has a 6X His tag as part of its fusion tag sequence that was used in affinity purification. The NusA-APO3G cells were resuspended and lysed in 50 mM sodium phosphate, pH 8.0, 0.3 M sodium chloride, 25 mM DTT, 10 mM imidazole, and 1 mM PMSF using a cell disruptor. The lysed cells were centrifuged at 14K for 30 minutes and the supernatant was incubated with His-Select (Sigma) nickel resin for 2 hours at 4°C. After 2 hours the slurry (protein-beads) was poured into a gravity column and fractions were collected. The protein was about 60% pure at this stage, then the pooled nickel fractions were cleaved with thrombin and purified on the FPLC using a

Sepharose 6 column. After thrombin cleavage no free APO3G was observed, but free NusA was observed suggesting the cleavage was successful and that APO3G either precipitated after cleavage or is in such low quantity that it could not be detected by SDS PAGE. Further analysis via western blot showed free APO3G to be present in the cleaved lanes, but the band intensity was faint suggesting that indeed the quantity of APO3G being produced is too small to detect via SDS PAGE.

In addition, in the expression and purification of NusA-APO3G some free NusA is expressed and purified along with NusA-APO3G. This is likely due to the ribosomes falling off the NusA-APO3G construct prior to synthesizing APO3G, or it is possible that an internal *E. coli* protease is cleaving the fusion protein. Small amounts of APO3G were obtained from nickel purification alone; but because of the contaminating NusA protein, further purification of NusA-APO3G was attempted. NusA-APO3G was purified as a fusion protein because it eliminates any contaminates that could interfere with cleavage and allows for NusA to keep APO3G soluble for as long as possible. Therefore, NusA-APO3G was purified using the same purification protocol through the nickel column, and instead of the cleaving reaction, the fusion protein was purified further using an anion exchange column (MonoQ) on the FPLC. The chromatogram produced had two distinct peaks. The first peak was free NusA and the second peak was a mixture of free NusA and NusA-APO3G, thus not all the contaminating free NusA was removed from the NusA-APO3G fractions (Figure A1.4). Further purification of NusA-APO3G was performed on a sizing column (S200), but the protein eluted in a high

Figure A1.4

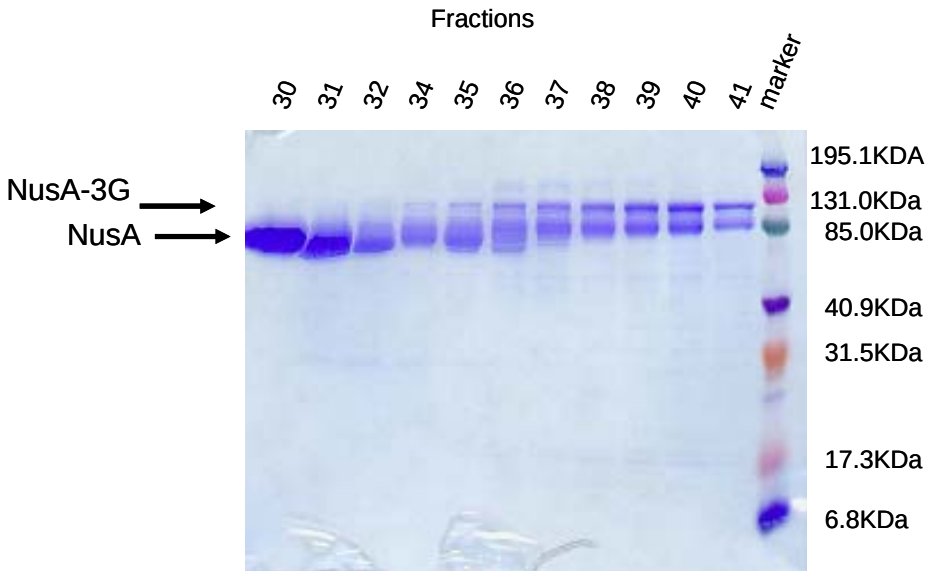
Fractions
30
31
32
34
35
36
37
38
39
40
41
marker
NusA-3G
NusA
195.1KDA
131.0KDa
85.0KDa
40.9KDa
31.5KDa
17.3KDa
6.8KDa

Figure A1.4: NusA-APO3G Purification. NusA-APO3G was expressed and purified as HIV-1 Vif was in Figure A1.3A.

molecular weight peak consistent with aggregation. In addition, thrombin cleavage of the NusA-APO3G fusion protein resulted also in APO3G aggregating.

Therefore, soluble APO3G protein was expressed using the NusA tag. This protein was purified with the largest contaminant being free NusA using both nickel purification and anion exchange purification. However, when further purification was attempted via size exclusion purification the fusion protein appeared to aggregate.

Co-expression (Vif and APO3G)

HIV-1 Vif has been shown by my previous expression attempts and those of others to be highly insoluble. APO3G is a cellular protein that has been shown to bind to HIV-1 Vif (Lecossier, 2003; Mangeat, 2003; Zhang, 2003; Bishop, 2004; Bishop, 2004; Harris, 2004; Liddament, 2004; Wiegand, 2004; Zheng, 2004; Doehle, 2005; Holmes, 2007). Therefore, my hypothesis was that co-expression of HIV-1 Vif with APO3G might stabilize the proteins and create a soluble protein complex. NusA constructs were used in coexpression experiments because in previous experiments some soluble HIV-1 Vif and APO3G were observed when they were expressed as NusA-fusions. Therefore, I hypothesized that coexpression of NusA-fusions potentially will aid in solubilizing coexpressed proteins.

HIV-1 Vif_{LAI} and APO3G were cloned into the pACYC-Duet coexpression vector, creating pDuet-Vif_{LAI} and pDuet-APO3G. First, I determined the fraction in which Vif would appear. To that end, pDuet-Vif_{LAI} was expressed in BL21(DE3) cells by inducing them overnight with 50 µM IPTG at 25°C in TB. Duet-Vif was expressed only

in insoluble fractions (Figure A1.5A). Subsequently, I tried to obtain soluble HIV-1 Vif and APO3G by cotransforming BL21(DE3) cells with pDuet-Vif_{LAI} and pNusA-APO3G and inducing them for 4 hours with either 1mM or 50 µM IPTG at 28°C in TB. Duet-Vif was expressed at low level only in the insoluble fraction. BL21(DE3)-competent cells were transformed with pDuet-Vif_{LAI} and these cells were used to create BL21(DE3) pDuet-Vif_{LAI}-competent cells. Both pNusA-Vif_{LAI} and pNusA-APO3G were transformed into the BL21(DE3) pDuet-Vif_{LAI}-competent cells. Both were expressed in TB and induced at 25°C with 50µM IPTG. Western blot analysis revealed that pNusA-Vif_{LAI} coexpressed with pDuet-Vif, but the proteins were insoluble (Figure A1.5A). On the other hand, pNusA-APO3G apparently did not coexpress with pDuet-Vif as only Vif protein was observed (Figure A1.5B). Similarly, competent BL21(DE3)pDuet-APO3G cells were created. pNusA-Vif was transformed into these cells and expressed by inducing in TB overnight at 25°C and 28°C, at 50 µM and 1 mM IPTG. Although HIV-1 Vif and APO3G were coexpressed in these cells, the majority was again found in the insoluble fraction. A small fraction of expressed pNusA-Vif was soluble, but no APO3G was present in the soluble fraction.

Although an extensive range of coexpression variables was tried, additional variables could be tried, i.e., (1) cotransformation of pDuet-Vif_{LAI} with pDuet-APO3G and pDuet-APO3G with pNusA-Vif, (2) pDuet-APO3G could be expressed in BL21(DE3)pDuet-Vif_{LAI}-competent cells, (3) pDuet-Vif_{LAI} could be expressed in BL21(DE3)pDuet-APO3G-competent cells, and (4) a bicistronic expression vector, pDuet-Vif_{LAI}-APO3G, could be created for use in coexpression trials.

Figure A1.5A

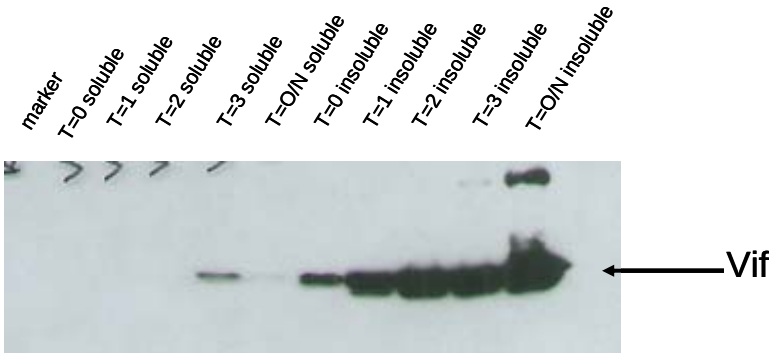

pDuet-Vif Expression

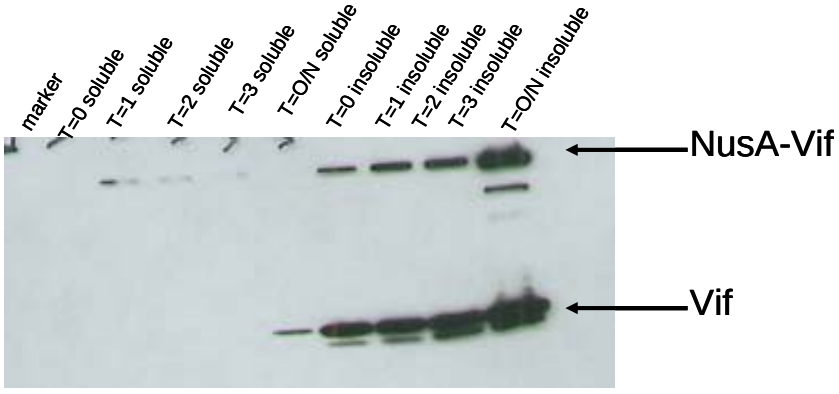

pNusA-Vif expression in pDuet-Vif compotent cells

Figure A1.5B

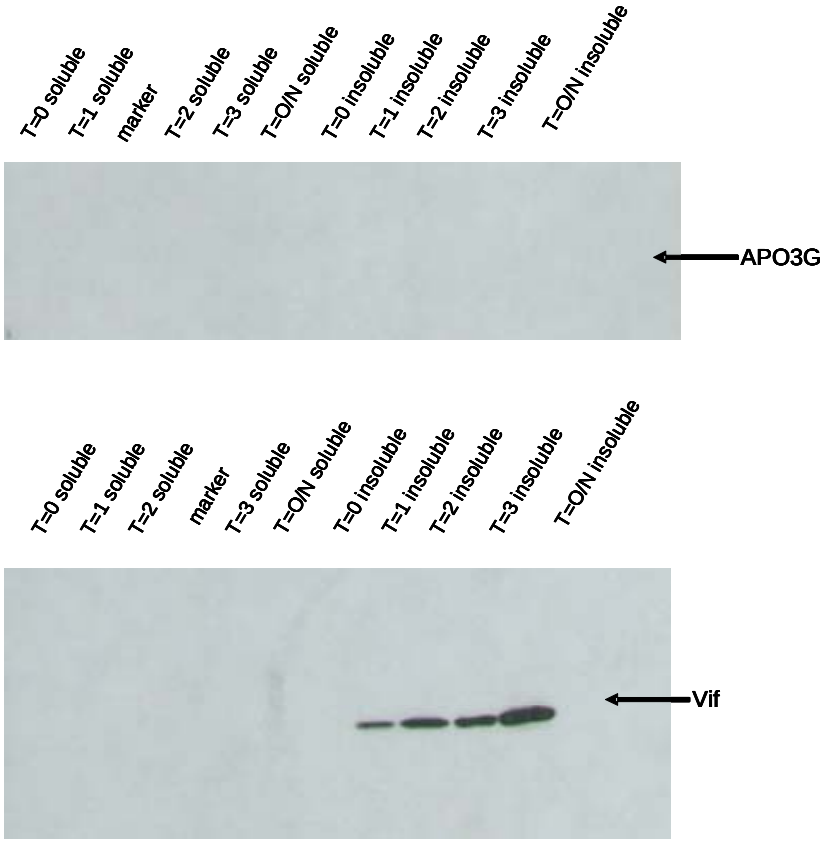

pNusA-APO3G expressed in pDuet-Vif competent cells

Figure A1.5: Coexpression of HIV-1 Vif and APO3G. (A.) HIV-1 Vif was cloned into the pDuet expression vector for use in coexpression experiments and analyzed via western blotting. *Top panel*: pDuet-Vif was expressed overnight in BL21(DE3) cells at 25°C in TB and induced with 50 µM IPTG. pDuet-Vif was expressed in the soluble fraction. *Bottom panel*: pNusA-Vif was expressed overnight in BL21(DE3)pDuet-Vif-competent cells at 25°C in TB and induced with 50µM IPTG. Both pNusA-Vif and pDuet-Vif were expressed in the insoluble fraction. **(B.)** pNusA-APO3G is coexpressed with pDuet-Vif. pNusA-APO3G was expressed in BL21(DE3)pDuet-Vif competent cells at 25°C in TB overnight and induced with 50 µM IPTG. Coexpression was analyzed via western blotting. pDuet-Vif was expressed in the insoluble fraction where as pNusA-APO3G was not expressed at all.

DISCUSSION

HIV-1 infections and AIDS have been successfully treated by current drug regimens, but these drugs are becoming less effective due to drug resistance. Drug resistance results when infectious agents such as viruses grow rapidly and evolve to produce proteins that evade current drugs, creating a need for novel drug targets. One such target is the interaction between HIV-1 Vif and the host cell antiviral agent, APO3G (cite refs).

The lack of available information on the structure of HIV-1 Vif is likely due to the difficulty of expressing and purifying milligram quantities of soluble protein. Therefore, my goal was to obtain soluble protein using different expression conditions, fusion proteins, and strains of Vif protein. The majority of the protein expressed was found in the insoluble fraction, or inclusion bodies, and could not be refolded. However, using the NusA tag facilitated purification of small quantities of soluble HIV-1 Vif and APO3G proteins. Unfortunately, the large NusA tag could not be separated from either protein, making them unsuitable for structural analysis. However, the NusA-Vif_{LAI} fusion protein was used in one biochemical experiment to obtain cross-links consistent with dimers and trimers (Chapter III).

Although large quantities of soluble HIV-1 Vif and APO3G were not obtained, the protocols I tried could be further optimized to obtain soluble protein. These optimization approaches include cloning full-length HIV-1 Vif into various tags known to improve solubility, e.g., MBP (maltose binding protein); varying other coexpression variables with APO3G and HIV-1 Vif; and optimizing protein expression in baculovirus

and in mammalian expression systems. Other approaches would be to express proteins in minimal M9 media, to express all the fusion protein I generated at lower temperatures, and to use C-terminal-tagged proteins. To obtain native protein for structural analyses, it would be necessary to further optimize the cleavage of NusA-fusion proteins or the MBP-Vif truncation mutants.

REFERENCES

Bishop, K. N., R. K. Holmes, A. M. Sheehy, N. O. Davidson, S.-J. Cho and M. H. Malim (2004). "Cytidine Deamination of Retroviral DNA by Diverse APOBEC Proteins." Current Biology **14**: 1392-1396.

Bishop, K. N., R. K. Holmes, A. M. Sheehy and M. H. Malim (2004). "APOBEC-mediated editing of viral RNA." Science **305**(5684): 645.

Bogerd, H. P., B. P. Doehle, H. L. Wiegand and B. R. Cullen (2004). "A single amino acid difference in the host APOBEC3G protein controls the primate species specificity of HIV type 1 virion infectivity factor." Proc. Natl. Acad. Sci USA **101**(11): 3770-3774.

Doehle, B. P., A. Schafer, H. L. Wiegand, H. P. Bogerd and B. R. Cullen (2005). "Differential Sensitivity of Murine Leukemia Virus to APOBEC3-Mediated Inhibition Is Governed by Virion Exclusion." Journal Of Virology **79**(13): 8201-8207.

Harris, R. S. and M. T. Liddament (2004). "Retroviral Restriction By APOBEC Proteins." Nature Reviews Immunology **4**: 868-877.

Holmes, R., M. Malim and K. Bishop (2007). "APOBEC-mediated viral restriction: not simply editing?" Trends Biochem Sci **32**(3): 118-28.

Kobayashi, M., A. Takaori-Kondo, Y. Miyauchi, K. Iwai and T. Uchiyama (2005). "Ubiquitination of APOBEC3G by an HIV-1 Vif-Cullin5-ElonginB-ElonginC complex is essential for Vif function." Journal of Biological Chemistry **280**(19): 18573-8.

Lecossier, D., F. Bouchonnet, F. Clavel and A. J. Hance (2003). "Hypermutation of HIV-1 DNA in the Absence of the Vif Protein." Science **300**(5622): 1112.

Liddament, M. T., W. L. Brown, A. J. Schumacher and R. S. Harris (2004). "APOBEC3F Properties and Hypermutation Preferences Indicate Activity against HIV-1 in Vivo." Current Biology **14**: 1385-1391.

Luo, K., Z. Xiao, E. Ehrlich, Y. Yu, B. Liu, S. Zheng and X.-F. Yu (2005). "Primate lentiviral virion infectivity factors are substrate receptors that assemble with cullin 5-E3 ligase through a HCCH motif to suppress APOBEC3G." Proc. Natl. Acad. Sci USA **102**(32): 11444-11449.

Mangeat, B., P. Turelli, S. Liao and D. Trono (2004). "A single amino acid determination governs the species-specific sensitivity of APOBEC3G to Vif action." Journal of Biological Chemistry **279**(15): 14481-14483.

Mangeat, B., P. Turelll, G. Caron, M. Friedll, L. Perrin and D. Trono (2003). "Broad antiretroviral defence by human APOBEC3G through lethal editing of nascent reverse transcripts." Nature **424**(6944): 99-103.

Mehle, A., E. R. Thomas, K. S. Rajendran and D. Gabuzda (2006). "A zinc-binding region in Vif binds Cul5 and determines Cullin selection." Journal of Biological Chemistry **281**(25): 17259-65.

Schrofelbauer, B., D. Chen and N. R. Landau (2004). "A single amino acid of APOBEC3G controls its species-specific interaction with virion infectivity factor (Vif)." Proc. Natl. Acad. Sci USA **101**(11): 3927-3932.

Wiegand, H. L., B. P. Doehle, H. P. Bogerd and B. R. Cullen (2004). "A second human antiretroviral factor, APOBEC3F, is suppressed by the HIV-1 and HIV-2 Vif proteins." The Embo Journal **23**(12): 2451-2458.

Xiao, Z., E. Ehrlich, K. Luo, Y. Xiong and X. Yu (2007a). "Zinc chelation inhibits HIV Vif activity and liberates antiviral function of the cytidine deaminase APOBEC3G." FASEB J **21**(1): 217-22.

Xiao, Z., E. Ehrlich, Y. Yu, K. Luo, T. Wang, C. Tian and X.-F. Yu (2006). "Assembly of HIV-1 Vif-Cul5 E3 ubiquitin ligase through a novel zinc-binding domain-stabilized hydrophobic interface in Vif." Virology **349**(2): 290-9.

Xiao, Z., Y. Xiong, W. Zhang, L. Tan, E. Ehrlich, D. Guo and X. Yu (2007b). "Characterization of a Novel Cullin5 Binding Domain in HIV-1 Vif." Journal of Molecular Biology **373**(3): 541-50.

Yang, B., L. Li, Z. Lu, X. Fan, C. A. Patel, R. J. Pomerantz, G. C. DuBois and H. Zhang (2003). "Potent Suppression of Viral Infectivity by the Peptides That Inhibit Multimerization of Human Immunodeficiency Virus Type 1 (HIV-1) Vif Proteins." The Journal of Biological Chemistry **278**(8): 6596-6602.

Yang, S., Y. Sun and H. Zhang (2001). "The Multimerization of Human Immunodeficiency Virus Type 1 Vif Protein." The Journal of Biological Chemistry **276**(7): 4889-4893.

Yang, X., J. Goncalves and D. Gabuzda (1996). "Phosphorylation of Vif and Its Role in HIV-1 Replication." The Journal of Biological Chemistry **271**(17): 10121-10129.

Zhang, H., B. Yang, R. J. Pomerantz, C. Zhang, S. Arunachalam and L. Gao (2003). "The cytidine deaminase CEM15 induces hypermutation in newly synthesized HIV-1 DNA." Nature **424**(6944): 94-98.

Zheng, Y.-H., D. Irwin, T. Kurosu, K. Tokunaga, T. Sata and B. M. Peterlin (2004). "Human APOBEC3F Is Another Host Factor That Blocks Human Immunodeficiency Virus Type 1 Replication." Journal of Virology **78**(11): 6073-6076.

APPENDIX II

EXAMINATION OF HIV-1 VIF AND APOBEC3G INTERACTIONS BY SURFACE PLASMON RESONANCE, SIZE-EXCLUSION CHROMATOGRAPHY, AND LASER LIGHT SCATTERING

METHODS

Surface Plasmon Resonance (SPR)

APOBEC3G (APO3G), obtained from the AIDS Research and Reference Reagent Program, was immobilized on a CM4 amine-coupling chip in a SPR machine (Biacore). The CM4 chip surface was activated with 50mM sodium hydroxide and primed by injecting a mixture containing EDC/NHS. After injecting the EDC/NHS, 50µl of 20µg/ml APO3G was injected to immobilize the protein on the chip. The CM4 chip was then washed with ethanolamine to block any unreacted sites; 3000 response units of APO3G were immobilized on the chip.

Binding of NusA-Vif_{LAI} to APO3G immobilized on the CM4 chip was tested by injecting 34µM NusA-$Vif_{LAI,}$ 34µM NusA, and buffer alone. After these single-concentration injections showed binding, I injected the CM4-APO3G chip with buffer-alone control (20mM Tris, pH 8.0, 150mM NaCl), 34µM NusA, and serial dilutions of NusA-Vif_{LAI} (34µM-532nM). The serial-dilution injections produced responses that were analyzed by Biaevalution software to produce kinetic-binding data. The software analysis subtracted the reference surface and blank buffer from experimental values (Chapter II, Methodology).

Size-Exclusion Chromatography—Laser Light Scattering (SEC-LS)

HIV-1 Vif, APO3G, and HIV-1 Vif-APO3G were separated by size-exclusion chromatography column followed by laser light scattering analysis at the Yale Keck facility. The low molecular weight or catalytically active form of APO3G (Chiu, 2006),

was isolated from RNA by incubating E. coli expressed APO3G with 50µg/ml RNase A (Chiu, 2005) for 1 hour at room temperature. The RNase-treated APO3G sample was filtered through a 0.22 µm filter and analyzed by Superdex 200 size-exclusion chromatography. Since the eluate of the Superdex 200 column contained a large aggregate, a tandem-column approach was used, i.e., each sample was first separated on a Superose 6 column, and then over a Superdex 200 column. HIV-1 Vif was analyzed in a similar fashion to APO3G, but not treated with RNase A. For the HIV-1 Vif-APO3G complex, APO3G was incubated with HIV-1 Vif and 50 µg/ml RNase A for 1 hour at room temperature and analyzed by tandem columns. All proteins were analyzed in 50 mM Tris, 150mM sodium chloride, and 1mM DTT, pH 8.0.

RESULTS

Dissociation kinetics of HIV-1 Vif-APO3G does not saturate

APO3G was immobilized onto a CM4 chip and serial dilutions of NusA-Vif_{LAI} were injected onto the immobilized sensor surface in order to obtain a dissociation constant for the Vif-3G interaction. A dose-dependent binding of NusA-Vif_{LAI} to the APO3G surface was observed (Figure A2.1A). However a graph of NusA-Vif_{LAI} concentration versus response units revealed that the reaction did not saturate. Higher concentrations of protein are necessary to achieve this saturation, which I unfortunately was unable to obtain. Even though the binding reaction did not saturate, an approximate K_d of 100µM was determined by fitting the data to the steady-state model (Figure A2.1B). It is possible, however, that this binding constant could be influenced by how

Figure A2.1A

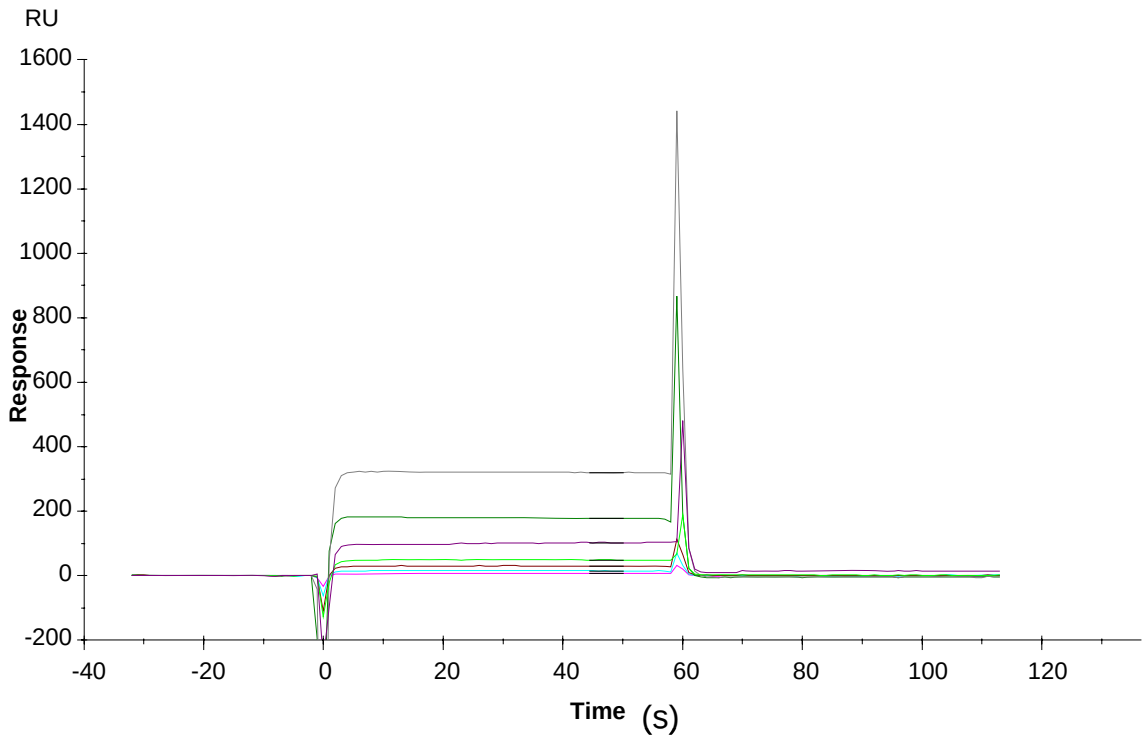
RU
1600
1400
1200
1000
800
600
400
200
0
-200
Response
-40
-20
0
20
40
60
80
100
120
Time (s)

Figure A2.1B

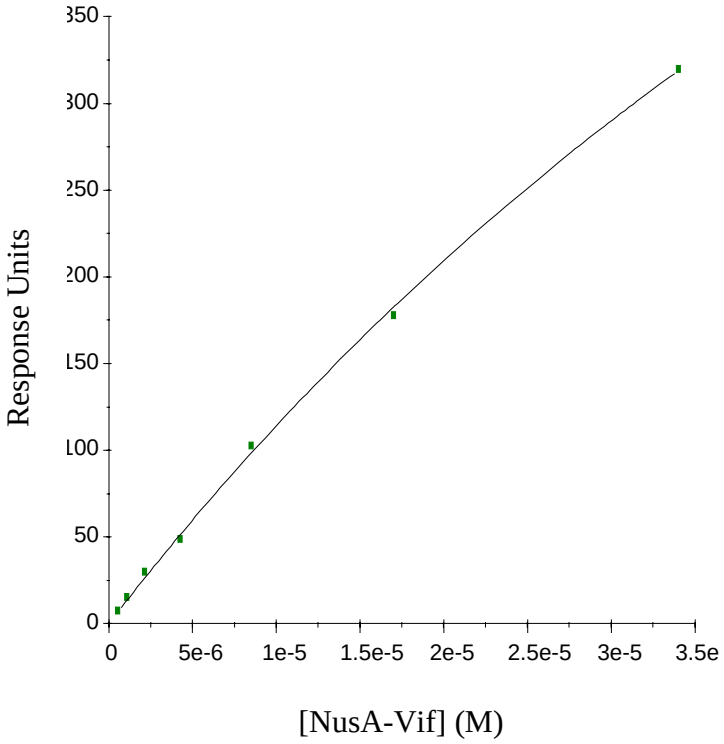
Response Units
350
300
250
200
150
100
50
0
0
5e-6
1e-5
1.5e-5
2e-5
2.5e-5
3e-5
3.5e
[NusA-Vif] (M)

Figure A2.1: NusA-Vif Binding to APO3G Sensor Surface. (A) Dose-dependent binding of NusA-Vif to APO3G surface. APO3G was immobilized on a CM4 sensor chip and different concentrations of NusA-Vif were incubated with the surface. A dose-dependent binding was observed for NusA-Vif to APO3G where as no NusA alone bound to the surface. **(B)** Analysis of NusA-Vif binding to APO3G surface. The concentration of NusA-Vif was plotted versus response units and an approximate K_d of 100μM was observed. The binding kinetics did not saturate, creating a need for further experiments to more accurately determine K_d.

APO3G was immobilized. The amine coupling reaction could have altered the APO3G structure or blocked the HIV-1 Vif binding site, thus causing a low dissociation constant.

Stoichiometry of HIV-1 Vif-APO3G interaction not determined due to insufficient amount of stable protein

HIV-1 Vif, APO3G, and HIV-1 Vif incubated with APO3G were analyzed using size-exclusion chromatography and laser light scattering at the Yale Keck facility. APO3G was analyzed using the Superdex 200. However large protein aggregates were observed, which saturated the light scattering detector. A tandem separation was performed using the Superose 6 and Superdex 200 SEC columns in order to separate the aggregates away from the remaining protein sample. However the majority (greater than 90%) of the sample analyzed was lost. Loss of the protein was likely due to either protein aggregation or the protein interacting with the column matrix (Figure A2.2A). Similar to the APO3G analysis, the HIV-1 Vif and HIV-1 Vif incubated with APO3G analysis had similar failed results--large protein aggregates were seen and the majority of the protein analyzed was lost (Figure A2.2B and C). In the HIV-1 Vif sample analysis, a peak was detected at the 18ml fraction that potentially corresponded to a 20kDa moiety; however the signal was too low for an accurate molecular weight determination (Figure A2.2B). Furthermore, because of the low abundance of the possible 20kDa moiety the presence or absence of oligomers could not be determined.

Figure A2.2A

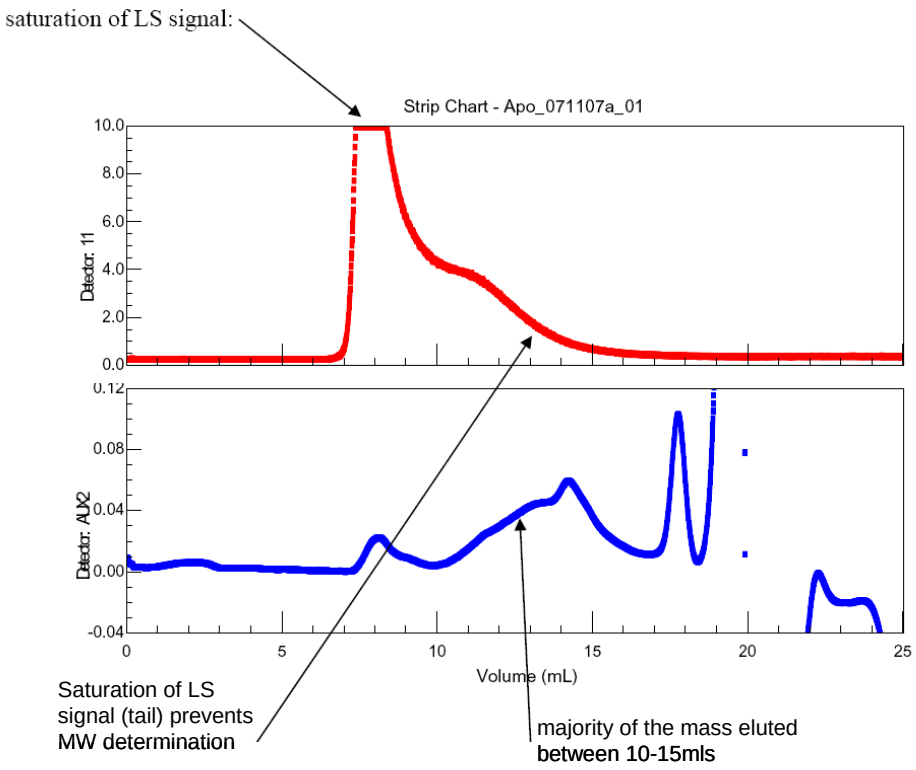
saturation of LS signal:
Strip Chart - Apo_071107a_01
Detector: 11
Detector: AUX2
Volume (mL)
Saturation of LS signal (tail) prevents MW determination
majority of the mass eluted between 10-15mls

Figure A2.2B

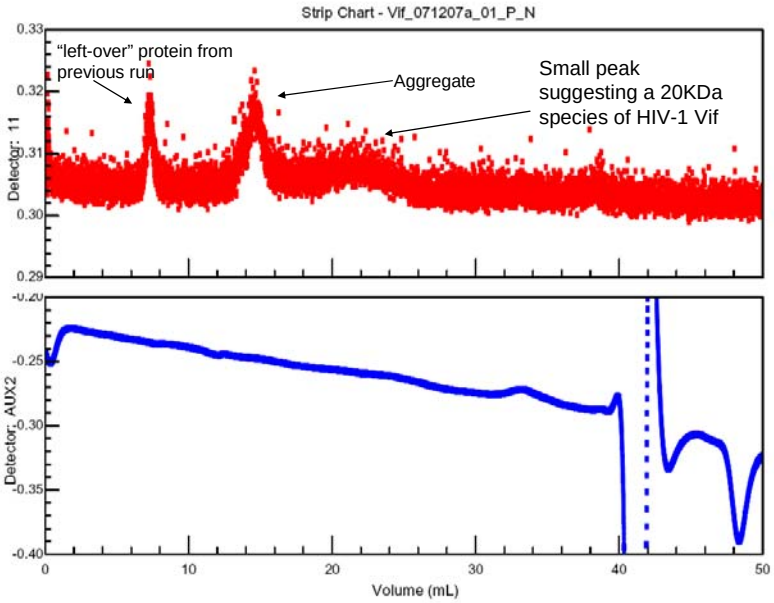
Strip Chart - Vif_071207a_01_P_N
"left-over" protein from previous run
Aggregate
Small peak suggesting a 20KDa species of HIV-1 Vif
Detector: 11
Detector: AUX2
Volume (mL)

Figure A2.2C

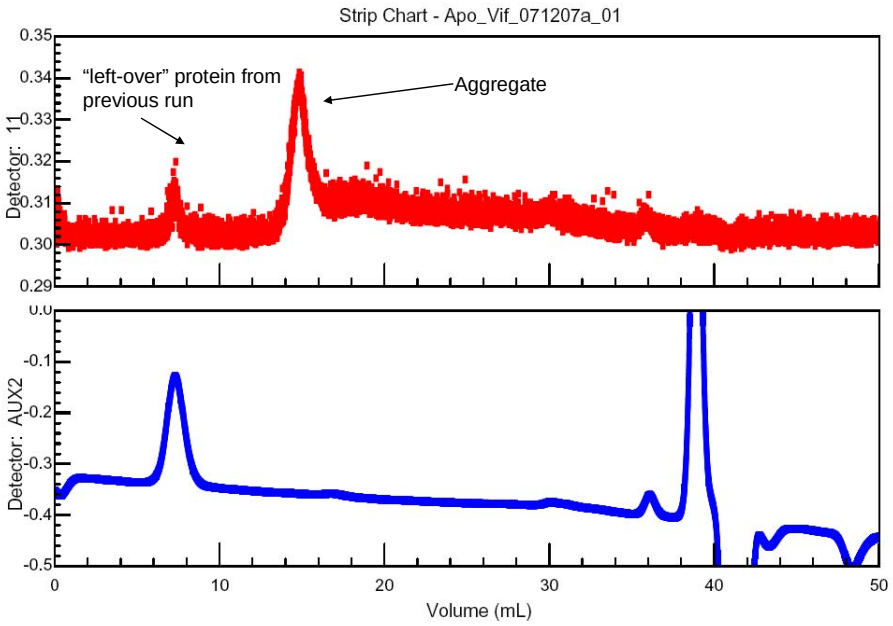
Strip Chart - Apo_Vif_071207a_01
"left-over" protein from previous run
Aggregate
Detector: 11
Detector: AUX2
Volume (mL)

Figure A2.2: SEC-LS Analysis of APO3G, HIV-1 Vif, and the Vif-APO3G complex. **(A)** Analysis of APO3G using SEC-LS. APO3G was incubated with 50µg/ml RNase A, purified using a Superdex 200 or a Superdex 200 followed by a Superose 6 Column, and analyzed using laser light scattering. Unfortunately, the APO3G sample aggregated and saturated the LS signal preventing molecular weight determination. **(B)** Analysis of HIV-1 Vif using SEC-LS. HIV-1 Vif was purified using a Superdex 200 or a Superdex 200 followed by a Superose 6 Column, and then analyzed using laser light scattering. The HIV-1 Vif sample aggregated and saturated the LS signal preventing molecular weight determination. However, a small peak in suggests a 20KDa Vif species may exist. **(C)** Analysis of APO3G incubated with HIV-1 Vif using SEC-LS. HIV-1 Vif and APO3G were incubated together in the presence of 50µg/ml RNase A, purified using a Superdex 200 or a Superdex 200 followed by a Superose 6 Column, and then analyzed using laser light scattering. The HIV-1 Vif-APO3G sample aggregated and saturated the LS signal preventing molecular weight determination.

DISCUSSION

To quantitate the strength of the APO3G-Vif interaction I used surface plasmon resonance (SPR), which measures a dissociation constant or K_d. Preliminary experiments using NusA-Vif_{LAI} as the analyte and APO3G immobilized on the sensor surface of the SPR machine determined an approximate K_d of 100μM. This result suggested that HIV-1 Vif and APO3G have a weak interaction that might be easily disrupted by inhibitors. However, the dissociation reaction did not saturate; thus, the K_d obtained was only a preliminary and approximate value. To obtain a more accurate K_d value, the experiments should be repeated several times at higher concentrations of NusA-Vif_{LAI} to drive the reaction to saturation. However, these experiments were precluded by the low solubility and low concentrations currently available for NusA-Vif_{LAI}. The reciprocal experiment also needs to be performed, i.e., with APO3G as the analyte and HIV-1 Vif immobilized on the sensor surface. When these experiments were attempted, protein aggregated in the flow cell, thus clogging the machine.

To determine the stoichiometry of the HIV-1 Vif-APO3G interaction, I used size-exclusion chromatography followed by laser light scattering. This analysis was hindered by two technical problems. First, the samples of HIV-1 Vif, APO3G, and the HIV-1 Vif-APO3G complex eluted from the column as aggregates that saturated the light scattering detector and prevented analysis of the remaining sample. Second, the majority of each sample appeared to interact with the column matrix, resulting in a 90-100% loss of protein for analysis. To repeat this type of analysis and to optimize column buffer conditions, more soluble and more stable proteins are needed.

REFERENCE

Chiu, Y.-L., V. B. Soros, J. F. Kreisberg, K. Stopak, W. Yonemoto and W. C. Greene (2005). "Cellular APOBEC3G restricts HIV-1 infection in resting CD4+ T cells." Nature **435**(7038): 108-14.